STUDIES OF THE WHITE AND SCARLET PROTEINS OF *Drosophila melanogaster*

A thesis submitted for

the Degree of Doctor of Philosophy

of the Australian National University

Susan Margaret Mackenzie

July, 1999

Membrane Biochemistry Group

Division of Biochemistry and Molecular Biology

John Curtin School of Medical Research

Australian National University

Statement

The work described in this Thesis was performed by the author, except where specifically stated in the text.

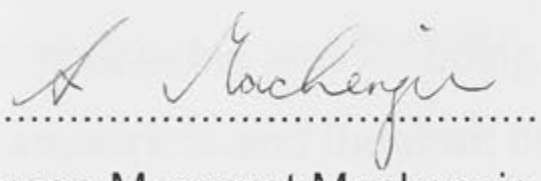

Susan Margaret Mackenzie

July, 1999

Acknowledgments

I would like to thank my supervisors Gary Ewart, Graeme Cox and Tony Howells for their excellent supervision, encouragement and inspiration they have provided me during the years of my post-graduate study. In particular, thanks to Tony Howells, a pioneer in the biochemical analysis of White in *Drosophila*, and Gary Ewart who pioneered the functional characterisation of White, Scarlet and Brown prior to my arrival on the scene. Thank you to Graeme for making me feel welcome in the group and also for being a source of inspiration. Thank you to Tony for helpful lab chats, lab lunches, being so approachable and for being there to make much needed comments on manuscripts and the draft thesis. Thank you to Gary for always being there, particularly near the end after Graeme and Tony had retired.

I acknowledge Rick Tearle's original unpublished postulations of possible sub-cellular locations of White and Scarlet suggesting residence in the pigment granule membrane, as described in his Thesis (ANU, 1986). This topic is the subject of Chapter 7.

Thank you to the membrane biochemistry group - Lyndall Hatch, Terry Sullivan, Anita Dennis, Kerry Mills, Brett Cromer, Louise Tierney, Andy Rodgers, Izzi Wu, Dianne Webb, Damian Buck, Anita Premenkur, Robyn Harris and also Peter Gage, Bryndis Birnir and Lurline Hardy for being friendly and helpful. I also thank Phillis for being terrific, and for shiny floors and empty bins. Thank you to Jelena Burum who tirelessly cleans the glassware and performs other essential duties everyday for the whole of the Biochemistry & Molecular Biology Department.

Thank you to the JCSMR Electron Microscopy Unit, particularly Cathy Gillespie who performed all of the work in relation to preparation of fly eye tissue for electron microscopy (Chapter 6) and whose encouragement and excellent technical expertise enabled the work described in Chapter 6 to culminate in a manuscript for publication. I also thank Cathy for training me on the use of the electron microscope and helping with interpretation. Thank you to Roger McCart for his patience in training me in the use of the confocal

microscope, in addition to printing many electron micrographs. I also thank Darren Moss for many prints of electron micrographs.

Thank you to Russell Taylor for all those large scale *E. coli* cultures, and also for smashing cells with the ribi French press, in addition to repairing and maintaining equipment.

Thank you to Stewart, Julie, Karen and Mark of the Photography Unit of JCSMR for so many photographs of gels, westerns, flies eyes and for advice on: drawing programs; scanning; posters; and slides, and for always being happy to offer advice and help with all sorts of things.

Thank you to Geoff Osborne and Sabine Greuninger for training me on the use of the FACS and IAsys machine, and also for much needed tips on data analysis and the use of the flow cytometry data analysis software.

Thank you to Sue Henderson from the JCSMR computer help desk with assistance with computer problems.

Thank you to Nick Gordon of Chris Parish's group for advice on the use of IAsys data analysis software and for providing very helpful tips on experimental design of interaction experiments.

Thank you to the members of the Biomolecular Resource Facility of the ANU - Cameron, Marjo, Jill, Kerry, Simon and Peter Milburn - for DNA sequencing, oligonucleotides, synthesised peptides, protein sequencing and generally for being helpful and providing a terrific service.

Thank you to Alan Senior who was a visiting fellow with the membrane biochemistry group while I was preparing the manuscript based on Chapter 3 for providing helpful comments.

Thank you to Peter East (CSIRO, Entomology) for his helpful advice on possible approaches with respect to immunolocalisation studies. I also thank Sally Stowe (EM Unit JCSMR) for a very helpful discussion with respect to the ultrastructure of the compound eye.

Thank you to Michael Clarkson for providing me with healthy live stocks of Canton S strain of *D. melanogaster* for electron microscopy experiments.

Thank you to the Division of Biochemistry and Molecular Biology which is made up of many kind hearted people, particularly Dr Paul Foster for allowing

me to remain in an office space at the JCSMR while I finished writing-up. Thank you to Bob Ayling, Barry Webb, Sue Lavender, Sue Petriella, Jan Lee, Babs and Carol for all their help with respect to ordering materials and other day to day problems.

Thank you to the John Curtin School of Medical Research for the PhD Scholarship which provided me with income for 3½ years thereby allowing me to study full-time.

Thank you to Gretchen Mathur (librarian, JCSMR Medical Library) for help and understanding while I occupied one of five library study rooms.

Thank you to my family for their support and encouragement over the years, and in particular my mother and father for their support while I was studying for the Higher School Certificate at night, and also during my under-graduate years. Without this support I would never have made it past first base and would still be doing unfulfilling work.

Thank you to Mr and Mrs Thomas for their kindness and generosity. Thank you to Don Thomas for his support and encouragement, cooking dinners, doing the laundry, cleaning the house, doing the shopping, watering the garden, setting up and maintaining my bike, and also for looking after me when I was ill. Thank you to "Fly" for being the best dog in the world.

Abstract

The *white*, *brown* and *scarlet* genes of *Drosophila melanogaster* encode proteins (White, Brown and Scarlet) which transport precursors of the fly's red and brown eye-colour pigments. These proteins belong to the ABC transporter superfamily and current models envisage that the White protein interacts with the Brown or Scarlet proteins to form two heterodimeric transport complexes of different specificities - namely a White/Brown complex which transports a precursor of red pigments; and White/Scarlet complex which transports a precursor of brown pigments. In the study described in this thesis four different experimental approaches were used in order to investigate structure and functional issues regarding these ABC transporters. These approaches included: 1) immuno-localisation of White and Scarlet in the compound eye of *D. melanogaster*; 2) genetic and biochemical analyses of mutant *white* alleles which result in a partial decrease in eye pigmentation; 3) heterologous expression of *white* and *scarlet* cDNAs in insect cells using a Baculovirus-mediated approach; and 4) expression of the predicted soluble ATP binding domains of White and Scarlet in *E. coli*.

Biochemical evidence prior to the commencement of this thesis implied that the White/Scarlet complex was located in the plasma membrane of pigment cells where they formed a transporter for tryptophan (Howells et al, 1977; Sullivan et al, 1980; Sullivan and Sullivan, 1975). To investigate this proposal, anti-White and anti-Scarlet specific antibodies were used in an immuno-electron microscopy localisation study using *D. melanogaster* eye tissue (Chapter 7). Secondary colloidal gold conjugated antibody labelling indicated that both White and Scarlet localise to the sub-cellular pigment granule membrane and not the plasma membrane as previously proposed. This finding provides fundamental insights into the role of White and Scarlet in the eye pigmentation pathway. This location indicates that White and Scarlet transports 3-hydroxykynurenine, the final pigment precursor found in the cytoplasm of the cell, which is converted to xanthommatin by enzymatic and chemical reactions within the pigment granule.

Genetic and biochemical analyses of mutant *white* and *brown* alleles from flies with partial decreases in red and/or brown eye pigments has previously identified residues within the transmembrane domain of *white* and *brown* encoded subunits which interact and are important for function (Ewart et al, 1994). This thesis describes the analysis of a further five *white* alleles (Chapter 3). The mutations identified fall into two categories: 1) those which occur within the transmembrane domain and which primarily decrease function of the White/Brown transporter (w^{cf}: G589E and w^{sat}: F590G); and 2) those which occur within the nucleotide binding domain and decrease function of both transporters equally (w^{crr}: H298N and w^{101}: G243S). In addition, a mutation was identified within an intra-helical loop region (w^{Et87}: G509D) which caused the most severe reduction in eye pigments. Peptide-protein Interaction analysis using an IAsys biosensor indicated that the White nucleotide binding domain binds to the wild-type loop and that the substitution G509D causes a decrease in binding (Chapter 6, Section 6.2.5).

Work towards the development of a heterologous Baculovirus-mediated expression system of *white* and *scarlet* cDNA is described in this thesis (Chapter 5). This system was tested as a model system for investigating: 1) sub-cellular location of the White and Scarlet proteins; and 2) the hypothesis, that White and Scarlet form a tryptophan transporter in the plasma membrane. White and Scarlet proteins were successfully expressed in insect cells and some of the protein was located in the plasma membrane. However no evidence for tryptophan uptake was obtained. This finding is in agreement with the immuno-EM localisation results indicating White and Scarlet are located in the pigment granule membrane where they function as an importer of 3-hydroxykynurenine into pigment granules, and not an importer of tryptophan at the plasma membrane.

Heterologous expression in *E. coli* of the nucleotide binding domain of White as a fusion protein to glutathione-S-transferase allowed the over-expression of this domain and subsequent affinity purification by glutathione-agarose chromatography (Chapter 6). Although this domain was predicted to be soluble

by sequence analysis, most of the protein was found in the insoluble cell debris and membrane fractions. This domain was successfully solubilised using non-denaturing detergents and it was subsequently partially purified, and shown to have ATP binding activity.

Abbreviations

A	Adenosine
ABC	ATP binding cassette
AMP	Adenosine monophosphate
ANU	Australian National University
APS	Ammonium persulphate
ATP	Adenosine triphosphate
bp	Base pairs
C	Cytosine
cDNA	Complementary DNA
CF	Cystic fibrosis
CFTR	Cystic fibrosis transmembrane regulator
CHAPS	3-[3(3-cholamidopropyl)dimethyl-ammonio]-1-propansulfonat
DNA	Deoxyribonucleic acid
DTT	DL-dithiothreitol
EDTA	Ethylenediamine tetraacetic acid
EM	Electron microscopy
TEM	Transmission electron microscopy
G	Guanosine
GTP	Guanosine-triphosphate
GST	Glutathione-S-transferase
HPLC	High performance liquid chromatography
IPTG	Isopropyl β-D-thiogalactoside
JCSMR	John Curtin School of Medical Research
kDa	Kilo daltons
Kb	Kilo base
LB	Luria Bertani
mA	Milli amps
MCS	Multiple cloning site
MDR	Multiple drug resistance

MTPBS	Mouse tonicity phosphate buffer
NBF	Nucleotide binding fold
OD	Optical density
PAGE	Polyacrylamide gel electrophoresis
PCR	Polymerase chain reaction
PMSF	Phenyl-methansulphonylfluoride
PVDF	Polyvinylidene difluoride
rpm	Revolutions per minute
SDS	Sodium dodecyl sulphate
ss	Single stranded
T	Thymidine
TCA	Trichloro acetic acid
TE	Tris-EDTA
TEMED	N,N,N'N'-tetramethyl-ethylenediamine
TM	Transmembrane
Tris	Tris[hydroxymethol amino-methane]
TX	Triton X
Vhr	Volt hour
w/v	Weight per volume
UV	Ultraviolet

TABLE OF CONTENTS

Publications

Mackenzie S M, Brooker M R, Gill T R, Cox G B, Howells A J and Ewart G D
Mutations in the *white* gene of *Drosophila melanogaster* affecting ABC transporters that determine eye colouration
In press, *Biochimica et Biophysica Acta*

Mackenzie S M, Howells A J, Cox G B, and Ewart G D
Immuno-electron microscopy localisation of White and Scarlet protein in the compound eye of *Drosophila melanogaster*
Submitted to *Molecular and General Genetics*

CHAPTER 1

INTRODUCTION

1. INTRODUCTION

The biological significance of membranes and the proteins and reactions which are associated with membranes should never be under-estimated. Cell membranes enable order within an otherwise vast metabolic soup and are an integral part of the majority of cellular processes including: cellular respiration; intercellular communication; flux of metabolites in and out of the cell; the list goes on and on. The importance of passage of metabolites by specific membrane proteins becomes obvious in disease states where failure of a single membrane protein (e.g. a transporter, channel or receptor) can result in metabolic perturbation of the whole organism resulting in death or severe disability. A number of exmples of this can be found among the superfamily of membrane transporters known as the ATP binding cassette (ABC) transporters, including:

i) **Cystic fibrosis** is the debilitating lung and pancreatic disease which results from mutation of the cystic fibrosis transmembrane regulator (**CFTR**) which controls chloride flux in specific tissues (Quinton, 1990; Rommens et al, 1989).

ii) **Stargardt disease** results from mutations within the ABCR gene (Allikmets et al, 1997) encoding a retinal rod photoreceptor protein which, when defective causes blindness.

iii) **Adrenoleukodystrophy** results from mutations in the ALD gene which encodes a peroxisomal membrane protein and when dysfunctional results in impaired peroxisomal oxidation of very long chain fatty acids which results in neurodegeneration (Mosser et al, 1993).

iv) **P-glycoprotein** is encoded by the MDR1 gene in humans (Fojo et al, 1985; Roninson et al, 1986). It is the over-expression of this gene which contributes to a multi-drug resistance phenotype in cancer cells which is a serious clinical problem in the treatment of cancer patients (Gottesman and Pastan, 1993; Roepe, 1995; Roepe et al, 1996). Over-expression of P-

glycoprotein enhances the efflux of cytotoxic anti-cancer drugs from the cells.

The work described in this thesis is focussed on the development of a model system for the study of the structure and function of ABC transporters. The genes *white*, *scarlet* and *brown* from *Drosophila melanogaster* encode membrane transporters involved in the biosynthesis and sub-cellular localisation of red and brown eye-colour pigments within pigment cells of the fly's compound eye. The products of these three genes belong to the ABC transporter superfamily, based on amino acid sequence similarity with members of the superfamily. This introductory chapter aims to review the current understanding regarding the structure and function of this very interesting superfamily of membrane transporters. The general protein topology of ABC transporters will be discussed, in addition to the different functional domains which make up an active ABC transporter. Evidence for inter-domain interactions and the significance of these interactions to the transport mechanism will be discussed. Particular reference will be made to two eucaryotic ABC transporters, P-glycoprotein and CFTR, which have been intensively studied for many years. Many of the insights gained from these systems may be applicable to the *Drosophila* proteins and other ABC transporters. An overview of the background literature regarding the *white*, *scarlet* and *brown* gene products will be given, concluding with the aims of the work described in the thesis.

1.1 ABC transporters: an introduction

The ABC transporter superfamily is made up of a large number (over 100 identified) of membrane permeases which are energised by ATP for the transport of substrate against a concentration gradient. Members of this superfamily share a number of characteristic structural and functional features. Sequence similarity between members of the family, at first glance, is limited largely to a number of highly conserved sequence motifs which are diagnostic for ABC transporters. This conservation is most apparent for the ATP binding domains, suggesting that this domain is highly conserved both in structure and function. The transmembrane (TM) domains are less conserved, however all

members of the family share a similar predicted membrane topology. The highly conserved nature of the ATP binding domains and the membrane topology of the TM domains is indicative of a similar ATP powered transport mechanism which has adapted for the transport of a vast range of substrates by alterations in the transmembrane domains which provide specificity. These issues are discussed in more detail below.

1.2 Overall Topology

ABC transporters are composed of two hydrophobic domains each usually consisting of 6 putative transmembrane α helices. In addition, they possess two cytoplasmic ATP binding domains which harbour the ATP binding cassette. The four domains can be associated, in various combinations, on the same or different polypeptide chains (which are closely associated in the three dimensional structure), as indicated in Fig. 1. Bacterial ABC transporters usually possess an additional subunit known as the periplasmic substrate binding protein which presents substrate to the transporter. CFTR is the only known eucaryotic ABC transporter which possesses an extra domain, known as the regulatory domain, which is linked in the same polypeptide (Fig. 2). The different combinations of fused and unfused functional units gives an indication of possible gene fusion and duplication events which have occurred during evolution and suggest that the ABC transporters known today arose from a separate ancestral hydrophobic membrane spanning domain, combining with a separate nucleotide binding domain (Croop, 1998).

Fig. 1 Topological categories of ABC transporters. ABC transporters can be grouped into a number of sub-groups based on whether or not the different functional domains are fused on the same polypeptide, or on separate polypeptides. This figure illustrates these sub-groups both diagramatically in A. and as a broad dendogram in B. which is suggestive of the evolutionary relatedness of the sub-groups. The diagram shown in B. was partly derived from Fath & Kolter (1993).

A.

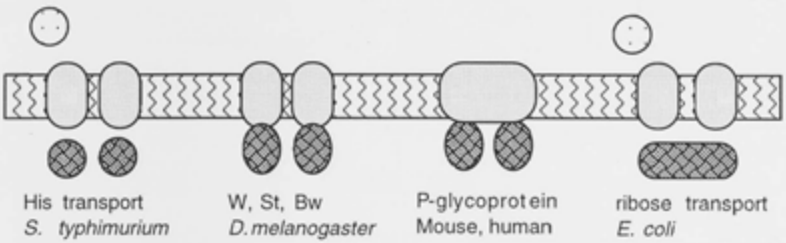

B.

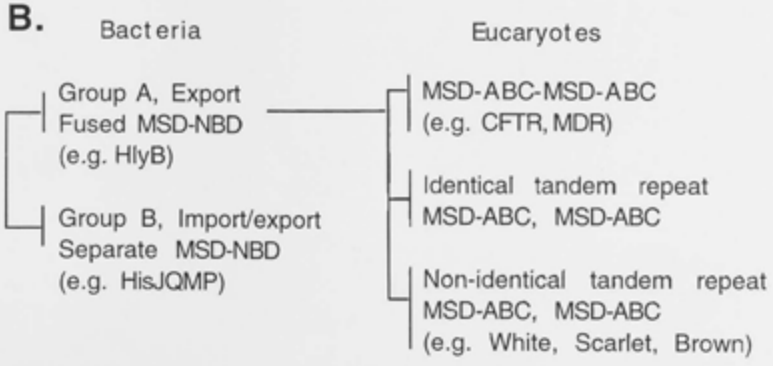

Fig. 2 Predicted topology of CFTR and P-glycoprotein

Shown here are simplified diagrammatic illustrations of the membrane topology of CFTR and P-glycoprotein. Both of these ABC transporters are made up from a single polypeptide chain. The putative membrane spanning α-helices are represented as grey filled cylinders and are numbered 1 to 12. Abbreviations: NBD, nucleotide binding domain; R domain, regulatory domain. This figure illustrates the relative positions of loops and transmembrane regions discussed in the text.

A. The predicted transmembrane topology of CFTR (Riordan et al, 1989). CFTR is the only known eucaryotic ABC transporter which harbours the accessory domain known as the R (regulatory) domain.

B. The predicted topology of P-glycoprotein (Gottesman and Pastan, 1988; Juranka et al, 1989).

A. CFTR

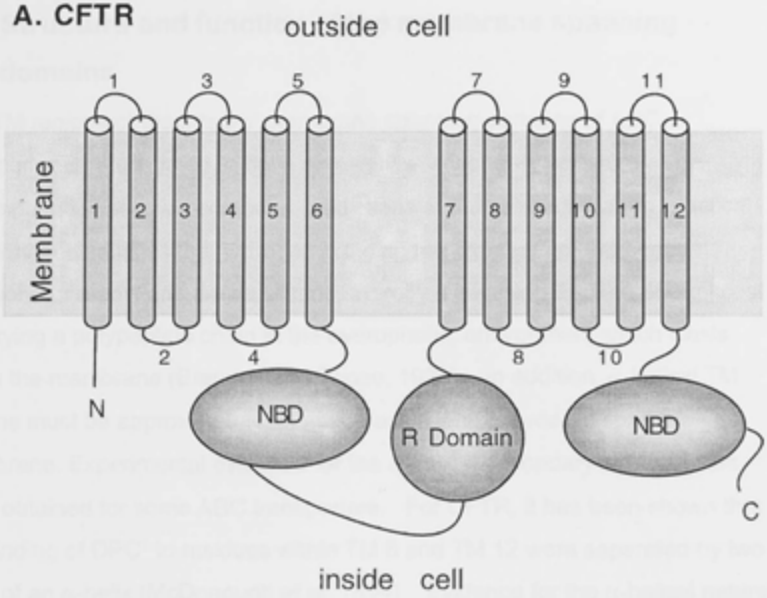

B. P-glycoprotein

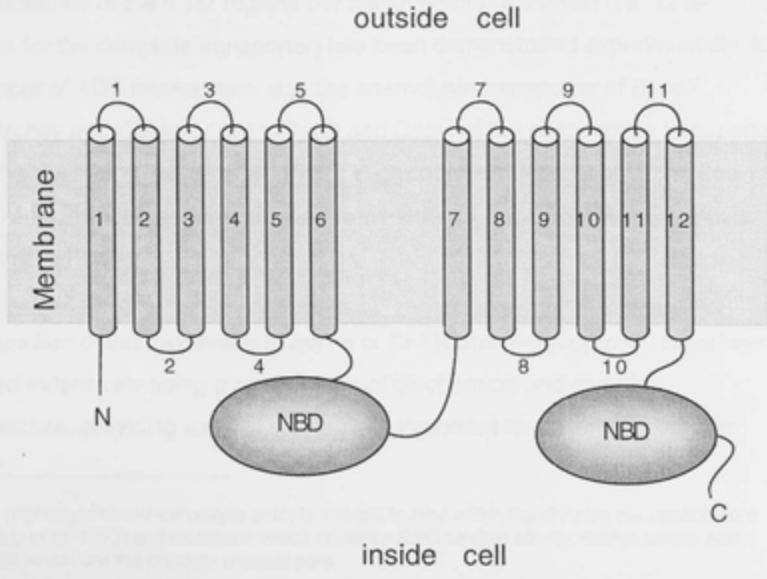

1.3 Structure and function of the membrane spanning domains

The TM regions of the integral membrane spanning domains of ABC transporters are assumed to have an α-helical secondary structure. This assumption is based on computer predictions and the theory that an α-helical conformation satisfies the hydrogen bonding requirements of the peptide backbone carbonyl and amide groups, thereby minimising the free energy cost of burying a polypeptide chain in the hydrophobic environment which exists within the membrane (Branden and Tooze, 1991). In addition, α-helical TM regions must be approximately 20 amino acids long in order to span the membrane. Experimental evidence for the α-helical secondary structure has been obtained for some ABC transporters. For CFTR, it has been shown that the binding of DPC[1] to residues within TM 6 and TM 12 were separated by two turns of an α-helix (McDonough et al, 1994). Evidence for the α-helical nature of TM 1 has also been obtained. Cysteine-scanning mutagenesis and sulfhydryl-specific reagents were used to label transmembrane residues and these were shown to have an α-helical periodicity (Akabas et al, 1994).

The existence of the 6 TM regions per transmembrane domain (i.e. 12 α-helices for the complete transporter) has been demonstrated experimentally for a number of ABC transporters e.g. the haemolysin transporter of *E. coli* (Gentschev and Goebel, 1992), OppB and OppC of the oligopeptide transporter of *S. typhimurium* (Pearce et al, 1992); P-glycoprotein (Kast et al, 1996; Loo and Clarke, 1995b); and the histidine transporter of *S. typhimurium* (Kerppola and Ames, 1992).

The function of the membrane domains of CFTR and P-glycoprotein have been studied extensively using a combination of biochemical and genetic approaches, providing insights into regions important for channel activity (in

---

[1] DPC (diphenylamine-2-carboxylic acid) is thought to bind within the chloride permeation pore (McCarty et al, 1993) and mutations which influence DPC binding affinity change amino acid residues which line the chloride channel pore.

CFTR) and substrate binding and specificity. In particular, TM regions 1, 5, 6, 11 and 12 of both P-glycoprotein and CFTR (see Fig. 2) have been extensively studied and shown to be important for the structure and function of these proteins. Some of these insights are reviewed below.

Substrate specificity of transmembrane domains

(a) P-glycoprotein

It has been well established using photo-affinity drug labelling and energy transfer techniques that P-glycoprotein recognises its substrate within the context of the membrane bilayer[2] (Bruggemann et al, 1989; Greenberger, 1993; Greenberger et al, 1991; Morris et al, 1994; Morris et al, 1991; Raviv et al, 1990). It was reported that photolabelled sites were located symmetrically near TM 6 and 12 (Greenberger, 1993). The model illustrated in Fig. 3 was proposed, where TM 6 and 12 interact to form part of the channel that participate in drug efflux (Greenberger, 1993) and therefore may be a region important for substrate specificity.

The specificity function of the TM domains was demonstrated by a number of studies using chimeric P-glycoprotein molecules (Buschman and Gros, 1991; Dhir and Gros, 1992). The conversion of MDR-3 (which does not have a drug efflux activity) into an active drug efflux pump, by substituting the extra-cellular loop between TM 11 and 12, as well as TM helix 12 from MDR1, was very strong evidence that these regions were of paramount importance for the transport activity of P-glycoprotein (Zhang et al, 1995a). In addition, it was observed that cross-resistance profiles altered (i.e. substrate specificity changed) depending on the replacements.

Further investigations with respect to the issue of substrate specificity have identified a number of residues which alter P-glycoprotein's specificity to some

---

[2] i.e. P-glycoprotein substrates intercalate into the lipid bilayer prior to being recognised by the transporter, which pumps it out of the bilayer.

Fig. 3 Model of the photoaffinity drug labelling site of P-glycoprotein.

This model is based on photoaffinity drug labelling studies where the major sites of IAAP labelling were proposed to be in contact with intracellular regions just beyond TM 6 and TM 11 and in close proximity to the ATP binding site. This figure illustrates TM 5 and 6, as well as TM 11 and 12 in close proximity and interacting in the formation of part of a channel that participates in drug eflux. This model also highlights a possible functional importance of intracellular loop regions in close proximity to the ATP binding domain. This figure was reproduced from Greenberger, (1993).

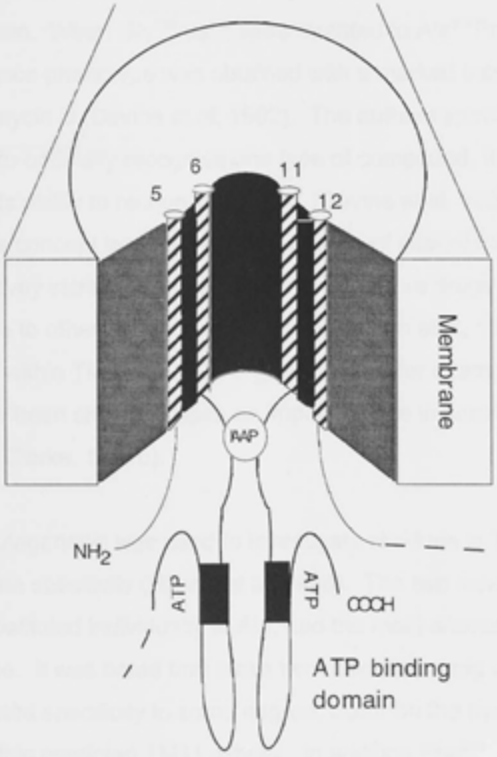

drugs, but not others. The serine residues Ser^{939} of mdr1[3] and Ser^{941} of mdr3, both within TM 11, were shown to have marked modulatory effects on cross-resistance (Dhir et al, 1993). It was shown that the introduction of the bulky side chains of tyrosine and tryptophan at these sites caused loss of colchicine and adriomycin resistance, while increasing the actinomycin resistance of cells containing mdr1 (3 fold) or mdr3 (4-8 fold) (Dhir et al, 1993).

This phenomenon was also observed for two adjacent residues in TM 6 of hamster P-glycoprotein. When $Gly^{338}Ala^{339}$ were mutated to $Ala^{338}Pro^{339}$, an altered cross-resistance phenotype was obtained with a marked increase in resistance to actinomycin D (Devine et al, 1992). The authors speculate that "if the site was altered to optimally recognise one type of compound, it might lose or be diminished in its ability to recognise others." (Devine et al, 1992). The authors note that this concept is consistent with reports of alterations of P-glycoprotein that convey increased resistance to one or more drugs, resulting in decreased resistance to others (Choi et al, 1988l; Roninson et al, 1991; Safa et al, 1990). Residues within TM6 of human P-glycoprotein (for example Val^{338} and Gly^{341}) have also been shown to have an important role in substrate specificity (Loo and Clarke, 1994b).

Alanine scanning mutagenesis was used to investigate residues in TM 11 important for substrate specificity (Hanna et al, 1996). The two residues Phe^{953} and Tyr^{949} when substituted individually to Ala, had the most dramatic effect on drug cross-resistance. It was noted that these two residues, along with other residues which affected specificity to some degree, occur on the hydrophilic face of the amphipathic predicted TM11 α-helix. In addition Phe^{953} and Tyr^{949} are highly conserved in both TM5 and TM11 of P-glycoproteins of other species, as well as other ABC transporters, including CFTR and its homologs in mouse, frog and dogfish (Hanna et al, 1996), also suggesting their functional importance. The residue Ile^{936} which reduced resistance to all four

---

[3] lower case "mdr" denotes mouse homologs of P-glycoprotein, while upper case denotes human homologs.

drugs tested, is also conserved in TM5 and 11 of P-glycoproteins in rodents, human and yeast. Isoleucine or leucine is also found in the analogous position in some prokaryotic ABC transporters (Hanna et al, 1996).

(b) Cystic fibrosis transmembrane regulator

It is very interesting to note that regions predicted to form TM 6 and 12 in CFTR, like P-glycoprotein, have also been found to be strongly associated with substrate binding and specificity functions (Anderson et al, 1991; Cheung and Akabas, 1996; McDonough et al, 1994; Tabcharani et al, 1993).

TM 6 was first implicated in substrate specificity when it was demonstrated that mutation of Lysine^{335} of TM 6 to an acidic residue caused a change in halide specificity of the CFTR ion channel (Anderson et al, 1991). It was also shown that the mutation of S^{341} and K^{335} within TM 6 can alter the binding of a voltage-dependent open channel blocker (diphenylamine-2-carboxylic acid (DPC)) (McDonough et al, 1994). In both TM 6 and TM 12, residues involved in DPC binding were separated by two turns of an α helix (McCarty et al, 1993; McDonough et al, 1994). It was proposed that residues within TM 6 and TM 12 line the chloride pore of CFTR.

In addition to TMs 6 and 12, TM 1 in combination with TM 6 have been extensively studied by cysteine-scanning mutagenesis[4] (Cheung and Akabas, 1996; Cheung and Akabas, 1997). Fig. 4 A and B illustrates α helical maps of TMs 1 and 6 showing residues which were found to be water accessible (highlighted by black squares) when substituted for cysteine. The figure shows that most of the water accessible positions are on one face of the helix, with some notable exceptions (Q^{353}, R^{352} and K^{335}) which are proposed to loop up back into the water accessible channel. This is illustrated in the working model proposed for the CFTR channel represented in Fig. 4C (Akabas et al, 1997). It was proposed by these authors that the cytoplasmic end of TM 6 loops back

[4] The cysteine-scanning-accessibility technique (Akabas et al, 1992) has been used to identify water-accessible residues of TM domains associated with channel activity by their reaction with sulfhydryl-specific methanethiosulfonate (MTS) reagents.

Fig. 4 Model of the CFTR channel

The helical-wheel plots of TM 1 and TM 6 shown in A and B show the relative positions of amino acid residues in the helices. Water-accessible residues (indicated by black squares) determined from MTS-accessibility studies (reviewed in (Akabas et al, 1997)). The model interpreting these data is shown in C where MTS-accessible residues line the channel lumen, while residues at the cytoplasmic end of TM 6 loop back into the channel lumen forming a selectivity filter. This figure was reproduced from (Akabas et al, 1997).

A CFTR M1 SEGMENT

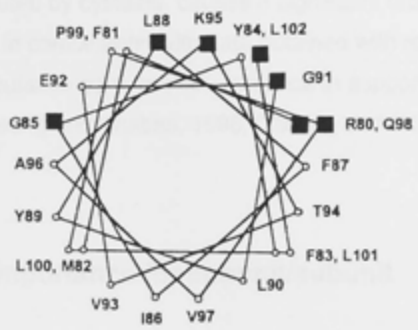

B CFTR M6 SEGMENT

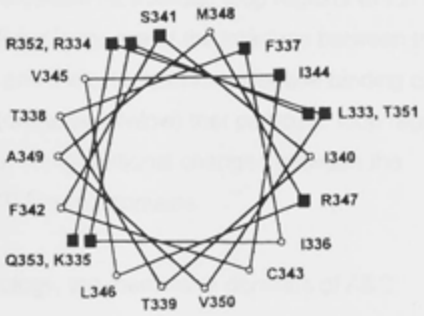

C

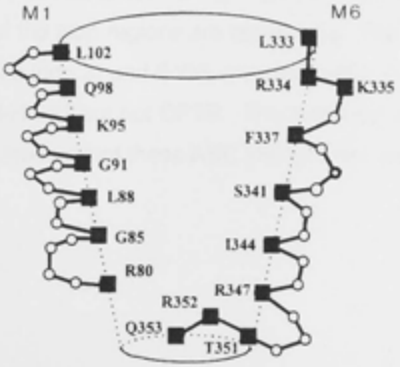

and may mediate resistance to current flow and form the anion-selectivity filter. In particular R^{352}, when substituted by cysteine, causes a significant drop in charge selectivity. This result, in combination with data obtained with respect to electrical distances within the putative pore, provide evidence in support of this model (Akabas et al, 1997; Cheung and Akabas, 1996; Cheung and Akabas, 1997).

1.4 Intracellular loops: importance for subunit/subunit interactions

It is clear from the work reviewed above that particular transmembrane helices are of functional importance for both substrate specificity and transport or channel activity in the case of CFTR. Also of functional significance with respect to transport function are certain intracellular loop regions which connect the TM helices. These intracellular loops are at the interface between the transmembrane (TM) domains and the cytoplasmic nucleotide binding domains (NBDs) and there is evidence (discussed below) that particular loop regions are important for the transduction of conformational changes between the membrane and cytoplasmic ATP binding domains.

With respect to sequence homology, the membrane domains of ABC transporters have a lower sequence conservation in comparison to the homology of the NBDs. However significant amino acid homology has been noted in the loop regions connecting the TM regions in sequence alignments of CFTR, MDR, STE6, HLYB and HAM1 as shown in Fig. 5 (Manavalan et al, 1993). In addition, the length of the loop regions are conserved. The sequence motifs LTLXXXXXXP (in loop 3) and GXXL (in loop 5) (Fig. 5) were noted in MDR, STE6, HLYB and HAM1 but not CFTR. This provides strong evidence for the evolutionary relatedness of these ABC transporters and that

Fig. 5 Amino acid conservation of transmembrane domains of a number of ABC transporters

This figure was reproduced from (Manavalan et al, 1993) and illustrates conservation of the putative transmembrane (indicated by the solid bars) and loop regions of ABC transporters with divergent functions from different organisms. Of particular interest is the homology between loop regions. There is also some degree of homology between some residues within the transmembrane regions.

Abbreviations:
Suffixes N and C after the identification code denote the N-terminal and C-terminal transmembrane domain, respectively; HMDR1 human MDR1; MMDR1, mouse MDR1; HCFTR, human CFTR; STE6, yeast α factor transporter; HlyB, *E. coli* haemolysin toxin exporter; RING4, human MHC-linked peptide transporter; HAM1, mouse MHC-linked peptide transporter

Colour key:
Yellow: Identical or very similar amino acid residues.
Blue: Residues that are more specific for the first transmembrane domain.
Pink: Residues that are more specific for the second transmembrane domain.
Green: Sequence motifs that are observed only in MDR, STE6, HlyB, RING4 and HAM1.

the folding topology of the membrane domain is probably similar (Manavalan et al, 1993).

Of particular interest is whether a sequence analogous to the EAA motif found in procaryotic ABC transporters is found in the eucaryotic transporters. In the prokaryotic models this motif which is around 30 residues long, occurs within intracellular loop 4 (Kerppola and Ames, 1992; Saurin et al, 1994a). Certain residues in the motif have been shown to be important for function and it has been suggested that the EAA motif interacts with the nucleotide binding domain (Kerppola and Ames, 1992). Strong evidence for this proposal has been provided by mutagenesis studies whereby certain EAA mutants of the *E. coli* maltose permease caused the failure of MalK to assemble with MalF and MalG (Mourez et al, 1997). In addition Mourez et al (1997) identified several mutations within the proposed helical-domain between Walker A and B motifs (Mimura et al, 1991) which restored activity in transport defective EAA motif mutants, providing strong evidence that these regions interact. It has also been noted that substrate specificity of procaryotic ABC transporters can be predicted by sequence variation in their EAA motif (Saurin et al, 1994b). Although a role in correct recognition between ATP binding domains (which are often separate polypeptide chains in procaryotes) and the membrane associated domain of procaryotic ABC transporters has been suggested (Saurin et al, 1994b) a role for this motif in substrate binding may also be possible.

In eucaryotic ABC transporters, an EAA-like motif of around 15 amino acids has been noted in loop 4 (intracellular loop between TMs 4 and 5)(Shani et al, 1995) (e.g. adrenoleukodystrophy protein (ALDp), Pxap, PMP70, TAP1, P-glycoprotein). It has been suggested that the ABC signature sequence[5] interacts with the TM domain through this EAA-like motif in eucaryotes (Shani et al, 1996) (see Fig. 6).

Fig. 6 The EAA-like motif of some eucaryotic ABC transporters

A. A hypothetical model (Shani et al, 1996) of the topology of the peroxisomal ABC transporter Pxa1p of *S. cerevisiae*. This ABC transporter is a member of a homologous family of eucaryotic peroxisomal ABC transporters implicated in the human genetic disorders of peroxisome biogenesis and function. A motif designated the "EAA-like motif" has been identified in peroxisomal ABC transporters and other eucaryotic ABC transporters. The relative positions of the Walker A, and B, and signature sequence (motif C), are shown. Shani et al, 1996 proposed that motif C interacts with the EAA-like motif.

B. Alignment of the EAA-like motifs of eucaryotic ABC transporters (from (Shani et al, 1996).

Abbreviations are as follows:
Pxa1p, from *S. cerevisiae*
Pxa2p, from *S. cerevisiae*
PMP70, from human
ALDP, from human
(*C. e* C44B7.8), *C. elegans* open reading frame C44B7.8
hTAP1, human TAP1
mMDR2, murine MDR2
dMDR4, *Drosophila* MDR 4

A

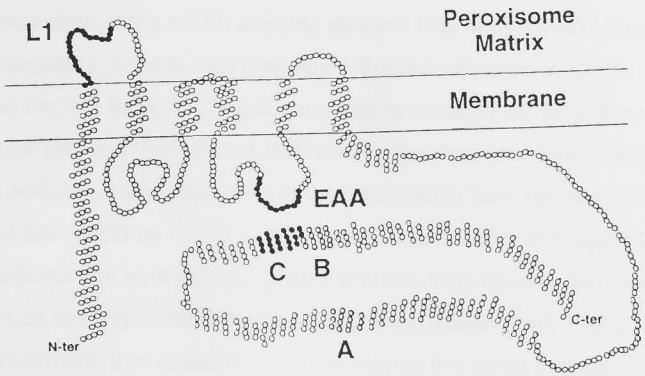

B

Pxa1p	NSEEIAFYQGTAVER	292-305
Pxa2p	SNEEIALLRGQKRELL	320-333
PMP70	NSEEIAFYNGNKREK	275-288
ALDP	NSEEIAFYGGHEVEL	289-302
C. e C44B7.8	NSEEIAFYNGNKPEK	283-395
hTAP1	TVRSFANEEGEAQKF	436-450
hMDR1	KNLEEAKRIGIKKAI	280-292
mMDR2	KHLENAKKIGIKKAI	279-291
hMDR3	KHLENAKEIGIKKAI	282-294
dMDR4	KLLIPAENTGRKKGL	284-296

Evidence for the functional significance of intracellular loop regions has been presented for CFTR, P-glycoprotein and ALDp. In CFTR it has been reported that the intracellular loop between TMs 4 and 5 is involved in stabilising the full conductance state of the CFTR chloride channel (Xie et al, 1995). These authors suggested that the loop interacts with other domains in CFTR (nucleotide binding folds, R domain and/or other intracellular loops) or with other cellular proteins that may be involved in transition between conductance states. In addition, some mutations in the intracellular loop between TMs 4 and 5 have a similar effect on CFTR activity as mutations within the nucleotide binding domains and so it was suggested that this loop couples the activity of the nucleotide binding domains to channel gating (Cotten et al, 1996). Similarly, mutations that cause CF disease map to the loops between TM 2 and 3 and these have been reported to impede transition of CFTR to the open state (Seibert et al, 1997). In particular, mutations introducing a positive charge into this loop ($G^{178}R$ and $E^{193}K$) have a severe effect on channel activity, which is consistent with the notion that electrostatic interactions between the cytoplasmic loops and other domains of the protein, are important (Seibert et al, 1997).

In the case of P-glycoprotein, a role of cytoplasmic loops in substrate specificity has been postulated (Loo and Clarke, 1994a). It has been demonstrated that mutating glycine residues in cytoplasmic loops between transmembrane helices 2 and 3; 4 and 5; and 8 and 9 alters substrate specificity (Loo and Clarke, 1994a).

Although it is clear from the abovementioned reports that the loop regions between TM helices are functionally important, it is not yet clear what their specific functions are.

---

[5] The ABC signature sequence (also known as motif C), a highly conserved motif within the nucleotide binding domain, is diagnostic for ABC transporters and is not found in other ATP or GTP binding proteins. This motif is discussed in Section 1.5.2 c.

1.5 ATP binding domain

The cytoplasmic ATP binding domains of the ABC transporter superfamily are thought to be the energy transducing machinery for powering the translocation of substrate, via the TM domains, from one side of the membrane to the other. As discussed below this domain is highly conserved in sequence, inferring conserved functional and structural elements common to all ABC transporters.

The ATP binding domains of the ABC transporters share significant sequence homology of between 30 and 50% (Croop, 1998; Higgins, 1992) and sequence alignment of different ABC transporters reveal a number of highly conserved sequence motifs which occur within a region encompassing 200 amino acids (Croop, 1998; Higgins, 1992; Higgins et al, 1986; Hyde et al, 1990; Mimura et al, 1991; Riordan et al, 1989). This is the region designated the "ATP binding cassette" from which the ABC transporter superfamily derives it's name.

The structure of this domain was believed to be similar to other ATP and GTP binding proteins including adenylate kinase, $p21^{ras}$ and EF-Tu. Crystallographic structures of these proteins have been solved and they harbour similar mononucleotide binding protein structural elements. The structure of $p21^{ras}$, which is a good example of the conserved folding pattern of this group of proteins is shown in Fig. 7. The core structure includes the P-loop motif (orange), followed by 2 β-strands and a domain composed of a helix-turn-strand motif which is a highly conserved structural element known as the Rossman fold (Rossman et al, 1974). The Rossman fold may be one of the most ancient protein motifs known and is conserved in many dinucleotide binding proteins (Bellamacina, 1996) as well as mononucleotide binding proteins. It is structures such as these that have provided the framework for a number of predicted models of the nucleotide binding domains of ABC transporters (Annereau et al, 1997; Bianchet et al, 1997; Hoedemaeker et al, 1998; Hyde et al, 1990; Mimura et al, 1991). However, the first solved crystal structure of an ATP binding

Fig. 7 Structure of the GTP-bound form of p21^{ras}

This ribbon diagram illustrates the 3D structure of p21^{ras} determined by x-ray diffraction analysis and is taken from Bourne et al, 1991. This structure is a good example of the conserved nature of ATP and GTP binding proteins. The Rossman fold made up of a number of β-strands is shown by grey arrows. The Walker A motif which forms part of the phosphate binding loop is coloured orange, and labelled G1. The Walker B harbouring a highly conserved Asp is coloured red and labelled G3. Other coloured regions labelled G2, G4 and G5 highlight other regions which may be conserved and important for function in Ras or other members of the GTP binding protein family.

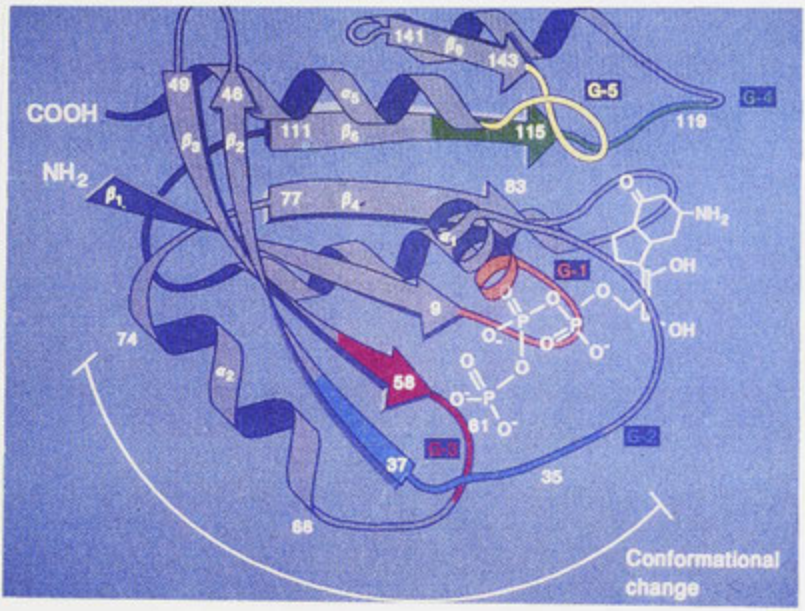

domain of an ABC transporter (HisP) has recently been published (Hung et al, 1998) and is markedly different from the predicted structures based on adenylate kinase, $p21^{ras}$, with only limited similarity to structures of recA (Story and Steitz, 1992) and the α- and β- subunits of bovine F_1ATPase (Abrahams et al, 1994). The uniqueness of the ABC transporter nucleotide binding domain, and its conserved nature among a large family, suggests an effective solution to a common metabolic problem i.e. the selective transport of molecules across membranes. The structure of HisP[6] and possible functional significance is discussed below.

1.5.1 Crystal structure of HisP

The crystal structure of HisP shows that, in agreement with previous biochemical data, the subunits form a dimeric structure. Each monomer was described as having an overall "L" shape made up of two arms (arm I and arm II) illustrated in Fig. 8. The ATP binding pocket is near the end of arm I. The six stranded β sheet spans both arms of the L. On one side of arm I the β-strand rich area forms an anti-parallel β sheet and it is through this structure that the two monomers contact each other, through hydrophobic interactions. Arm II is α-helix rich and this region is less conserved in sequence among ABC transporters (except for the signature sequence). This region is appropriately placed for interactions with the TM domain. There is strong genetic evidence indicating that arm II is embedded in the membrane by interaction with the TM subunits HisQ and HisM. Mutations in arm II of HisP have been shown to decrease the affinity of HisP for HisQ and HisM (Petronilli and Ames, 1991). It is assumed that the conformation of the TM domain has been appropriately changed (normally a role of the HisJ protein) to allow binding and transport of the substrate. The ABC signature sequence is located within the α helical rich part of arm II, well placed for its predicted role in transduction of conformational changes between the ATP binding site and the TM domain. However the exact role of this sequence is not obvious. This region is buried within arm II with only

---

[6] The crystal structure of HisP was unknown at the outset of this PhD project.

Fig. 8 Crystal structure of the HisP dimer

The view of the HisP dimer shown here is along an axis perpendicular to its two-fold axis. The top and bottom of the dimer are suggested to face towards the periplasmic and cytoplasmic sides respectively (Hung et al, 1998). ATP is illustrated by the ball and stick diagram at the nucleotide binding fold.

LSGGQQ (residues 154-158) being partially exposed. A role for this sequence in structural stability has been proposed (Hung et al, 1998). However the sequence conservation and interesting and varied effects on function noted in other systems (described in Section 1.5.2c) indicate a possible role in protein/protein interaction, possibly with particular intra-helical loop regions of the TM domain. The positioning of the signature sequence suggests this role is carried out in an indirect way due to the distance of the sequence from the surface predicted to interact with the TM domain.

1.5.2 The sequence and structural motifs of the ATP binding cassette

1.5.2.a The Walker motif A

This sequence motif, which was reported to be common to many distantly related ATP and GTP binding enzymes (Walker et al, 1982), and in ABC transporters, consists of the consensus sequence GXXXXGK[TS]. Structural data obtained for a number of ATP or GTP binding proteins which harbour this motif reveal that this sequence encodes a conserved secondary structure known as the P-loop or phosphate binding loop (Saraste et al, 1990). A representative structure of the P-loop is shown in Fig. 9. The P-loop consists of a loop between a β-strand and an α-helix (Pai et al, 1990). Using the $p21^{Hras}$ P-loop structure as an example (Pai et al, 1990; Tong et al, 1989) the significance of this structure is partly due to the amide nitrogens of the glycine loop which provide a positively polarised electrostatic field for the binding of the mononucleotide. The inherent dipole of the α helix is also thought to be important for binding the γ-phosphate (Saraste et al, 1990). The conserved lysine is thought to perform a dual role of binding to the β and γ-phosphates of ATP or GTP, in addition to stabilising the transition state by neutralising both the charges at the γ-phosphate and increasing the charge at the leaving phosphate group (Bossemeyer, 1994). The recently solved crystal structure of HisP is consistent with previously solved structures harbouring the conserved P-loop.

Fig. 9 The phosphate binding loop

This figure illustrates a stereo view of the mononucleotide-binding fold P-loop of $p21^{ras}$. The GTP analogue GMP-PNP shown, and the Mg^{2+} is shown as a black dot. This figure was reproduced from (Bossemeyer, 1994). This loop contains the conserved Walker A motif.

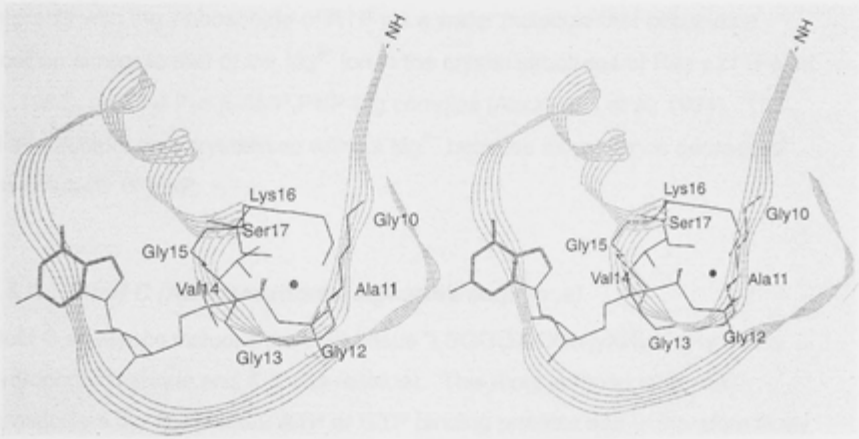

1.5.2.b Walker motif B

The sequence motif named motif B (Walker et al, 1982) was also identified in many ATP binding proteins. This motif is not as well characterised as the Walker A P-loop motif, however in ABC transporters it includes the consensus ILLLD. The function of the highly conserved aspartic acid has been assigned to the co-ordination of the Mg^{2+}-phosphate interaction by analogy with the other GTP/ATP binding proteins which harbour typical Walker A and B motifs (Yoshida and Amano, 1995) and this was confirmed by the crystal structure obtained for HisP. The relative positions of the residues thought to be involved in ATP binding are illustrated in Fig. 10. Asp^{178} of the Walker B motif of His P interacts with the γ phosphate of ATP via a water molecule that occupies a position similar to that of the Mg^{2+} ion in the crystal structures of Ras p21 (Pai et al, 1989), and the $F_1\alpha,\beta$-AMP.PNP-Mg complex (Abrahams et al, 1994). This HisP structure was crystallised without Mg^{2+} because its presence decreased the solubility of HisP.

1.5.2.c Motif C (ABC transporter signature sequence)

Motif C sequence includes the consensus "LSGGQXXXRHyXHyA" (Hy is any hydrophobic residue and X is any residue). This motif is found in all ABC transporters but not in other ATP or GTP binding proteins and is therefore likely to perform a function specific to this superfamily (Ames and Lecar, 1992; Ames et al, 1992). Mutation analyses of this motif indicates a mixed bag of possible functional roles depending on the system under study. These include: protein stability (Bakos et al, 1997); protein/protein interactions involved in transducing signals from the NBD to the membrane domain (Mimura et al, 1991; Shani et al, 1996; Shyamala et al, 1991); the mechanism of ATP hydrolysis inferred by analogy with the GTPase reaction (Carson and Welsh, 1995); substrate specificity in P-glycoprotein (Hoof et al, 1994).

Fig. 10 Residues of HisP involved with interactions with ATP

This figure shows the atomic details of the interactions of HisP with ATP. Hydrogen bonding is shown by dashed lines, aromatic interactions are shown as vertical lines. Interactions between ATP and specific amino acid residues (boxed) are indicated; interactions to protein main chain atoms are shown as lines to the atoms. Residues included in the Walker A and walker B motifs are shown in green and red respectively. Water molecules are labelled Wat and are circled. This diagram was reproduced from (Hung et al, 1998).

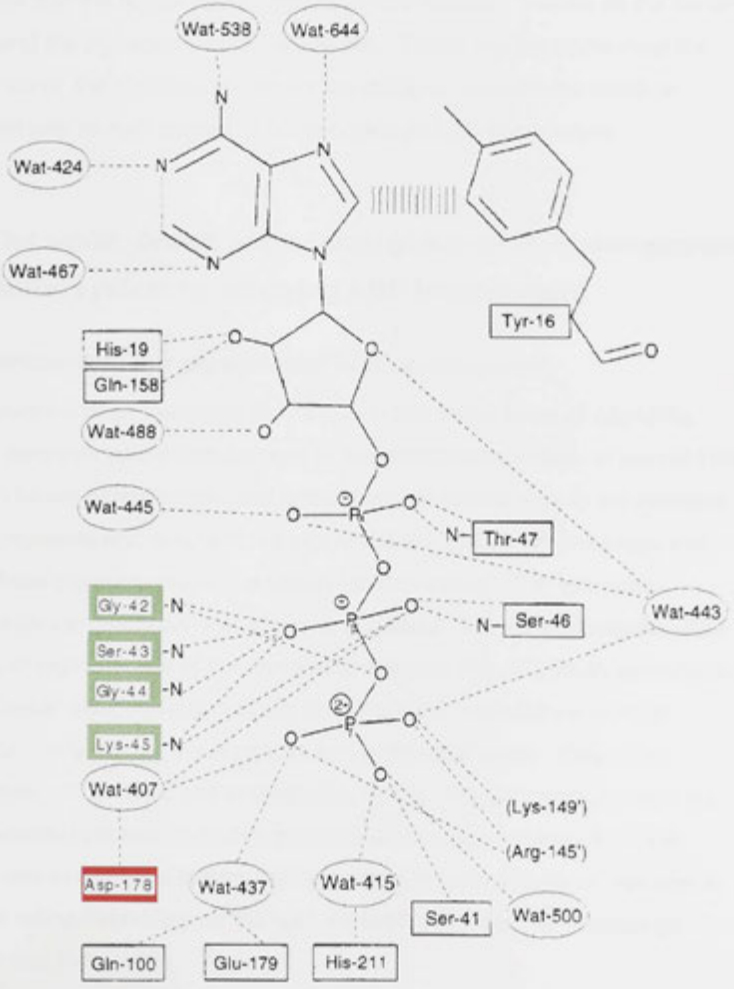

Although mutations at some positions of the motif have a detrimental effect on activity, there are some which rescue function in CFTR and Ste6. In CFTR R553Q (the 6th residue of the motif) partially corrects cystic fibrosis (Dörk et al, 1991) in a patient carrying both ΔF508 (which causes severe cystic fibrosis) and R553Q. Similarly, R553Q restored alpha-peptide transport in a STE6-ΔF508 CFTR chimera in yeast thereby partially correcting the processing and channel defects caused by the ΔF508 mutation. These authors have suggested that the region containing the ΔF508 mutation (known as the center region) and the signature sequence interact. These reports make clear the importance of the signature region for the transport mechanism which is consistent with its high degree of conservation in ABC transporters.

1.6 The *white, brown* and *scarlet* genes of *D. melanogaster*: Model system for studying ABC transporters

1.6.1 Introduction: eye pigmentation in *D. melanogaster*

Eye-colouration of *D. melanogaster* is due to two major types of pigments, namely, xanthommatin which belongs to the ommochrome class of pigment and results in brown pigmentation; and drosopterin, which belongs to the pteridine class of pigments and results in red pigmentation. In flies with wild-type eye-colour, these pigments result in a brown-red eye-colour. The eye-colour pigments play an important role in vision in insects. They are deposited within granules of pigment cells of the compound eye (see Fig. 11) which surround the photoreceptor cells, thereby optically isolating each ommatidium from its neighbour. In so doing, the pigments enhance visual acuity, (Stark and Wasserman, 1972; Stark and Wasserman, 1974). Pigment granules also act as a moveable light screen and migrate radially towards or away from the retinula cells in response to light and dark, allowing either more or less light to reach the retina depending on the light availability (Bernard and Stavenga, 1979; Lo and Pak, 1981).

Fig. 11 Cartoon of the insect compound eye

The top section of this figure illustrates the repetitive array of ommatidia which make up the compound eye. The bottom section illustrates longitudinally and in cross-section, the cells which make up a single ommatidium. Pigment cells surround both the cone region, as well as the photoreceptor cells, thereby forming a sheath of light screening cells between each ommatidium. This figure was reproduced from Keeton & Gould, 1986.

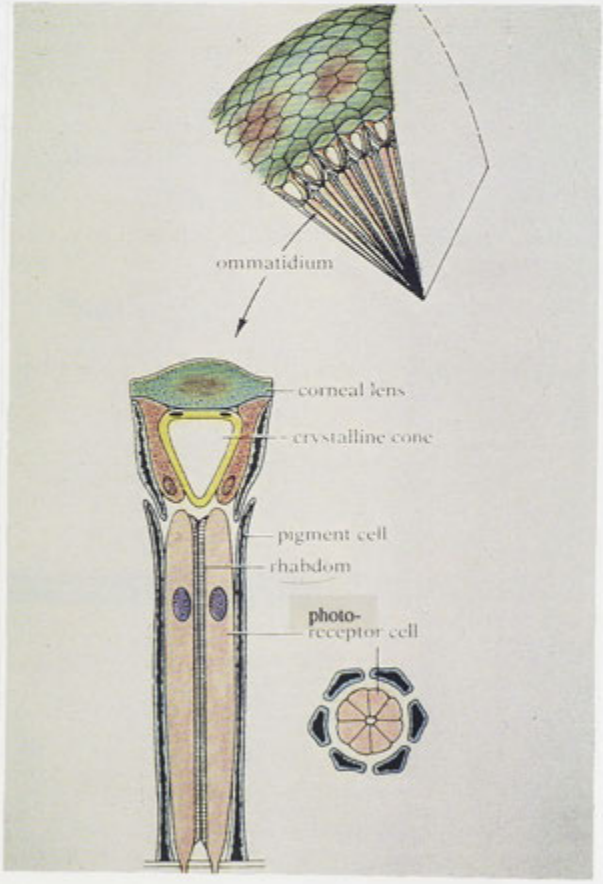

1.6.2 Role of *white*, *scarlet* and *brown* genes in the tryptophan → xanthommatin biosynthetic pathway

The developmentally regulated process of the synthesis and deposition of eye pigments in *D. melanogaster* is a complex multi-step process involving a large number of genes (reviewed in (Phillips and Forrest, 1980)). Some of these genes are structural and encode enzymes involved in the biosynthesis of pigments from precursor molecules, others may play regulatory roles, while others are believed to be involved in transport of precursor molecules to appropriate sub-cellular locations. The *white*, *brown* and *scarlet* genes are believed to fall into the last mentioned category. These genes encode proteins bearing all the conserved motifs of the ABC transporter superfamily and their role in eye pigmentation is discussed below.

The study of eye pigmentation in insects, particularly in *D. melanogaster*, has a very long history since the discovery of eye pigment mutants in about 1910 (Morgan, 1910). These mutants have been used with great success for the study of the genetics[7], developmental biology and biochemistry of the pigmentation pathways (Summers et al, 1982). Of particular interest with respect to this thesis is the tryptophan → xanthommatin biosynthetic pathway (Fig. 12) which leads to the deposition of xanthommatin within pigment granules of the compound eye. To provide a perspective as to where the *white* and *scarlet* gene products might fit into this pathway, this introductory section will review the current understanding of this pathway with respect to its regulation during development through the larval, pupal and adult stages, and the roles of specific enzymes.

---

[7] *D. melanogaster* eye-colour mutants provided fundamental demonstrations of Mendelian inheritance (reviewed in (Zeigler, 1961)).

Fig. 12 The xanthommatin biosynthetic pathway in insects

The biosynthesis of the major brown pigment, xanthommatin, involves a series of oxidation steps, each catalysed by a different enzyme (reviewed in Summers et al, 1982). The enzymes of the pathway are highlighted in grey and the known structural genes are shown in brackets.

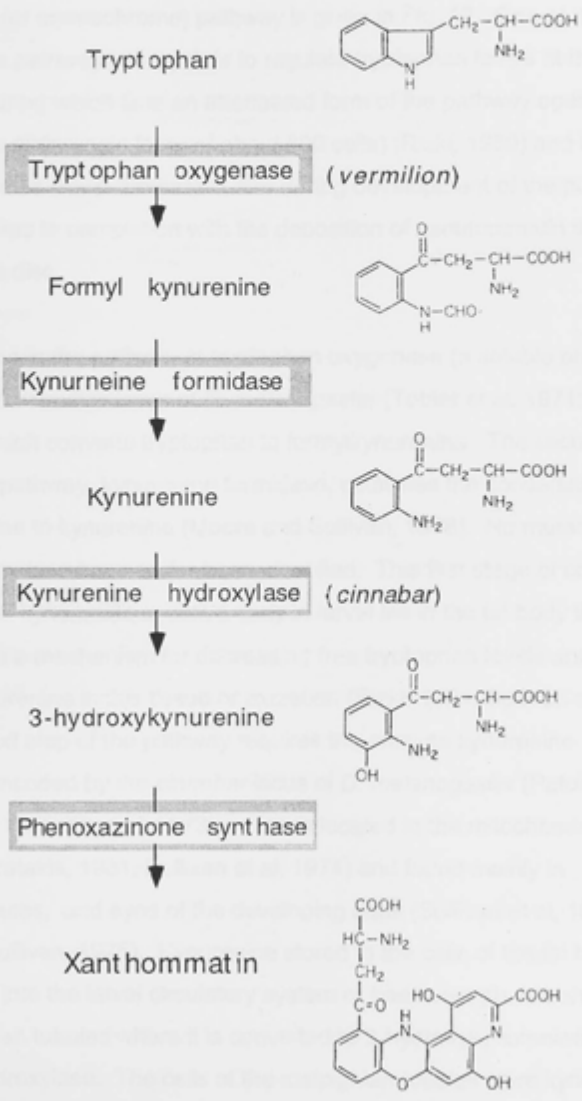

Tryptophan → xanthommatin pathway

Tryptophan is an essential amino acid in insects and comprises an indolyl moiety capable of donating electrons in chemical interactions with other compounds. The biological activity of this amino acid means that it can be toxic at high levels and therefore its metabolism requires strict regulation. The xanthommatin (or ommochrome) pathway is given in Fig. 12. One of the key functions of the pathway in insects is to regulate tryptophan levels at the larval stage of life, during which time an attenuated form of the pathway operates in the larval fat body (a single layer of about 800 cells) (Rizki, 1980) and the malpighian tubules (renal tubules). Later during development of the pupae the pathway operates to completion with the deposition of xanthommatin in the developing eye disc.

The first enzyme in the pathway is tryptophan oxygenase (a soluble enzyme encoded by the *vermilion* locus of *D. melanogaster* (Tobler et al, 1971; Walker et al, 1986)) which converts tryptophan to formylkynurenine. The second enzyme in the pathway, kynurenine formidase, catalyses the conversion of formylkynurenine to kynurenine (Moore and Sullivan, 1978). No mutants of kynurenine formidase have so far been identified. This first stage of conversion of tryptophan → kynurenine is active early in larval life in the fat body tissue and is thought to be a mechanism for decreasing free tryptophan levels and for storage of kynurenine in this tissue or excretion (Rizki, 1961; Sullivan and Kitos, 1976). The next step of the pathway requires the enzyme kynurenine hydroxylase (encoded by the *cinnabar* locus of *D. melanogaster* (Paton and Sullivan, 1978; Sullivan et al, 1973)) which is located in the mitochondrial outer membrane (Stratakis, 1981; Sullivan et al, 1974) and found mainly in malpighian tubules, and eyes of the developing adult (Sullivan et al, 1973; Sullivan and Sullivan, 1975). Kynurenine stored in the cells of the fat body, once released into the larval circulatory system or haemolymph, is transported to the malpighian tubules where it is converted to 3-hydroxykynurenine by kynurenine hydroxylase. The cells of the malpighian tubules store kynurenine and 3-hydroxykynurenine within vesicles (Bonse, 1969; Yagi and Ogawa,

1996). It is thought that these stores of xanthommatin precursors are released during tissue rearrangement which occurs during metamorphosis (Gilmour, 1961; Wigglesworth, 1972) into the circulatory system (haemolymph) where they are transported to the pigment cells of the developing eye (Summers et al, 1982). It has been shown by cell lineage experiments (Nissani, 1975) that eyes of wild-type *D. melanogaster* are capable of producing xanthommatin from tryptophan but depend on transported kynurenine and/or 3-hydroxykynurenine to produce normal quantities of xanthommatin. This finding indicates that the controlled production, storage and release of these precursors in the fat body of the larvae and malpighian tubules of the larvae and pupae is a very important process in the production of wild-type levels of xanthommatin.

The gene-enzyme relationship of tryptophan oxygenase; (*vermilion*) and kynurenine hydroxylase; (*cinnabar*) have been extensively studied using the mutant forms of the genes and some of these studies are described below. Mutant *vermilion* larvae when fed or microinjected with kynurenine or 3-hydroxykynurenine, are subsequently able to produce xanthommatin (Beadle and Law, 1938; Ephrussi, 1942; Green, 1952). Transplantation experiments where developing *vermilion* mutant eye discs were transplanted into wild-type hosts resumed synthesis of xanthommatin (Beadle and Ephrussi, 1936). Similarly mutants of the *cinnabar* locus could resume xanthommatin synthesis when 3-hydroxykynurenine was provided by feeding, injection or transplantation into a wild-type host (Beadle and Ephrussi, 1936; Beadle and Law, 1938; Ephrussi, 1942). These genes are categorised as having a non-autonomous phenotype which contrasts with the autonomous phenotype of mutants of *white* and *scarlet* which cannot resume xanthommatin biosynthesis even when all of the precursors are artificially supplied as for *vermilion* and *cinnabar* (Beadle and Ephrussi, 1936).

It has since been shown that tissues of both the malpighian tubules and the developing eye from w^{o} and st^{o} mutants, are defective in uptake of tryptophan and kynurenine (Sullivan et al, 1980; Sullivan and Sullivan, 1975) in comparison

to these tissues from wild-type flies. In addition, increased rates of excretion of exogenously supplied kynurenine and 3-hydroxykynurenine from w^o and st^o mutant larvae, also indicate a defect in uptake and storage of these compounds in the cells of malpighian tubules (Howells et al, 1977). This biochemical evidence, coupled with the transplantation data described above, provides strong evidence that the gene products of *w* and *st* are required for transport of precursors of xanthommatin.

The DNA sequences of the three genes *white*, *brown* and *scarlet* are now known (Dreeson et al, 1988; O'Hare et al, 1984; Tearle et al, 1989) and the protein sequences derived from the translated cDNAs has revealed that all three proteins harbour all the amino acid sequence motifs typical of the ABC transporter superfamily (reviewed in (Ewart and Howells, 1998)). This is evident from sequence alignments of White, Scarlet and Brown with other ABC transporters (see Fig. 13). The hydropathy profiles of *w*, *bw* and *st* are also consistent with the ABC transporter superfamily in that each harbours a hydrophilic ATP binding domain and a hydrophobic domain predicted to consist of six hydrophobic membrane spanning α-helices (see Fig. 14). Thus *w*, *bw* and *st* each encode a half transporter and it has been proposed that interaction between White/Scarlet, or White/Brown result in two different ABC transporters each with two nucleotide binding domains and two transmembrane domains comprised of 12 hydrophobic α-helices. Since genetic and biochemical analysis shows that White is required for transport of precursors of both red and brown pigments, Scarlet is only required for transport of brown precursors, and Brown is only required for transport of precursors of red pigments, it was proposed that White and Brown interact to form a transporter for guanine (Dreeson et al, 1988), while White and Scarlet interact to form a transporter for tryptophan (Tearle et al, 1989) (see Fig. 15).

The biochemical data with respect to pigment precursor transport defects of w^o, bw^o and st^o mutants discussed above, implies that these proteins are located in the plasma membrane of specific cell types in order to allow the high level of

Fig. 13 Amino acid sequence alignment of nucleotide binding domains of ABC transporters

This sequence alignment illustrates sequence conservation of the ATP binding cassette. A comparison of the nucleotide binding domains of White, Brown and Scarlet, are compared with those from CFTR, MDR1 and HisP. Highlighted in colour are sequences included in the Walker motif A and B, as well as the highly conserved ABC signature sequence. CFTR and MDR1 (both from human) have two nucleotide binding domains and these are indicated as (1), the N-terminal NBD, and (2), the C-terminal NBD. The sequence alignment was performed as described in the experimental procedures.

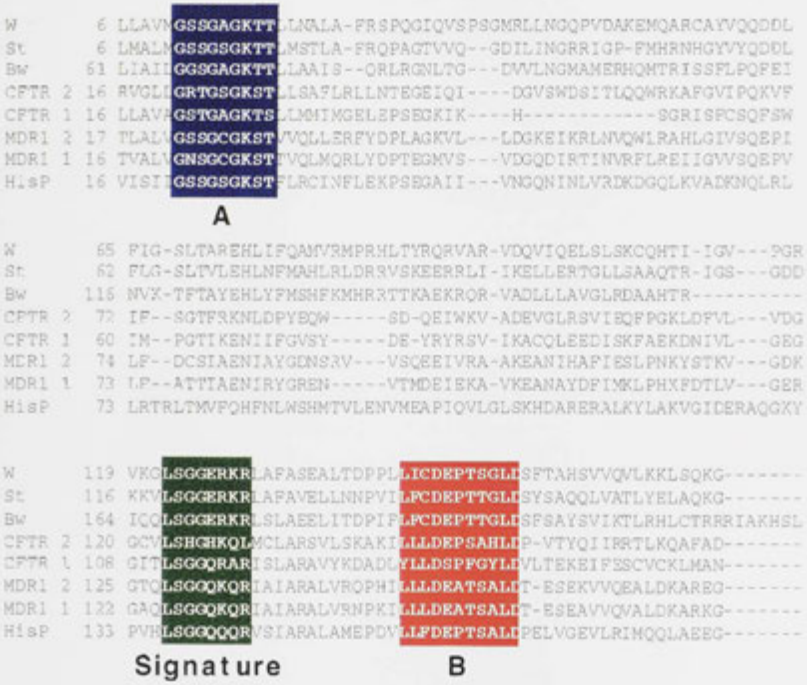

Fig. 14 Hydropathy analysis of White, Scarlet and Brown proteins

This figure illustrates a comparison of hydropathy profiles of White, Scarlet and Brown, with those from CFTR and MDR1 from human. Hydrophobic transmembrane domains are predicted at regions showing downward inflection, and are highlighted by the hatched bar. Upward inflections are indicative of hydrophilic regions associated with the nucleotide binding domains. White, Scarlet and Brown all show a single transmembrane domain, and single nucleotide binding domain, while MDR and CFTR both harbour two nucleotide binding domains and transmembrane domains on the same polypeptide chain. The hydropathy analysis was performed as described in the Section 2.6.10.

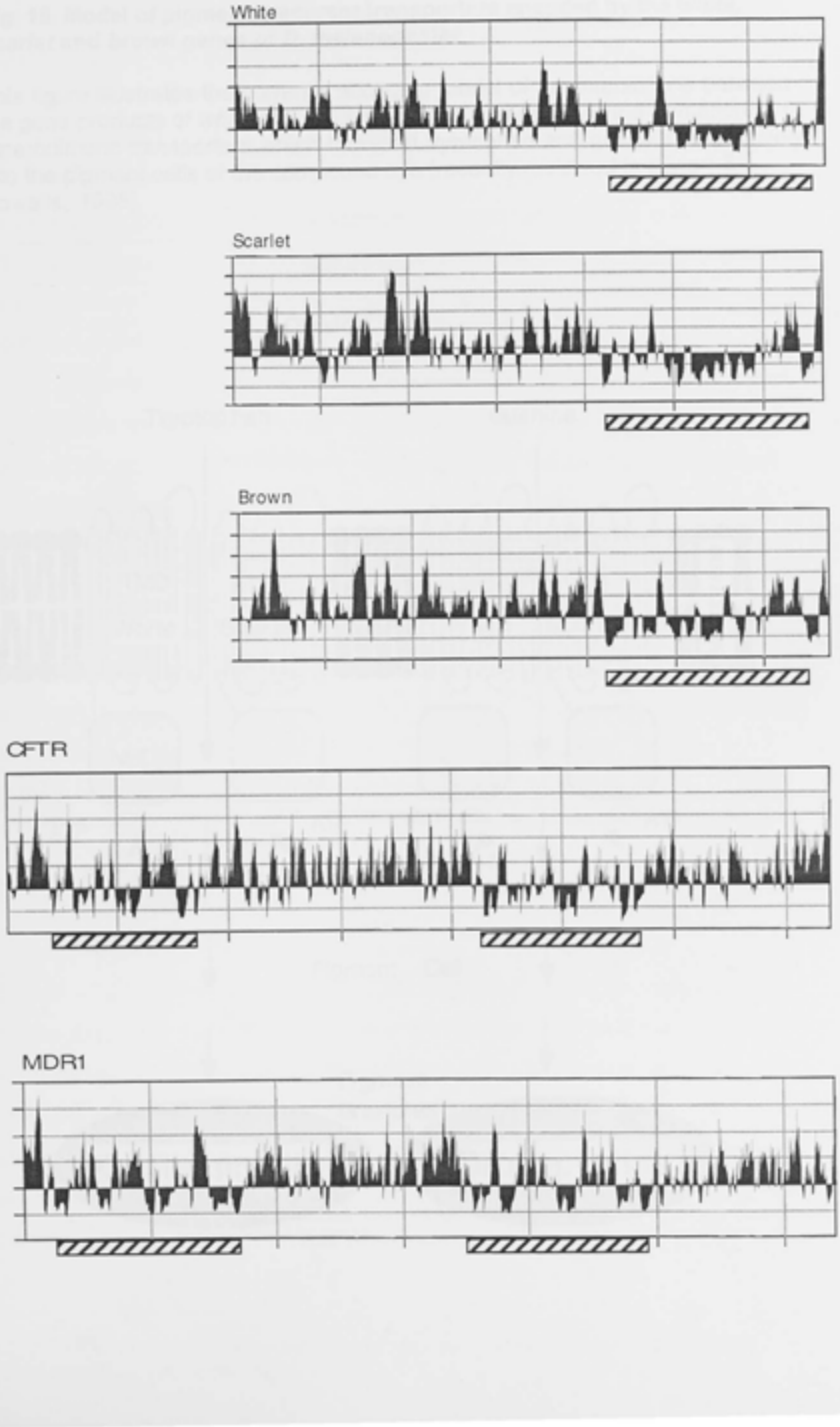
White
Scarlet
Brown
CFTR
MDR1

Fig. 15 Model of pigment precursor transporters encoded by the *white*, *scarlet* and *brown* genes of *D. melanogaster*

This figure illustrates the currently accepted model of the interactions between the gene products of *white* and *scarlet*, or *white* and *brown* in the formation of heterodimeric transporters which transport tryptophan and guanine respectively, into the pigment cells of the compound eye (recently reviewed in (Ewart & Howells, 1998).

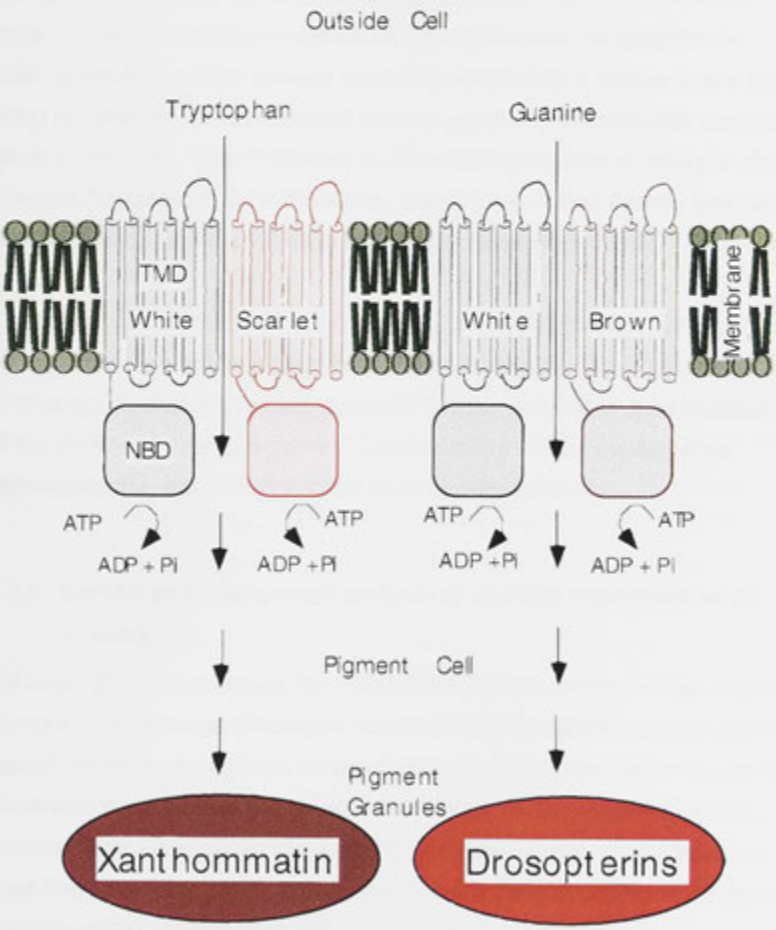

uptake required for the purposes of either storage (in larval malpighian tubules) and/or pigmentation in the pigment cells of the eye.

1.7 Experimental aims

The *Drosophila* pigment precursor transporters represent a novel and powerful experimental system for the study of ABC transporters. Although there are amorphic alleles of the *white* gene (e.g. w^{1118}), there are no known lethal mutations of *white*, *scarlet* or *brown*, so these genes are not essential for viability, however mutant animals are easily detected by a change in eye-colour. Many of these have been collected over the years and are available from mutant strain collections[8]. The P-element mediated transformation of embryos allows site-specific mutations to be introduced into transgenic flies thereby providing another vehicle for the production of flies with mutant eye-colour.

The overall aim of this thesis is to develop a variety of systems, utilising genetics, biochemistry and recombinant DNA technology, as well as electron microscopy, to characterise the structure, function and sub-cellular localisation of the White and Scarlet proteins. Outlined below are the experimental approaches that were taken in order to achieve these aims.

1.7.1 Genetic and biochemical analysis of partially pigmented *white* mutants

Although w^{o} mutations cause the complete loss of red and brown eye pigments giving a pure white eye phenotype, many *white* mutant alleles cause a partial loss of pigments. It has been an ongoing interest of this laboratory to identify alterations in amino acid sequence in the existing partially pigmented *white* mutants. The *white* alleles chosen for genetic and biochemical analysis are ones that have been previously reported to have gene structures undiscernible from the wild-type *white* gene (by Southern blotting), indicating that the gene is

---

[8] *Drosophila* stock centres can be accessed through the internet site known as "Flybase", http://flybase.bio.indiana.edu

intact and does not harbour any gross genetic lesions. These alleles are likely to harbour codon changes. In addition, the partial loss of eye-colour pigments shows that the White protein is at least partially functional, indicating that the altered protein is capable of assembling into a folded state capable of inserting into the membrane. This approach has been used very successfully by this laboratory to identify transmembrane regions of the White and Brown proteins which may interact and play a role in substrate specificity (Ewart et al, 1994; Ewart and Howells, 1998). The analysis of additional partially pigmented *white* alleles is presented in Chapter 3 and has led to the identification of amino acid replacements in the White protein which affect function. The consequences of these mutations on the levels of red and/or brown eye-colour pigments has been determined[9].

1.7.2 Expression of *white* and *scarlet* genes in insect cells

Extensive genetic and biochemical studies have been performed, which have led to the current transporter model discussed above, however, direct biochemical evidence for the transport function and its characteristics are still lacking. One aim of this thesis is to express an active White/Scarlet transporter in an insect cell line using the Baculovirus-based expression of *white* and *scarlet* cDNA. Work towards the development of this system is described in Chapter 5. The Baculovirus-based system has been used successfully for the characterisation of many membrane transport and channel proteins, including ABC transporters (Carter et al, 1992; Cope et al, 1994; Germann et al, 1990; Meyer et al, 1994; O'Riordan et al, 1995; Sarkadi et al, 1992; Tate and Blakely, 1994), and was therefore considered a good starting point for the heterologous expression and characterisation of White and Scarlet proteins. The goals are to provide a convenient system for assaying transport activity, specifically, to test tryptophan uptake activity. In addition, it could provide a convenient system for analysing site-directed mutants, thereby providing a powerful model system for pursuing questions regarding structure-function relationships in these proteins.

[9] This work has been accepted for publication (Mackenzie et al, 1999).

1.7.3 Production of antibodies recognising White and Scarlet proteins

As an adjunct to the aims described in Sections 1.7.2, 1.7.4 and 1.7.5, antibodies specifically recognising White and Scarlet proteins were required in order to demonstrate protein expression and determine the localisation of expressed proteins by immuno-labelling techniques.

This work (described in Chapter 4) involved raising antisera in rabbits against synthetic peptides representing protein epitopes of White and Scarlet respectively, followed by the demonstration of specificity.

1.7.4 Immuno-localisation studies of White and Scarlet proteins in the compound eye

The current model for the White/Scarlet transporter assumes that it is localised in the plasma membrane of pigment cells, where it functions as a tryptophan transporter (Ewart et al, 1994; Ewart and Howells, 1998), however there is no direct evidence for this hypothesis. In order to investigate this issue, an immuno-localisation study was performed on sections of adult eyes, using colloidal gold immuno-labelling at the electron-microscope level. The study was aimed at gaining a fundamental understanding of the sub-cellular localisation of White and Scarlet, and how this information relates to the tryptophan → xanthommatin biosynthetic pathway. This work is presented in Chapter 7.

1.7.5 Expression of the nucleotide binding domains of White and Scarlet in *Escherichia coli*

Over-expression of heterologous proteins in *E. coli* has been shown to be a powerful technique for the production of high levels of proteins - difficult to obtain from the natural source - for subsequent purification and in vitro structure-function analysis. This technique has been applied successfully to the characterisation of nucleotide binding domains of a number of ABC transporters (Ko et al, 1997; Koronakis et al, 1993; Randak et al, 1995), and was therefore tested for the production of the nucleotide binding domains of White and Scarlet. The success of such a system would not only allow the characterisation of the ATP binding and hydrolysis activity of these domains, but also lead to the

possibility of obtaining enough pure material for crystallisation and x-ray crystallographic analysis. A crystal structure for the nucleotide binding domain of only one bacterial member of the superfamily has been reported, and therefore the solving of the structure for a eucaryotic nucleotide binding domain is a high priority in this field. Work towards this goal is presented in Chapter 6.

CHAPTER 2

EXPERIMENTAL PROCEDURES

2. EXPERIMENTAL PROCEDURES

2.1 Fly techniques

2.1.1 Maintenance of *D. melanogaster* strains

Standard methods were used for the maintenance of *D. melanogaster* stocks (Roberts, 1986). Flies were cultured in 250 ml milk bottles on a medium made up of the following components: For 100 ml of media - 10 g agar, 26.3 g sucrose, 52.7g dextrose, 90.9 g maize meal, 15.9 g dried yeast, 11 ml water. Flies were generally maintained at 25°C and transferred to bottles containing fresh medium once a fortnight. When anaesthetised flies were required di-ethyl ether was used. The *D. melanogaster* strains used in this work are listed in Table 1.

2.1.2 Extraction of drosopterin and xanthommatin eye pigments

Modified small-scale methods described previously (Evans and Howells, 1978; Ryall and Howells, 1974) were used to extract xanthommatin and drosopterin pigments, respectively, from adult, 10 day old *D. melanogaster*. The ages of flies used for extraction of pigments were standardised to 10 days old since eye-colour changes as the fly matures. For extraction of xanthommatin pigments, 20 adult heads were homogenised in 0.3 ml of 2M HCl using a small homogeniser. The homogenate was transferred to an eppendorf tube and vortexed intermittently with 0.4 ml n-butanol and 1 mg sodium meta bisulphite for 10 min. The tube was then centrifuged in an Eppendorf bench top centrifuge for 2 mins and 200 µl of the upper (butanol) layer was removed and the absorbance measured at 492nm. n-butanol was used as a blank. For extraction of drosopterin pigments 10 adult heads were homogenised in a 1:1 mixture (0.4 ml each) of 0.1% aqueous ammonia and chloroform using a small homogeniser. The homogenate was transferred to an eppendorf tube and

Table 1 *D. melanogaster* strains

white allele	Flybase ID	Discoverer	Source
w^{+}	FBgn0003996	(Morgan, 1910)	A J Howells
w^{cf}	FBa10018222	(Nicoletti, 1960)	Drosophila Stock Center, California Institute of Technology, Pasadena
w^{crr}	FBa10018230	(Judd, 1964)	Drosophila Stock Center, California Institute of Technology, Pasadena
w^{ET87}	-	M.M. Green and A.J. Howells, unpublished	A J Howells
w^{sat}	FBa10018300	(Bridges, 1935)	Drosophila Stock Center, California Institute of Technology, Pasadena
w^{101}	FBa10018145	(Pastink et al, 1988b)	DNA was obtained from A. Pastink

centrifuged for 2 minutes. 200 μl of the upper (aqueous) phase was removed and the absorbance measured at 485 nm. 0.1% aqueous ammonia was used as a blank. Duplicate xanthommatin and drosopterin extractions were performed. Duplicate readings were averaged and results were expressed as a percentage of the of absorbance readings obtained from extractions from heads of the *D. melanogaster* wild-type strain Canton-S. The heads of the *D. melanogaster* strain w^{1118} which lacks pigmentation were used as a negative control.

2.1.3 Solubilisation of proteins from fly heads for SDS PAGE analysis

Fly head tissue was homogenised in a buffer containing 6 M urea and 5% SDS and incubated at 65°C for 1 hr, followed by centrifugation for 2 mins in a bench top centrifuge, prior to adding 10 x SDS PAGE sample buffer and separation of proteins by SDS PAGE as described in Section 2.6.1.

2.2 General Molecular Biology Techniques

2.2.1 Synthesis and preparation of oligonucleotides

Oligonucleotides were synthesised by the Biomolecular Resource Facility at the ANU. The oligonucleotides were subsequently precipitated from 100μl aliquots of the ammonia solution they were supplied in by addition of 1ml of n-butanol followed by centrifugation for 1 min at room temperature in a benchtop eppendorf microcentrifuge. The pellet was dried under vacuum, resuspended in water and quantitated by absorbance at 260nm as described in Section 2.2.2.

2.2.2 Spectrophotometric analysis of DNA

DNA in solution was diluted 1/200 and assayed at 260 and 280 nm using a Hitachi U-1100 Spectrophotometer. The DNA concentration was then determined, based on 1 optical density unit at 260 nm being equivalent to

50 μg/ml dsDNA or 20 μg/ml for oligonucleotides (Sambrook et al, 1989). DNA purity was assessed by dividing OD_{260} by OD_{280}, which is between 1.8 and 2.0 for DNA uncontaminated with RNA or protein (Sambrook et al, 1989).

2.2.3 Polymerase chain reaction

This technique was used to amplify DNA fragments from plasmids or genomic DNA. Polymerase chain reaction (PCR) (Mullis and Faloona, 1987; Saiki et al, 1985) was performed in the Perkin Elmer Cetus Thermal Cycler, using sterile 0.5ml thin walled polypropylene microcentrifuge tubes (Perkin Elmer Cetus). A typical reaction mix included *Pfu* DNA Polymerase buffer (supplied with the enzyme from Stratagene) (20mM Tris-Cl pH8.2, 10mM potassium chloride, 6mM ammonia sulphate, 2mM magnesium chloride, 0.1% Triton X-100 10ng/ml nuclease free Bovine Serum Albumin), 20pmol of each of two opposite-facing primers (primers are detailed in Section 2.14), 200mM of each dNTP, 250ng of template DNA 2.5 units of *Pfu* DNA Polymerase (Stratagene)(from the hyperthermophilic marine archaebacterium, *Pyroccocus furiosus*), sterilised distilled water to a total volume of 50 μl . The PCR reaction mix was mixed gently and overlayed with mineral oil (Perkin Elmer Cetus). An estimate of the optimum annealing temperature for a primer was calculated by adding 2°C for each A and T nucleotide present in the primer and 4°C for each G and C nucleotide and subtracting 5°C from the result. The tubes were pre-heated to the denaturing temperature for 1 minute then subjected to 25 to 30 cycles of the following typical temperature and time profile:

Denaturation:	94°C for 45 seconds
Annealing:	55°C for 1 minute
Extension:	72°C for 3 minutes

Following 25 to 30 cycles, a final cycle with a 10 minute extension time was run. The PCR reactions were stored at 4°C or -20°C.

2.2.4 Chromosomal DNA extraction from *D. melanogaster*

Chromosomal DNA was extracted from *D. melanogaster* strains using a modified method described previously (Bender et al, 1983). 100 μl of freshly made Lifton Solution (0.2M sucrose, 0.05M EDTA, 0.5% SDS, 100mM Tris pH 9) was added to approximately 20 flies in an eppendorf tube. The flies were crushed with a small glass rod until most of the fly matter was broken up. A further 100 μl Lifton Solution was added and the flies were further crushed until the fly tissue was no longer aggregating. The fly homogenate was incubated at 65°C for 30 minutes. 50 μl of a solution containing 3 M potassium and 5 M in acetate was added to the fly homogenate, mixed gently and incubated on ice for 60 mins. The mixture was centrifuged at 10,000 rpm for 10 mins at 4°C. The supernatant was carefully removed and transferred to a fresh eppendorf tube. The chromosomal DNA was purified by successive phenol, phenol/chloroform/isoamyl alcohol, and chloroform/isoamyl alcohol extractions by adding an equal volume of solvent, vortexing and then centrifuging in a benchtop Eppendorf microcentrifuge for 5 minutes at room temperature. The upper phase was removed and treated with RNAase A (2 μg) for 15 minutes at 37°C. The DNA was ethanol precipitated at room temperature by the addition of two volumes of ethanol, standing for 5 minutes, and centrifuging at 8000 rpm for 15 minutes. The pellet was washed with 70% ethanol, dried in a vacuum desiccator, and resuspended in 40 μl of TE buffer.

2.2.5 Purification of PCR products, and products from restriction digests

Products from PCR experiments and DNA digested by restriction enzymes for sub-cloning purposes, were purified using a BresaClean Kit (Bresatech). The PCR reaction is removed from the PCR tube and transferred to a clean Eppendorf tube being careful not to carry over any mineral oil. Three volumes of NaI solution was added to the reaction, followed by 5μl of well resuspended BresaClean silica resin. The solution was mixed and incubated for 5 mins to allow the DNA to bind to the silica resin. The solution was then centrifuged to 5 secs at top speed in a bench top centrifuge and the supernatant removed. The

silica/DNA pellet was resuspended gently with 500µl of BresaClean wash solution followed by centrifugation at top speed in a bench top centrifuge. The wash solution was removed as completely as possible and the pellet was dried under vacuum in a SpeediVac Concentrator (Savant). The silica/DNA pellet was then resuspended in sterile distilled water and incubated for 5 mins at 50°C. The silica resin was pelleted by centrifugation at top speed for 1 min in a bench top centrifuge and the supernatant containing the PCR products were transferred immediately to a fresh tube. The DNA containing solution was centrifuged again for 30 sec and transferred to a new tube, in order to remove any residual silica resin.

2.2.6 Agarose Gel Electrophoresis

Agarose gel electrophoresis was used to separate DNA fragments by size. Generally 0.9g of agarose powder (Sigma) was dissolved in 100 ml TAE buffer (40mM Tris-HCl, 20mM sodium acetate, 1mM EDTA, pH 7.8) and was poured into a 15 x 18cm tray, with combs inserted to create sample wells. Samples were loaded in 20 µl volumes with loading dye (470mM sucrose, 0.75mM bromophenol blue, 48mM EDTA) and run at a constant current of approximately 180mA, until the bromophenol blue dye front had migrated three-quarters of the length of the gel. After 20 min of staining the gel in a 1ug/ml ethidium bromide solution, the DNA was visualised under UV light as fluorescent bands, and photographed.

2.2.7 Growth of *E. coli* cultures for molecular biology work

E. coli strains were grown in liquid culture in LB Broth (1.0% (w/v) Tryptone, 0.5% (w/v) Yeast extract, 0.5% (w/v) sodium chloride, pH 7); or on agar plates (10% Bacto-agar dissolved in LB broth) with the addition glucose (1ml of 2M glucose/100ml of LB broth) and the appropriate antibiotic. The Table in Section 2.13 details the strains used in this work and their antibiotic resistance status in addition to the growth temperature. When a new *E. coli* strain was made by transformation with a recombinant plasmid a primary source of

inoculum was made by growing the strain on an agar plate overnight, and resuspending the cells with a sterile glass rod in 2 mls of a solution of 10% glycerol and LB broth. The resuspended cells were transferred to a sterile vial and stored at -20°C or -70°C. This primary source of inoculum was then used in future experiments where the cells would be thawed, a loop full of cells would be taken and streaked onto an LB agar plate, or used to inoculate LB broth, and the glycerol stock would be returned to the freezer. Small scale cultures for small scale purification of plasmids were grown in McCartney bottles, with a maximum of a 3ml culture volume. Liquid cultures were grown in baffled conical flasks with the culture volume not exceeding ½ the volume of the flask. Flasks without baffles were sometimes used and in this culture volume would not exceed 1/10 the volume of the flask to ensure good aeration. Liquid cultures were placed in a shaking air incubator.

2.2.8 Small scale purification of plasmid DNA

A commercially available kit from Qiagen was used to purify plasmid DNA from *E. coli* on a small scale. 3ml overnight *E. coli* cultures were harvested by centrifugation at 5000 rpm for 2 mins. The cells were resuspended in 300µl of Cell Resuspension Solution. 300µl of Cell Lysis Solution was added and mixed gently by inverting the tube several times. 350µl of Neutralisation Solution was then added and gently mixed by inverting the tube several times. A thick, White precipitate formed after addition of the neutralisation solution and this was pelleted by centrifugation at top speed in a microfuge for 15 mins. The supernatant containing the plasmid DNA was removed carefully, avoiding the White precipitate containing cell wall and chromosomal DNA, and transferred to a Qiagen column. The supernatant was passed through the column and discarded, the plasmid DNA remains bound to the membrane in the column. The column was washed with column wash solution by centrifugation. The wash solution was discarded and the column was centrifuged again for 1 min to remove as completely as possible any remaining column wash solution. 50µl of sterile distilled water was then added to column membrane and incubated for 5

mins at room temperature before centrifuging for 1 min collecting the supernatant containing the plasmid DNA in a fresh eppendorf tube.

2.2.9 Large Scale purification of Plasmid DNA by CsCl Density Gradient

When a large quantity of high purity plasmid DNA was required, for example, for sequencing of extensive regions of DNA, a CsCl density gradient purification was performed. The method described here was adapted from (Sambrook et al, 1989). An overnight 1 L *E. Coli* culture harbouring the desired plasmid was grown in the presence of the appropriate selective antibiotic(s) (see Section 2.13. The bacteria were harvested by centrifugation at 5,000 rpm for 15 mins in an GSA Sorvall rotor. The bacterial pellet was resuspended in 20 ml of solution containing 50mM Tris, pH 8, 25% sucrose and left on ice for 5 mins. 80 mg of lysozyme dissolved in 4mls of 0.25M Tris pH 8, was added to the cells, swirled gently and left on ice for 5 mins. 2 mls of 0.5M EDTA pH 8.0 was then added and mixed by swirling and incubated for 5 mins on ice. 16 mls of a buffer containing 0.3% TritonX-100, 50 mM Tris, pH 8.0, 62.5 mM EDTA was added, swirled to mix, and incubated for 15 mins on ice. The lysozyme treated cells were then centrifuged for 15 mins at 20,000 rpm in an SS34 Sorval rotor at 4°C to pellet chromosomal DNA attached to *E. Coli* cell wall, and other insoluble material. The supernatant containing the plasmid DNA was decanted into a fresh tube, holding the pellet with a spatula to ensure it stayed in place. The volume of the supernatant was measured and ¼ this volume of 5 M NaCl was added, followed by ¼ volume (including NaCl) of 50% w/v PEG 6,000 in 50 mM Tris pH 8.0. This was gently mixed, intermittently for 15 mins on ice, then incubated on ice for between 2 and 18 hours. The solution was then centrifuged at 4,000 rpm for 5 mins in a GSA Sorvall rotor. The supernatant was removed and the plasmid DNA pellet resuspended in 7 ml of TE buffer (10 mM Tris, 1 mM EDTA, pH 8.0). 7.2 g CsCl was added to the resuspended pellet and dissolved by mixing with a spatula in tubes for use in an SE12 rotor. This mixture was centrifuged for 20 mins at 15,000 rpm in an SE 12 rotor at 15°C. The protein layer at the surface of the solution was removed with a spatula as completely as possible. The supernatant was transferred to a Ti50

Beckman rotor tube and 0.3 ml of 10 mg/ml ethidium bromide was added. The solution was protected from light once the ethidium bromide was added. The solution was then centrifuged in an Beckman ultracentrifuge at 39,000 rpm at 15°C for 41 to 42 hrs. The centrifuge was slowed with the brake off to avoid disturbing the CsCl gradient. The plasmid band was extracted by inserting an 18 gauge needle attached to a 5 ml syringe barrel, and transferred to a sterile tube. The ethidium bromide was removed from the DNA solution by adding isopropanol (stored over NaCl saturated TE buffer). The solution was vortexed to mix and the isopropanol phase containing ethidium bromide removed. This isopropanol extraction procedure was repeated until no further red colour could be seen in the isopropanol phase. CsCl was removed from the DNA solution by dialysis against one tenth the concentration of TE buffer, at 4°C. To ensure complete removal of CsCl, the DNA solution was de-salted using a NAP25 de-salting column (Pharmacia). The concentration and purity were analysed by spectrophotometry as described in Section 2.2.2. The level of supercoiled plasmid DNA was analysed by agarose gel electrophoresis as described in Section 2.2.6.

2.2.10 Site Directed Mutagenesis

Two methods were used to alter specific DNA sequences in plasmid constructs. Both methods employ oligonucleotide directed mutagenesis. Whenever possible mutations were designed in order to introduce a restriction endonuclease site to allow identification of site-directed mutants by restriction analysis.

2.2.10.a Site directed mutagenesis using Uracil-containing DNA

This method described previously (Kunkel et al, 1991) is an oligonucleotide-directed mutagensis technique. A single stranded DNA template containing a small number of uracil residues in place of thymine (Kunkel, 1988) is prepared by passaging the appropriate plasmid through an *E. coli dut⁻ ung⁻* strain. This strain lacks the enzymes: dUTPase (*dut*) resulting in an elevated level of dUTP, which competes with TTP for incorporation into DNA; and uracil N-

glycosylase (*ung*$^-$) which normally removes uracil from DNA. The double *dut*$^-$ *ung*$^-$ mutant can be used to produce plasmid DNA or single stranded DNA containing uracil. The uracil-containing DNA was then used as a template for the synthesis of a complementary strand containing the oligonucleotide-directed mutant DNA sequence. The product of this reaction is then passaged through an *ung*$^+$ *E. coli* strain which inactivates the non-mutant template strand by the action of uracil N-glycosylase which removes uracil from DNA producing apyrimidinic sites in the template strand which reduces the biological activity of the template strand. This selection procedure results in the plasmids arising from the complementary strand containing the mutation.

Infection of *dut*$^-$, *ung*$^-$ strain AN3828 with phagemid particles: The plasmid vector pBlueScriptSK$^+$ (a phagemid vector) harbouring the cDNA encoding the White nucleotide binding domain was used to produce ssDNA template in an *E. coli dut*$^-$, *ung*$^-$ strain by first transforming $CaCl_2$ competent cells with the plasmid vector (Section 2.3.9). Transformant colonies were then grown as an overnight culture and 1ml of this culture was used to inoculate 50 ml of 2 x YT (1.6% (w/v) Bactotryptone, 1% Bacto yeast extract, 0.5% NaCl) and incubated with shaking at 37 °C until an OD_{600} of 0.3 was reached. The helper phage M13K07 (which contains a kanamycin resistance gene) was added to obtain a M.O.I. of around 20. After 1 hr of further incubation at 37°C, 70 μl of 50 mg/ml kanamycin solution was added in order to select helper phage infected cells, and the incubation was continued for between 6 and 24 hrs. The cell culture was then centrifuged at 5,000 rpm in an SS34 rotor at 4°C for 20 mins. The supernatant containing the phagemid particles was then transferred to a fresh tube.

Comparison of phagemid titres in *ung*$^+$ and *ung*$^-$ *E. Coli* strains: The phagemid titre was compared in *ung*$^+$ and *ung*$^-$ *E. Coli* strains before extraction and purification of ssDNA, to check that the uracil content of the phagemid vector was high enough for use in the in vitro mutagenesis. This was done by first inoculating 50 ml 2 x YT with 1 ml of overnight culture. When the culture reached a cell density of OD_{600} of 0.3 the culture was infected with 10 μl of

U-DNA phagemid supernatant. The culture was grown for 2 hrs. Samples of the phagemid infected cultures were diluted 100 fold and 50 µl spread evenly onto Agar plates containing LB Glucose, ampicillin, tetracycline and glucose. The plates were incubated overnight at 37°C. If the *ung*⁻ plate yielded 10,000 fold more ampicillin resistant colonies than the *ung*⁺ plate, the uracil content was considered sufficient for in vitro mutagenesis.

Preparation of ssDNA for template for site directed mutagenesis: 30 ml of Phagemid supernatant prepared as described above was incubated on ice for 1 hr with ¼ volume of 20% PEG, 2.5 M NaCl. This solution was then centrifuged at 5,000 g for 15 min at 4°C to pellet phagemids. The pellet was drained well. The pellet was resuspended in 200 µl of high salt extraction buffer (100 mM Tris pH 8, 300 mM NaCl, 1 mM EDTA) by vortexing vigorously then left on ice for 1 hr. This solution was transferred to an eppendorf tube and centrifuged at 5,000 g for 15 mins at 4°C. The ssDNA was extracted twice with phenol and twice with chloroform/isoamyl alcohol (24:1). The ssDNA partitions to the aqueous phase while phagemid proteins partition to the organic phase. The ssDNA was precipitated by adding 0.1 volume of 3 M sodium acetate (pH 5.0) and 2 volumes of ethanol. The solution was incubated at -20°C for at least 30 mins. The ssDNA was pelleted by centrifugation at top speed in a bench top centrifuge at 4°C. The ssDNA pellet was washed by slowly adding 0.5 ml of 70% ethanol, then removing the ethanol of aspiration being careful not to disturb the ssDNA pellet. The pellet was dried under vacuum and resuspended in 50 µl of sterile distilled water and 5µl was used for analysis by agarose gel electrophoresis (Section 2.2.6).

Annealing mutagenic oligonucleotide to ssDNA template: In a 25 µl reaction volume in an eppendorf tube,1 µg of template ssDNA template was mixed with 10 ng of phosphorylated oligonucleotide and 1.25 µl of 20 x SSC (3 M NaCl, 300 mM sodium citrate). The eppendorf tube was placed in a float in 500ml of water at 70°C and then cooled to room temperature or 26°C.

Synthesis of the complementary strand: In a reaction volume of 50 µl, 20 µl of the annealing reaction described above was added to 5 µl of 10 x T4 DNA polymerase buffer, 500 µM of each dNTP, 0.4 mM ATP, and 1 unit of T4 DNA

polymerase. The reaction mix was incubated for 30 min at room temperature then a further 1 unit of T4 DNA polymerase was added, and 2 units of T4 ligase. This was incubated at 37°C for 2 hrs. The reaction was terminated by adding EDTA to 15 mM.

Transformation of *E. coli dut⁺ ung⁺* strain XL1Blue with mutagenesis synthesis products: 10 µl of the mutagenesis synthesis reaction was used to transform $CaCl_2$ competent *E. Coli* strain XL1Blue (Section 2.3.9), including the following control transformations: 250ng of plasmid DNA, as a positive control; no DNA as a negative control; 0.5 µl of ssU-DNA. The transformed cells were plated out onto selective agar plates and incubated at 37°C overnight. Well separated transformant colonies were single colony purified then single colonies were used to perform small scale plasmid purifications (Section 2.2.8). If the mutation was designed to introduce a new restriction site, plasmid DNA from several single colonies were screened by restriction analysis and agarose gel electrophoresis (Section 2.2.6) to confirm the introduction of the new site. Plasmids with the correct restriction pattern were then sequenced to confirm the correct sequence.

2.2.10.b Site directed mutagenesis using PCR

This method is based on a method described by Stratagene, and called QuikChange™ Site-Directed Mutagenesis. An overview of the method is illustrated in the flow-chart in Fig. 1. A standard double stranded plasmid vector prepared by either small or large scale purification (Sections 2.2.8 and 2.2.9 respectively) can be used as template DNA. The mutagenesis reaction mix in a volume of 50 µl contains the following: 50 ng of dsDNA template, 125 ng of each oligonucleotide (oligonucleotides were phosphorylated as described in Section 2.3.4), 5 µl of 10x *Pfu* reaction buffer, 1 µl of 10 mM dNTP mix (2.5 mM each NTP), distilled water to a final volume of 50 µl, 1 µl of native *Pfu* polymerase (2.5 U/µl). The *Pfu* polymerase was added last. The reaction mix was overlayed with a drop of mineral oil and the following temperature cycle was followed for 18 cycles, after heating the reaction to the denaturing temperature of 95°C for 1 min: denaturation at 95°C for 30 sec, primer

Fig. 1 Overview of the QuikChange™ site-directed mutagenisis method

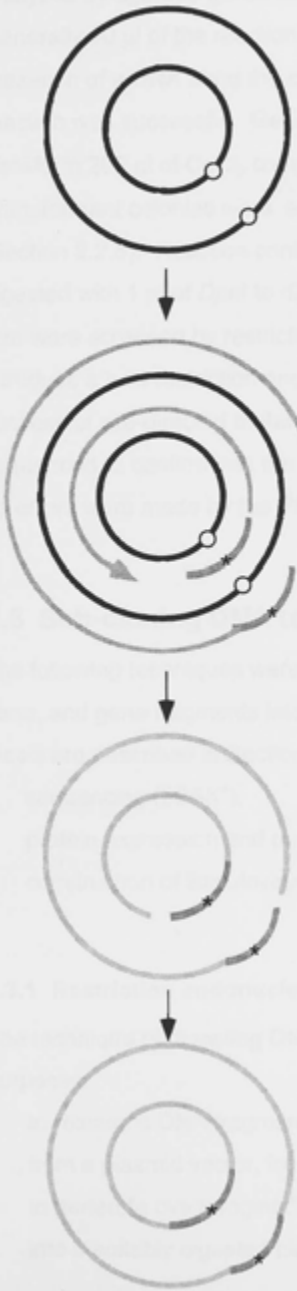

Template plasmid highlighting target site for SDM O

Temperature cycling:
Cycle of denaturing plasmid template, annealling oligonucletide primers ▬ containing the desired mutation (*), and synthesis of a mutant strand —

Removal of template DNA:
Digest the methylated, nonmutated parental DNA template with *Dpn* I

Transformation:
Transform the circular, nicked dsDNA into XL1-Blue competent cells

After transformation, the XL1-blue repair the nicks in the mutated plasmid

annealing at 55°C 1 min, DNA polymerisation at 68°C 2 mins/kb of plasmid length. The reaction was stored at 4°C. The products of the PCR were analysed by agarose gel electrophoresis as described in Section 2.2.6. Generally 10 μl of the reaction mix was loaded onto the agarose gel. The presence of a DNA band the correct size was a good indication that the reaction was successful. Generally 20 μl of the reaction mix was used to transform 200 μl of $CaCl_2$ competent *E. Coli* as described in Section 2.3.9. Transformant colonies were screened by small scale plasmid purification (Section 2.2.8). Reaction containing PCR products the correct size were then digested with 1 μl of *Dpn*I to digest the template DNA. Plasmids of the correct size were screened by restriction analysis if the mutation was designed to introduce a new restriction endonuclease site to allow quick identification of successful site-directed mutants. The gene containing the mutation was then sequenced to confirm that the altered sequence was correct, and to check that no errors were made by the *Pfu* polymerase.

2.3 Sub-cloning DNA techniques

The following techniques were used for the cloning of the *D. melanogater white* gene, and gene fragments into various plasmid vectors (plasmids used for this thesis are described in Section 2.4) for use for various uses, such as:

* sequencing (pBSK$^+$);
* protein expression and purification in *E. coli* (p2GEX and related plasmids)
* construction of Baculovirus transfer vectors (pAcUW31).

2.3.1 Restriction endonuclease digestion of DNA

The technique of digesting DNA at specific sites was used for the following purposes:

* to release a DNA fragment containing a gene or gene fragment of interest from a plasmid vector, for sub-cloning into a different plasmid vector;
* to generate overhanging "sticky" ends, or "blunt ends", suitable for ligation into a suitably digested plasmid vector;

* screening recombinant plasmids and site directed mutants by restriction analysis.

Sizes of DNA fragments resulting from restriction digests were predicted using the MacVector program (Section 2.6.10). Restriction digests were usually performed in a 20 μl volume including plasmid DNA, 2 μl 10 x buffer (recommended by the supplier), distilled water and 1 unit of restriction enzyme. The reaction mix was incubated at 37°C for 1 hr. 5 μl of the reaction was then analysed by agarose gel electrophoresis (Section 2.2.6).

2.3.2 Production of "blunt ends" by DNA Polymerase Klenow fragment

When convenient restriction sites flanking the DNA to be cloned were not available, a "blunt end" ligation technique was often used. Both the vector DNA and DNA to be inserted were digested with the appropriate enzymes, producing overhanging ends, which were then modified by end-filling by DNA Polymerase Klenow fragment to produce a "blunt end" for cloning. Following restriction enzyme digestion with the appropriate enzymes, the digested DNA was mixed in a reaction containing 25 μM dNTPs and 1 unit of Klenow, in a volume of 50 μl. The reaction was incubated at room temperature for 10 mins. The reaction was stopped with the addition of SDS to 1% and EDTA to 10 mM. The DNA was then purified as described in Section 2.3.6

2.3.3 Removal of terminal phosphates from linearised vector DNA

Removal of terminal phosphates from linearised DNA vectors was carried out in order to minimise re-ligation of the vector DNA. The vector DNA was digested with the appropriate enzyme, and on completion of the restriction reaction, 5 to 10 units of Calf Intestinal Alkaline Phosphatase (CIP) was added directly to the digestion reaction and incubated for 15 min. If the buffer used for restriction digestion contained 100 mM NaCl or more, the reaction was diluted to medium salt level of 50 mM (King and Possee, 1992). The CIP reaction was stopped by adding EDTA to 25 mM and SDS to 1%. The linearised, phosphatased vector DNA was then purified using the BresaClean method (Section 2.2.4).

2.3.4 Phosphorylation of oligonucleotides

25-300 pmol of oligonucleotide primer was mixed with the following ingredients: 10 mM ATP, 1 x One-Phor-All buffer PLUS (Pharmacia), and 5 units of T4 polynucleotide kinase was added to the reaction mix. The reaction was incubated at 37°C for 30 minutes prior to heat inactivation at 65°C for 10 mins.

2.3.5 Purification of DNA fragments

Following enzymatic reactions performed in the process of preparing vector and insert DNA for ligation, such as restriction enzyme digestion, Klenow end-filling and phosphatasing, the resulting DNA was purified to remove enzymes and other reagents which could interfere with a ligation reaction. The BresaClean kit (Bresatech) was used. Three volumes of sodium iodide solution was added to the reaction followed by 5 μl of well resuspended BresaClean silica resin and incubated for 5 mins at room temperature. The silica resin/DNA was pelleted and washed as described in Section 2.2.4.

2.3.6 Purification of DNA fragments from agarose gels

This method involved digesting a plasmid vector containing a gene of interest to be sub-cloned into a different vector, with the appropriate restriction enzymes. The DNA fragments resulting from the digest were then separated by agarose gel electrophoresis and stained with ethidium bromide (Section 2.2.6). The DNA fragments were visualised using a UV light box and the correct band was removed using sterile scalpel and transferred to an eppendorf tube. The DNA fragment was purified from the agarose gel and ethidium bromide using the BresaClean Kit (BresaTech). 1ml per gram of gel of sodium iodide solution was added to the DNA/gel slice and this was incubated at 55°C with occasional gentle mixing until the gel had completely dissolved. 5 μl of well resuspended BresaClean silica resin was added and incubated for 5 mins at room

temperature. The silica resin/DNA was pelleted and washed as described in Section 2.2.4.

2.3.7 Ligation of DNA

For routine sub-cloning 50 µl ligation reactions were performed, using a total DNA concentration of 200 ng and a vector:insert molar ratio of approximately 1:5. The reaction mix contained the following:
31 µl distilled water, 2.5 µl 1M Tris, pH7.5, 5 µl 0.1M $MgCl_2$, 5 µl 1 mg/ml BSA (nuclease free), 2.5 µl 0.1M DTT, 0.5 µl 0.1M spermidine, 0.5 µl 0.1 M ATP, 20 ng linearised vector (usually 50 µg/ml) and 180 ng of prepared insert DNA followed by 1 µl T4 DNA ligase. For reactions where overhanging "sticky" ends were to be ligated the reaction was performed at room temperature for 30 mins. Blunt end ligations were usually more successful when incubated overnight at room temperature with the addition of PEG (to 15%) in the reaction mix as recommended by Boehringer.

2.3.8 Preparation of Competent *E. coli* using $CaCl_2$

1 L of LB broth was inoculated with 50 ml of overnight culture and incubated at 37°C with vigorous aeration until an OD_{600} of 1 was obtained. The culture was then chilled on ice for 10 minutes and harvested by centrifugation at 7,000 rpm for 10 minutes. The supernatant was removed and the cells were resuspended gently (by pipetting up and down with a sterile pasteur pipette) in 10 ml of cold 0.1M $CaCl_2$ cells and then incubated on ice for 20 minutes. The cells were harvested again at 7,000 rpm for 10 minutes, the supernatant removed, and the cells were resuspended gently in 1ml of a cold solution of 0.1M $CaCl_2$:glycerol (85:15). 50µl aliquots were then transferred to pre-chilled Eppendorf tubes, rapidly frozen in liquid nitrogen and stored at -70°C.

2.3.9 Transformation of competent *E. coli* with plasmid DNA

A 50ml aliquot of frozen, competent cells (prepared as described in Section 2.3.8) were thawed on ice for 5 minutes. 0.9ml of ice-cold $CaCl_2$ was added and the cells mixed gently by pipetting up and down. 100 µl aliquots of these cells were transferred to chilled eppendorf tubes and 5 µl of ligation mix was added and mixed gently, followed by a 30 minute incubation on ice. The tubes were transferred to a water bath warmed to 43.5°C for 45 seconds then immediately returned to ice. This step is known heat-shock and facilitates the uptake of exogenous DNA by *E. coli*. 1ml of LB broth (1.0% (w/v) Tryptone, 0.5% (w/v) Yeast extract, 0.5% (w/v) sodium chloride, pH7) was added to each tube and the cells are incubated at 37°C for an hour to allow recovery of expression of antibiotic resistance genes. The cells are harvested by centrifugation at 5,000 rpm for 2 minutes, the supernatant was removed and the cells were resuspended in 250 µl of fresh LB broth. The cells were then plated onto LB agar plates containing the appropriate antibiotic followed by an overnight incubation at 37°C.

2.3.10 Characterisation of plasmids from individual transformant *E. coli* colonies

Inoculum from single transformant colonies was taken from the agar plate and mixed with a 50 µl aliquot of colony cracking solution (50mM sodium hydroxide, 10% SDS, 0.4M EDTA, 10% glycerol, 2% Bromocrescol green). After mixing, the reactions were incubated at 65°C for 30 minutes. The size of plasmids in the lysed cells were analysed by agarose gel electrophoresis (Section 2.2.6) and compared to cells transformed with the parental vector without insert. Colonies containing larger sized plasmids were selected for further analysis by small scale plasmid purification (Section 2.2.8) restriction digest (Section 2.3.1) and further agarose gel electrophoresis of the DNA fragments from restriction analysis.

2.4 Plasmid vectors

2.4.1 Plasmid vector pBluescript®SK +/-

This plasmid vector (obtained from Stratagene, GenBank #52325 (SK+), 52324 (SK-)) was used for general recombinant DNA sub-cloning and site directed mutagenesis using *E. coli*. The physical map of pBluescriptSK+ is shown in Fig. 2 The + or - suffix denotes the direction of the f1 filamentous phage origin of replication allowing recovery of either the sense (+) or antisense (-) strand. The plasmid is based on pUC19. The SK designation indicates the polylinker is orientated such that *lacZ* transcription proceeds from *Sac*I to *Kpn*I.

2.4.2 Plasmid vector pGEX4T1

This plasmid vector (obtained from Pharmacia) (see Fig. 3A) was used for expression of heterologous proteins in *E. coli* as C-terminal fusions to the enzyme glutathione-S-transferase from *Schistosoma japonicum*. This plasmid is based on pGEX-1 first described by (Smith and Johnson, 1988).

2.4.3 p2GEX

This plasmid was based on p2GEX-4T-1 (see Fig. 3B) and harbours a second GST coding region which was cloned into the *Ssp*1/*Sma*I site which is 5' of the ampicillin resistance gene and under control of the Ptac promoter element. This plasmid was constructed in Graeme Cox's laboratory, JCSMR, ANU.

2.4.4 Plasmid vector pAcUW31

The plasmid pAcUW31 (Clontech) (Weyer and Possee, 1991) is a baculovirus transfer vector for dual expression of two genes simultaneously. The physical map of pAcUW31 is illustrated in Fig. 4. The polyhedrin and p10 baculovirus promoter elements are arranged back-to-back transcribing in opposite directions. The polyhedrin promoter is followed by a unique *Bam*HI cloning site for insertion of foreign genes and the polyhedrin polyadenylation signals. The

Fig. 2 Plasmid vector pBluescript SK $^{+}$

Illustrated in this figure is the physical map of pBluescriptSK^{+}. Abbreviations and description of the features are listed below.

f1 (+) origin	(6-642 bp) f1 filamentous phage origin of replication allowing recovery of the sense strand of the *lacZ* gene when a host strain containing the Bluescript phagemid is co-infected with the helper phage.
ColE1 origin	(1032-1912 bp) Plasmid origin of replication used in the absence of helper phage
LacZ	(lac promoter: 816-938 bp) This portion of the *lacZ* gene provides α-complimentation for blue/white colour selection of recombinant phagemids. An inducible lac promoter upstream from the *lacZ* gene permits fusion protein expression with the β-galactosidase gene product.
MCS	(657-759 bp) Multiple cloning site flanked by T3 and T7 promoters.
Ampicillin	(1975-2832 bp) Ampicillin resistance gene for antibiotic selection of the phagemid vector.

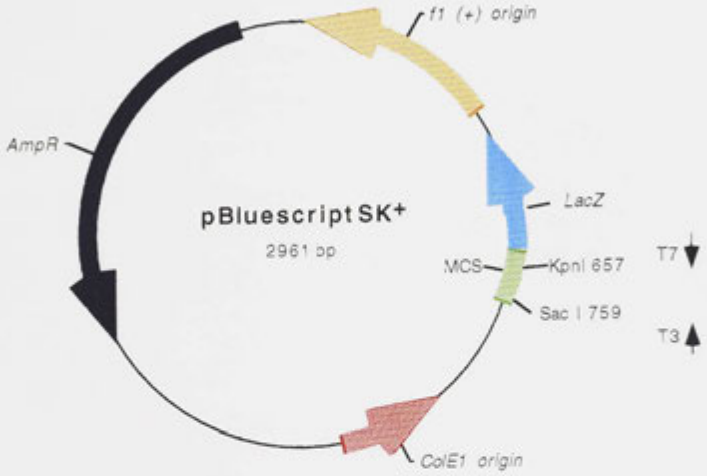
f1 (+) origin
AmpR
pBluescript SK+
2961 bp
LacZ
MCS
KpnI 657
Sac I 759
T7
T3
ColE1 origin

MCS


T3 promoter
β-Galactosidase
T7 promoter
T7 Primer
M13 -20 Primer
M13 Rev Primer

Fig. 3 Plasmid vectors pGEX4T1 and p2GEX

This figure illustrates the physical maps of the plasmid vectors:

A. pGEX4T1; and
B. p2GEX

Abbreviations and descriptions of the features are listed below:

Tac promoter	*tac* promoter : strong promoter element (hybrid of the *tryp* and *lac* promoters) induced by IPTG
GST	Glutathione-S-transferase gene region encoding 26 Kd GST protein
MCS	Multiple cloning site. 5' region harbours DNA sequence encoding site for thrombin cleavage to cleave GST and fusion partner
Amp^R	Ampicillin resistance gene
pBR322 ori	*E. coli* origin of replication
$lacI^q$	*lac* gene represser. Repression is inhibited by IPTG

A

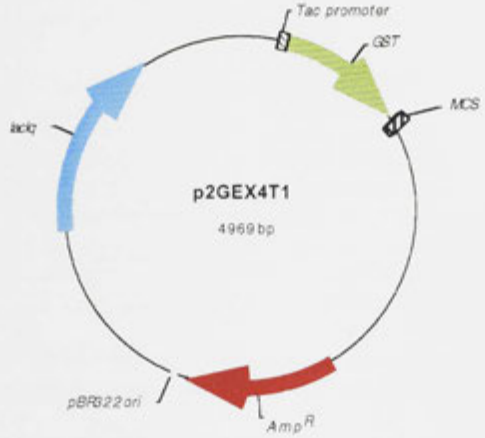

B

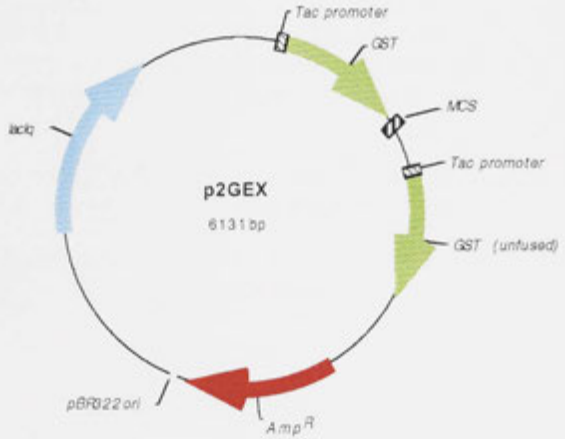

Multiple cloning site (MCS)

Fig. 4 Plasmid vector pAcUW31

This figure illustrates the physical map of the Baculovirus transfer plasmid vector pAcUW31. Abbreviations and descriptions of the features are listed below:

*Ac*MNPV	DNA sequences derived from the baculovirus *Autographa californica* multiple nuclear polyhedrosis virus. This sequence in conjunction with the sequence labelled *Ac*NPV flank the region of the vector which harbours cloning sites for insertion of foreign genes and forms the region which undergoes homologous recombination with linear wild-type *Ac*MNPV DNA.
*Ac*NPV	DNA sequence derived from the baculovirus *Autographa californica* multiple nuclear polyhedrosis virus.
poly A+	Polyadenylation signal for the polyadenylation modification of the 3' end of the transcribed insert DNA
M13 ori	M13 origin of replication which can be use to package single stranded DNA of the coding strand of genes cloned behind the polyhedrin promoter and the non-coding strand of the genes cloned behind the p10 promoter (top strand in figure)
p10 Prom	p10 promoter element from *Autographa californica* nuclear polyhedrosis virus
Polyhedrin Prom	Polyhedrin promoter element from *Autographa californica* nuclear polyhedrosis virus
pBR322 ori	Origin of replication propagation in *E. coli*
Ap-R	Ampicillin resistance gene

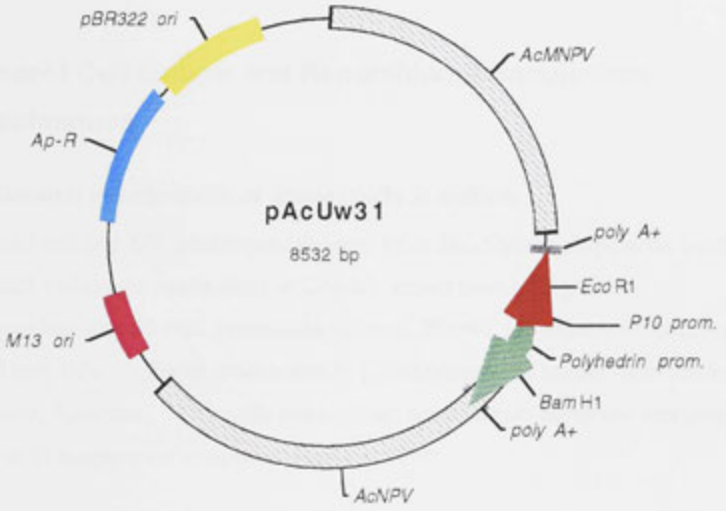

Cloning sites

SV40 poly A+ signal ....GAATTCAGATCTGTGATT0 ← P_{p10} TCTAGA

Eco RI *Bgl* II *Xba* I

$P_{Polyhedrin}$ → TAAATATCGGATCCGG..... poly A+ signal

Bam HI

p10 promoter is followed by unique *Bgl*II and *Eco*RI cloning sites and a polyadenylation signal from SV40.

2.5 Insect Cell culture and Recombinant Baculovirus techniques

2.5.1 General maintenance of insect cells in culture

The insect cell line Sf9 (Invitrogen) derived from *Spodoptera frugiperda* ovarian cells (Sf21 cells) was maintained in Grace's insect media (Sigma) supplemented with 20 ml/L yeastolate (Gibco), 20 ml/L lactalbumin hydrolysate (Gibco) and 10% v/v foetal bovine serum (Commonwealth serum laboratories, Melbourne, Australia). The cells were grown either as an adherent monolayer culture or in suspension in spinner flasks at 27°C.

Grace's media was prepared in 10 L lots from powdered stocks (Sigma) using double distilled water. Yeastolate (Gibco) and lactalbumin hydrolysate (Gibco) were added to 2% final volume. The pH was adjusted to 5.9-6.0 with 10 M potassium hydroxide prior to filter-sterilisation through a 142 mm Millipore stainless steel sanitary filterholder (a tri-clamp sanitary inlet outlet system). A glass fibre pre-filter (Gelman Sciences, type A/E, 127 mm diameter) was used in conjunction with a 0.2 mm pore diameter membrane filter (Gelman Sciences, Supor 200, 142 mm diameter) to filter-sterilise the media by pressure filtration. At this point the osmolality of the solution was checked and adjusted, if necessary, by the addition of sterile water. Osmolality values of 300-330 mosmol l^{-1} were considered acceptable. When Sigma Grace's media was used osmolality values did not vary significantly and the addition of water was rarely required. Media was then dispensed into 500 ml sterile Schott bottles and incubated at 37°C for two days to check for possible contamination. This stock media, referred to as incomplete TNM-FH, was stored at 4°C. Complete media was prepared as required by the addition of heat inactivated foetal bovine serum (FBS) to 10 % v/v. Heat inactivation of FBS was performed at 56°C for

30 min. This media, termed complete TNM-FH, had a final pH of 6.0-6.2 and osmolality of 330-360 mosmol.l^{-1} . Storage was at 4°C in the dark.

Sf9 cells were grown and maintained in spinner culture which allowed a more precise monitoring and control of their growth and provided sufficient numbers of cells for experimentation. Cells (1 x 10^7) were thawed at 27°C from stocks frozen in liquid nitrogen and seeded into a 25 cm^2 tissue culture flask (Corning) containing 5.0 ml complete TNM-FH. The cells were grown at 27°C until a confluent monolayer had formed (5-7 days); the media was generally replaced once during this time. In order to obtain enough cells to seed a 50 ml spinner (Bellco) the cells were passaged into 75 cm^2 flask and resuspended from the flask bottom by agitation achieved by pipetting fresh complete TNM-FH over the cells 4-6 times. These cells were then seeded into a 75 cm^2 flask and grown to confluence at 27°C. The cells were passaged into three 75 cm^2 flasks containing 10 ml complete TNM-FH. When a confluent monolayer of cells had grown (3 days), the cells were resuspended and seeded into a 50 ml spinner containing 10 ml complete TNM-FH. The cell density was adjusted to 0.5 x 10^6 cells/ml with complete TNM-FH and incubated at 25°C on a magnetic platform stirred at 50 rpm. The slightly lower temperature of the spinner cultures, compared to 27°C used for flask cultures and viral incubations, meant cells took 4 to 5 days to reach stationary phase and consequently decreased the handling time. Growth (cell density) was monitored by counting the cells using a haemocytometer and viability determined using trypan blue (4%, sigma); 10 ml of trypan blue was added to 100 ml cells with viable cells excluding the blue dye. Cultures of 95-98% viable cells were considered acceptable. The spinner culture was allowed to grow to stationary phase, 2-3 x 10^6 cells/ml, before being diluted down to 1.0-2.0 x 10^5 cells/ml.

Every two weeks cells that had been grown in spinner culture were transferred to a sterile 50 ml tube (Falcon) and centrifuged at 1000 rpm for 10 min. The media was decanted and replaced with 30 ml fresh complete TNM-FH. The cells were resuspended gently and transferred to a clean, sterile spinner

containing 10 ml complete TNM-FH. The cell density was adjusted to 2.0-5.0 x 10^6 cells/ml in a volume of 50 ml. This procedure removed cell debris and the build up of cell components secreted by the growing cells into the media which may inhibit growth. A monolayer culture ($25cm^2$ flask) was always maintained as a backup in case the spinner culture became contaminated or decreased viability.

2.5.2 Production of recombinant Baculovirus

A flow chart illustrating the steps involved in production of a recombinant Baculovirus is provided in Fig. 5.

2.5.2.a Co-transfection method

The cotransfection of Sf9 insect cells with linear viral AcNPV DNA (BacPAK6) (Clontech) and baculovirus transfer vector was carried out using the lipofectin method originally described by (Felgner et al, 1994) and specifically described for use with linear AcNPV DNA in the manufacturers protocol (Clontech).

Sf9 cells were grown in spinner culture to a density of between 0.5-0.7 x 10^6 cells/ml were seeded into 35mm tissue culture places (Nunc) at 1.5 x 10^6. When the cells had formed a monolayer (approximately 20 mins), the media was replaced with 2.0 ml serum free TNM-FH. This washing step was repeated a second time to ensure that the component in serum which inhibits lipofectin-mediated transfection was removed. Plasmid DNA, prepared by either a mini-prep protocol or CsCl isopycnic (density gradient) centrifugation (Section 2.2.8) was filter sterilised and diluted in sterile TE buffer to a final concentration of 100 ng/ml. The following reagents were mixed in sterile polystyrene tubes:

	Cotransfection	Control
Sterile water	40 µl	45 µl
Plasmid DNA	5 µl	5 µl
Linear viral DNA	5 µl	0 µl
Lipofectin solution (0.1mg/ml)	50 µl	50 µl

Fig. 5 **Construction of recombinant baculovirus**

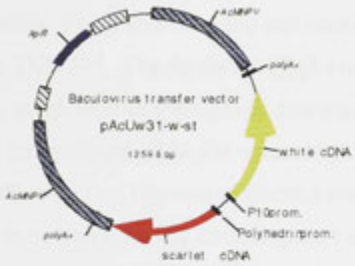

Construct transfer vector harbouring genes of interest

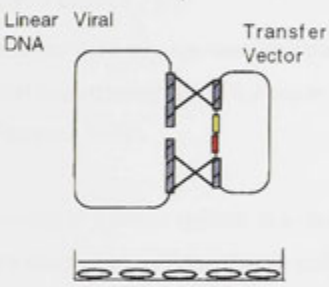

Co-transfection of linear viral DNA and transfer vector resulting in recombination between homologous sequences shown in blue

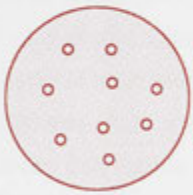

Co-transfection supernatant used to perform plaque assays

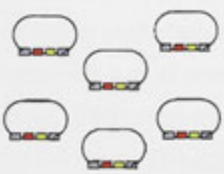

Amplification of recombinant viral progeny from single plaque. Recombinant virus used to infect cells and screen for protein expression of foreign genes.

The lipofectin reagent (Clontech) was added last, then mixed gently and incubated at room temperature for 15 min to allow lipofectin-DNA complexes to form. Meanwhile, the media from the cell monolayers was replaced with 1.5 ml of serum free TNM-FH. The lipofectin-DNA complexes were added drop-wise to the media, which was swirled gently and incubated at 27°C for 5 hr. After this time, 1.5 ml complete TNM-FH was added and the samples incubated at 27°C for a further 72 hr. The cotransfection media, containing recombinant viruses, was then harvested by centrifugation at 1000 rpm for 10 min in a bench top centrifuge and the supernatant stored at 4°C.

2.5.2.b Plaque assay:

Individual recombinant viruses were isolated and purified from the cotransfection supernatant using a plaque assay essentially as described in (King and Possee, 1992).

Sf9 cells growing in spinner culture at a density of between 0.5-0.7 x 10^6 cells/ml were seeded into 60mm tissue culture plates (Nunc) at 1.5 x 10^6 cells and allowed to form a monolayer. The cotransfection supernatant was diluted to 10^{-1}, 10^{-2} and 10^{-3} in serum free media just prior to infection. Duplicate samples were prepared at each dilution. The media was removed from the cell monolayer and 1.0 ml of diluted cotransfection supernatant overlayed. The samples were incubated at room temperature with gentle agitation on a slowly rocking platform for 90 min. Approximately 15 min prior to the end of the infection sterile liquefied Sea Plaque agarose (3.0%) (FMC) was allowed to cool slightly before adding complete media, diluting the agarose to 1%. At the end of the incubation period the diluted cotransfection supernatant was removed and 4 ml of the 1% Sea Plaque agarose which had cooled sufficiently but had not solidified, was added to each plate and then allowed to solidify. Finally the agarose was overlayed with 1 ml of complete TNM-FH to provide sufficient nutrients for cell growth. Each plate was then sealed with parafilm and incubated at 27°C for 5-8 days. The agarose overlays were then stained with Neutral Red (Sigma) (0.5% w/v in PBS). Live cells take up the dye while cells

killed by viral infection would not, thus viral plaques appear clear in a background of red cells.

At least 10 well separated plaques for each sample were picked from the highest dilution on which plaques could be visualised. Each agarose plug was taken up in a pasteur pipette and expelled into 1 ml serum free TNM-FH media. Plugs were left overnight at 4°C to allow diffusion of the virus particles into the media before being used for further rounds of plaque purification and subsequent P1 viral supernatant production.

2.5.2.c Identification of Recombinant Viruses

Individual plaques were used to prepare a seed stock (P1) from which recombinant isolates were identified by Western blotting. Infected cells were harvested at least 30 hpi, cell proteins separated by SDS PAGE and Western blotting 2.6.1, using anti-White and anti-Scarlet antibodies 2.11 as described below.

2.5.2.d Preparation of P1 seed stock:

Sf9 cells growing in spinner culture at a density of 0.5-0.7 x 10^6 cells/ml were seeded at 1.5 x 10^6 cells into 25 cm^2 flasks containing 2.0 ml complete TNM-FH. When the cells had formed a monolayer the media was removed and 1.0 ml of virus suspension from a single plaque pick used to infect the cell monolayer. The flasks were incubated for 90 min at room temperature on a slowly rocking platform. The inoculum was removed, the cells overlayed with 5 ml complete TNM-FH, and then incubated at 27°C for 6 days. Medium, containing viral particles, was harvested by centrifugation at 1000 rpm for 10 min in a bench top centrifuge and stored at 4°C.

2.5.2.e Screening of Recombinant Viral Isolates by Western blot Detection of the White and Scarlet protein

Sf9 cells growing in log phase in spinner culture, 0.5-1.2 x 10^6 cells/ml, were seeded to form a confluent monolayer in wells of a 96 well plate (Nunc) which contained 100 µl of complete TNM-FH. This volume varied between

approximately 120-200 μl of cells depending on cell density. The media was removed and 40 μl of each of each P1 supernatant added to individual wells and incubated at room temperature for 90 min. The virus was removed prior to adding 200 μl of complete TNM-FH and the cells incubated at 27°C for 24-72 hr.

The infected cells were resuspended in the incubation media and transferred to 1.5 ml eppendorf tubes. The samples were centrifuged in a microfuge at 14000 rpm for 2 min. The liquid was aspirated off and 0.5 ml PBS added to wash the cells. Following a second centrifugation the liquid was removed and 50 μl of reducing electrophoresis sample buffer added. The samples were then boiled for 5 min and the proteins separated on a 12% SDS polyacrylamide gel (Section 2.6.1). The proteins were transferred to a PVDF membrane (Novex) and the White and Scarlet proteins were detected by Western blotting using anti-White or anti-Scarlet polyclonal antibodies (Chapter 4).

2.5.2.f Amplification of Recombinant Viral Stocks:

To produce a large volume of high titre viral supernatant (P3) a positively identified recombinant P1 viral supernatant was propagated according to the protocol described in King & Possee. The procedure involves the passaging of a P1 viral stock (5ml) through an intermediate passage (P2) to provide a suitable volume (10ml) of ideally similar or lower titre virus for subsequent production of a large volume of amplified viral progeny. Continued passaging and amplification of recombinant virus is reported to result in viral instability and accumulation of defective interfering virus particles (King and Possee, 1992); hence amplification of the virus was performed from a small viral population to produce progeny of similar derivation.

2.5.2.g Production of P2 Recombinant Viral Supernatant:

Sf9 cells growing in spinner culture at a density of 0.5-0.7 x 10^6 cells/ml were seeded at 5 x 10^6 cells into 75 cm^2 flasks (Corning) containing 10 ml complete TNM-FH and allowed to form a monolayer. The P1 supernatant was diluted eight fold with incomplete TNM-FH (2.0 ml per infection). The media was

removed from the monolayer and the cells overlayed with the 2.0 ml of diluted P1 supernatant. Infection was performed at room temperature for 90 min with the flasks on a slowly rocking platform. The virus was then removed and the cells overlayed with 10 ml of complete TNM-FH and incubated at 27°C for 4-6 days. The propagation time was monitored by the degree of cell lysis, i.e. cells floating, indicative of viral infection. When approximately 60-80% of the cells had lysed the P2 viral stock was harvested by centrifugation of the supernatant at 1000 rpm for 10 min in a bench top centrifuge and stored at 4°C. Typical incubation times were 5 to 6 days.

2.5.2.h Production of P3 Recombinant Viral Supernatant:

A spinner flask was seeded (0.5×10^6 cells/ml) and the cells grown to confluency (approximately $2\text{-}3 \times 10^6$ cells/ml, at which time it was diluted down to $0.1\text{-}0.2 \times 10^6$ cells/ml (approx. 2 days) the cells were infected at a MOI of 0.1-0.2 pfu/cell according to the following calculation:

$$\text{Volume of P2 viral supernatant added} = \frac{[\text{MOI (pfu/cell)} \times \text{number of cells}]}{\text{titre of virus (pfu/ml)}}$$

Volume of cell culture	50 ml
cell count	0.5×10^6 cells/ml
total cell number	2.5×10^7 cells/ml
Virus titre (P2)	x pfu/ml
multiplicity of infection (MOI)	0.2-0.2 pfu/cell

The spinner was then placed on a magnetic stirrer and incubated at 27°C for 6 days. To harvest the supernatant the spinner was placed at 4°C overnight and the next day the supernatant spun at 1000 rpm for 10 min in a bench top centrifuge. This P3 supernatant was stored at 4°C and its titre determined by plaque assay.

2.5.2.i Infection of Sf9 cells with recombinant Baculovirus

All assays included uninfected and an infected negative control cells. The virus used for the negative infected control was a recombinant Baculovirus constructed by Brett Cromer containing the cDNA encoding the human Gaba 1 subunits α1 and β1. Cells expressing a heterologous gene product unrelated to the White or Scarlet protein was considered to be a better control than the wild-type AcNPV infected cells which produce large amounts of polyhedrin making them optically very different to cells expressing recombinant virus which does not express the polyhedron gene. Sf9 or Hi5 cells growing at a density of 0.5-0.9 x 10^6 cells/ml were seeded in 30cm^2 tissue culture plates (Nunc) at 1.5 x 10^6 cells and allowed to form a monolayer. Duplicates of each sample were prepared as follows. Recombinant viral supernatants were diluted in incomplete TNM-FH for infection at MOIs of 50 Pfu/cell. Typically P3 (1 x 10^8 Pfu/ml or better) were diluted 4 fold and P2 stocks (1 x 10^7 Pfu/ml) were diluted 1 fold. The media was removed and 1.0 ml of diluted recombinant viral supernatant added to the cell monolayer and incubated for 90 min at room temperature on a slowly rocking platform. The virus was then removed and the cells overlayed with 3.0 ml of complete TNM-FH and incubated at 27°C for times ranging from 24-48 hours post infection (hpi).

2.5.3 Inhibition of glycosylation in Sf9 cells

In experiments examining the effect of inhibition of N-glycosylation by tunicamycin (Sigma), the inhibitor was dissolved in DMSO at a concentration of 1 mg/ml and added 3 hpi to the media overlay at a final concentration of 1 mg/ml. The delay in tunicamycin addition was to ensure that the cells had recovered sufficiently following infection in serum free media. The time of addition was well before promoter activation of the foreign proteins (12 hpi). Cell proteins from tunacamycin treated cells and those not treated with tunacamycin were analysed by SDS PAGE and Western blotting to detect changes in apparent molecular weight due to the presence or absence of glucose residues.

2.5.4 Flow cytometry analysis of recombinant Baculovirus infected cells

2.5.4.a Labelling of infected Sf9 cells for FACS analysis and confocal microscopy

The viral supernatant was removed and the cells were resuspended in PBS and transferred to polystyrene tubes. The cells were harvested by centrifugation at low speed in a bench top MSE centrifuge at 1,000 rpm for 5 min. Duplicate samples were prepared for analysis of (1) plasma membrane protein targeting, and (2) cytoplasmic protein targeting which required solubilisation of the membrane with SDS. The main difference between the preparation of these duplicate samples was that for plasma membrane targeting analysis, the primary and secondary antibodies were incubated with the cells prior to fixation in order to minimise protein damage due to the fixation procedure which may alter epitopes recognised by the antibodies. The samples prepared for cytoplasmic targeting analysis required fixing prior to SDS treatment to preserve the cell's structure during membrane permeabilisation. The SDS treatment precedes antibody incubation to allow the antibody access to the inside of the cell.

1. Plasma membrane protein targeting

The liquid was aspirated off and samples for analysis of plasma membrane targeting were resuspended in a solution containing PBS, 1% BSA and typically a 1:10 dilution of purified polyclonal primary antibody, or a 1:100 dilution of serum containing polyclonal primary antibodies. The cells were incubated for a minimum of 30 mins at room temperature, or at 4°C over-night. At this stage the cells were transferred to small tubes pelleted by centrifugation at 1,000 rpm for 5 min in a benchtop centrifuge, the antibody solution removed and replaced with 0.4ml of PBS to wash the cells. The small tubes allowed smaller volumes to be used in order to decrease the loss of cells due to the cells sticking to a larger surface area. The cells were then incubated for 30 min at room temperature with 100µl of a solution containing PBS, 1% BSA and a 1:50

dilution of a goat anti rabbit antibody conjugated to FITC. The samples were protected from light after addition of the FITC conjugated secondary antibody to prevent photobleaching of FITC fluorescence. The cells were then washed with PBS and resuspended in 100ul of Zamboni's Fixative (2% formaldehyde, 15% saturated picric acid in 0.1M phosphate buffer, pH 7.4) for 90 mins at room temperature. The cells were washed twice with PBS.

2. Cytoplasmic membrane targeting

The cells were harvested in the same way as above, and resuspended in 0.4 ml of PBS and transferred to small tubes. The PBS was removed and replaced by 100µl of Zamboni's fixative (as in 1 above) and the cells were incubated for 90 mins at room temperature. The cells were washed twice with PBS, then incubated for 30 mins at room temperature with 100µl of a solution containing PBS, 1% BSA and 0.1% SDS. The cells were washed twice with PBS then incubated with primary and secondary antibodies as described in 1. above.

2.6 Protein Biochemistry Techniques

2.6.1 Electrophoresis of proteins

Proteins were separated by electrophoresis essentially as described previously by (Laemmli, 1970) using either a Novex XCell II apparatus and pre-cast polyacrylamide gels (Novex), or polyacrylamide gels were manually poured and a Biorad Mini-PROTEAN II Cell (10 x 7cm) as follows:

Non-denaturing conditions (native PAGE)

Stacking gel: 12mM Tris, pH 6.8, 1.95% (29:1) acrylamide/Bis, 0.1% TX-100

Resolving gel: 38mM Tris, pH 8.8, 7.5% (29:1) acrylamide/Bis, 0.1% TX-100

Denaturing conditions (SDS PAGE)

Stacking gel: 1.95% (29:1) acrylamide/Bis, 12mM Tris, pH 6.8, 0.1% (w/v) SDS

Resolving gel: 12% (29:1) acrylamide/Bis, 38mM Tris, pH 8.8, 0.1% (w/v) SDS

APS and TEMED were added last to initiate polymerisation. The resolving gel was poured first and was set under a thin layer of water-saturated butanol which straightened the surface and excluded oxygen. After the resolving gel

had set the stacking gel was poured and a 10 well comb was inserted to form sample wells. Once the stacking gel was set, the plates were transferred from the casting try to the BioRad Mini Protean buffer tank, and covered with SDS Running Buffer.

Samples were prepared for SDS PAGE by adding 2x SDS sample buffer (0.5M Tris-HCl, pH 6.8, 10% SDS, 0.1% Bromophenol blue, 20% glycerol, 2% DTT) to an equal volume of sample (usually 50µl). Or alternatively, a one tenth volume of SDS-Z buffer (40mM Tris-HCl pH 8, 10% (w/v) glycerol, 16% (w/v) SDS, 4% DTT) to dilute protein solutions. Samples were then incubated for 2 minutes at 100°C, then centrifuged for 1 minute in a benchtop microfuge. Samples were prepared for native PAGE by adding an equal volume of 2x native sample buffer (1.5M Tris-HCl, pH 8.8, 0.1% bromophenol blue, 20% glycerol, 0.2% TX-100) 20ml samples were loaded into the wells. Gels were run at 35mA per gel in SDS running buffer (25mM Tris-HCl, 190mM glycine, 3.5mM (w/v) SDS) for denaturing conditions and native running buffer (5mM Tris-HCl, 38.4mM glycine) for non-denaturing conditions until the dye front was at the bottom of the gel (denaturing conditions) or run off the bottom of the gel (non-denaturing conditions). Low range molecular weight markers and prestained molecular weight markers were from Biorad and Novex (SeeBlue™). Gels were stained either with Coomassie R-250 (PhastGel™ Blue R, Pharmacia Biotech)(1.25% (w/v), Coomassie R-250 dye, 10% (v/v) acetic acid, 50% (v/v) methanol, 25% (v/v) ethanol) and destained overnight in destain solution (25% (v/v) ethanol, 8% (v/v) acetic acid), or silver stained. After staining and destaining, gels were desalted in water and incubated in gel drying solution (5% (w/v) glycerol, 30% (v/v) methanol), then dried between sheets of cellophane (pre-soaked in gel drying solution) (Novex) using a Novex gel drying frame.

2.6.2 Silver staining of polyacrylamide gels

This method relies on differential reduction of silver ions that are bound to the side chains of amino acids. The method was carried out as described

(Sambrook et al, 1989). Proteins were fixed after electrophoresis in a solution of ethanol:glacial acetic acid:water (30:10:60) for 4 to 12 hours. If Coomassie Blue staining was used initially, the gel was destained overnight. The fixing solution was discarded and the gel was incubated with shaking at room temperature with 30% ethanol 30 minutes. This step was repeated. The ethanol was discarded and deionized water was added and the gel was incubated for 10 minutes at room temperature. This step was repeated twice. The last of the water washes was discarded and a solution of 0.1% silver nitrate was added and the gel was incubated with shaking for 30 minutes at room temperature. The silver nitrate was discarded and the gel was washed on both sides with a gentle stream of deionized water for 20 seconds each side. Freshly made aqueous solution of 2.5% sodium carbonate and 0.02% formaldehyde was then added. The gel was incubated at room temperature with gentle agitation until the stained bands of protein appeared. When the desired contrast was obtained the reaction was quenched by the addition of a solution of 1% acetic acid and the gel was incubated for 2 to 3 minutes. The gel was then washed in deionized water several times.

2.6.3 Detection of Protein by Western blot

For Western blot detection proteins were transferred to nitrocellulose essentially as described by (Towbin et al, 1979). The semi-dry transfer technique, using a Multiphor^{R}II electrophoresis system (Pharmacia), was used to electrophorese proteins from the polyacrylamide gel onto the nitrocellulose membrane (Schleicher and Schuell) or PVDF membrane (Novex), following the manufacturer's assembly instructions as follows. Two layers of 3 MM filter paper, cut to the exact same dimensions as the resolving gel (9 x 6 cm), were soaked in semi-dry transfer buffer (39 mM glycine, 48 mM Tris, 0.0375% w/v SDS, 20% v/v methanol). Six sheets were stacked onto the graphite anode followed by a piece of nitrocellulose the same size. The gel was then mounted followed by the final six sheets presoaked filter paper. Electrophoretic transfer proceeded at 0.8 mA per cm^2 (e.g. 0.8 x (9 x 6) = 43.2 mA for 50 min.

At the completion of the transfer step the nitrocellulose was incubated in blocking buffer (10 mM Tris pH 7.5, 10% milk powder, 0.9% NaCl, 0.05% Tween 20 (Biorad)) for 40-60 min on a rocking platform. The blot was washed in Tris buffered saline with Tween 20 (TTBS) solution (10 mM Tris-HCl pH 7.5, 0.9% NaCl, 0.05% Tween) three times, each for 5 mins. The primary polyclonal antibody (either anti-White or anti-Scarlet (Section 2.11) specific for either the White or Scarlet proteins was diluted 500 fold in blocking buffer to a final volume of 10 ml and the blot immersed in the solution. The blot was incubated at either 4°C overnight, or 2 hours at room temperature. The blot was washed in TTBS solution three times, each for 5 min, prior to immersing in secondary antibody (goat-anti-rabbit immunoglobulins conjugated with alkaline phosphatase) (DAKO) diluted 1 in 1000 in TTBS for two hours at room temperature. The blot washed with TBS (omitting Tween 20) three times, each for 5 min, prior to detection of immunoreactive bands by incubation with a solution containing alkaline phosphatase substrate (Western Blue® Stabilised Substrate for Alkaline Phosphatase (Promega)). Once the immunoreative bands reached the desired intensity the membrane was washed with distilled water thee times, each for 5 mins and dried.

2.6.4 Tryptophan uptake assay of whole insect cells

Tryptophan transport activity of insect cells was performed using L-[5-^{3}H]Tryptophan (Amersham International plc). 16 wells of 3 x 24 well plates were seeded with 150 μl of 100 x 10^{4} cells/ml and left for between 30 mins to overnight to form a cell monolayer. This allowed for four wells or quadruplicate samples, of four different times. The media was removed from each well followed by the addition of either BV-*w,st* P3 stock; or control virus (expressing the human Gaba 1 subunits α1 and β1 obtained from Brett Cromer, JCSMR, ANU); or media containing no virus for an uninfected control. The cell monolayers were incubated for 90 min at room temperature with gentle rocking on a rocking platform. The viral supernatant was removed and fresh media (0.5

ml) containing approximately 1 μCi/ml of L-[5-^{3}H]Tryptophan, was added to the monolayers. The cells were incubated at 25°C. Cells were harvested over a time course of 6 hpi, 24 hpi, 31 hpi and 48 hpi. The cell monolayers were resuspended by pipetting up and down gently then were transferred to separate eppendorf tubes for harvesting by centrifugation. The cells were washed twice with PBS, then resuspended in 0.5 ml PBS and stored at -20°C until counting. Cells were then added to 3 ml of scintillation fluid and counted in a scintillation counter.

2.6.5 Separation of cell fractions by differential centrifugation

2.6.5.a Fractionation of E. coli cells

Harvested cells were resuspended in 50mM Tris-HCl pH 7.4 and 20% glycerol, in a volume of 2ml/g wet weight of cells for large cell cultures (20-40L) or in a minimum volume of 50ml for 1L cultures. Cells were then lysed using a RF-1 Ribi Cell Fractionator (Sorvall) at a pressure of 20,000 p.s.i. 0.05g DNAase was added to the lysate to degrade the DNA released from the lysed cells to reduce the viscosity of the suspension. The lysate was centrifuged at 15,000 rpm in a Sorvall SS34 rotor for 30 minutes to pellet the cell debris (cell wall, and insoluble aggregates such as inclusion bodies), and the supernatant was centrifuged for a further hour at 60,000 rpm in a Beckman Ti70 rotor (approx. 100,000 g) to separate the membrane fraction (pellet; lipids and integral membrane proteins) from the cytosol (supernatant; this fraction contains soluble proteins).

2.6.5.b Fractionation of Sf9 insect cells

Sf9 cells growing as suspension culture or cell monolayer were harvested by centrifugation at 1,000 rpm and washed in PBS. Cells were resuspended in 10mM Tris, pH 7.4, 200 mM Sucrose and then lysed using a dounce tissue homogeniser (Wheaton) by 15 strokes with the loose-fitting pestle followed by 5 strokes with the tight-fitting pestle. The cell lysate was centrifuged at low speed (1,000 rpm or 121 g) in an SS34 rotor for 5 minutes to separate insoluble

material. The supernatant from the low speed centrifugation was centrifuged at 60,000 rpm (around 100,000 g) in a Ti 60 (Beckman) rotor for 1 hr to separate crude membranes from soluble cytoplasmic fraction of the cell.

2.6.6 Separation of cell fractions by percoll density gradient

Sf9 cells harvested by centrifugation at 1,000 rpm and washed in PBS. Cells were resuspended in 10mM Tris, pH 7.4, 200 mM Sucrose and then lysed using a dounce tissue homogeniser (Wheaton) by 15 strokes with the loose-fitting pestle followed by 5 strokes with the tight-fitting pestle. Percoll (Pharmacia) was added to the cell lysate to a final concentration of 11.9%. The solution was centrifuged at 20,000 rpm in a Ti 50 Sorvall rotor for 30 minutes. Fractions were removed by gentle aspiration with a pasteur pipette.

2.6.7 ATP binding assays of protein immobilised to glutathione-agarose

This method was developed in this laboratory. 10 μCi of [α-^{32}P]-ATP (Amersham International, plc) was added to 100 μl sample volume of protein immobilised to glutathione-beads (50% bead slurry), (described in Section 2.9.1). Samples were gently mixed and incubated at room temperature for between 30 sec to 2 mins. The beads were then washed by filtration three times with 150 μl of sample buffer prior to resuspension in 100 μl of sample buffer which was then transferred to a scintillation vial containing 3 ml of scintillation liquid. The radiation was then counted by a scintillation counter (Packard Tri Carb 300) for 5 minutes.

2.6.8 [α-^{32}P]-8-Azido-ATP photocrosslinking

This method was modified from previously described methodology (Czarnecki et al, 1979) and utilizes the photoreactive ATP analog 8-azido-ATP. Exposure of 8-azido-ATP to UV irradiation converts the azido group into a highly reactive nitrene which can form a covalent bond with amino acids at the nucleotide-binding site of the protein being studied. [α-^{32}P]-8-Azido-ATP (ICN

Pharmaceuticals) was added to 50 µl sample volume on ice, to a final concentration of 10.3 µM. The sample was mixed gently incubated for approximately 30 seconds, then irradiated with UV radiation at 254 nm for between 30 sec and 1 min on ice. Samples were then TCA precipitated and proteins were separated by SDS PAGE on a 12% Tris-Glycine polyacrylamide gel. The gel was then stained with Coomassie blue, destained, then incubated in a solution of 5% glycerol and 30% methanol twice for 10 minutes with two changes of solution. The gel was then dried onto chromatography paper using a Biorad slab drier and autoradiographed at -70°C for periods ranging from overnight to two weeks.

2.6.9 Detection of ATPase activity in non-denaturing polyacrylamide gels

Detection of phosphate release due to ATP hydrolysis activity in polyacrylamide gels under non-denaturing condition was performed as described previously by (Weinbaum and Markman, 1966) and modified by (Fayle, 1978). Protein were separated by non-denaturing PAGE prior to incubating the gel with an ATP/lead staining buffer (35 mM Tris-HCl, 270 mM glycine, 14 mM magnesium sulphate, 0.2% (w/v) lead nitrate, 8 mM ATP, pH 7.4). The gel was incubated at 37°C overnight to allow the white precipitate to form.

2.6.10 Precipitation of proteins with trichloro acetic acid

Proteins samples to be concentrated prior to SDS PAGE analysis were precipitated by adding trichloro acetic acid (TCA) to a final concentration of 10% (w/v). Samples were then chilled for 10 minutes at 4°C, then centrifuged in a benchtop microcentrifuge for 5 minutes at 4°C. The supernatant was removed and the pellet was washed with ethanol. The sample was resuspended in 1 x SDS PAGE loading buffer (40 mM Tris-HCl, pH 8.0, 10% glycerol, 1.6% SDS, 10 mM DTT) and prepared for SDS PAGE.

2.7 Computer analysis of protein and DNA sequences

Protein analyses including hydrophilicity analysis, antigenic index, sequence alignments, calculation of isoelectric points were performed using the computer program MacVector version 6.0.1.

Sequence comparisons were performed using CLUSTAL W alignment program (Higgins et al, 1996) using the Macvector computer program. The settings used were as follows: pairwise alignment mode: slow; pairwise alignment parameters: open gap penalty 10; delay divergent 40%; extend gap penalty 0.1; gap distance 2; similarity matrix used was blossom; multiple alignment parameters: open gap penalty, 10; extend gap penalty, 0.1; delay divergent, 40%; gap distance 2; similarity matrix, blossom.

2.8 Over-expression of heterologous GST-fusion proteins in *E. coli* and solubilisation of membrane and cell debris fractions

This method describes the over-expression of GST -wNBD fusion proteins for subsequent affinity purification first described by (Smith and Johnson, 1988). Recombinant GST fusion proteins were over-expressed in protease deficient *E. coli* strains (AN3700 or AN3701) by induction with 0.1 mM IPTG during late log phase and grown at 30°C for between 2 and 3 hours. Cells were harvested by low speed centrifugation at 4°C and resuspended in 2 ml/g of fresh weight of cell pellet of a buffer containing 50 mM Tris-HCl, 10% glycerol, pH 7.4, and a protease inhibitor cocktail (Complete™ (Boehringer)). The resuspended cells were lysed by a ribi French pressure cell. The cell lysate was subjected to differential centrifugation to separate membrane, cytoplasm and insoluble material (Section a). Membrane and cell debris fractions were resuspended in buffers containing non-denaturing detergents at concentrations above the critical micellar concentration (CMC) i.e. the minimal concentration at which detergents begin to form micelles . such as TX-100 (0.1%) (Sigma), CHAPS (1.0%)(Boehringer), deoxycholic acid (0.25%)(Sigma), and NaCl (0.1M).

Solubilisation buffers also contained 50 mM Tris-HCl, 20% glycerol and protease inhibitors (Complete™ (Boehringer)) and were pH 7.4. After resuspending membrane and cell debris pellets in solubilisation buffer they were incubated overnight at 4°C with constant stirring.

2.9 Protein purification techniques

2.9.1 Glutathione-agarose chromatography

This method of affinity purification was performed essentially as described by (Smith and Johnson, 1988). GST-wNBD fusion proteins were partially purified from non-denaturing detergent solubilised membrane and cell debris *E. coli* fractions by the addition of pre-swollen glutathione-agarose beads (Sigma). In general 0.2 ml of beads were added to solubilised fraction obtained from a 1 L cell culture. The glutathione-agarose beads were incubated with the solubilised cell fraction containing GST-wNBD fusion protein at 4°C with gentle rocking for periods ranging from between 2 hrs to overnight. The solution was then passed through a column containing a sintered glass filter at its base, thereby collecting the glutathione-agarose beads with bound fusion protein at the base of the column and unbound proteins and impurities were removed by filtration. The glutathione-agarose beads with bound fusion protein were then washed with 20 volumes of solubilisation buffer (omitting protease inhibitors which could interfered with thrombin digestion) used to solubilise the cell fraction. Samples of the beads were removed for analysis by SDS PAGE and Western blotting. Fusion protein was eluted from the glutathione-agarose beads by incubation with 100 mM reduced glutathione. Typically 0.5 ml of beads were incubated with 1 ml of 100 mM reduced glutathione (reduced glutathione was always prepared fresh in a strongly buffered solution containing the same detergent and NaCl concentration used for solubilisation, 20% glycerol, and 1 M Tris pH 9 was added until the pH rose to pH 7.4). The beads were incubated with 100 mM reduced glutathione for 10 minutes with gentle rocking prior to collecting the supernatant by filtration. This was repeated two or three times resulting in several 1 ml fractions containing partially purified fusion protein samples of

which were then analysed by SDS PAGE and Western Blotting. Samples of fusion protein were then digested with human thrombin (10 units/ml) (Sigma) overnight at 4°C. The extent of digestion was analysed by SDS PAGE and Western blot detection of a change in molecular weight of the fusion protein (~ 75.5 Kd) to a molecular weight of ~ 47.5 Kd representative of the wNBD released from the fusion protein. Protease inhibitors were then added to the digested sample in order to prevent further non-specific thrombin digestion. Samples were then buffer exchanged into the original buffer used for solubilisation of the fusion protein (excepting that the glycerol concentration was decreased to 10%) using a PD-10 buffer exchange column following the instructions of the supplier (Pharmacia), in order to remove glutathione.

2.9.2 Purification of hexa-histidine tagged proteins

This method of protein purification utilising immobilised metal chelate affinity chromatography was based on the method described by (Janknecht et al, 1991) and was used as a secondary purification step subsequent to partial purification of the White nucleotide binding domain (wNBD) by glutathione-agarose chromatography. The metal chelating absorbent resin (Ni-NTA resin) (Quiagin) was added to samples containing $wNBD_{6his}$ (0.2 ml of resin was added per 5 ml protein sample) and incubated at 4°C for 1 hr prior to eluting unbound proteins. Proteins bound to the resin were eluted by incubation with imidazole. The resin was incubated with rocking for 10 mins with generally 1 ml of sample buffer with imidazole. This eluting step was repeated, each time increasing the concentration of imidazole (between 10 mM and 1M). Samples of each eluent were then analysed for the presence of wNBD and other contaminants by SDS PAGE and Western blotting.

2.9.3 Dye-ligand chromatography

This technique was performed essentially as described above for metal-chelate chromatography however resins with immobilised dye molecules were used as the affinity chromatography resin, namely Cibacron Blue 3GA (Sigma) and

Reactive Red 120-agarose (Sigma). The technique is based on one previously described for purifying proteins with a nucleotide binding fold (Thompson et al, 1975). Increasing concentrations of $MgCl_2$ and ATP (1 mM to 50 mM) buffered to pH 7.4 in an appropriate solubilisation buffer (i.e. the buffer used for initial solubilisation and partial purification of GST-wNBD from cell debris or membrane cell fractions) was used to attempt to elute proteins from the resin.

2.9.4 Cation exchange high-performance liquid chromatography

HPLC was carried out on a dual-pump Bio-Rad gradient module fitted with titanium 1/16" tubing. Detection was carried out using a Linear Instruments Uvis-204 ultraviolet/visible absorbance detector. Operation was under the control of a Bio-Rad model 700 Chromatography Data Station. Ion exchange chromatography was performed using a strong cation exchange column, Bio-Gel™ MA7S Cation Exchange Column (Bio-Rad). The column and pumps were pre-equilibrated with buffer to be used for chromatography (10% glycerol, 50 mM Tris-HCl, 1% CHAPS, pH 7.4) prior to loading the sample. Buffers to be used for cation exchange HPLC were filtered prior to use, through 0.5 μM filter paper (Millipore). A linearly increasing NaCl concentration over time was used to elute proteins from the cation exchange column. The elution profile was obtained using absorbance readings at 280 nm and a flow rate of 1 ml/minute. Fractions were collected every minute and samples from each fraction analysed by SDS PAGE and Western Blotting.

2.10 IAsys Biosensor techniques

The protein-peptide interaction analysis experiments were performed using an IAsys auto plus biosensor machine (Fisons Applied Sensor Technology, Cambridge, UK). The cuvettes designed for use in this machine had two wells allowing experiments to be performed in each well to be performed simultaneously.

2.10.1 Immobilisation of peptides to CMD matrix surface of cuvette

This technique involves immobilisation of synthetic biotinylated peptides (synthesised by the Biomolecular Resource Facility, ANU) via interaction with avidin which was immobilised to the carboxy methyl dextran (CMD) matrix surface of the IAsys auto plus cuvette. Coupling of avidin occurs through primary amino groups reacting with N-Hydroxysuccinimide (NHS) in a reaction mediate by 1-ethyl-3-(3-dimethylaminopropyl) carbodiimide (EDC) (see Fig. 6). The instructions supplied by IAsys were followed exactly, as follows. The CMD matrix was first activated by addition of NHS (0.013 g/ml) and EDC (.076 g/ml) to the cuvette which was pre-equilibrated at room temperature with phosphate buffered saline (0.01 M phosphate buffer, 0.0027 M KCl, 0.137 M NaCl, 0.05% Tween 20) (PBS/T). The CMD matrix was activated for 7 mins at room temperature and the unreacted activation mixture was removed and the cuvette washed with PBS/T buffer for 2 minutes. Avidin (50 μg/ml in 10 mM acetate buffer, pH 4.5) was added to the activated cuvette and incubated for 10 mins. The non-coupled avidin was removed and the cuvette washed with PBS/T for 2 mins. 1 M ethanolamine, pH 8.5 was added to the cuvette and incubated for 2 mins. The ethanolamine was removed and the cuvette washed with PBS/T for 5 mins. The synthetic biotinylated peptides were dissolved at a concentration of 50 μg/ml in 10 mM Acetate buffer pH 4.45 (both peptides were soluble in this buffer) and were added to the cuvette whereupon the biotin group binds irreversibly to the avidin immobilised on the CMD matrix surface. Fig. 7 illustrates the IAsys responses recorded during the immobilisation procedure which are indicative of the level of protein immobilised to the CMD surface. This figure shows that the levels of avidin, and subsequently, wild-type or mutant biotinylated peptide immobilised to the cuvette CMD surfaces to an approximately equal degree.

Fig. 6 Chemistry of immobilisation of biomolecules to carboxy methyl dextran

The standard coupling chemistry available for immobilization of biomolecules on carboxy methyl dextran (CMD) coated IAsys sample cells by reaction via N-hydroxysuccinimide (NHS) in a reaction mediated by (1-ethyl-3-(3-dimethylaminopropyl (EDC) as shown in this figure.

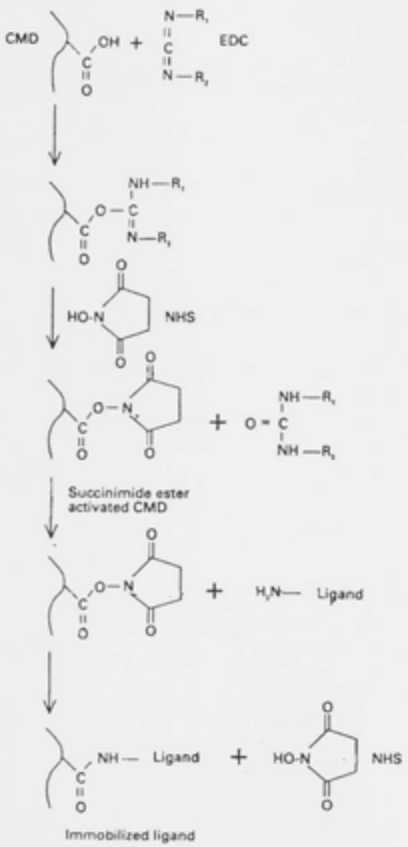

Fig. 7 Immobilisation of synthetic peptides to the avidin-CMD matrix of an IAsys cuvette

This figure shows the profiles obtained from the IAsys biosensor during immobilisation of biotinylated synthetic peptides to avidin which was previously immobilised to the CMD matrix of the cuvette surface. Immobilisations were carried out at the same time, using an IAsys two well cuvette. The same concentrations of avidin, and synthetic peptide (wild type peptide is shown in blue, while the peptide containing a single amino acid alteration is shown in red) were added to each well respectively. Events are numbered as follows:

1. Baseline obtained after immobilisation of avidin. The profiles prior to immobilisation of avidin are not shown here.

2. Buffer wash.

3. 1 M ethanolamine to block unreacted succinimide esters.

4. Buffer wash.

5. Addition of biotinylated peptide.

6. Buffer wash.

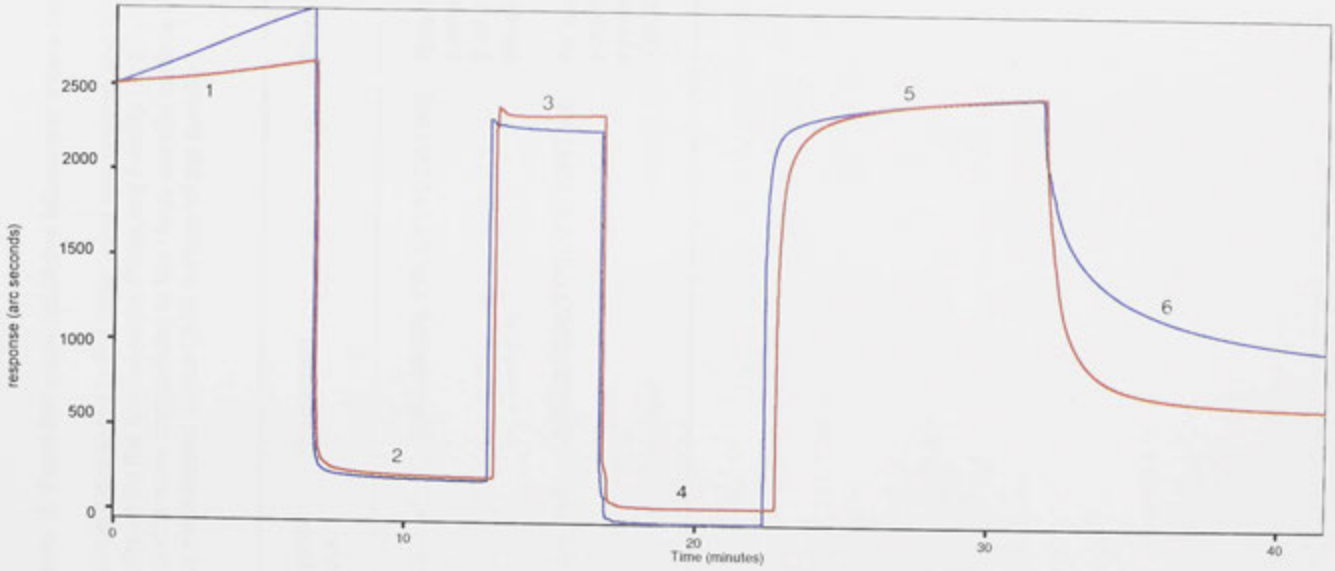
response (arc seconds)
2500
2000
1500
1000
500
0
1
2
3
4
5
6
0
10
20
30
40
Time (minutes)

Table 2 Peptides used for IAsys biosensor interaction analysis

The peptides listed in this table were synthesised and biotinylated at the amino-terminus by the Biomolecular Resource Facility (ANU). The biotinylated peptides were immobilised to the IAsys cuvette surface by way of avidin which was immobilised to the CMD surface of the cuvette.

Peptide name	Sequence	Description
WL2-3 *w*$^{+}$	CMREARSRLYRCDTYFLGKTIAE	Representative of a loop between TM helices 2 and 3 of the predicted White structure
WL2-3 mut	CMREARSRLYRCDTYFLDKTIAE	As above however contains substitution identified in the eye-colour mutant w^{ET87} (G509D)

2.10.2 Peptide-protein interaction experiments

Interaction analysis between peptides immobilised to the IAsys auto plus cuvette were carried out as follows. The buffer used for all experiments i.e. equilibration, sample and wash buffer, was phosphate buffered saline (PBS) (0.01 M phosphate buffer (0.01 M Na_2HPO_4, 1.76 mM KH_2PO_4), 0.137 M NaCl, 0.0027 M KCl, pH 7.4), 0.1% TX-100, 10% glycerol, pH 7.4. All experiments were carried out at 25°C with constant stirring set at 80% of the maximum stirring. The cuvette was pre-equilibrated with buffer and a baseline was obtained prior to addition of experimental samples. Protein samples for interaction analysis containing White nucleotide binding domain (wNBD) were partially purified by over-expression in *E.coli*, solubilised from membrane the *E. coli* fraction using TX-100 and partially purified using glutathione-agarose chromatography (as described in Section 2.8), however PBS was the buffer of choice. Generally a number of consecutive experiments were performed to obtain binding curves at a number of different concentrations. A binding curve was recorded over a period of 5 mins, after which time the cuvette was washed three times with buffer, followed by regeneration with 6 M guanidine HCl, pH 4.4 for 2 mins. This washing and regeneration step was performed subsequent to each experiment.

2.10.3 Analysis of binding data

The interaction between immobilised peptides and wNBD was analysed in real-time by a resonant mirror optical biosensor device (Buckle et al, 1993; Cush et al, 1993) using the IAsys auto plus biosensor machine. The IAsys biosensor was provided with a digital DECpc $450D_2LP$ computer. Data obtained with the biosensor were transferred directly to the Fast Fit computer program (Fison Applied Sensor Technology). This program uses an iterative curve-fitting to derive the observed rate constant and the maximum response at equilibrium due to ligand binding at the particular ligand concentration. The association of a soluble ligand with an immobilised macromolecule when only one binding site

is available for the ligand can be described by the pseudo-first-order equation:

$$R_t = R_0 + E(1 - e^{-K_{obs}t}) \qquad \text{(Cush et al, 1993)}$$

Where:

R_t = the IAsys response at time t in units of arc-seconds

R_0 = the IAsys response at time t = 0 in units of arc-seconds induced by the addition of the ligand solution to the buffer in the cuvette (this represents a net displacement of the biosensor signal, and its value is determined by the Fast Fit program for each binding curve analysed

t = 0 in units of arc-seconds induced by the addition of the ligand solution to the buffer in the cuvette (this represents a net displacement of the biosensor signal, and its value is determined by the Fast Fit program for each binding curve analysed

E = the maximum IAsys response in units of arc-seconds due to bound ligand at equilibrium

K_{obs} = the observed rate constant (termed k_{on} in Fast Fit, i.e. $k_{on} = k_{obs}$) given by:

$$k_{obs} = k_{off} + k_{on}[\text{ligand}] \qquad \text{(George et al, 1995)}$$

2.11 Production of antibodies in rabbits recognising *white* and *scarlet* protein epitopes

2.11.1 Peptides used for raising antibodies

Polyclonal antibodies were raised in New Zealand White rabbits against peptides synthesised by the Biomolecular Resource Facility at the Australian National University. Peptides for injection into rabbits were coupled via a C-terminal cysteine to a lysine core matrix, also called multiple antigen peptide (MAP) system. This system is based on a small immunogenically inert core molecule of radially branched lysine dendrites onto which a number of peptide antigens are anchored (Lu et al, 1991). The sequences of the synthetic peptides are shown in Table. 3.

Table 3 Peptides used for raising anti-White and anti-Scarlet antibodies in rabbits

Epitope	Epitope Code	Peptide sequence
Predicted extracellular loop region between TMs 5 and 6 of the White protein	wECL	RYANEGLLINQWADVEPGEC
N-terminus of the White protein. This is also at the N-terminus of the intracellular ATP binding domain	wNT	MGQEDQELLIRGGSKHPSAC
N-terminus of the scarlet protein. This is also at the N-terminus of the intracellular ATP binding domain	stNT	MSDSDSKRIDVEAPERVEQC

2.11.2 Immunisation of rabbits with Multi-Antigenic Peptides

Blood was collected before injection of peptide as a negative pre-immune serum control. For the first or primary injection, MAP coupled peptide was dissolved in MTPBS (150 mM NaCl, 16 mM Na_2HPO_4, 4 mM NaH_2PO_4, pH 7.4) to 50 μg/ml and was emulsified with an equal volume of Freund's Complete Adjuvant (Freund and McDermott, 1942) (Sigma) by vigorous vortexing for several minutes. The peptide/adjuvant mix was considered thoroughly emulsified when a 20 μl drop of the mix did not disperse when placed onto water. 3 ml of peptide/adjuvant mix was injected sub-cutaneously at several sites along the back of the rabbit. Not less than four weeks after the primary injection the rabbit was injected again in the same way as described for the primary injection, however using Freund's incomplete adjuvant instead of Freund's complete adjuvant. A third injection or boost was given not less than four weeks after the previous boost. Seven days after the respective 2nd and 3rd

boosts, blood was collected from the anaesthetised rabbit, through the marginal ear vein. Serum was separated from whole blood by first allowing a clot to form at 37°C for 1 hr then incubating at 4°C overnight. Serum was transferred to a centrifuge tube and centrifuged for 20 minutes at 4°C to pellet any remaining insoluble material. The serum was stored in aliquots at -20°C.

2.11.3 Detection of anti-peptide polyclonal antibodies in rabbit serum

The appearance of polyclonal antibodies in rabbit serum specific to the MAP-peptides used in immunisation was monitored enzyme-linked immunosorbent assay (ELISA) (Engvall and Perlmann, 1971). ELISAs were performed in 96 well micro-titre plates. Wells were coated with the appropriate peptide by incubating with 50 µl of 50µg/ml peptide in PBS overnight at 4°C or 2 hours at room temperature. A set of control wells were included which were not exposed to MAP-peptide. The wells were washed twice with PBS. Serial dilutions in blocking solution (10% skim milk in PBS) of pre-immune and post-immune serum to be tested were prepared over a range of between 1:10 to 1:1000. 50µl of each dilution was added to the MAP-peptide coated wells or control wells (with no peptide) and incubated for 1 hour at room temperature. Wells were washed twice with PBS. 50µl of secondary anti-rabbit alkaline phosphatase conjugated antibody was then added to each well and incubated for 1 hr at room temperature. Wells were washed twice with PBS then once with pH 9.5 buffer (10mM Diethanolamine, 0.5mM $MgCl_2$, pH 9.5). 50 µl of alkaline phosphatase substrate (1mg/ml p-nitrophenylphoshate in pH 9.5 buffer) was then added per well. The yellow colour was then allowed to develop and the optical density between 405 nm and 630 nm was recorded in a micro-titre plate reader.

2.11.4 Purification of polyclonal anti-peptide antibodies from serum by immunoaffinity purification

Polyclonal antibodies against synthetic MAP-peptides in rabbits were purified by immunoaffinity purification using a SulfoLink® Kit from Pierce. Synthetic

peptides equivalent to those used to produce antibodies (without the coupled MAP) possessing a C-terminal cysteine were covalently immobilised via an iodoacetyl group on a crosslinked agarose support. The preparation of the SulfoLink® immunoaffinity column was carried out as described in detail in the instructions provided with the kit by Pierce. The appropriate serum containing polyclonal antibodies against the respective peptide was diluted 1:10 in PBS. 10 ml of diluted serum was passed through the column 3 times.

2.12 Transmission electron microscopy techniques

2.12.1 Preparation of *Drosophila* eye tissue

The fly eyes were carefully dissected away from the head tissue and primary fixation was performed in 2%/1% paraformaldehyde/glutaraldehyde in 0.1 M sodium cacodylate buffer (pH 7.4) for 1.5 hrs. The tissue was washed for 15 mins three times in 0.1 M sodium cacodylate buffer (pH 7.4). Secondary fixation was performed using 1% osmium tetroxide in 0.1 M sodium cacadylate buffer (pH 7.4) for 30 mins followed by three 15 minute washes in 0.1 M sodium cacodylate buffer (pH 7.4). The tissue was dehydrated through a graded series of ethanol:water (30% to 70%) for 15 mins, three times, followed by two 15 min washes in 70% ethanol prior to infiltration of LR White resin for 1 hr in 50:50 alcohol:resin, followed by overnight incubation with 100% resin, and a further 2 hrs in 100% fresh resin, and for a further 24 hrs in 100% resin at 55°C.

2.12.2 Immuno-gold labelling of *Drosophila* eye tissue and Sf9 cell sections

Thin sections (80 nm) were collected on Formva coated and carbon coated nickel grids (slot grids were used for *Drosophila* eye sections) (ProSciTech) and incubated with primary affinity-purified antibody (either anti-White at 1:10 dilution, or anti-Scarlet at 1:40 dilution) diluted in 0.05 M Tris buffered saline (TBS) pH 7.6 overnight at 4°C. The sections were washed twice for 10 mins in 0.05M TBS pH 7.6. The sections were then washed in TBS containing 1%

bovine serum albumin (BSA) (Fraction V, Boehringer) for 10 mins, followed by incubation with EM-grade goat-anti-rabbit gold conjugated antibody (EM Sciences) (diluted 1:20) in 0.02 M TBS (pH 8.2) containing 1% BSA for 1 hr at room temperature. The sections were washed in TBS containing 1% BSA, then washed a further two times in TBS for 10 mins each wash, prior to washing in distilled water for 10 mins, two times. The sections were post-stained with 2% uranyl acetate for 15 mins and lead citrate for 10 mins and allowed to dry prior to visualisation using a Hitachi H-7000 electron microscope.

2.12.3 Preparation of insoluble material obtained from percoll gradient

A drop of the protein sample was placed on Formva coated and carbon coated grids (ProSciTech) supported on lenspaper, and incubated for 1 minute to adhear to the Formvar coating. The grid was gently swirled in 2% uranyl acetate followed by brief swirling in water to wash excess material off the grid, then placed briefly in 90% ethanol. The grids were then visualised using a Phillips CM10 microscope.

2.12.4 Preparation of Sf9 insect cells for immuno-electron microscopy

Sf9 cells were harvested by centrifugation washed with PBS buffer prior to primary fixation with 1%/3% paraformaldehyde/glutaraldehyde in 0.1 M sodium cacodylate buffer (pH 7.4) for 1.5 hours. The cells were then washed three times for 15 mins each wash with 0.1 M sodium cacodylate buffer (pH 7.4). A secondary fixation was performed as follows: the cells were incubated with 1% osmium tetroxide in 0.1 M sodium cacodylate buffer (pH 7.4) for 45 mins. The cells were then washed 3 times for 15 minutes each wash with 0.1 M sodium cacodylate buffer (pH 7.4). The cells were then dehydrated through a graded series of ethanol:water (30% to 100%) for 15 mins, three times, followed by two 15 min washes in 70% ethanol prior to infiltration of LR White resin for 1 hr in 50:50 alcohol:resin, followed by overnight incubation with 100% resin, and a further 2 hrs in 100% fresh resin, and for a further 24 hrs in 100% resin at 55°C.

2.13 *E. coli* strains

Strain	Genotype	Antibiotic Resistance and growth temp		Source
XL1Blue	recA1, endA1, gyrA96, thi-1, hsdR17, supE44, relA1, lac, [F' proAB, lacI^{q}ZΔM15, Tn10(tet^{R})	Tetracyline	37°C	Stratagene
AN3700	lac(am), pho(am), mal(am), trp(am), supC(ts), rpsL(Strep^{R}), rpoH165-Tn10(Tet^{R})	Streptamycin Tetracyline	30°C	Laboratory strain
AN3701	pESL(Cap^{R})/lacZ(am,trp(am), pho(am), mal(am), trp(am), supC(ts), rpsL(Strep^{R}), rpoH165-Tn10(Tet^{R})	Streptamycin Tetracyclin Chloram-phenicol	30°C	Laboratory strain
AN3828	HfrKL16 PO/45 [lysA(61-62)], dut1, ung1, thi1, relA1, Zbd-279: : Tn10(Tet^{R}, supE44	Tetracyline	37°C	Previously called RZ1032 (Kunkel, 1985)

2.14 Sequence of oligonucleotides

[a]Recognition sequences for restriction by *Eco*RI, *Hind*III, *Bam*HI and *Pst*I endonucleases and underlined.
[b]Binding sites are numbered with +1 as the A of the translation start codon in the published *white* genomic or cDNA as indicated (O'Hare et al, 1984; Pepling and Mount, 1990).
[c] + indicates the coding strand; - indicates the complementary strand.

Primer	Sequence (5' to 3')[a]	Site of 3' base binding[b]	Use	Strand[c]
91-136	AACCGAATTCGTAGGATACTTCG	3102	PCR Exon 2-6 white	+
91-135	GCAGAGAATTCGATGTTGCAATCGC	123	PCR Exon 1 white	-
91-134	TTGAAGCTTGAGTGATTGGGGTG	-81	PCR Exon 1 white	+
91-73	GATGAAGCTTATCTTGTTTTTATTGGCAC	5714	PCR Exon 2-6 white	-
91-72	GATGTGCAGCTAATTTCGCC	5431	Sequencing white	-
91-71	CTTTTACGAGGAGTGGTTCC	4537	Sequencing white	-
91-70	GATCGTGTGCTGACATTTGC	3872	Sequencing white	-
91-69	ACACCTACAAGGCCACCTGG	4467	Sequencing white	+
96-74	CAATGAATTCCGTTTTAACTGAAACAAAC TGG		PCR, st NBD	+
96-74	CATAGCGGCCGCCCGCAACCATTGAATC GTGG		PCR, st NBD	-
91-68	CCACGACATCTGACCTATCG	3824	Sequencing white	+
91-22	GTTCCGGTGCCCTGCAGACGACCCTG	+ 392 cDNA	SMD white	+
96-71	CCTGATCCTCTTGGCCCATTCAGATCTG	+ 16	SDM white	-
96-70	CAGATCTGAATGGGCCAAGAGGATCAGG	-9 of start	SDM white	+
96-62	GATCCGTGATGGTGATGGTGATGT		6 his DNA insert	-
96-61	GATCACATCACCATCACCATCACG		6 his DNA insert	+
94-6	TATAGGATCCATGGGCCAAGAGGATCAG G	1 (cDNA)	PCR, w NBD	+
94-5	TAAGGAATTCTTATAGGAGGAGTGGTTC C	1296 (cDNA)	PCR, w NBD	-

CHAPTER 3

GENETIC AND BIOCHEMICAL ANALYSIS OF *white* MUTANTS

3. GENETIC AND BIOCHEMICAL ANALYSIS OF *white* MUTANTS

3.1 Introduction

The *white* gene has a very long history, dating back to early this century when white eye-colour was among the first mutant traits of *D. melanogaster* to be observed (Morgan, 1910). Since that time the *white*, gene and mutants of this gene, have played a vital role in the development of the field of genetics and this gene has been extensively characterised at the genetic, molecular, and biochemical levels (Hazelrigg, 1987; O'Hare et al, 1984; Sullivan et al, 1979; Sullivan et al, 1980; Sullivan and Sullivan, 1975; Summers et al, 1982; Zachar and Bingham, 1982). Due to the ease of identification of mutant *white* alleles by the change in eye-colour, the gene has provided an important phenotypic marker and has been a useful model system for the study of many phenomena in classical *Drosophila* genetics as well as a number of genetic regulatory mechanisms occurring in higher eucaryotes (Hazelrigg, 1987). The *D. melanogaster* experimental system also provides a powerful tool for producing transgenic flies (via P-element transformation (Rubin and Spradling, 1983)), which can be used to investigate the correlation between mutant eye-colour phenotype and mutations in the *white* gene.

The *white* gene has been used to study the nature of mutations caused by a number of mutagens, including chemicals and x-rays (Pastink et al, 1987; Pastink et al, 1988a; Pastink et al, 1988b). For example, the alkylating agent methyl methanesulfonate (MMS) has been shown to introduce genetic translocations and deletions which significantly alter the structure of the gene. On the other hand N-ethyl-N-nitrosourea (ENU) and ethyl methane sulfonate (EMS), which are also alkylating agents, as well as X-ray induced mutagenesis under the appropriate conditions, have been shown to introduce small alterations and single base changes in the *white* gene, which do not alter the overall structure of the gene (Pastink et al, 1987; Pastink et al, 1988a; Pastink

et al, 1988b). A very large collection of mutant *white* alleles has been built up using these techniques, in addition to many *white* alleles which have arisen spontaneously in laboratory populations. Many of the flies carrying these mutant *white* genes can be obtained from various *Drosophila* stock centres.

Zachar and Bingham, (1982) selected a sample of *white* mutants for molecular characterisation using the Southern blotting technique and comparing restriction fragment maps to the wild-type counterpart gene from Oregon-R or Canton-S (Zachar and Bingham, 1982). These mutants are shown in Table 1 and can be grouped into two categories. Those in one category have major genetic aberrations, such as large insertions of non-*white* DNA or deletions either within the gene or in upstream regulatory elements. These mutations would be assumed to disrupt the coding sequence in a major way or may prevent expression.

The other category of mutant alleles (highlighted with asterisks) were identified as having the same gene structure as their wild-type counterpart strain (Canton-S or Oregon R), and do not harbour any major molecular alterations. An interesting characteristic of this category of *white* alleles is that homozygous flies express an abnormal eye-colour distinguishable from the others in the category where either red and/or brown pigment deposition has been partially reduced to different extents in each of the mutants. This gives an indication that the mutation has not ablated protein assembly and that the level of function of the pigment precursor transporters are different in each of the mutants. Fig. 1 shows a comparison of the eye-colour of some of these mutants which will be further characterised in this chapter.

It has been a major focus of our group to further characterise this category of partially pigmented *white* mutants, which potentially carry point mutations, with a view to gaining insights into regions of the White protein which are important

Table 1. Molecular structure of a sub-set of mutant *white* alleles.

The mutant *white* alleles listed were analysed by Southern Blotting and restriction mapping to determine the cause of the mutant phenotype. All of these mutants were characterised by Zachar and Bingham, 1982, with the exceptions of the w^{101} allele which was produced and characterised by Pastink, 1988, and w^{ET87} which was induced by EMS mutagenesis and identified by our group, (M.M. Green and A.J. Howells, unpublished). Mutants which have retained some level of eye pigmentation and have a normal genetic structure compared to the wild-type counterpart strain (Oregon-R, or Canton-S), are highlighted with an asterisk.

white mutant	Cause of mutation	Genetic structure change
* w^{col}	X-ray	No change (Canton-S)
* w^{cf}	X-ray	No change (Oregon-R)
* $w^{\beta 5a25}$	X-ray	No change (Oregon-R)
* $w^{\beta ex}$	Spontaneous	No change (Canton-S)
* w^{crr}	Spontaneous	No change (Oregon-R)
* w^{bat}	Spontaneous	No change (Canton-S/Oregon-R)
* w^{101}	ENU	No change (M56i Amherst)
* w^{ET87}	EMS	No change (Canton-S)
w^{bf1}	Spontaneous	9.5 kb insertion
w^{a1}	Spontaneous	Copia insertion
* w^{a2}	Spontaneous	No change
* w^{a3}	Spontaneous	No change
w^{a4}	Spontaneous	10 kb insertion
w^{1}	Spontaneous	5.7 kb insertion
w^{e}	Spontaneous	Additional insertions into the w^{1} element
w^{h}	Spontaneous	Additional insertions into the w^{1} element
w^{ch}	Spontaneous	Identical to w^{e}
w^{zm}	Spontaneous	7.5 kb insertion
w^{ap55}	Spontaneous	5.8 kb insertion
w^{Ap1}	Spontaneous	8.6 kb insertion
w^{Ap2}	Spontaneous	0.2 kb deletion
w^{DZL}	Spontaneous	13-14 kb insertion
w^{11E4}	X-ray	Deletion
w^{Ap3}	X-ray	15 kb deletion
w^{Ap4}	X-ray	1.2 kb deletion

Fig. 1 Eye-colour phenotypes of *D. melanogaster* mutant *white* alleles

The top photograph displays eye-colour phenotypes of wild-type flies in comparison to phenotypes generated by null mutations in the *scarlet, brown* and *white* genes: clockwise from left, wild-type eye-colour (w^+), eye-colour when no brown pigment is present (st^-), eye-colour when no red or brown pigments are present (w^-), and when no red pigment is present (bw^-). The four photographs at the bottom of the page represent four of the *D. melanogaster* strains displaying partially pigmented mutant eye-colour phenotypes due to a mutant *white* allele.

w^+, st^-, w^-, bw^-

w^{sat}

w^{cf}

w^{crr}

w^{Et87}

for structure and function. This approach has been used very successfully by our group, in the characterisation of the *white* allele w^{CO2}, which was shown to affect transport of drosopterin (i.e. red pigment) precursors, only when in combination with either of the *brown* alleles bw^{6} or bw^{T50} (Ewart et al, 1994). When a wild-type w^{+} or bw^{+} encoded subunit is present function is restored and the phenotype is normal. The positions of the mutations identified in these mutants all occur at the extracellular end of predicted transmembrane (TM) α helices of the White and Brown proteins in locations appropriate for possible interactions. The w^{CO2} change is within TM 5, and bw^{T50} or bw^{6} within the predicted TM helices 5 and 6 respectively. Since these mutations result in reduced red pigments, leaving brown pigments uncharged, coupled with the predicted role of White/Brown in transport of guanine, it is postulated that TM helix 5 of the White protein and TM helix 5 and 6 of the Brown protein interact in the formation of a guanine specific transporter (Ewart et al, 1994). The putative model resulting from this work is illustrated in Fig. 2. Since brown pigment deposition is not affected in these mutants, the region in White responsible for the substrate (tryptophan) specificity resides in a different and as yet unidentified location. In addition, the mutant w^{Bwx} which is due to a deletion of an isoleucine residue within TM 5 (see Fig. 2) completely knocks out red pigment synthesis without affecting the deposition of brown pigments. This further strengthens the proposal that helix 5 of White is part of the lining of a pore specific for guanine.

The characterisation of the amino acid changes in w^{CO2}, w^{Bwx}, bw^{T50}, bw^{6} as described above gave a very strong indication of the potential of this approach to provide information with respect to the structure and function of the pigment precursor ABC transporters of *D. melanogaster*. Honours and Graduate Diploma students T. Gill and M. Brooker, respectively, have continued this approach and have identified point mutations in the alleles w^{ET87} and w^{101}. Work undertaken to characterise the alleles w^{crr}, w^{cf} and w^{sat} and their effects on pigmentation will be described in this chapter.

Fig. 2. Proposed interaction between transmembrane helices 5 of White and transmembrane helices 5 and 6 of Brown.

This figure is taken from Ewart & Howells, 1998 and represents a model of the physical interactions which occur between the transmembrane helix 5 of White and 5 and 6 of Brown, interpreted from mutant data discussed in the text.

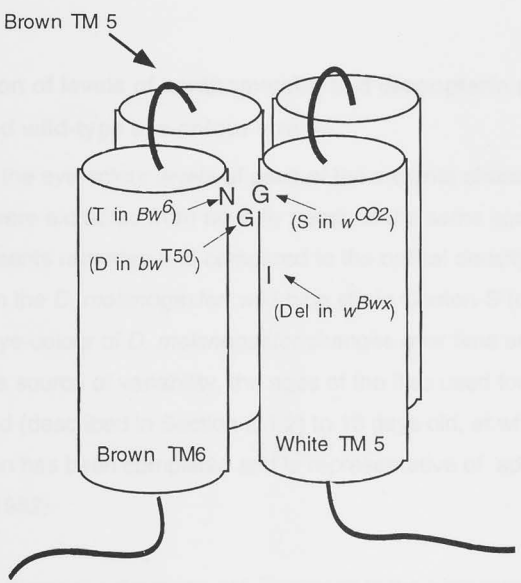

This chapter firstly describes the measurement of the levels of red and brown eye pigments present in flies carrying w^{crr}, w^{cf}, w^{sat} and w^{ET87} in comparison to wild-type eye pigment levels. Secondly, amplification by PCR and sub-cloning of each of the *white* alleles will be described, and the identification of the mutations by sequence analysis will be presented. The significance of the effect of each mutation on pigment levels will be discussed in the context of the current model of the White protein and ABC transporters in general.

3.2 Results

3.2.1 Comparison of levels of xanthommatin and drosopterin pigments in mutant and wild-type eye-colour strains

In order to define the eye-colour levels of each of the mutants chosen for this study, pigments were extracted from adult fly heads of the same age, optical density measurements recorded and compared to the optical density obtained from extracts from the *D. melanogaster* wild-type strain Canton-S (described in Section 2.1.2). Eye-colour of *D. melanogaster* changes over time and in order to standardise this source of variability, the ages of the flies used for extractions were synchronised (described in Section 2.1.2) to 10 days old, at which time pigment deposition has been completed and is representative of adult flies (Summers et al, 1982).

The results of the pigment extractions are illustrated in the histogram in Fig. 3 and expressed as a percentage of the wild-type pigment levels. In all four mutants drosopterin pigments are reduced to less than 30% of wild-type. Xanthommatin levels however are reduced to very low levels in w^{crr} and w^{ET87} mutant flies, while w^{cf} and w^{sat} retain levels of around 60% and 80%, respectively. On the basis of levels of red and brown eye pigments the four mutants can be separated into two groups:

1. both pigments reduced to low levels (w^{crr} and w^{ET87});
2. only red has been reduced to low levels, while brown is reduced only marginally (w^{cf} and w^{sat}).

Fig. 3. Comparison of levels of eye colour pigments xanthommatins (brown pigments) and drosopterins (red pigments) extracted from the compound eyes of flies carrying mutant *white* alleles.

Eye colour pigments were extracted from adult 10 day old flies as described in Chapter 2. Pigment levels are expressed as a percentage of the optical densities obtained for pigment extractions from wild type *D. melanogaster* strain Canton-S. Duplicate values from duplicate extractions were obtained and the mean value plotted in the histogram. The error bars represent the standard error of the mean. Photographs of representative flies containing these alleles are shown in Fig. 1.

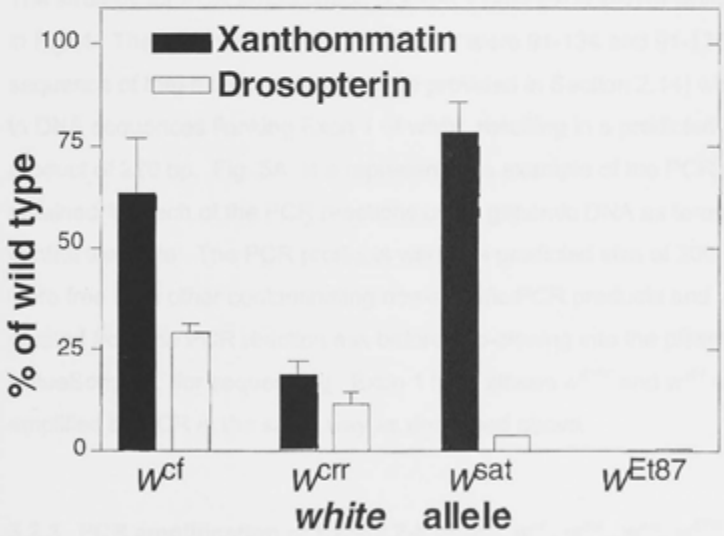

3.2.2 PCR amplification of Exon 1 of w^{crr}, w^{cf}, w^{sat}, w^{col}, w^{ET87}, and w^{101} mutant alleles

The coding regions of the *white* gene were amplified as two PCR fragments: a 220 bp fragment encompassing Exon 1, and a 2.6 Kb fragment encompassing Exons 2-6. This was done to omit the large 3 Kb intron 1 and allow more efficient amplification of the coding regions of the gene (see Fig. 4).

Genomic DNA prepared from mutant *D. melanogaster* strains (as described in Section 2.2.4) was used as template for PCR reactions amplifying Exon 1 of the *white* gene (described in Section 2.2.3). Positive controls were included in which a plasmid harbouring the full *white* gene was used as the DNA template. The strategy for PCR amplification of Exon 1 (and Exon 2-6) of *white* is shown in Fig. 4. The oligonucleotide primers used were 91-134 and 91-135 (the sequence of these oligonucleotides are provided in Section 2.14) which anneal to DNA sequences flanking Exon 1 of *white*, resulting in a predicted PCR product of 220 bp. Fig. 5A is a representative example of the PCR products obtained for each of the PCR reactions using genomic DNA as template, and control template. The PCR products were the predicted size of 200 bp and were free from other contaminating non-specific PCR products and were purified from the PCR reaction mix before sub-cloning into the plasmid vector pBlueScriptSK$^+$ for sequencing. Exon 1 from strains w^{ET87} and w^{101} were amplified by PCR in the same way as described above.

3.2.3 PCR amplification of Exons 2-6 of w^{crr}, w^{cf}, w^{sat}, w^{col}, w^{ET87}, and w^{101} mutant alleles

Exons 2-6 of the *white* gene from the alleles w^{crr}, w^{cf}, w^{sat}, w^{col}, and w^{ET87} were amplified by PCR, using genomic DNA extracted from the mutant *D. melanogaster* strains as described above for Exon 1. For w^{crr} and w^{sat} two sets of oligonucleotide primers were tested, (91-73, 91-136) and (95-51, 91-136). Occasionally the PCR reactions performed were unsuccessful when the

Fig. 4 Strategy for PCR amplification and sequencing of the coding regions of mutant *white* alleles.

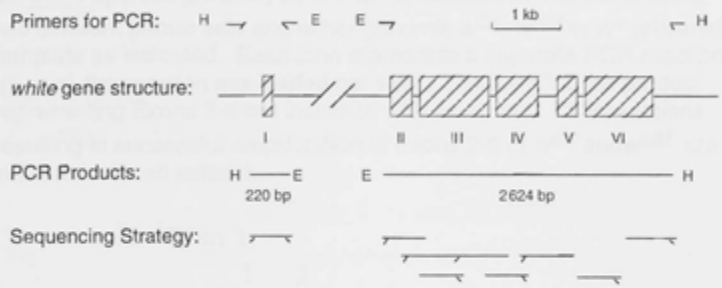

Coding regions of the *white* gene were amplified by PCR as two DNA fragments using genomic DNA prepared from mutant fly strains as template DNA as described in Chapter 2. This PCR strategy omits the large 3 Kb intron 1 of the *white* gene which occurs between Exons 1 and 2 and allowed more efficient amplification of the coding regions of the gene. Exon 1, a 220 bp fragment was amplified using primers 91-134 and 91-135. Exons 2-6, a 2624 bp fragment was amplified using primers 91-136 and 91-73, or 95-51 and 91-136 (the sequences of these oligonucleotides are given in Section 2.12). Two primer sets were used to increase the success rate of amplifying the desired 2.6 Kb fragment in the event that one primer set was not as efficient as the other set (see text). Each primer had a recognition sequence for restriction by either *Eco*RI(E) or *Hind*III(H) incorporated at their 5' ends to allow subsequent cloning of the PCR-generated fragments to pBluescriptSK$^+$ for sequencing.

Fig. 5 PCR Amplification of coding sequences of mutant *white* alleles

A. 0.9% agarose gel analysis of the 220 bp PCR products (highlighted with an arrow) representing Exon 1 of a mutant *white* allele (lane 1) and wild type *white* gene as a positive control (lane 2). A representative PCR product is shown. This result was the same for all of the *white* mutants.

B. 0.9% agarose gel analysis of PCR products from reactions using two different primer sets and either genomic w^{crr}, w^{sat} or w^{+} (plasmid) template as indicated. Each lane represents a separate PCR reaction (5 ul of the reaction mix loaded per well). The 2.6 Kb DNA product representing Exons 2-6 are indicated with an arrow. PCR reactions resulting in successful amplification of Exons 2-6 of w^{crr} and w^{sat} are indicated with an asterisk.

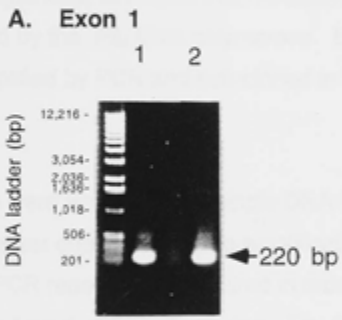

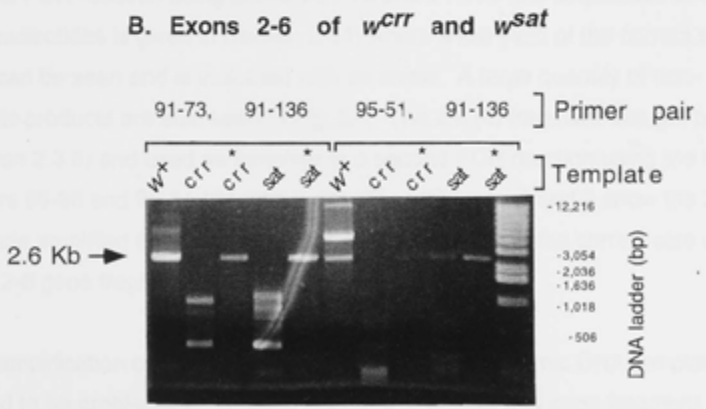

primer pair 91-73 and 91-136 was used. Consequently a second pair of primers was designed (95-51, 91-136). Both of these sets of primers anneal to sequences at the 5' end and 3' ends flanking Exons 2-6 of the *white* gene. The strategy for PCR amplification of Exons 2-6 of the *white* gene is illustrated in Fig. 4. The sequences of these primers are detailed in Section 2.14. Fig. 5B shows the amplified PCR products from duplicate PCR reactions using the different primer sets. The 2.6 Kb amplified DNA fragment is indicated with an arrow. This is the correct size for the Exons 2-6 gene fragment. Lanes highlighted with an asterisk represent successful duplicate PCR amplifications for each of w^{crr} and w^{sat} derived Exons 2-6,which were used for sub-cloning into the plasmid vector pBlueScriptSK^{+}. Independent sub-clones from two separate PCR reactions were sequenced, to ensure that mutations identified were not due to an error introduced by the *Pfu* DNA polymerase. Exons 2-6 of the strains w^{ET87} and w^{101} were amplified by PCR and sub-cloned in the same way as described above.

The w^{cf} Exons 2-6 were amplified as a single DNA fragment as described for w^{sat} and w^{crr}. However due to competing amplification of non-specific products, a second nested PCR reaction was required in order to generate a sufficient quantity of amplified product for sub-cloning. Fig. 6A shows PCR products from the first PCR reaction using primers 91-73 and 91-136 (the sequences of these oligonucleotides is given in Section 2.14) where a low yield of the correct size DNA can be seen and is indicated with an arrow. A large quantity of non-specific products are also seen in Fig. 6A. The 2.6 Kb fragment was gel purified (Section 2.3.6) and used as template in a second PCR reaction using the nested primers 96-96 and 95-51 (Section 2.14). Fig. 6B lanes 1 and 2 show the 2.6 Kb products amplified from duplicate PCR reactions which is the correct size of the Exon 2-6 gene fragment.

PCR amplification of Exon 2-6 of the w^{col} allele from genomic DNA template proved to be problematic. Several attempts to amplify this gene fragment, using different quantities of template DNA, different genomic DNA extractions.

Fig. 6 PCR amplification of Exons 2-6 of the *wcf* allele.

A. Lane 1 represents the products of a primary PCR reaction which amplified a low yield of the 2.6 Kb Ex 2-6 white fragment and a large quantity of non-specific products.

B. The 2.6 Kb product obtained from A. lane 1 was purified and used in a secondary PCR reaction using a nested set of primers (as described in the text), which resulted in a higher yield of the desired product. PCR products from duplicate PCR reactions are shown in lanes 1 and 2.

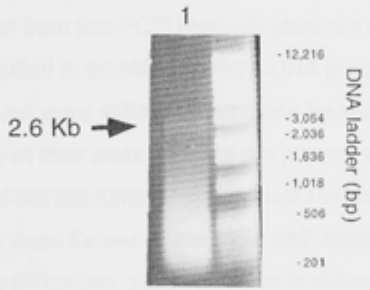

A Primary PCR reaction

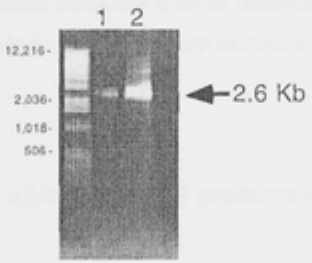

B Secondary PCR reaction

and different annealing temperatures in the PCR reaction were carried out, however no 2.6 Kb product was obtained. To further investigate the possible cause of this problem, a number of separate PCR reactions were carried out using different sets of primers (designed for sequencing the Exon 2-6 region of the *white* gene). These anneal internal to the primers normally used (which anneal to sequences outside the coding regions of Exons 2-6), in an attempt to identify which region of the w^{col} was causing the problem. A variety of results were obtained from this PCR analysis (data not shown). Some of the PCR reactions resulted in amplification of a DNA product of approximately the correct size, but were difficult to subclone because they lacked restriction enzyme sites at their ends (most of the primers were designed for sequencing reactions and did not harbour appropriate restriction enzymes sites for cloning). Most of them were formed in low yield and required further amplification. In view of these difficulties, it was decided to discontinue analysis of this mutant in order to devote time to other parts of the thesis project. This mutant *white* allele has been previously analysed by Southern blotting and was deemed to have a normal restriction map compared to the wild-type counter-part strain (Zachar and Bingham, 1982). The sensitivity of this technique is such that deletions or insertions down to approximately 50 bp can be detected. It is possible that this mutant harbours a small deletion, insertion or rearrangement which was not detected using restriction analysis but which affects the primer binding sites.

3.2.4 Sub-cloning *white* allele PCR products into pBluescriptSK$^+$ plasmid vector

The PCR products were cloned (described in Chapter 2, Section 2.3) by "sticky-end" ligation into the multiple cloning site of the plasmid vector pBluescriptSK$^+$ (described in Chapter 2, Section 2.4.1). The PCR products were purified, digested with *Eco*RI and *Hind*III followed by ligation into the *Eco*RI/*Hind*III site of the multiple cloning site of pBlueScriptSK$^+$. Following transformation, plasmid DNA was isolated from transformed colonies.

Fig. 7A is a representative restriction analysis of the pBSK⁺ constructs harbouring Exon 1 of *white*. It can be seen that *Eco*RI and *Hind*III digests result in the release of the 200 bp Exon 1 *white* gene fragment. Fig. 7B is a restriction analysis of the pBSK⁺ constructs harbouring Exon 2 to 6 derived from w^{crr} and w^{sat} flies. In this case, an *Eco*RI and *Hind*III digest results in the release of a 2.6 Kb fragment which is the predicted size of Exons 2-6 of the *white* gene. Similar results were obtained for w^{ET87} and w^{101} (data not shown).

The DNA fragments separated by agarose gel electrophoresis resulting from *Eco*RI and *Hind*III double digest of two Exon 2-6 w^{cf} sub-clones are shown in Fig. 8A. The digest products are different compared to the other *white* exons 2-6 sub-cloned in that the fragment representing Exon 2-6 is about 2 Kb instead of 2.6 Kb which is the predicted size. The *Eco*RI and *Hind*III digest shown in the set of lanes labelled **1** in Fig. 8A, shows three products of around: 300 bp, 2900 bp, 2300 bp. This restriction pattern suggests that the 2.6 Kb Exon 2-6 DNA fragment has been cleaved into two fragments, of about 300 bp and 2.3 Kb. The *Hind*III digest resulted in a single fragment of around 5.5 Kb, the predicted size of the construct. This suggests that there is a second *Eco*RI site around 300 bp from either the 5' or 3' end of the gene fragment. This is confirmed by the *Eco*RI digestion which yields two products about 2100 and 3200 bp. As will be described in Section 3.2.5, the introduced *Eco*RI site is due to one of the w^{cf} mutations and the restriction map of pBSK⁺Exon 2-6 is as illustrated in Fig. 8B. The set of lanes labelled 2 in Fig. 8A does not show the 300 bp fragment. In this case the cloning of the entire Exon 2-6 must have occurred due to a partial digestion by *Eco*RI prior to ligation into the plasmid vector since the *Eco*RI site is actually present in the sequenced plasmid (Section 3.2.5).

Fig. 7 Restriction analysis of purified plasmid DNA from transformed *E. coli.*

A. A representative pBSK+Exon1 subclone digested with *Eco*RI and *Hind*III resulting in release of the 200bp Exon 1 and 2.9 Kb vector DNA.

B. pBSK+Exon 2-6 subclones of w^{sat} and w^{crr} digested with *Eco*RI and *Hind*III resulting in release of the 2.6 Kb Exon 2-6 DNA fragment and 2.9 Kb vector DNA.

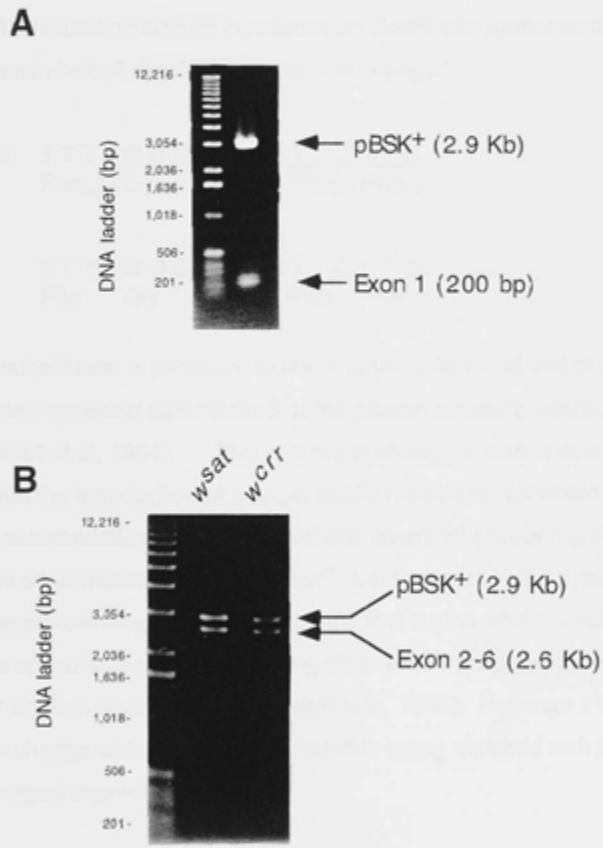

3.2.5 Amino acid substitutions and eye-colour pigment levels in the *white* alleles w^{cf} and w^{sat}: mutations affecting transmembrane spanning helix 5 of the white protein

The sequences obtained from the cloned PCR products were compared to the published wild-type Canton-S strain *white* genomic (O'Hare et al, 1984) and cDNA (Pepling and Mount, 1990) sequences. Two nucleotide changes affecting the amino acid sequence were identified in the w^{cf} **allele**: **G589E**, and **L49R.** The mutation G589E introduces an *Eco*RI site (underlined in the sequence shown below) due to the nucleotide change:

w^{cf} sequence:	T T T	G G C	G A A	T T C	T T C
	Phe_{587}	Gly_{588}	**Glu_{589}**	Phe_{590}	Phe_{590}
Wild-type sequence	T T T	G G C	G G C	T T C	C T G
	Phe	Gly	Gly	Phe	Phe

The G589E substitution is predicted to occur at the C-terminal end of putative transmembrane spanning alpha helix 5 of the protein structure previously modelled (Ewart et al, 1994). This is a major change in amino acid chemistry, with the introduction of a larger acidic residue which would be predicted to substantially alter the physical and chemical environment around this site. The other mutation identified in w^{cf}, L49R occurs in the cytoplasmic domain of the protein near the amino terminus in a region which is not conserved in amino acid sequence among other ABC transporters, nor in homologs of *white* in other species (Zwiebel et al, 1995). However it is not a conservative change with a hydrophobic residue being replaced with the positively charged arginine.

In Section 3.2.1 it was shown that this mutant has low levels of drosopterin (red pigments) (30% of wild-type levels), while xanthommatin (brown pigments) are closer to wild-type levels (65%). This result indicates that the mutation/s identified in w^{cf} reduces the uptake of precursors for drosopterins (red

pigments) while having a lesser effect on the uptake of precursors of xanthommatins (brown pigments).

In the ***w^{sat}* allele**, only one nucleotide change was identified which altered the amino acid sequence and this resulted in the substitution **F590G**. This substitution represents a major change in residue chemistry, with a large hydrophobic residue being replaced by glycine. This residue is adjacent to G589 which has been substituted in the *w^{cf}* allele. F590 is located on the extracellular, C-terminal end of transmembrane helix 5 in the White protein model (Ewart et al, 1994).

It was shown in Section 3.2.1 that flies carrying this mutation have very low levels of drosopterin pigments (5%) while the xanthommatin levels were almost at wild-type levels (80%). This result suggests that the F590G substitution has caused a significant loss of function of the transporter for precursors of drosopterins, while the transporter function for precursors of xanthommatin are near wild-type levels.

3.2.6 Amino acid substitutions of the *white* alleles w^{crr} and *w^{101}*: mutations identified within the cytoplasmic region of the white protein

The coding regions of the *white* allele *w^{crr}*, and *w^{101}* were cloned and sequenced as described for *w^{cf}* and *w^{sat}*. The only alteration to amino acid sequence found in the ***w^{crr}* allele** was the substitution **H298N**. Although this represents a substantial change in residue chemistry with the histidine residue being replaced with uncharged, polar asparagine, it is a relatively conservative substitution with respect to size and hydrogen bonding potential. H298 is located within the region encompassing the ATP binding cassette and the possible significance of this residue will be discussed in Section 3.3. It was shown in Section 3.2.1 that both xanthommatin and drosopterin pigment levels in flies carrying this allele are significantly reduced (10% and 20% respectively). This result suggests that the H298N substitution has caused a significant loss

of function of both transporters for precursors of drosopterins, and xanthommatins.

In the ***w*^{101} allele** two nucleotide changes were identified which altered the amino acid sequence: **G243S and L49R**. Both of these residues are located within the ATP binding domain. G243S alters a highly conserved residue within the ABC transporter "signature sequence" (described in Section 1.5.2 c) and represents a major change with the replacement of the small uncharged glycine residue with a larger residue, (serine) with hydrogen bonding potential. The L49R substitution resides near the amino terminus within the cytoplasmic domain of the protein and is the same change identified in the w^{cf} allele. This suggests that this substitution might be a polymorphism present in the strains from which these mutants were derived. The pigment levels of flies carrying the w^{101} allele could not be assayed because flies were not available (DNA for analyses was obtained from Dr A Pastink). However, the eye phenotype is reported to be partially pigmented (Pastink et al, 1988a) suggesting that there are detectable levels of both eye-colour pigments.

3.2.7 Amino acid substitutions of the *white* allele w^{ET87}: a mutation identified within an intracellular loop region connecting TM helices 2 and 3

In the w^{Et87} allele the only nucleotide change identified resulting in a change in amino acid sequence was the substitution **G509D**. This is a major alteration in residue chemistry with a small glycine residue substituted with a larger charged aspartic acid residue. G509 is located in the transmembrane domain in a predicted intracellular loop between transmembrane helices 2 and 3 of the proposed White protein structure. It was shown in Section 3.2.1 that both pigment levels of flies carrying this allele are dramatically reduced. Drosopterins were 0.2% and xanthommatin was undetectable. This result suggests that the G509D substitution has effectively eliminated the activity of both transporters.

3.3 Discussion

The White protein of *D. melanogaster* is an unusual member of the ABC transporter family in that it is a subunit of two different transporters: the combination of White and Brown subunits makes a drosopterin precursor transporter, while the combination of White and Scarlet subunits forms an xanthommatin precursor transporter. The fact that each of these transporters is required for normal deposition of red or brown pigments, respectively, in *Drosophila* eyes, makes eye-colour phenotype a convenient way to assess the function of *white* alleles (Ewart and Howells, 1998). The five mutant *white* alleles analysed in this work were selected from amongst many of the known *white* alleles on the criterion of partial eye pigmentation. Our expectation was that such non-knockout phenotypes would be caused by mutations changing single base pairs in the gene and so reveal individual amino acids in the White protein with functional roles.

In the work presented here, DNA sequence analysis of the w^{crr}, w^{sat}, w^{cf}, w^{101}* and w^{ET87}* alleles has identified point mutations which alter amino acids in the encoded White protein (see Table 2). The relative positions of these mutations, and other previously reported mutations in relation to the predicted structure of White are shown in Fig. 9. As will be discussed below, five of these changes affect residues in regions or motifs conserved among members of the ABC transporter superfamily. The mutations G243S in w^{101} and H298N, in w^{crr}, affect motifs within the nucleotide binding domain and correlate with reduced function in both of the White-containing transporters. Similarly, the mutation G509D in w^{ET87}, located in the cytoplasmic loop between helices 2 and 3, severely reduces function of both transporters. In contrast however, the mutations G589E and F590G in w^{cf} and w^{sat} respectively, affect function of the White/Brown guanine transporter more than the White/Scarlet tryptophan transporter.

---

* Sequence analysis of these alleles performed by earlier students in this laboratory.

Table 2. Point mutations identified in the *white* genes of *white* alleles of *D. melanogaster*

[a] Mutation sites are numbered with +1 as the A of the translation start codon in the published *white* genomic DNA sequence (O'Hare et al, 1984).
[b] Mutations previously reported in the *white* and *brown* genes (Ewart et al, 1994).

white allele	Mutation in DNA[a]	Amino Acid Change	Predicted location in protein
w^{101}	T to G (3270)	Leu 49 to Arg	N-terminal region of the nucleotide binding domain
	G to A (3925)	Gly 243 to Ser	Nucleotide binding domain
w^{crr}	C to A (4090)	His 298 to Asn	Nucleotide binding domain
w^{cf}	GC to AA (5315)	Gly 589 to Glu	Transmembrane helix 5
	T to G (3270)	Leu 49 to Arg	N-terminal region of the Nucleotide binding domain
w^{sat}	TT to GG (5317)	Phe 590 to Gly	Transmembrane helix 5
w^{Et87}	G to A (5075)	Gly 509 to Asp	Intracellular loop between transmembrane helices 2 & 3
w^{Bwx} [b]	Δ (5290) ATC	Ile 581 deleted	Transmembrane helix 5
w^{CO2} [b]	G to A (5311)	Gly 588 to Ser	Transmembrane helix 5
bw^{6} [b]	A to C (1913)	Asn 638 to Thr	Transmembrane helix 6
bw^{750} [b]	G to A (1733)	Gly 578 to Asp	Transmembrane helix 6

Fig. 9. Model of the topology of the protein products encoded by the *white* and *brown* genes of *D. melanogaster*.

This figure is a simplified representation of the model of Ewart et al, 1994, based on hydropathy analysis, and illustrates the relative positions of the amino acids which are altered due to mutations in the *white* gene described in this work and highlighted in red. These include F590G and L49R (w^{sat}), G589E (w^{cf}) and H298N (w^{crr}). In addition, the previously reported mutations in the *brown* gene (referred to in the text), bw^{T50} (G578D), bw^{6} (N638T), and *white* gene w^{co2} (G588S) are also shown. The mutations w^{101} (L49R and G243S) and w^{Et87} (G509D) identified by Michael Brooker and Tim Gill respectively are also shown. The black vertical rods represent putative membrane spanning alpha-helices; circles represent the ATP binding domains; lines connecting the transmembrane helices represent intra or extra-cellular loop regions.

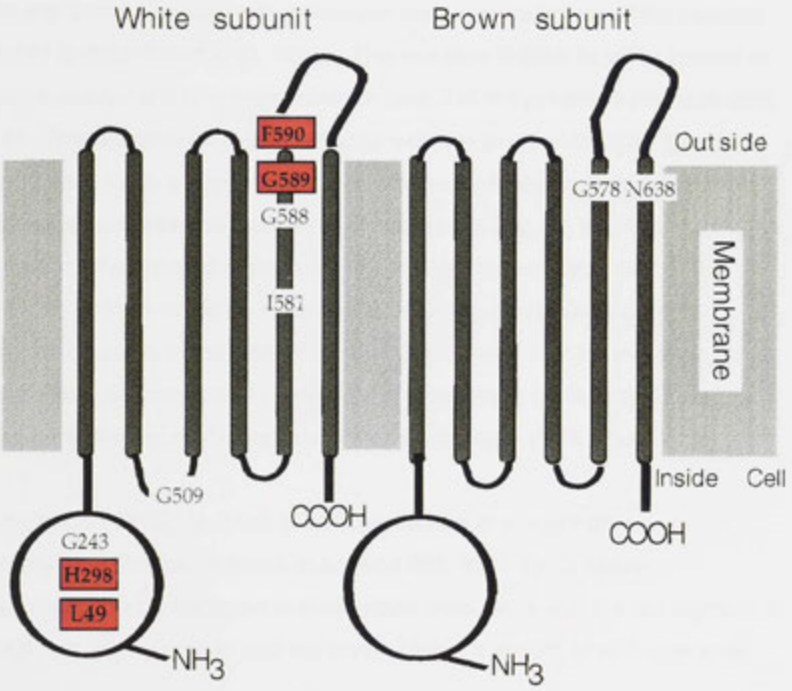

From these and previous (Ewart et al, 1994) results, we conclude: (1) that proper functioning of the nucleotide binding domain of the White subunit is essential to activity of both transporters; and (2) that the transmembrane helix 5 of the White subunit has different roles in the mechanisms of the two different transporters. These mutations are discussed further below in relation to the effects of identical or similar mutations in other ABC transporters.

3.3.1 Mutations identified in the transmembrane domain of the White and Brown proteins

There is a clustering of mutations at the extracellular end of TM α helix 5 of White and these correlate with decreased red pigmentation in all the mutants identified to date (Ewart et al, 1994). The mutation **G589E in w^{cf}** is located at the extra-cellular end of transmembrane helix 5 of the predicted structure (see Fig. 9). This alteration is a major change with the small uncharged glycine being replaced with a larger, acidic side chain which would substantially alter the physical and chemical environment around this site. In addition, the introduction of a charged residue into the hydrophobic environment of the membrane domain would be expected to be energetically unfavourable. Pigmentation levels in the G589E mutant flies indicate that the mutation has a greater effect on transport of precursors of drosopterin (30% of wild-type) compared to transport of precursors for xanthommatin (65% of wild-type).

The mutation **F590G** identified in w^{sat} also results in a major change in chemistry, and like the mutation at position 589, the F590G mutation preferentially affects transport of drosopterin precursors with the red pigment at about 5% of wild-type level and the brown pigment at 80% of wild-type level.

An adjacent mutation (G588S) in the *white* allele w^{CO2} (Ewart et al, 1994) (see Fig. 9) was also shown to decrease transport of drosopterin precursors, but only when combined with either of the *brown* alleles bw^{D} or bw^{T50} which also have amino acid substitutions in the extracellular ends of TM 5 and TM 6 (see

Fig. 9). The w^{CO2} mutation is silent when a wild-type *brown* allele is present as are the two *brown* alleles when w^+ is present. This suggests a functional interaction between the TM 5 of White and TM 5 and 6 of the Brown subunit (Ewart et al, 1994). It is interesting to note the gradation of effect on the presence of red pigments, with w^{CO2}(588) having the least effect, w^{cf} (589) having an intermediate effect while w^{bat} (590) has the greatest effect.

The functional significance of transmembrane helix 5 for transport of precursors of drosopterins was also highlighted by the *white* allele w^{Bwx} (ΔIle581) (Ewart et al, 1994) which completely abolished the presence of red pigments, while brown pigment synthesis was unaffected. It has been proposed that this region is associated with the function of the mouth of a pore specific for guanine and that helix 5 of the *white* encoded subunit interacts with helices 5 and 6 of the *brown* encoded subunit in formation of a guanine specific transporter (Ewart et al, 1994).

Studies on CFTR suggest that the pore through which substrate passes is funnel shaped, and that the narrow end of the funnel is the region associated with specificity and rate of flow of solute (Akabas et al, 1997). It would be interesting to investigate whether this structural feature also applies in the White/Brown transport complex if an appropriate model system was available. The mutant data collected so far suggests that the predicted extracellular ends of TM 5 of White and TM 5 and 6 of Brown may form the gate region of the transport route (Ewart et al, 1994), which would account for the sensitivity of this region to mutations. It is possible that residues in this region interact in a way which imparts a selectivity filter, and in combination with subtle conformational changes propagated by ATP binding/hydrolysis at the ATP binding domains, side groups manoeuvre in a way which opens and closes the transport route, possibly by a slight rotation of one or more of the helices.

The White, Brown and Scarlet systems of *D. melanogaster* appear to be analogous to other ABC transporters. It has been reported in the P-glycoprotein

system, and CFTR that substrate specificity resides in the transmembrane domain. There is biochemical evidence to suggest that transmembrane helices 5, 6, 11 and 12 are involved in drug binding and specificity in P-glycoprotein (Devine et al, 1992; Greenberger, 1993; Hanna et al, 1996; Loo and Clarke, 1994a). In CFTR, residues within and flanking transmembrane helix 6 have been proposed to line the ion conducting channel (Cheung and Akabas, 1996; McDonough et al, 1994; Tabcharani et al, 1993) and influence halide ion specificity (Anderson et al, 1991; Cheung and Akabas, 1997). In particular, the cytoplasmic end of TM 6 is postulated to loop back into the channel thereby affecting electrical resistance and anion selectivity (Cheung and Akabas, 1997). This model is described in more detail in Chapter 1, Section 1.3.

It was recently reported that the White, Scarlet and Brown proteins' closest relatives based on sequence homology of the nucleotide binding domains are the human and mouse homologs of White, and the yeast drug resistance proteins Snq2, Bfr1 and Pdr5 (Croop, 1998). In order to investigate possible homology between the transmembrane domains of these proteins a sequence alignment was performed and the relevant regions of this alignment are shown in Fig. 10. A number of conserved residues were noted, in particular, TM 5 of homologs of White, Scarlet and Brown show marked homology to Pdr5, Bfr1 and Snq2 which is highlighted in Fig. 10A. Of particular interest is the almost 100% conserved Gly which corresponds to the G589E mutation. This observation is suggestive of a conserved structural/functional element. It is noteworthy that guanine and tryptophan are similar to substrates of the MDR family of ABC transporters which generally consist of a series of indole and alkaloid compounds which are mostly cationic yet relatively lipophilic (Beck and Qian, 1992). It has been noted that the transmembrane domains of the P-glycoprotein family and related proteins with similar substrate specificity profiles contain a much higher percentage of aromatic amino acids (Pawagi et al, 1994). Computer modelling of transmembrane α-helices of P-glycoprotein indicate that many of the transmembrane helices can interact in a way which

Fig. 10 Protein sequence alignments of White, Scarlet and Brown proteins with other ABC transporters

The multiple alignments were performed using the CLUSTAL W alignment program (described in Chapter 2, Section 2.6.10). Numbers on the left and right hand side of the protein sub-sequences indicates the amino acid residue number as published in the SwissProt database. Residues boxed in black are present in all (or most) sequences. Boxed residues occur more than once in that position.

A. Alignment of transmembrane helices (TM) 5 of White, Brown and Scarlet from *D. melanogaster* and homologs of White from mouse and humans*, and transmembrane regions of yeast multiple drug resistance proteins. The number of the TM region is indicated on the far right hand side of the respective sequence. The residue altered in the w^{cf} mutant (G589E) is circled.

B. A region of the nucleotide binding domain of White, Scarlet and Brown harbouring a highly conserved histidine residue. The residue altered in the w^{cm} mutant (H298N) is circled. The same histidine is also present in HisP.

C. Alignment of loop regions between transmembrane helices 2 and 3 of White, Brown and Scarlet from *D. melanogaster* and White from mouse and human. The residue altered in the w^{ET87} mutant (G509D) is circled. Loop regions from yeast multiple drug resistance proteins are also shown (the position of the loop is indicated in brackets on the right).

D. Alignment of the ABC transporter "signature sequence" of White, Scarlet, Brown from *D. melanogaster*, human MDR1, human CFTR and HisP. The residue altered in the w^{101} mutant (G243S) is highlighted with a circle.

Abbreviations:
dWhite, dBrown, dScarlet - protein sequences from *D. melanogaster*
mWhite - protein sequence from mouse White
hWhite - protein sequence from human White

---

* Homologs of the *Drosophila* White protein have been identified in mouse and humans (Chen et al, 1996; Croop et al, 1997; Savary et al, 1996), however homologs of Brown and Scarlet have not been identified in mammals. The function of mammalian homologs of White has not yet been determined.

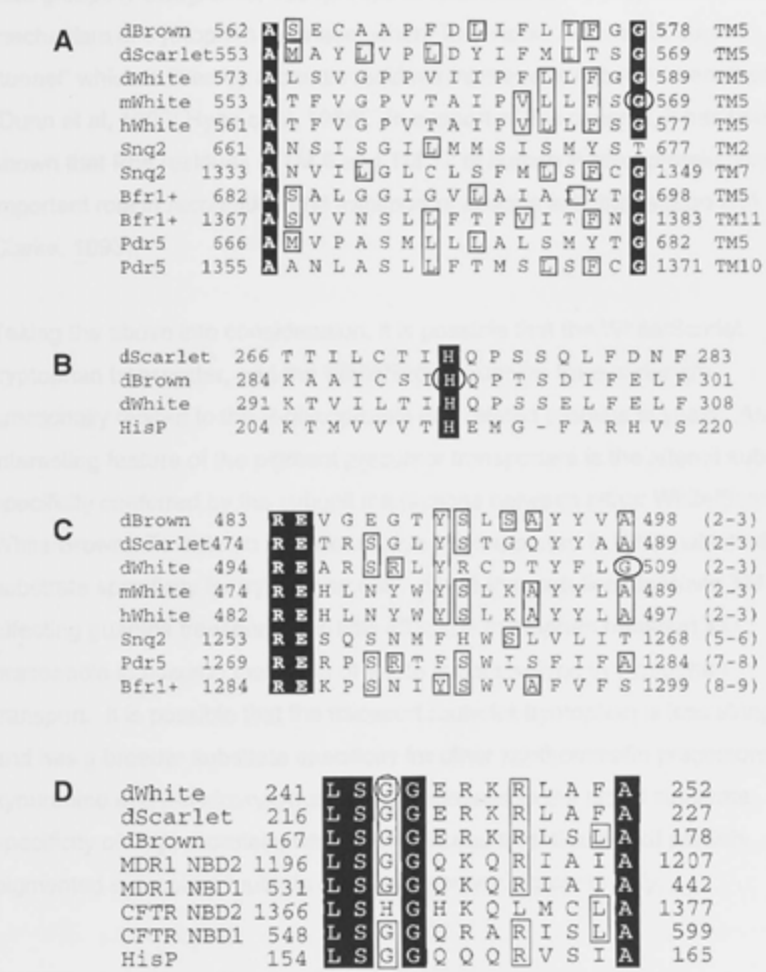
A
dBrown 562 A S E C A A P F D L I F L T F G G 578 TM5
dScarlet 553 A M A Y L V P L D Y I F M T T S G 569 TM5
dWhite 573 A L S V G P P V I I P F L L F G G 589 TM5
mWhite 553 A T F V G P V T A I P V L L F S G 569 TM5
hWhite 561 A T F V G P V T A I P V L L F S G 577 TM5
Snq2 661 A N S I S G I L M M S I S M Y S T 677 TM2
Snq2 1333 A N V I L G L C L S F M L S F C G 1349 TM7
Bfr1+ 682 A S A L G G I G V L A I A Y T G 698 TM5
Bfr1+ 1367 A S V V N S L L F T F V I T F N G 1383 TM11
Pdr5 666 A M V P A S M L L L A L S M Y T G 682 TM5
Pdr5 1355 A A N L A S L L F T M S L S F C G 1371 TM10
B
dScarlet 266 T T I L C T I H Q P S S Q L F D N F 283
dBrown 284 K A A I C S I H Q P T S D I F E L F 301
dWhite 291 K T V I L T I H Q P S S E L F E L F 308
HisP 204 K T M V V V T H E M G - F A R H V S 220
C
dBrown 483 R E V G E G T Y S L S A Y Y V A 498 (2-3)
dScarlet 474 R E T R S G L Y S T G Q Y Y A A 489 (2-3)
dWhite 494 R E A R S S L Y R C D T Y F L C 509 (2-3)
mWhite 474 R E H L N Y W Y S L K A Y Y L A 489 (2-3)
hWhite 482 R E H L N Y W Y S L K A Y Y L A 497 (2-3)
Snq2 1253 R E S Q S N M F H W S L V L I T 1268 (5-6)
Pdr5 1269 R E R P S R T F S W I S F I F A 1284 (7-8)
Bfr1+ 1284 R E K P S N I Y S W V A F V F S 1299 (8-9)
D
dWhite 241 L S G G E R K R L A F A 252
dScarlet 216 L S G G E R K R L A F A 227
dBrown 167 L S G G E R K R L S L A 178
MDR1 NBD2 1196 L S G G Q K Q R I A I A 1207
MDR1 NBD1 531 L S G G Q K Q R I A I A 442
CFTR NBD2 1366 L S H G H K Q L M C L A 1377
CFTR NBD1 548 L S G G Q R A R I S L A 599
HisP 154 L S G G Q Q Q R V S I A 165

facilitates the formation of a pore lined by aromatic side groups and that a typical P-glycoprotein substrate (rhodamine 123) can intercalate between these side groups (Pawagi et al, 1994). Also of relevance is the proposed "tunnelling" mechanism of tryptophan synthase, where free indole diffuses through a "tunnel" which is lined by aromatic residues from one active site to another (Dunn et al, 1990; Hyde et al, 1988). In support of this concept, it has been shown that Phe residues in TM 6 and TM 12 of human P-glycoprotein play an important role in recognition and transport of specific substrates (Loo and Clarke, 1993).

Taking the above into consideration, it is possible that the White/Scarlet tryptophan transporter, and the White/Brown guanine transporter are functionally related to the P-glycoprotein and related proteins in yeast. An interesting feature of the pigment precursor transporters is the altered substrate specificity conferred by the subunit interactions between either White/Scarlet or White/Brown. To date no mutations have been reported in White which affect substrate specificity for tryptophan only. Since the mutations in White TM 5 affecting guanine transport have little effect on tryptophan transport it is reasonable to assume that TM 5 of White is not involved in tryptophan transport. It is possible that the transport route for tryptophan is less stringent, and has a broader substrate specificity for other xanthommatin precursors (i.e. kynurenine and 3-hydroxykynurenine), analogous to the broad substrate specificity of P-glycoprotein, which would account for the lack of partially pigmented eye-colour mutants deficient in brown pigments only.

3.3.2 Mutations identified in the ATP binding domain and intracellular loop regions of the White protein

The mutation identified in w^{crr}, **H298N** changes a histidine residue in the ATP binding domain which is highly conserved in ABC transporters, but not other nucleotide binding proteins. In the sequence alignment in Fig. 10B, H298 of White aligns with H211 of HisP which according to the crystal structure of HisP, is involved in hydrogen bonding to δ-phosphate of ATP via a water molecule

(wat-415) which is adjacent to the water molecule proposed to be the attacking water during ATP hydrolysis (wat-437) (Hung et al, 1998) as illustrated in Fig. 11A. H211 of HisP is positioned near the carboxy-terminal end of β-strand 10 forming part of a β-sheet which is involved in the ATP binding site, as well as an interface between the ATP binding site and the α-helical rich arm II which interacts with the membrane domain (Hung et al, 1998). β-10 is joined to α-6 of arm II via a loop, and the carboxy-terminal end of this helix protrudes from the structure thereby being appropriately placed for interaction with the membrane domain (Hung et al, 1998) (illustrated in Fig. 11B). Significantly, the residue K204 located on a loop arising from the carboxy-terminal end of α-6 has been shown to be accessible from the periplasm and therefore involved in formation of a hydrophilic pore, or a substrate binding site (Baichwal et al, 1993). Taking the above into consideration, it can be imagined that the consequences of the mutation of H298 of White could have a far reaching consequence on the transport function, both with respect to ATP binding and/or hydrolysis and subsequent propagation of conformational changes. It is interesting to note that when the homologous residue in the ATP binding domain of the histidine permease of *S. typhimurium* is mutated to either D, R or Y, transport function is abolished, while ATP binding is not affected (Shyamala et al, 1991). This suggests that this residue is not crucial for ATP binding, however may affect ATP hydrolysis activity (which was not tested in this report) or be involved in conformational changes subsequent to ATP binding (Shyamala et al, 1991) which is consistent with the above interpretation of the crystal structure of HisP. The presence of only very low levels of both eye pigments in flies carrying the w^{pr} allele suggests that the transporters for both drosopterin and xanthommatin pigment precursors have been severely affected despite the presence of either the normal *brown* or *scarlet* encoded subunits. The presence of some pigment however, indicates that replacement of H298 with a residue containing an amine may be tolerated while another residue may not be tolerated.

The H298N mutant results in a more or less equal decrease in transport of both precursors for red and brown pigments indicating that the White nucleotide

Fig. 11 Position of H211 in the crystal structure of HisP

The diagrams shown in this figure have been reproduced from (Hung et al, 1998).

A. Residues of the nucleotide binding fold of His P which interact with ATP. Hydrogen bonds are represented by dashed lines, and aromatic stacking is indicated by vertical lines. The residue H211 which is analogous to H298 of White is highlighted and interacts with the γ phosphate of ATP via a water molecular.

B. Illustration of the secondary structure of HisP derived from the x-ray crystal structure of the HisP dimer (the monomer only is shown). Cylinders and arrows represent α helices and β strands, respectively. ATP is shown in yellow (A, adenine; R, ribose; P, phosphate group). The approximate position of H211 in β strand labelled β10 is indicated by a circle. The connection between β10 and α6 (shown in blue) is also highlighted as a grey line.

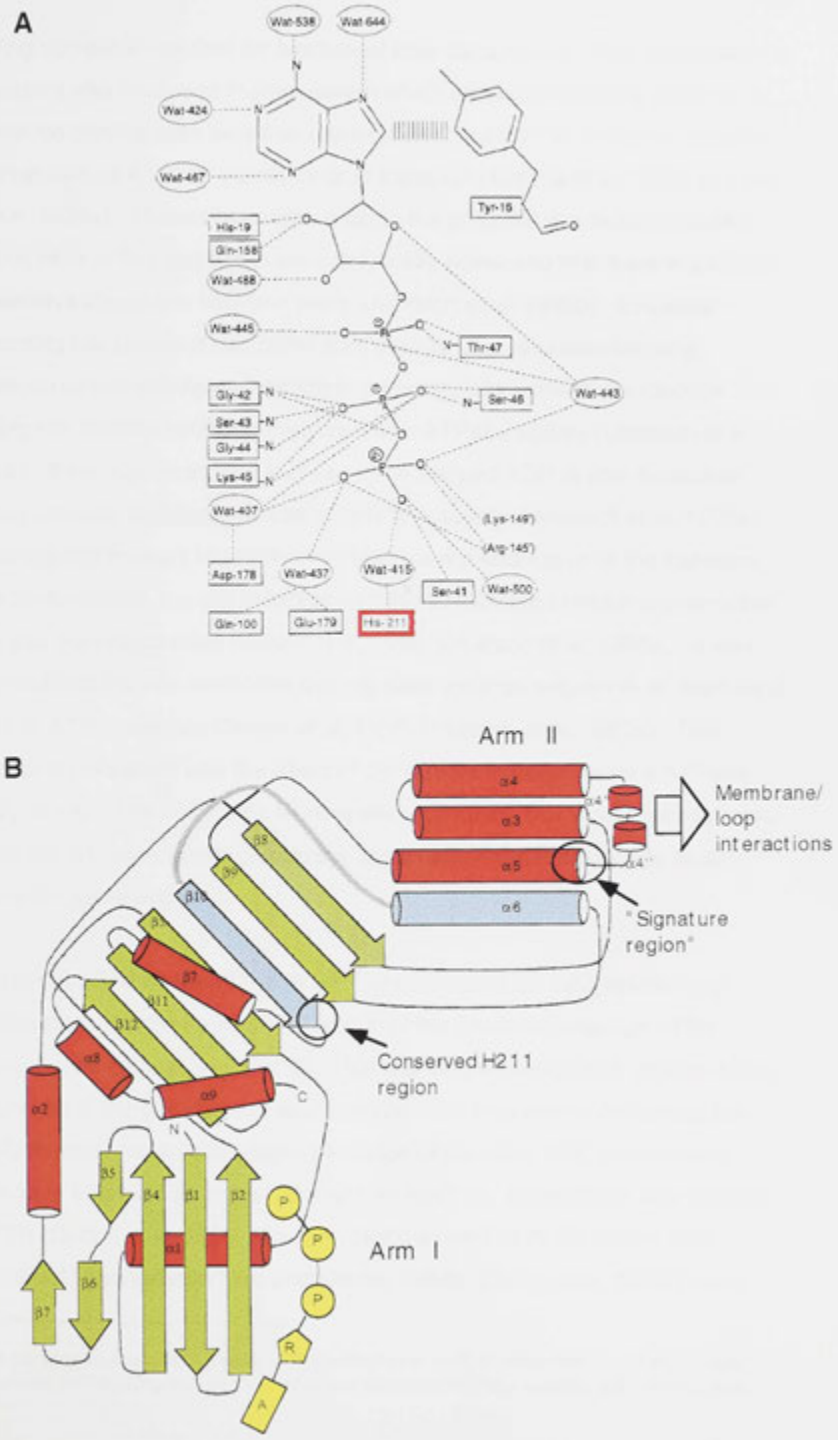
A
Wat-538
Wat 644
Wat-424
Wat-467
Tyr-16
His-19
Gln-158
Wat-488
Wat-445
Thr-47
Gly-42
Ser-43
Gly-44
Lys-45
Ser-46
Wat-443
Wat-437
(Lys-149')
(Arg-145')
Asp-178
Wat-437
Wat-415
Ser-41
Wat-500
Gln-100
Glu-179
His-211
B
Arm II
α4
α3
α5
α6
Membrane/
loop
interactions
"Signature
region"
Conserved H211
region
Arm I
N
C
P
R
A

binding domain is required for function of both transporters. This observation is consistent with studies of P-glycoprotein which show that blocking either of its nucleotide binding sites by either chemical modification[10] or mutation, resulted in elimination of ATPase activity or drug transport (Azzaria et al, 1989; Loo and Clarke, 1995a). These observations led to the proposal that both nucleotide binding sites in P-glycoprotein are catalytically active and that there is a strong cooperative interaction between them (Urbatsch et al, 1995b). Evidence supporting this proposal has come from the use of a vanadate-trapping technique where orthovanadate (Vi) traps nucleotide within the nucleotide binding site thereby inhibiting P-glycoprotein ATPase activity (Urbatsch et al, 1995b). It was demonstrated that vanadate-trapped ADP at one nucleotide binding site was sufficient to block all ATPase activity (Urbatsch et al, 1995a). Assuming that trapped Mg-ADP-Vi complex is representative of the transition state conformation, the site is locked into this conformation which prevents the other site from functioning (Senior et al, 1995; Urbatsch et al, 1995a). It was proposed that the two nucleotide binding sites undergo sequential or alternating cycles of ATP hydrolysis (Senior et al, 1995; Urbatsch et al, 1995a). This proposal is consistent with the effect of the H298N mutation since if ATPase activity at the White nucleotide binding site is reduced, this would consequently reduce the ATPase activity of both the Brown and Scarlet nucleotide binding sites to the same degree.

The mutation **G509D identified in w^{2187}** occurs within the cytoplasmic loop between transmembrane helices 2 and 3 of the predicted structure of the *white*-encoded subunit (see Fig. 9). This is a major change with glycine being replaced by a charged aspartic acid residue. The loop region containing the G509D mutation may be analogous to loops of the other ABC transporters which have been shown to be important for function. Intracellular loop regions of CFTR (Cotten et al, 1996; Xie et al, 1995) as well as ALDp (Shani et al, 1996) and P-glycoprotein (Loo and Clarke, 1994a; Zhang et al, 1995b) have

---

[10] P-gp harbouring a single Cys residue in the Walker A motif of either NBD 1 or NBD 2 were used, where ATP binding was blocked at one or the other NBD by reaction with NEM-Cl (Loo

been reported to be functionally important. In CFTR it has been reported that the intracellular loop between transmembrane spanning helix 4 and 5 is involved in stabilising the full conductance state of the CFTR chloride ion channel (Xie et al, 1995). These authors suggested that the loop interacts with other domains (nucleotide binding folds, R domain and/or other intracellular loops) in CFTR or with other cellular proteins that may be involved in the transition between conductance states. In addition, mutations in intra-cellular loop 4 having a similar effect on CFTR activity as mutations within the nucleotide binding domains have been reported (Cotten et al, 1996) and it was suggested that this loop couples the activity of the nucleotide binding domains to channel gating. In the case of P-glycoprotein it has been demonstrated that mutating glycine residues in cytoplasmic loops between transmembrane helices 2 and 3; 3 and 4; and 5 and 6 alters substrate specificity (Loo and Clarke, 1994a).

In order to investigate possible homology between intrahelical loop regions of White, Scarlet and Brown and the yeast MDR proteins Pdr5, Bfr1 and Snq2 a sequence alignment was performed. The loop between helices 2 and 3 of White, Scarlet and Brown showed marked homology with loop regions of the yeast MDR proteins, in particular a 100% conserved Arg-Glu pair. These aligned sequences are illustrated in Fig. 10C. According to the predicted topology of these proteins, the Bfr1 aligned sequence is analogous to the intracellular loop of White, Brown and Scarlet. However, this region is within predicted extracellular loops of Pdr5 and Snq2. It is speculated that this conserved glutamic acid is inherited from the EAA motif of procaryotes. The observation that the conserved RE motif is found on the extracellular side of the membrane in Pdr5 and Snq2, may be indicative of topological rearrangements which have occurred during evolution.

Certain eucaryotic ABC transporters possess, within an intracellular loop region, a 15 amino acid motif resembling the EAA motif of procaryotic ABC

---

and Clarke, 1995a).

transporters (Shani et al, 1995). Although the loop between transmembrane helices 2 and 3 of the *white* encoded subunit has low similarity to this EAA-like motif, it nevertheless is an important region for function for both the guanine and tryptophan transporter since the w^{E87} G509D substitution causes almost complete knock-out of pigment levels compared to wild-type. This intracellular loop region of the *white*-encoded subunit may perform a similar functional role to loops of other ABC transporters containing the EAA-like motif. In the case of procaryotes, it has been suggested that the EAA motif interacts with the nucleotide binding domain (Kerppola and Ames, 1992; Mourez et al, 1997). It has also been observed that the EAA motif has a higher degree of conservation among procaryotic ABC transporters which transport similar substrates (Saurin et al, 1994b). A role of this motif in correct recognition between ATP binding domains (which are often separate polypeptide chains in procaryotes) and the membrane associated domain of procaryotic ABC transporters has been suggested (Saurin et al, 1994b). It was recently demonstrated (Mourez et al, 1997) that the EAA motifs of the *E. coli* maltose permease forms an important site of interaction between the ATP binding domain of MalK and the transmembrane domains MalF and MalG. In addition Mourez et al, (1997) (Mourez et al, 1997) identified several mutations in the region between the Walker A and B motifs (Mimura et al, 1991) which restored activity in transport deficient EAA motif mutants, providing strong evidence that these regions interact. Particularly interesting are the mutations at positions Val^{149} and Val^{154} which are positioned between the LSGGQ signature sequence and the Walker B motif (Mourez et al, 1997). These observations strongly suggest a structural/functional link between the LSGGQ region and the loop harbouring the EAA motif and this concept is discussed further below with respect to the recently solved structure of the ATP binding domain of the histidine permease of *Salmonella typhimurium* (Hung et al, 1998).

In w^{101}, two mutations were found, **G243S and L49R**. The w^{101} mutation G243S (underlined in the sequence below) is located within the highly conserved signature sequence which has the consensus sequence

"LSGGQXXXRHyXHyA", (Hy is any hydrophobic residue, and X is any residue) and is illustrated in the sequence alignment in Fig. 10D. The replacement of the single hydrogen atom of the side chain of glycine with the polar hydroxyl moiety of serine with hydrogen bonding potential represents a significant alteration in residue size and chemistry. Possible consequences of this change may include a loss of flexibility and/or an alteration of the intramolecular interactions which may occur between this residue and others in the cytoplasmic domain. Mutations in the signature motif have been shown to adversely influence function in several systems. In the histidine permease of *Salmonella typhimurium* the mutation S155F (the 2nd residue of the motif) decreased histidine transport to 6% of wild-type, while ATP binding function was unchanged (Shyamala et al, 1991). In the STE6 alpha-factor transporter the mutations S507R, S507I, and S507N (the 2nd residue of the motif) as well as G509D and G509S (the 4th residue of the motif) were reported to cause severe defects in alpha-factor transport without affecting the level of expression or localisation of the protein (Browne et al, 1996). However, the analogous residues in human P-glycoprotein (S532R and G534D) result in very low expression levels, while K536Q altered the substrate specificity increasing resistance to colchicine of CHO cells containing the mutant gene (Hoof et al, 1994). On the other hand, it has been reported that mutations in this region of human P-glycoprotein eliminate expression (L531R, G534V) or eliminate the ATPase activity (G534D, I541R, R538M) and it was concluded that the ABC-signature region is essential for MDR1 protein stability and function, but alterations in this motif do not modulate P-glycoprotein-drug interactions directly (Bakos et al, 1997). In human CFTR S549R (Kerem et al, 1990) (the 2nd residue of the motif) and G551D (Cutting et al, 1990) (the 4th residue of the motif) drastically reduces function causing severe cystic fibrosis. On the other hand the mutation R553Q (the 6th residue of the motif) partially corrects cystic fibrosis (Dörk et al, 1991) in a patient carrying both ΔF508 (which causes severe cystic fibrosis) and R553Q. Similarly, restoration of α-peptide transport in a STE6-ΔF508 CFTR chimera in yeast was achieved by the mutation R553Q and showed that the R553Q mutation partially corrected the processing and

channel defects caused by the ΔF508 mutation (Teem et al, 1993). It was suggested that the region containing the ΔF508 mutation and the signature sequence interact (Teem et al, 1993). An involvement of the Q in the LSGGQ motif in the mechanism of ATP hydrolysis was proposed[11] when it was reported that mutation of the Q in CFTR NBD1 and the analogous residue in NBD 2 altered the closed and open states of the CFTR chloride channel (controlled by ATP hydrolysis) in a way which correlated with the hypothesis that the Q in the LSGGQ motif plays a role in the mechanism of ATP hydrolysis at the NBDs. The crystal structure of HisP rules out a direct mechanistic role of this residue in the ATPase reaction, nevertheless this and other mutant data discussed above highlights an important structural and functional connection between ATP binding/hydrolysis, the signature sequence and transport or channel function.

The signature motif in the crystal structure of the ATP binding subunit of the histidine permease of *Salmonella typhimurium* forms the first half of an alpha helix (α5) within a region of the protein designated arm II and which interacts with the membrane domains HisQ and HisM (Hung et al, 1998). According to this structure only the residues LSGGQ (residues 154 to 158 in HisP) are partially exposed to the cytoplasmic side of the protein (Hung et al, 1998). A role in the structural integrity of the folded HisP molecule was suggested (Hung et al, 1998). It is interesting to note that the α5 helix of the HisP crystal structure is mostly buried between the α helices of arm II of the protein, however it is physically connected via a loop to the β strand harbouring the highly conserved aspartic acid believed to be involved in the co-ordination of Mg^{2+} during ATP binding and hydrolysis (Hung et al, 1998). Conformational changes which occur upon ATP binding and/or hydrolysis may well be propagated via this connection to arm II proposed to interact with the membrane domains HisQ and HisM (Hung et al, 1998).

---

[11] This proposal was based on possible homology between LSGGQ motif and the DX[G/A]GQ motif of GTPases. The Q in this motif is involved in the mechanism of GTP hydrolysis (Bourne et al, 1991).

3.4 Conclusion

Analysis of mutant *white* and *brown* alleles from *D. melanogaster* flies with partial eye pigmentation has revealed a number of amino acid residues with signficant roles in the structure and function of this ABC transporter. A mutational hot spot has been identified at the extracellular end of TM helices 5 of White, and 5 & 6 of Brown which is involved in substrate specificity as well as function. Mutations identified within the nucleotide binding domain and intracellular loop region of White have been shown to decrease transport of both eye-colour pigments consistent with the concept that these regions of the White protein are essential for transport by both pigment precursor transporters. An interpretation of the accumulated mutant data previously published and the data presented in this chapter, has been presented and is consistent with the previous model (Ewart et al, 1994). A more detailed model for the involvement of particular residues in the gating mechanism for the transport of guanine will be described in Chapter 7.

It has not been shown definitively in this work that the mutant proteins assemble correctly in the membrane. However, since:

i) each mutation has a different effect on pigmentation;
ii) there is a consistency of the effects (residues in close proximity have similar effects); and
iii) the regions identified are also critical in other transporter systems;

it is reasonable to conclude that any decrease in function is unlikely to be a result of decreased protein assembly efficiency. This is particular evident in the transmembrane mutants which affect drosopterin levels only. If the mutations at any of these sites caused reduced assembly, this presumably would alter assembly of both transporters and pigment levels would be reduced to an equal extent. Nevertheless, direct evidence on assembly would strengthen these arguments. Analysis of eye tissue by immuno-electron

microscopy, described in Chapter 7 would be a useful technique for investigating this issue further.

The mutations identified in this work provide an excellent starting point for further investigation of the mechanism of transport, substrate specificity, and the ATP binding/hydrolysis function, once the model systems in Chapters 5 and 6 are developed to their full potential. In addition, the transposable element (P-element) transformation system available in *Drosophila*, provides a powerful technique for production of transgenic flies conaining site-directed mutations, and could be used to confirm the phenotypic effects of these mutations in the intact fly.

CHAPTER 4

PRODUCTION OF POLYCLONAL ANTIBODIES TO THE WHITE AND SCARLET PROTEINS OF *Drosophila melanogaster*

4. PRODUCTION OF POLYCLONAL ANTIBODIES TO THE WHITE AND SCARLET PROTEINS OF *D. melanogaster*

4.1 Introduction

This chapter describes the production of polyclonal antibodies that recognise specific epitopes of the White and Scarlet proteins of *D. melanogaster*. These antibodies provide a means of detecting White and Scarlet, not only in the heterologous expression systems described in Chapters 5 and 6, but also for the sub-cellular localisation of White and Scarlet in *Drosophila* eye tissue described in Chapter 7. Polyclonal antibodies were raised in rabbits against synthetic peptides corresponding to amino acid sub-sequences of White and Scarlet (described below). An overview of the method used to effectively induce production of antibodies against the synthetic peptides is also described.

4.2 Methods

4.2.1 Selection of antigenic sites

Synthetic peptides representing sub-sequences of White and Scarlet protein (shown in Table 1) were synthesised by the Biomolecular Resource Facility (ANU). The amino terminal region of White and Scarlet were considered to be feasible first choices since these regions are predicted to be accessible in the native folded state of the proteins, are relatively hydrophilic and have a degree of antigenicity as predicted by computer analysis (see Fig. 1). It was envisaged that antibodies raised against this region of both White and Scarlet would be useful both for SDS PAGE analysis of the denatured protein, in addition to labelling the protein in the native folded state. For the White protein, a second antigenic peptide was chosen, corresponding to a region predicted to comprise an extracellular loop between transmembrane spanning regions 5 and 6 (see Fig. 2), in order to obtain antigenic determinants at both extracellular and

Table 1 Peptides used for polyclonal antibody production

Location	Name	Peptide sequence
Predicted extracellular loop region between TMs 5 and 6 of the White protein	wECL	RYANEGLLINQWADVEPGEC
Amino terminus of the White protein.	wNT	MGQEDQELLIRGGSKHPSAC
Amino terminus of the Scarlet protein.	stNT	MSDSDSKRIDVEAPERVEQC

Fig. 1 Analysis of hydrophilicity and antigenicity of peptides chosen for the raising of antibodies

The hydrophilic nature of the peptides representing protein sub-sequences of White and Scarlet was analysed using the MacVector protein analysis software as described in Chapter 2, Section 2.6.10.

The hydrophilicity plots are based on the Kyte-Doolittle scale (Kyte and Doolittle, 1982), originally used for hydrophobicity profiles. This figure illustrates hydrophilicity by the reversal of the sign. The values are assigned using a combination of the water-vapour transfer free energies for amino acid side chains and the preference of amino acid side chains for the interior or exterior environments. The window size of 7 is useful in locating small hydrophilic regions that may protrude from the protein surface and thus provide a potential antigenic site. Values above the axis denote hydrophilic regions which may be exposed on the outside of the molecule; values below the axis indicate hydrophobic regions which tend to be buried inside the molecular or inside other hydrophobic environments such as membranes.

The antigenic index profile is designed to locate possible exposed surface peaks of a protein which are potential antigenic sites (Jameson and Wolf, 1988). This analysis combines information from hydrophilicity, surface probability, backbone flexibility predictions along with secondary structure predictions of Chou-Fasman (Chou and Fasman, 1978) and Robson-Garnier (Garnier et al, 1978; Robson and Suzuki, 1976) in order to produce a composite prediction of the surface contour of a protein. Regions that plot above the graph axis are predicted to be exposed at the protein's surface.

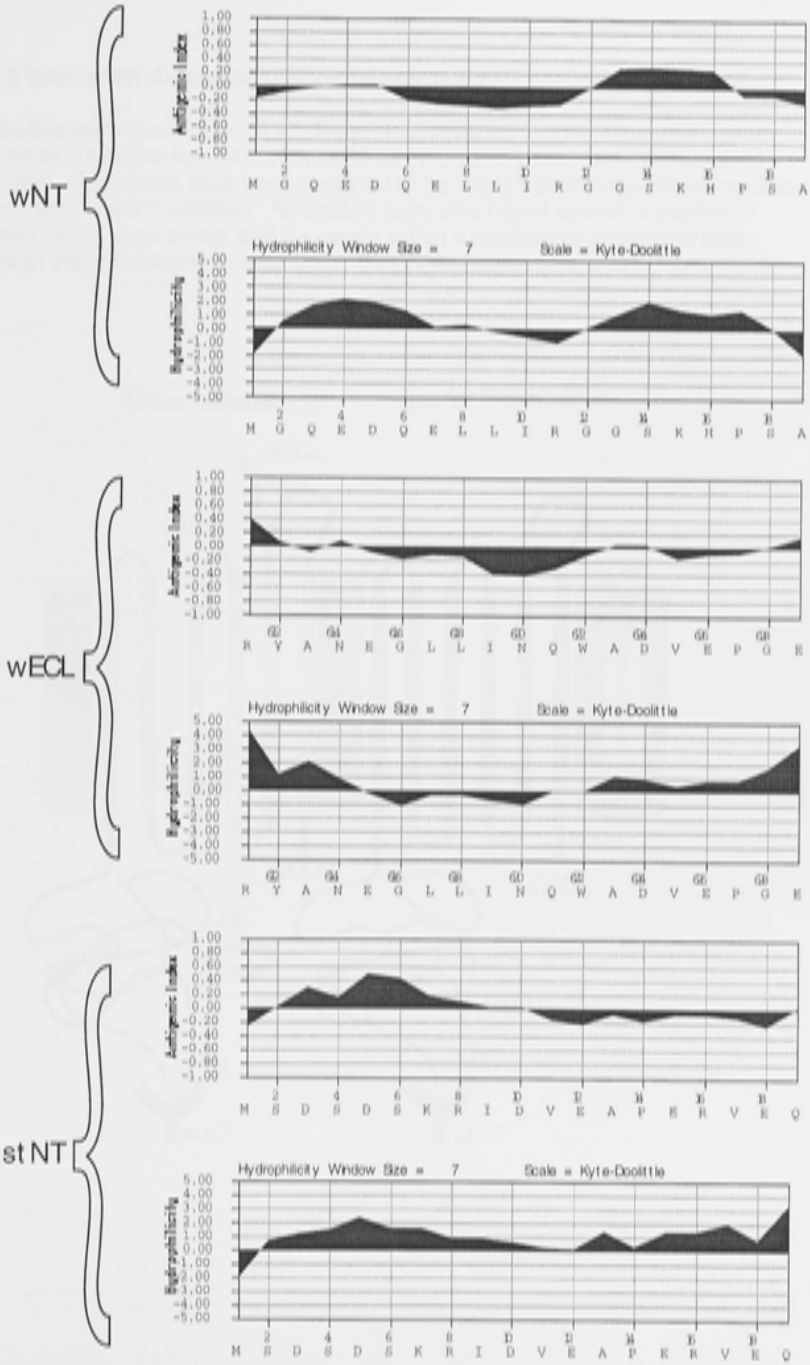
wNT
Antigenic Index
Hydrophilicity Window Size = 7
Scale = Kyte-Doolittle
Hydrophilicity
M G Q E D Q E L L I R G G S K H P S A
wECL
R Y A N E G L L I N Q W A D V E P G E
stNT
M S D S D S K R I D V E A P E R V E Q

Fig. 2 Sites of White and Scarlet protein targeted for antibody production

Antibodies were raised against synthetic MAP-peptides representing amino acid regions at the amino terminus of both White (shown in green) and Scarlet (shown in purple). Both these sites were predicted to be located at an intracellular location as indicated in the illustration. Antibodies were also raised against a peptide corresponding to an amino acid sequence within a predicted extracellular loop between transmembrane helices 5 and 6 of White, which is shown in blue.

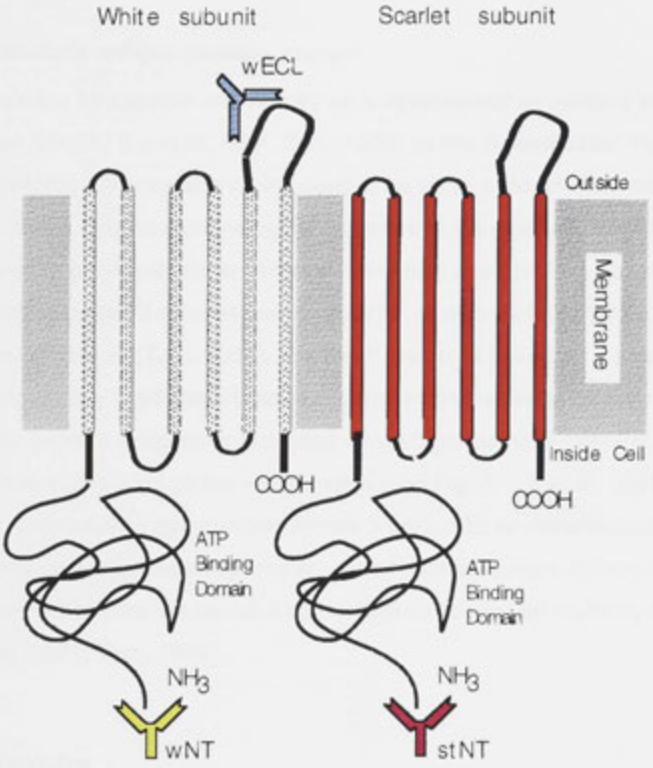

intracellular sides of the membrane. It was considered necessary to obtain such an antibody, recognising an extracellular epitope, to enable plasma membrane localisation of White to be assessed after heterologous expression in insect cells. This predicted loop region harbours two potential glycosylation motifs. The peptide sequence chosen for antibody production does not encompass either of these motifs in order to avoid the potential inhibition of antibody binding to the antigenic site by sugar residues.

4.2.2 Multiple antigen peptide system

The peptides for injection into rabbits were synthesised as multiple antigen peptides (MAPS) (Lu et al, 1991; Tam, 1988) by the Biomolecular Resource Facility (ANU). This system is proposed to be a more reliable and efficient means of inducing an immunological response to the synthetic peptide, compared to previously described and commonly used protein-carrier methods which utilise proteins such as serum albumin, or keyhole limpet hemocyanine as a protein carrier (Tam, 1988). The MAP system is based on a small immunogenically inert core of radially branched lysine dendrites onto which the synthetic peptide antigens are coupled via carboxy-terminal cysteine residues to chloroacetyl groups on the lysine matrix (see Fig. 3) (Lu et al, 1991; Tam, 1988). The resulting macromolecule has a unique three-dimensional configuration which has a high molar ratio of peptide antigen to core molecule and does not require the use of a carrier protein to elicit an antibody response (Lu et al, 1991; Tam, 1988).

4.3 Results

4.3.1 Detection of anti-peptide antibodies in rabbit serum by ELISA

Two rabbits were injected with each synthetic MAP-peptide (wNT, stNT, wECL) as described in Chapter 2, Section 2.11. Blood was taken from each rabbit prior to the first injection to provide a pre-immune negative control. Blood was collected seven days post-injection which corresponds to the approximate time

Fig. 3 Multiple antigen peptide

Diagrammatic representation of synthetic peptides anchored to a poly-lysine core matrix forming a multiple antigen peptide (MAP). The C-terminal cysteine of the antigenic peptide were conjugated to the lysine core matrix by reaction with chloroacetyl groups as described previously (Lu, 1991).

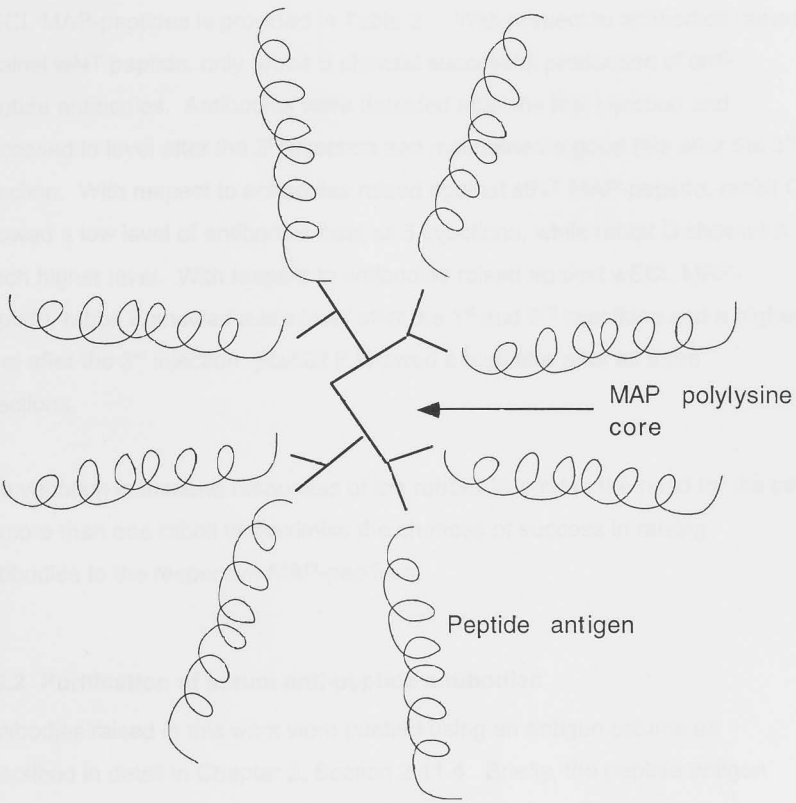

the antibody titre would be at its highest. Serum was separated from whole blood and serially diluted. The presence of anti-peptide antibodies were detected by ELISA as described in Chapter 2, Section 2.11.3.

A summary of the ELISA results for antibodies raised against wNT, stNT and wECL MAP-peptides is provided in Table 2. With respect to antibodies raised against wNT peptide, only rabbit B showed successful production of anti-peptide antibodies. Antibodies were detected after the first injection and increased in level after the 2nd injection and maintained a good titre after the 3rd injection. With respect to antibodies raised against stNT MAP-peptide, rabbit C showed a low level of antibodies from all 3 injections, while rabbit D showed a much higher level. With respect to antibodies raised against wECL MAP-peptide, rabbit E showed a low level after the 1st and 2nd injections and a higher level after the 3rd injection. Rabbit F showed a high titre after all three injections.

The variation in immune responses of the rabbits illustrates the need for the use of more than one rabbit to maximise the chances of success in raising antibodies to the respective MAP-peptides.

4.3.2 Purification of serum anti-peptide antibodies

Antibodies raised in this work were purified using an antigen column as described in detail in Chapter 2, Section 2.11.4. Briefly, the peptide antigen was coupled via a carboxy terminal cysteine residue to an immobilised iodoacetyl group on a crosslinked agarose support. Serum containing the highest levels of anti-peptide antibodies were diluted 1:10 in PBS and applied to the antigen column during which time the anti-peptide antibodies bind to the antigen column. The column was washed with buffer prior to eluting the anti-peptide antibody at high pH and also at low pH. 1ml fractions were collected and screened by dot blot for the presence of antibody and to determine which fractions contained the highest concentration of antibodies. Antibody containing fractions were pooled and dialysed against PBS. The purified

Table 2 Detection of serum antibodies raised against synthetic peptides

Antibodies were raised against synthetic MAP conjugated peptides in rabbits as described in Chapter 2, Section 2.11. Two rabbits were injected with the same MAP-peptide and blood was collected seven days post injection and the serum was serially diluted and screened by ELISA assay against the respective synthetic peptide used for injection. The presence of antibodies was detected by way of a colour reaction with the use of a secondary anti-rabbit alkaline phosphatase conjugated antibody. The table represents the relative level of antibodies in pre-immune serum (PI) which was taken prior to injection and after the first, second and third boosts. The strength of the colour reaction of alkaline phosphatase is indicated using several ticks for a strong reaction, one tick for a weak colour reaction and a dash for no colour reaction.

Peptide	Rabbit	Boost	Serum Dilution			
			10^{-1}	10^{-2}	10^{-3}	10^{-4}
wNT	A	PI	-	-	-	-
		1	-	-	-	-
		2	-	-	-	-
		3	-	-	-	-
	B	PI	-	-	-	-
		1	✓	✓✓	✓	-
		2	✓✓	✓✓✓	✓	-
		3	✓✓✓	✓✓✓	✓	-
stNT	C	PI	-	-	-	-
		1	✓	-	-	-
		2	✓	-	-	-
		3	✓	-	-	-
	D	PI	-	-	-	-
		1	✓	✓✓	-	-
		2	✓✓✓	✓✓	-	-
		3	✓✓✓	✓✓	-	-
wECL	E	PI	-	-	-	-
		1	✓	-	-	-
		2	✓	-	-	-
		3	✓	✓✓✓	✓	-
	F	PI	-	-	-	-
		1	✓	✓✓	✓	-
		2	✓✓	✓✓✓	✓	-
		3	✓✓	✓✓✓	✓	-

antibodies were then tested for specificity by dot blot against peptide antigen, and by Western blot analysis using Sf9 cells expressing White and Scarlet protein, uninfected cells, and cells infected with a control recombinant baculovirus which does not harbour *white* or *scarlet* cDNA (data not shown). The Western blot analysis of Sf9 cell lysates (Fig. 4) shows that the major immunoreactive bands correspond to the predicted molecular weight of the White protein (75.6 kDa) where wNT or wECL antibody was used, and the Scarlet protein (74.5 kDa) where the stNT was used. Immuno-reactive bands were not observed in either the uninfected or control virus infected cells. This indicates that all three purified antibodies are highly specific for White and Scarlet proteins.

Specificity of wNT and stNT antibodies was also tested using an *E. coli* expression system (described in Chapter 6). Three groups of cells were prepared for SDS PAGE, and Western blot analysis:

A Cells which do not express White or Scarlet (the background *E. coli* strain)
B Cells which express the White nucleotide binding domain
C Cells which express the Scarlet nucleotide binding domain

Proteins from these three groups of cells were separated by SDS PAGE followed by Western blot analysis testing both crude antiserum and purified antibody (Fig. 5). It can be seen from Fig. 5 that prior to purification of the antibodies, a large amount of non-specific binding was observed. However, where anti-wNT was used (Fig. 5A, lane 2), a distinctive and unique immunoreactive band is seen at approximately 72 kDa, in the lane representing cells expressing the GST-White nucleotide binding domain fusion protein (GST-wNBD) but not in the control lanes. This corresponds very well to the predicted molecular weight of the fusion protein (72 kDa). Bands corresponding to low molecular weight proteins were also observed, presumably indicative of proteolysis of the GST-wNBD fusion protein. Similarly, a distinctive and unique immunoreactive band is seen in the lane representing cells expressing the GST-Scarlet nucleotide binding domain (GST-StNBD), where anti-stNT antibody was used (Fig. 5C, lane 3). This immunoreactive band is smaller (in the vicinity of 55

Fig. 4 Western blot analysis of specificity of anti-White and anti-Scarlet antibodies in a heterologous Sf9 expression system

A Baculovirus based expression system (described in Chapter 5) was used to analyse the specificity of antibodies raised against synthetic peptides. Sf9 cells were infected with recombinant Baculovirus harbouring both *white* and *scarlet* cDNAs, harvested 30 hours post infection and cell proteins were separated by SDS PAGE and analysed by Western blot (indicated on the blots by W/S) using the purified antibody as indicated. Immunoreactive protein bands were detected by secondary antibody conjugated with alkaline phosphatase. Control cells included uninfected cells, as well as a control Baculovirus infected cells (indicated by Control Inf) which do not harbour *white* or *scarlet* cDNA.

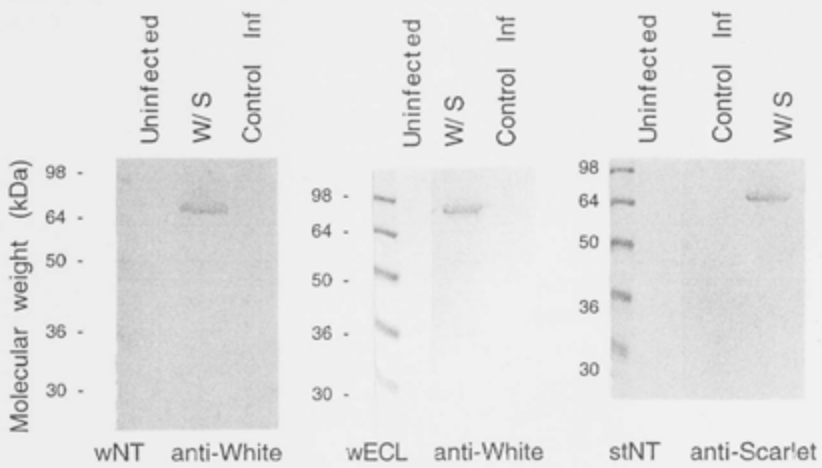

Fig. 5 Western blot analysis of specificity of anti-peptide antibodies using an *E. coli* heterologous expression system

An *E. coli* heterologous expression system (Chapter 6) was used to test the specificity of anti-peptide antibodies obtained from rabbit serum, both before and after purification using an antigen column (described in Chapter 2, Section 2.11.4). Three strains of *E. coli* were used in this experiment as follows:

Lane

1. Cells not expressing White or Scarlet protein

2. Cells harbouring p2GEXwNDB, which express the White nucleotide binding domain as a GST* fusion protein

3. Cells harbouring p2GEXstNBD, which express the Scarlet nucleotide binding domain as a GST fusion protein

The *E. coli* strains were grown on Luria plates supplemented with glucose, Ampicillin (50 μg/ml) and 0.01 mM IPTG. The control background strains was grown without addition of Ampicillin. Samples of cells were resuspended from the plate and prepared for SDS PAGE by boiling in SDS PAGE sample buffer followed by vortexing for 30 secs to shear chromosomal DNA. Proteins were separated by SDS PAGE on a 12% Tris-glycine polyacrylamide gel prior to Western transfer and blotting. The anti-peptide antibody used for each blot is indicated. Antibody binding was detected by way of a secondary anti-rabbit alkaline phosphatase conjugated antibody.

---

* GST: glutathione S-transferase.

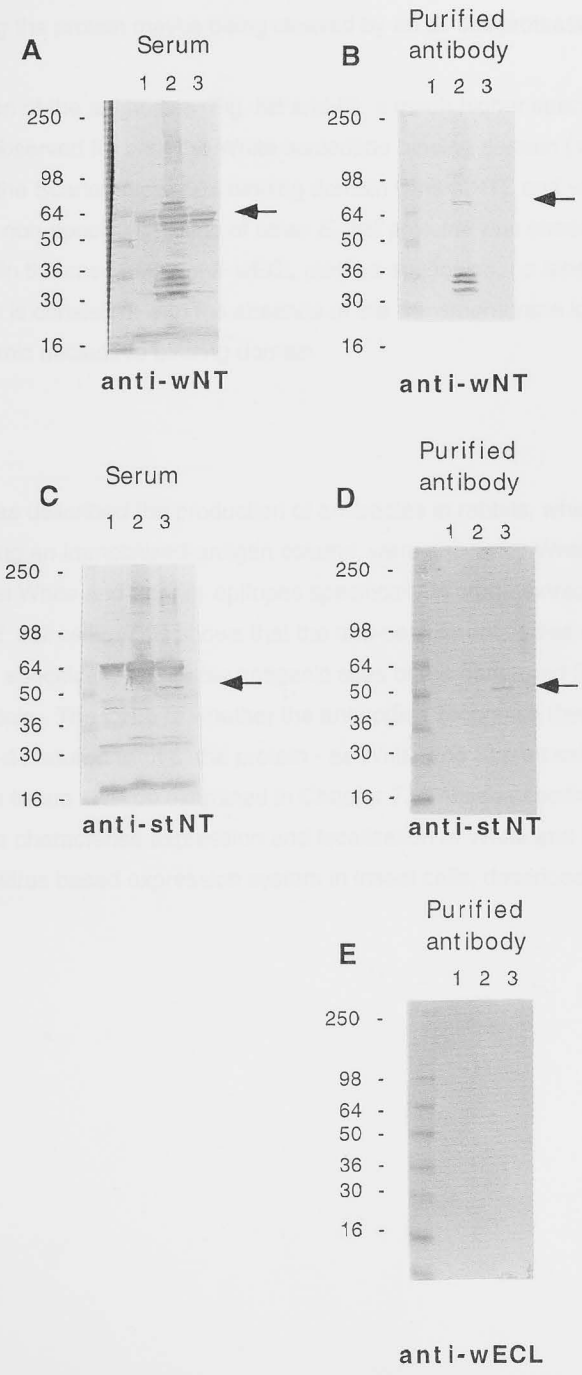
A
Serum
1 2 3
250
98
64
50
36
30
16
anti-wNT
B
Purified antibody
1 2 3
250
98
64
50
36
30
16
anti-wNT
C
Serum
1 2 3
250
98
64
50
36
30
16
anti-stNT
D
Purified antibody
1 2 3
250
98
64
50
36
30
16
anti-stNT
E
Purified antibody
1 2 3
250
98
64
50
36
30
16
anti-wECL

Kd) than the predicted molecular weight for the GST-StNBD fusion protein (70 kDa), indicating the protein maybe being cleaved by an *E. coli* protease.

After purification of the antibodies (Fig. 5B and D), a much higher specificity of labelling was observed for both the White nucleotide binding domain (wNT antibodies) or the Scarlet nucleotide binding domain (anit-stNT), and very little background or non-specific labelling of other *E. coli* proteins was observed in the control lanes. In the case of the anti-wECL purified antibodies, no labelling was detected which is consistent with the absence of the transmembrane loop region in the cytoplasmic nucleotide binding domain.

Summary

This chapter has described the production of antibodies in rabbits, which after purification using an immobilised-antigen column, were shown by Western blotting, to label White and Scarlet epitopes specifically in crude extracts from both Sf9 and *E. coli* cells. This shows that the anti-peptide antibodies described in this chapter, specifically recognise antigenic sites of the denatured SDS solubilised protein. The issue of whether the antibodies recognise these sites in the native non-denatured form of the protein - as White and Scarlet exists in *Drosophila* eye tissue - will be examined in Chapter 7. These antibodies will also be used to characterise expression and localisation of White and Scarlet using a baculovirus based expression system in insect cells, described in Chapter 5.

CHAPTER 5

EXPRESSION OF WHITE AND SCARLET PROTEINS FROM *D. melanogaster* IN INSECT CELLS

5. EXPRESSION OF WHITE & SCARLET PROTEINS FROM *D. melanogaster* IN INSECT CELLS

5.1 Introduction

The aim of the work described in this Chapter was to develop a heterologous eucaryotic expression system for the structural and functional characterisation of the *white* and *scarlet* gene products. The baculovirus expression system was chosen because it is a well established technique for expression of eucaryotic membrane proteins (Grisshammer and Tate, 1995; King and Possee, 1992) (an overview is provided below) and has been used successfully to study a number of ABC transporters (Germann et al, 1990; Meyer et al, 1994; O'Riordan et al, 1995; Sarkadi et al, 1992) and many transport and channel forming proteins (Carter et al, 1992; Cope et al, 1994; Tate and Blakely, 1994). Furthermore, insect derived cell lines were considered an appropriate choice for expression of *D. melanogaster* proteins. The advantages of this system include: the high expression levels which may be achieved; the eucaryotic background has been shown to perform post-translational modifications such as glycosylation, palmitoylation, myristoylation, addition of glycosylphosphatidylinositol (GPI) anchors and site-specific proteolytic cleavage (Grisshammer and Tate, 1995); and proteins are targeted in a similar way as they would be in the proteins' native cell background (King and Possee, 1992).

The baculovirus used in this expression system is derived from *Autographa californica* and is a double-stranded DNA-containing virus, surrounded by a lipid membrane (reviewed in (Fraser, 1992)). New viruses bud from the infected cell from about 8 hours post infection (hpi) and the cells die about 4-5 days post-infection. Baculovirus genes are classified into four groups depending on the time post-infection they are expressed: immediate early genes (0 - 4 hpi); delayed early genes (4-8 hpi); late genes (8-24 hpi) and the very late genes

(12-18 hpi, until cell death). The very late genes which include genes encoding polyhedrin protein and p10 protein are driven by promoter elements which result in very high expression and for this reason have been largely the promoters of choice for the over-expression of foreign genes (King and Possee, 1992). The function of polyhedrin in the native virus is to provide a protective capsule in which virus particles are protected from the external environment once released from the host cell. The function of the p10 protein is not clear, however, it is thought to play some role in polyhedra formation (Williams et al, 1989). Both the p10 and polyhedrin genes are not essential when the virus is used under laboratory cell culture conditions, so these genes can be deleted and a gene of interest can be inserted downstream of the polyhedrin or p10 promoter elements. The baculovirus genome is large in size (128 Kb) and is therefore difficult to manipulate for the purpose of inserting foreign genes. However, specialised plasmid vectors (known as baculovirus transfer vectors) have been developed which enable the insertion of foreign genes with relative ease. The baculovirus transfer vector is based on a bacterial plasmid allowing propagation in *E. coli* and manipulation using standard molecular biology techniques. The transfer vector used in the work described here, harbours both the p10 and polyhedrin promoters (Chapter 2, Section 2.4). The promoters are oriented back to back and are flanked by sequences from the wild-type virus. Co-transfection of cells by both linearised viral DNA and transfer vector DNA results in homologous recombination resulting in insertion of the foreign genes and promoter elements into the wild-type viral genome and production of recombinant viral particles. The linearised viral DNA used in these constructions has been digested at three positions with the restriction endonuclease *Bsu361* (Clontech) which deletes the polyhedrin gene and part of a downstream gene that is essential for viral replication. The transfer plasmid contains flanking regions that include the essential gene, ensuring that greater than 90% of the viable progeny virus are recombinants (Kitts and Possee, 1993). An outline of the steps involved in production of a recombinant baculovirus is illustrated in Fig. 1.

Fig. 1 Construction of recombinant baculovirus for heterologous expression of the *white* and *scarlet* cDNA from *D. melanogaster*

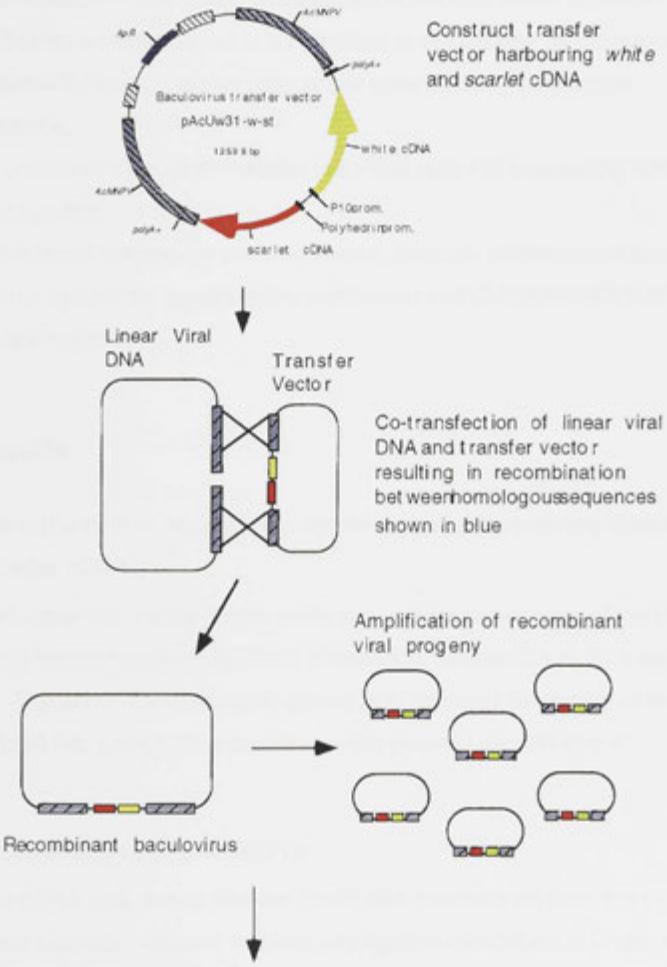

Once the recombinant baculovirus harbouring White and Scarlet cDNA was constructed, and successful expression had been achieved, the following objectives were envisaged:

1. Determination of the cellular localisation of the expressed proteins. White and Scarlet were predicted to be targeted to the plasma membrane where functional White/Scarlet complex would form a biologically active transporter.
2. Test uptake of tryptophan relative to control cells not expressing White or Scarlet protein.
3. If a functional transporter was expressed, then the system should provide a powerful system for construction, expression and characterisation of site directed mutants.

5.2 Results

5.2.1 Construction of baculovirus transfer vector harbouring White and Scarlet cDNA

The cDNA encoding the full length *white* and *scarlet* genes were cloned into the baculovirus transfer vector pAcUW31 (Chapter 2, Section 2.4.4) by a two step process. The *white* cDNA was sub-cloned first, followed by cloning of the *scarlet* cDNA into pAcUW31*w* resulting in the plasmid pAcUW31*w,st*.

5.2.1.a Construction of pAcUW31w

The *white* cDNA was cloned into the *Eco*RI site downstream from the p10 baculovirus promoter element by blunt end ligation (described in Chapter 2, Section 2.3). The *white* cDNA was removed from its previous plasmid vector by restriction digestion with *Eco*RI and *Kpn*I. The *white* cDNA fragment was separated from the vector fragment by agarose gel electrophoresis and subsequently purified from the agarose gel (described in Chapter 2, Section 2.3.6) followed by treatment with Klenow fragment to produce blunt ends

(Chapter 2, Section 2.3.2). The pAcUW31 plasmid DNA was digested with *Eco*RI followed by treatment with Klenow fragment (to produce blunt ends) and alkaline phosphatase (Sections 2.3.2 and 2.3.3) to prevent re-ligation of vector DNA. The *white* cDNA fragment and digested pAcUW31 plasmid DNA were then ligated and transformed into *E. coli* strain XL1Blue. Transformant colonies were screened by colony cracking assay (Chapter 2, Section 2.3.10) and colonies harbouring plasmid DNA larger than the circular vector plasmid were used to prepare small scale plasmid preparations which were analysed by restriction mapping. Fig. 2A is a plasmid map detailing the predicted DNA fragment sizes resulting from digestion with *Bgl*I restriction enzyme. Fig. 2B is an agarose gel analysis of plasmids digested with *Bgl*I. Plasmids showing the correct restriction map are highlighted with an asterisk. The resulting construct was named pAcUW31*w*.

*5.2.1.b Construction of pAcUW31*w,st

The *scarlet* cDNA was cloned into the *Bam*HI site downstream of the polyhedrin promoter element in the pAcUW31*w* vector. The *scarlet* cDNA fragment was released from its previous plasmid vector by restriction digestion with *Pst*I and *Hind*III and separated from the vector DNA by agarose gel electrophoresis. The *scarlet* cDNA fragment was purified from the gel and treated with Klenow fragment to produce a blunt ended fragment as described above for the *white* cDNA fragment. The pAcUW31*w* plasmid was digested with *Bgl*I, treated with Klenow to produce blunt ends, treated with alkaline phosphatase, and purified (as described in Chapter 2, Sections 2.3.2, 2.3.3 and 2.3.5). The prepared pAcUW31*w* vector and blunt ended *scarlet* cDNA were ligated and transformed into the *E. coli* strain XL1Blue. Colonies harbouring plasmid DNA larger than the pAcUW31*w* circular plasmid were used to prepare small scale purified plasmid DNA which was then analysed by restriction mapping which is illustrated in Fig. 3. Fig. 3A illustrates the plasmid map and predicted fragments resulting from a digest with *Bgl*I, where both *white* and *scarlet* are in the correct orientation with respect to their respective promoter elements. Fig. 3B is the agarose gel analysis of plasmids digested with *Bgl*I. The plasmids showing

Fig. 2. Restriction analysis of putative recombinant transfer vector plasmid pACUW31*w*.

A. Diagrammatic representation of the predicted sizes of fragments after a *Bgl*1 digest when the*white* cDNA is in the correct orientation. Full details of the pAcUw31 plasmid are provided in Chapter 2.

B. Restriction analysis of purified plasmid DNA of transformant colonies diagnosed to contain *white* cDNA from cracking assay. The plasmids showing the correct restriction pattern are signified with an asterisk.

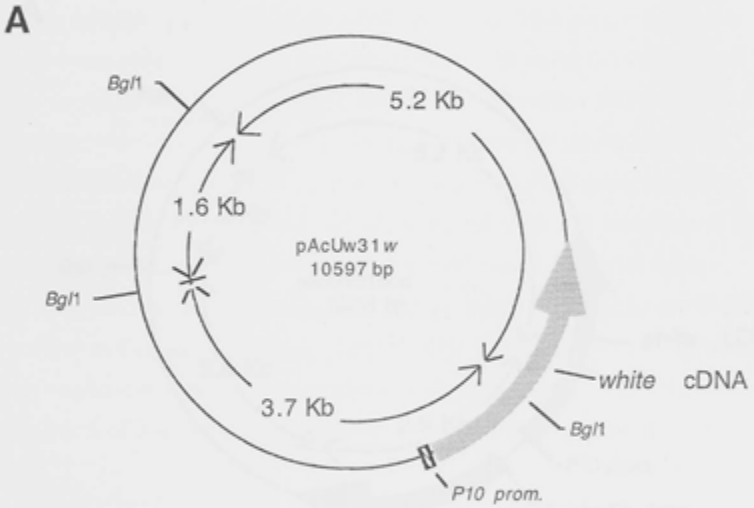

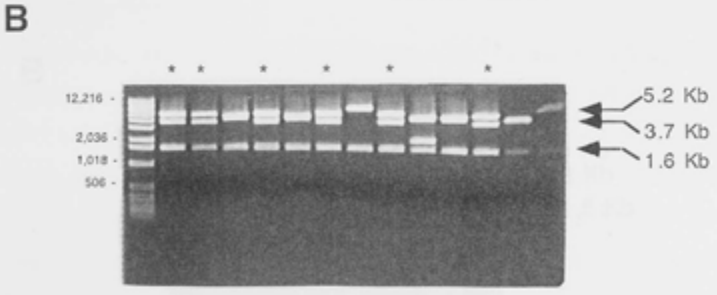

Fig. 3 Restriction analysis of putative recombinant transfer vector plasmids pACUW31*w,st.*

A. Diagrammatic representation of the predicted sizes of fragments after a *Bgl*1 digest when both *white* and *scarlet* cDNA are in the correct orientation.

B. Restriction analysis of purified plasmid DNA of transformant colonies diagnosed to contain white cDNA from cracking assay. The plasmids showing the correct restriction pattern are signified with an asterisk.

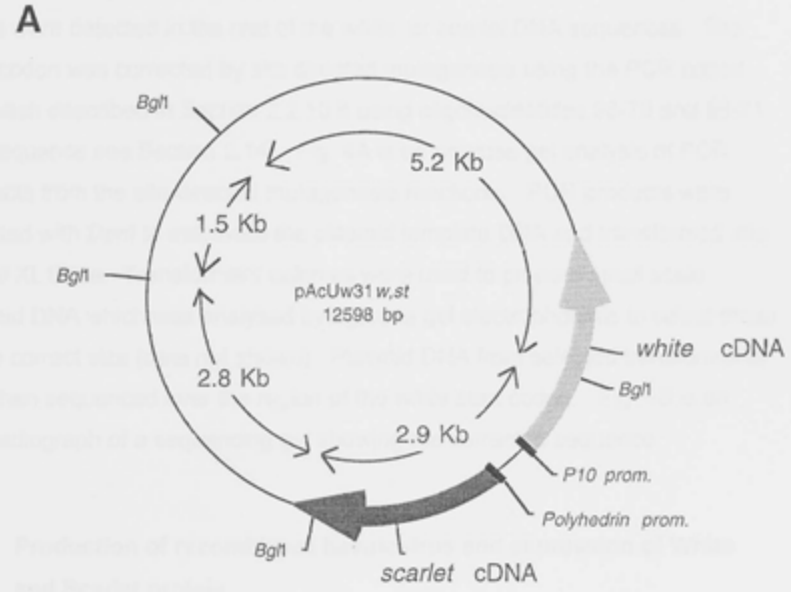

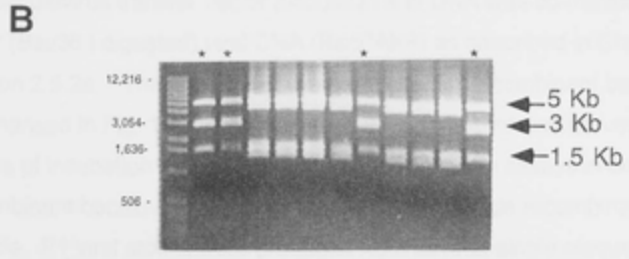

DNA fragment sizes consistent with the predicted *Bgl*I restriction map are highlighted with an asterisk. The resulting construct was named pAcUW31*w,st*.

5.2.1.c Site directed mutagenesis of pAcUW31w,st to correct the white *start codon*

Sequence analysis of pAcUW31*w,st* revealed that the start codon for the *white* cDNA was incorrect, possibly due to degradation of the 5' end of the *white* cDNA prior to ligation into pAcUW31. Apart from the start codon, no other errors were detected in the rest of the *white* or *scarlet* DNA sequences. The start codon was corrected by site directed mutagenesis using the PCR based approach described in Section 2.2.10 b using oligonucleotides 96-70 and 96-71 (for sequence see Section 2.14). Fig. 4A is an agarose gel analysis of PCR products from the site directed mutagenesis reactions. PCR products were digested with *Dpn*I to inactivate the plasmid template DNA and transformed into *E. coli* XL1Blue. Transformant colonies were used to prepare small scale plasmid DNA which was analysed by agarose gel electrophoresis to select those of the correct size (data not shown). Plasmid DNA from selected transformants was then sequenced over the region of the *white* start codon. Fig. 4B is an autoradiograph of a sequencing gel showing the corrected sequence.

5.2.2 Production of recombinant baculovirus and expression of White and Scarlet protein

The baculovirus transfer vector pAcUW31*w,st* DNA was co-transfected with linear (*Bsu*36 I digested) viral DNA (BacPAK8) as described in Chapter 2, Section 2.5.2a. The principle of the production of recombinant baculovirus is summarised in Fig. 1. The co-transfection supernatant was harvested after 5 to 6 days of incubation and then used to perform plaque assays in order to isolate recombinant baculovirus particles derived from a single recombinant baculovirus particle. P1 viral stocks were produced from several single plaque picks (described in Chapter 2, Section 2.5.2b). The cells used in the production

Fig. 4 Correction of start codon of *white* cDNA in pAcUW31*w,st* by site directed mutagenesis

A. Seven mutagenesis reactions were performed (as described in Chapter 2, Section 2.2.10) each containing the basic reaction mix (1x *Pfu* polymerase reaction buffer, 20 mM of each dNTP, 100 ng/μl DNA template, 100 ng/μl of each forward and reverse primer, 2.5 units/μl of native *Pfu* polymerase). The following additives were trialed as follows:

Lane Additive

Molecular weight marker
1. 10 μg/ml BSA
2. 5% (v/v) formamide
3. 5% (v/v) DMSO
4. 5% (v/v) glycerol
5. 15 mM ammonium sulfate
6. No additives
7. Template DNA

In lane 6 can be seen a DNA product of similar molecular weight as the template DNA. The DNA from this reaction was digested with *Dpn*I then transformed by electroporation into *E. coli* strain XL1Blue. Plasmid DNA was purified from transformant colonies and sequenced over the region of the start codon.

B. Autoradiograph of sequencing gel showing the corrected start codon of *white* cDNA in pAcUW31*w,st*.

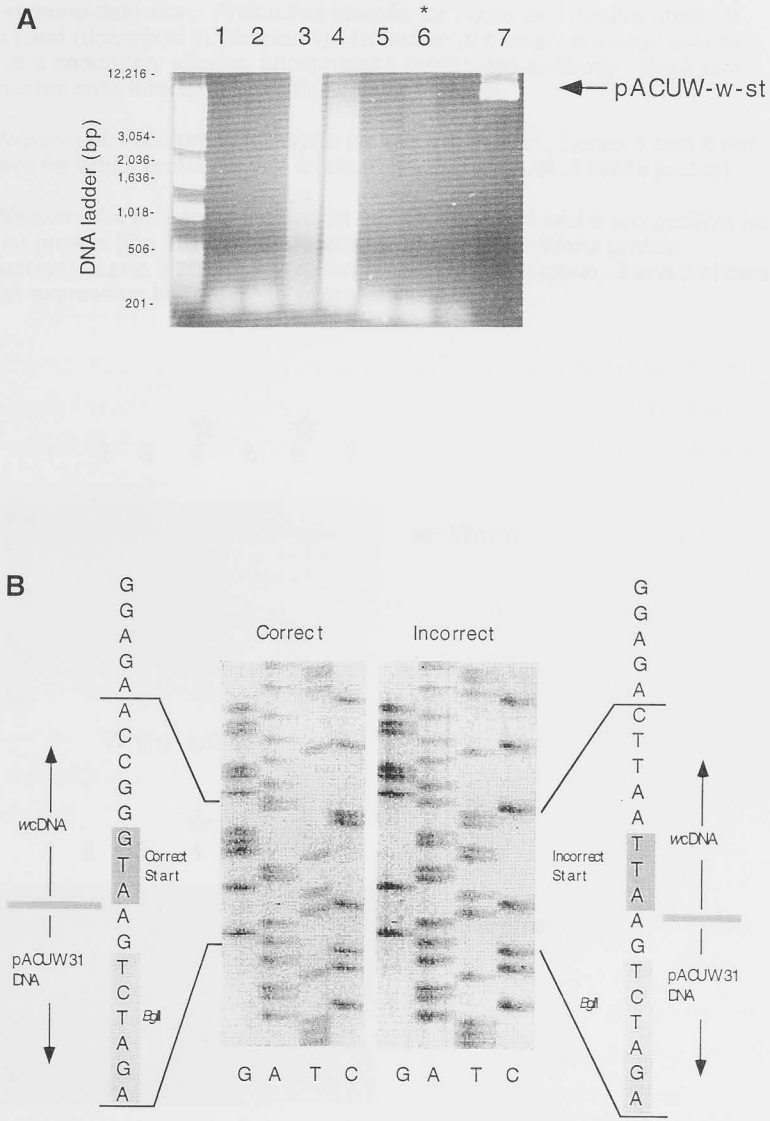
A
1 2 3 4 5 6 7
*
12,216 -
3,054 -
2,036 -
1,636 -
1,018 -
506 -
201 -
DNA ladder (bp)
pACUW-w-st
B
Correct
Incorrect
G A T C G A T C
wcDNA
pACUW31 DNA
Correct Start
Incorrect Start
BglI
BglI
wcDNA
pACUW31 DNA

Fig. 5. Expression of White and Scarlet protein by Sf9 cells infected with putative recombinant baculoviruses.

Virus particles derived from single viral plaque picks were used to infect Sf9 cells in 25 cm^2 flasks. After 5 days the supernatant was harvested and the cells were washed and prepared for SDS PAGE followed by western transfer and immuno-detection. Antibodies specific for White and Scarlet proteins were used (described in Chapter 4). Detection of primary antibody was by way of a secondary alkaline phosphatase conjugated antibody. Each lane represents cells infected from different plaque picks.

A. Western blot screening for White protein expression. Lanes 4 and 6 are positive for White protein. Lane 5 shows a very low level of White protein.

B. Western blot screening for Scarlet protein. Lanes 4 and 6 are positive for Scarlet protein (the identical lanes are also positive for White protein expression). Lane 5 shows a very low level of scarlet protein. Lane 7 shows scarlet expression but no White expression.

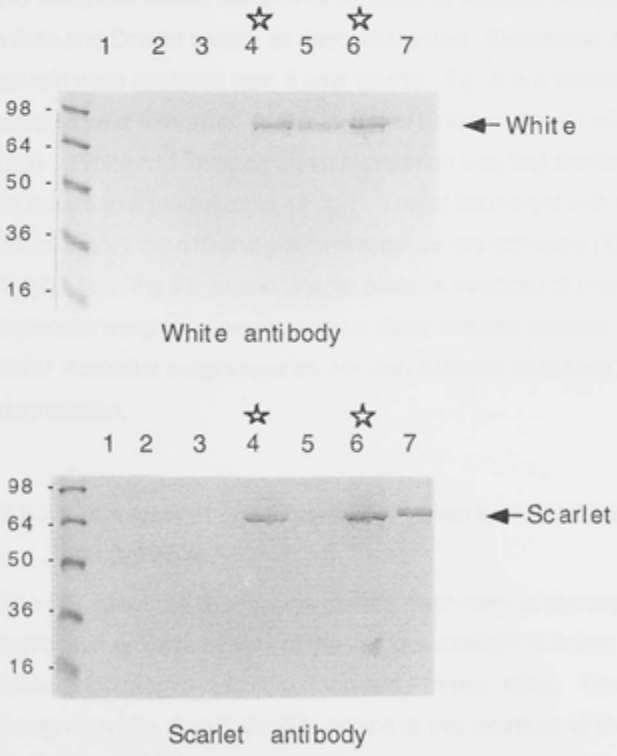

of P1 supernatant were harvested and analysed by Western blotting to test for White and Scarlet protein expression. Fig. 5 is a Western blot of cells used in the production of P1 recombinant baculovirus. Lanes 4 and 6 are positive for both White and Scarlet proteins and the molecular weights are approximately that predicted for White (75.6 Kd) and Scarlet (74.5 Kd). The recombinant baculovirus was named BV-*w,st* and the P1 supernatant was used to produce high titre P2 and P3 viral stocks for use in further experimental work.

*5.2.2.a Western blot analysis of the expression of White and Scarlet protein in BV-*w,st *infected cells over time*

Confirmation of successful production of a recombinant baculovirus expressing the *white* and *scarlet* cDNA was obtained by immuno-detection of expressed White and Scarlet protein as described above. Expression of White and Scarlet protein were analysed over a time course. Fig. 6 is a Western blot of BV-*w,st* infected cells harvested over a period of between 0 to 64 hours post infection (hpi). White and Scarlet protein expression was first detected at 16 hours and increases to a maximum at 48 hpi. This is consistent with the time post infection that the p10 and polyhedrin genes are activated (King and Possee, 1992). Both the White and Scarlet proteins migrated at their predicted molecular weights representing the major immuno-reactive product. Some lower molecular weight species are also detected indicating a minor degree of degradation.

5.2.2.b Analysis of glycosylation of White and Scarlet protein expressed in Sf9 cells

The Sf9 insect cell line has the cellular machinery to glycosylate heterologously expressed proteins by way of the well documented N-linked process that occurs in the endoplasmic reticulum (King and Possee, 1992). The consensus recognition site, Asn-X-Ser/Thr occurs at two locations of the White protein and once for the Scarlet protein, within a loop region between transmembrane helices 5 and 6, which has been postulated to be extracellularly accessible

Fig. 6 Expression of White and Scarlet protein in Sf9 insect cells infected with recombinant baculovirus.

Sf9 cells (30 x 10^4 cells) were infected with BV-*w,st.* were harvested over a time course. The cellular proteins were separated by SDS PAGE, transferred onto PVDF membranes and incubated with polyclonal antibodies raised against the White protein (wNT) **A**, or the Scarlet protein (stNT) **B**. Detection was by way of a secondary antibody conjugated to alkaline phosphatase. The White (75,667 kDa) and Scarlet (74,546 kDa) proteins are labelled and run at their predicted molecular weights.

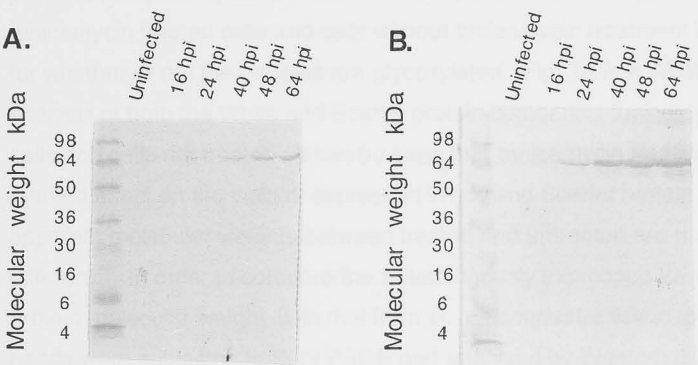

(Ewart et al, 1994). For proteins targeted to the plasma membrane, glycosylation is a good indicator for plasma membrane insertion due to the asymmetric orientation of oligosaccharide chains which are added on the luminal side of the ER and Golgi apparatus. This means that glycosylated regions of plasma membrane proteins face the outside of the cell membrane (Alberts et al, 1989). Glycosylated proteins migrate more slowly, appearing as a higher molecular weight protein on polyacrylamide gels, in comparison to the nonglycosylated counterpart (King and Possee, 1992). In order to investigate whether White or Scarlet undergo glycosylation processing, infected cells were treated with tunicamycin, which is an inhibitor of N-linked glycosylation. Glycosylation has a significant effect on the apparent molecular weight of proteins analysed by SDS PAGE so a comparison between protein from tunicamycin treated cells and cells without tunicamycin treatment is a good test for whether or not the proteins are glycosylated. Fig. 7A is a Western blot analysis of both the White and Scarlet protein comparing tunicamycin treated cells and cells not treated. It can be seen that tunicamycin treatment has had a marked effect on the yield of expressed White and Scarlet protein, however the apparent molecular weights between treated and untreated are not visibly different. In order to compare the heterologously expressed White and Scarlet protein molecular weight, with that from *D. melanogaster* tissue, proteins from fly heads were subjected to SDS PAGE and analysed by Western blot. Fig. 7B shows that the molecular weight of the proteins cross-reacting with the White or Scarlet antibodies are significantly higher than the predicted molecular weight for the nonglycosylated form of the proteins. This provides evidence that the White and Scarlet proteins may be glycosylated in vivo, however are not glycosylated in Sf9 cells.

5.2.3 Localisation of White and Scarlet protein expressed in Sf9 cells

Western blot analysis confirmed that both *white* and *scarlet* genes were being expressed under the control of the baculovirus p10 and polyhedrin promoters.

Fig. 7 Analysis of molecular weights of White and Scarlet protein expressed in Sf9 cells and extracted from *Drosophila* tissue

A. Analysis of the effect of tunicamycin on the apparent molecular weight of White and Scarlet protein expressed by Sf9 cells was performed as described in Chapter 2, Section 2.5.3. Cells were infected with BV-*w,st*. Tunicamycin was added 5 hpi to 1μg/ml. Cells were incubated for 42 hours prior to harvesting and preparing the cells for SDS PAGE on a 12% Tris-glycine gel. The gel was analysed by Western blotting using anti-wNT and anti-stNT antibodies respectively, as indicated below each Western blot.

B. Western blot analysis of White and Scarlet protein extracted from *D. melanogaster* heads. Fly heads were homogenised in solubilisation buffer as described in Chapter 2, Section 2.1.3 and solubilised proteins were separated by SDS PAGE on a 12% Tris-glycine gel. The gel was then analysed by Western blotting using anti-wNT and anti-stNT antibodies respectively and visualisation using an alkaline phosphatase conjugated secondary antibody.

Lanes:

1 Solubilised extract from fly heads
2 Cell lysate from Sf9 cells expressing White and Scarlet protein

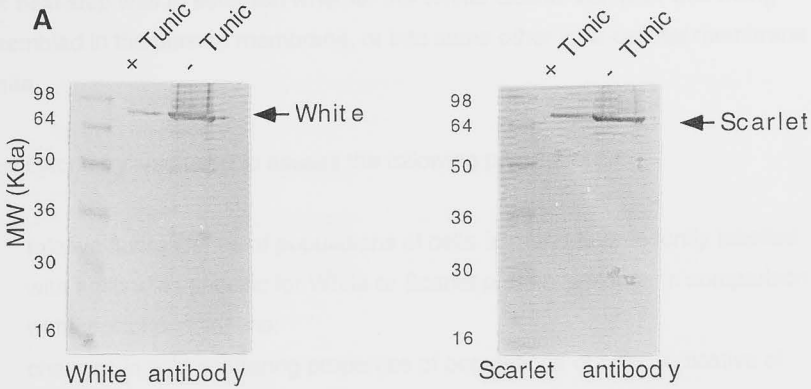
A
+ Tunic
- Tunic
MW (Kda)
98
64
50
36
30
16
White
White antibody
+ Tunic
- Tunic
98
64
50
36
30
16
Scarlet
Scarlet antibody

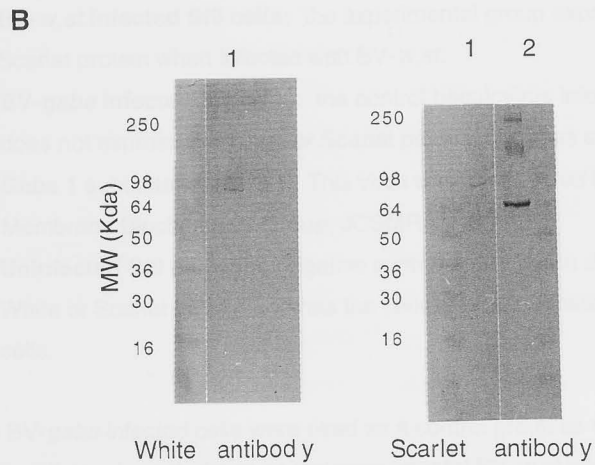
B
1
MW (Kda)
250
98
64
50
36
30
16
White antibody
1
2
250
98
64
50
36
30
16
Scarlet antibody

The next step was to establish whether the White/ Scarlet complex was being assembled in the plasma membrane, or into some other intra-cellular membrane or site.

Flow cytometry was used to assess the following parameters:

* relative fluorescence of populations of cells immuno-fluorescently labelled with antibodies specific for White or Scarlet protein epitopes in comparison with control populations;
* changes in light scattering properties of populations of cells, indicative of baculovirus infection.

Three groups of differently treated Sf9 cells were used in the experiments described in this section:

1. **BV-*w,st* infected Sf9 cells**: the experimental group expressing White and Scarlet protein when infected with BV-*w,st*.
2. **BV-*gaba* infected Sf9 cells**: the control baculovirus infected group which does not express the White or Scarlet protein, but does express the human Gaba 1 subunits $\alpha 1$ and $\beta 1$. This virus was constructed by Brett Cromer, Membrane Biochemistry Group, JCSMR, ANU.
3. **Uninfected Sf9 cells**: the negative control group which does not express White or Scarlet protein and has the cellular characteristics of uninfected cells.

The BV-*gaba* infected cells were used as a control group as they would have the same cellular characteristics as the experimental BV-*w,st* infected cells, minus the White and Scarlet protein. The uninfected cells gave a good indication of the changes in fluorescence during normal growth. In addition, the

change in light scattering properties before and after infection gives an indication of the percentage of cells infected in the infected groups.

5.2.3.a Flow cytometry analysis of non-permeabilised Sf9 cells: plasma membrane labelling using wECL antibody

The distribution plots in Fig. 8A illustrates the comparison of relative fluorescence of Sf9 cells labelled with anti-wECL antibody followed by the secondary FITC-conjugated anti-rabbit antibody. The BV-*w,st* infected cells have a geometric mean relative fluorescence of 174 which is 1.6 fold higher than BV-*gaba* infected cells (which have a geometric mean of 107) and three fold higher than uninfected cells (which have a geometric mean of 54). The distribution plots for the two infected groups do overlap, however approximately 50% of the cells (indicated under the marker line M1) in the BV-*w,st* infected cells have a higher fluorescence value than the brightest cells of the BV-*gaba* control group.

The three density plots shown in Fig. 8B, C and D give an indication of the correlation between BV-*w,st* infection and increased fluorescence due to immuno-fluorescence. The side-scatter parameter on the x axis, is plotted against relative fluorescence on the y axis. Each plot is divided into four quadrants. In the plot for the uninfected group, around 60% of the cells show a side scatter in the lower, left quadrant. This side scatter distribution is indicative of uninfected Sf9 cells. For both the infected groups the side scatter has increased substantially shifting the majority of the cells to the right hand quadrants. This change in distribution is indicative of baculovirus infected Sf9 cells. For BV-*w,st* infected cells around 80% of the cells lie in the two right hand quadrants (compared to 36% in the uninfected group). In comparison with the BV-*gaba* density plot, although the 76% of cells have increased side scatter, the fluorescence intensity has not increased to the extent of the BV-

Fig. 8 Flow cytometry and immuno-fluorescence labelling of Sf9 cells using anti-wECL antibody

A. The three overlayed distrubution plots provides a comparison of relative immuno-fluorescence of cells infected with BV-*w,st* virus, BV-*gaba* virus, and uninfected cells. Cells were harvested 30 hpi and were incubated with the primary antibody, wECL (1:100) prior to fixation followed by labelling with secondary FITC-conjugated anti-rabbit antibody as described in Chapter 2, Section 2.5.4. The marker line labelled M1 indicates the number of cells with fluorescence that fall in this range. The distribution plots are normalised with respect to cell number.

B., **C.** and **D.** Density plots showing side scatter against relative fluorescence as frequency distribution. The colour coding represents an increase in frequency or density where blue is least frequent, green is intermediate and red is the highest frequency. Each plot is separated into four quadrants and the percentage shown in each corner represents the percentage of cells which occur in that quadrant. This allows a direct comparison of the population shift which occurs when side scatter increases due to Baculovirus infection, in addition to the increase in relative fluorescence due to immuno-labelling between cells expressing White and Scarlet protein, and those which do not.

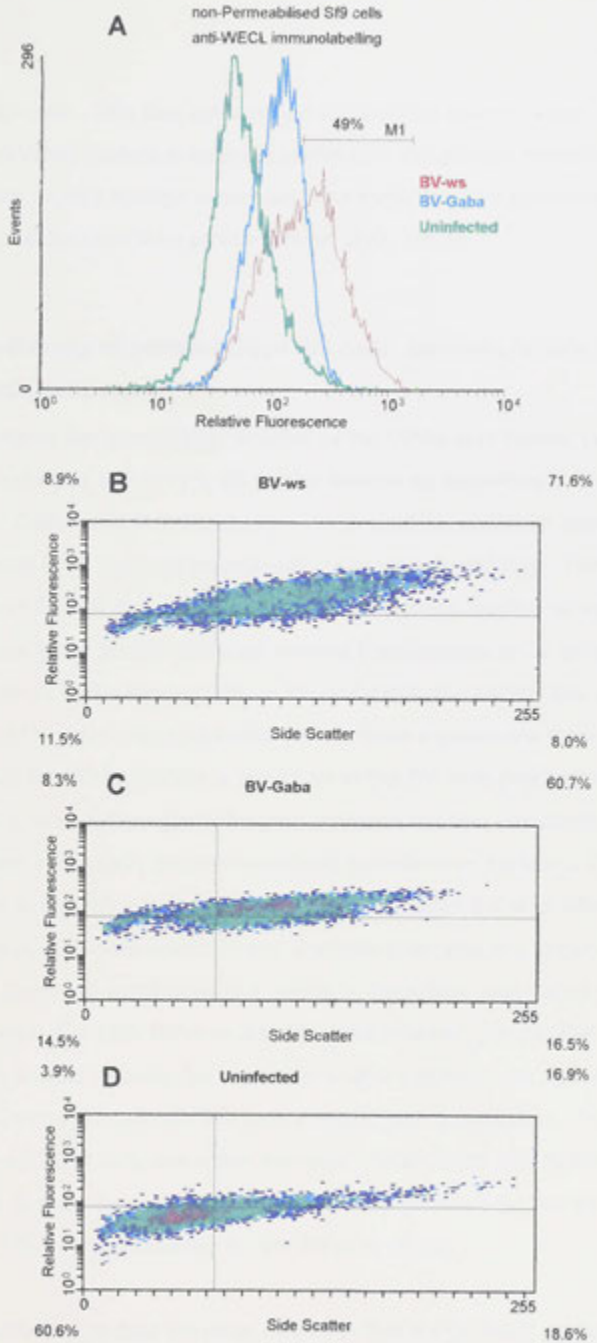
A
non-Permeabilised Sf9 cells
anti-WECL immunolabelling
296
Events
0
49%
M1
BV-ws
BV-Gaba
Uninfected
10^0
10^1
10^2
10^3
10^4
Relative Fluorescence
8.9%
B
BV-ws
71.6%
Relative Fluorescence
0
255
Side Scatter
11.5%
8.0%
8.3%
C
BV-Gaba
60.7%
14.5%
16.5%
3.9%
D
Uninfected
16.9%
60.6%
18.6%

w,st population of cells. This flow cytometry data provides evidence that at least some of the White protein is being assembled in the plasma membrane and that the White protein epitope is exposed extracellularly in agreement with the proposed model for the White protein (Ewart et al, 1994).

5.2.3.b Flow cytometry of permeabilised Sf9 cells: intracellular labelling with wECL antibody

In order to investigate the intracellular location of the White and Scarlet protein, cells were permeabilised with 0.01% SDS after fixation as described in Chapter 2, Section 2.5.4. Cells were then incubated with anti-wECL antibody, washed, then incubated with FITC-conjugated anti-rabbit secondary antibody. The distribution plots in Fig. 9A plot relative fluorescence against number of cells. The BV-*w,st* group has a geometric mean relative fluorescence of 30 which is six fold higher than both the control groups BV-*gaba* infected (which has a geometric mean of 5), and uninfected cells (which have a geometric mean of 7). This indicates that the White protein is produced in the BV-*w,st* infected cells and that there is a more noticeable difference between the test and control cells than was indicated in the cells not permeabilised described in Section 5.2.3a. The density plots in Fig. 9B illustrate the correlation between BV-*w,st* infection and increased relative fluorescence. In the uninfected density plot, around 80% of cells lie in the lower left-hand quadrant, which is the region associated with uninfected Sf9 cells. For both BV-*w,st* and BV-*gaba* infected groups, the populations have shifted towards the high side scatter values in the right hand quadrants which is associated with Sf9 cells infected with baculovirus. For both infected groups, ~70% of cells are within the region associated with higher side scatter. Relative fluorescence however has remained constant for the BV-*gaba* infected control group, and increased for the BV-*w,st* group.

This immuno-fluorescence data provides evidence that a significant amount of expressed White protein is intracellular. Taking into consideration the results from Section 5.2.3a which show the White protein is targeting the plasma membrane, it can be said that although some White protein reaches the plasma

Fig. 9 Flow cytometry and immuno-fluorescence labelling of permeabilised Sf9 cells using anti-wECL antibody

A. The three overlayed density plots provides a comparison of relative immuno-fluorescence of cells infected with BV-*w,st* virus, BV-*gaba* virus, and uninfected cells. Cells were harvested 30 hpi prior to fixation and permeabilisation with 0.01% SDS before incubation with the primary antibody, wECL (1:100) and then labelled with a secondary FITC-conjugated anti-rabbit antibody as described in Chapter 2, Section 2.5.4. The marker line labelled M1 indicates the number of cells which fall under the horizontal line. The distribution plots are normalised with respect to cell number.

B., **C.** and **D.** Density plots showing side scatter against relative fluorescence as frequency distributions. The colour coding represents an increase in frequency or density where blue is least frequent, green is intermediate and red is the highest frequency. Each plot is separated into four quadrants and the percentage shown in each corner represents the percentage of cells which occur in that quadrant. This allows a direct comparison of the population shift which occurs when side scatter increases due to Baculovirus infection, in addition to the increase in relative fluorescence due to immuno-labelling between cells expressing White or Scarlet protein, and those which do not.

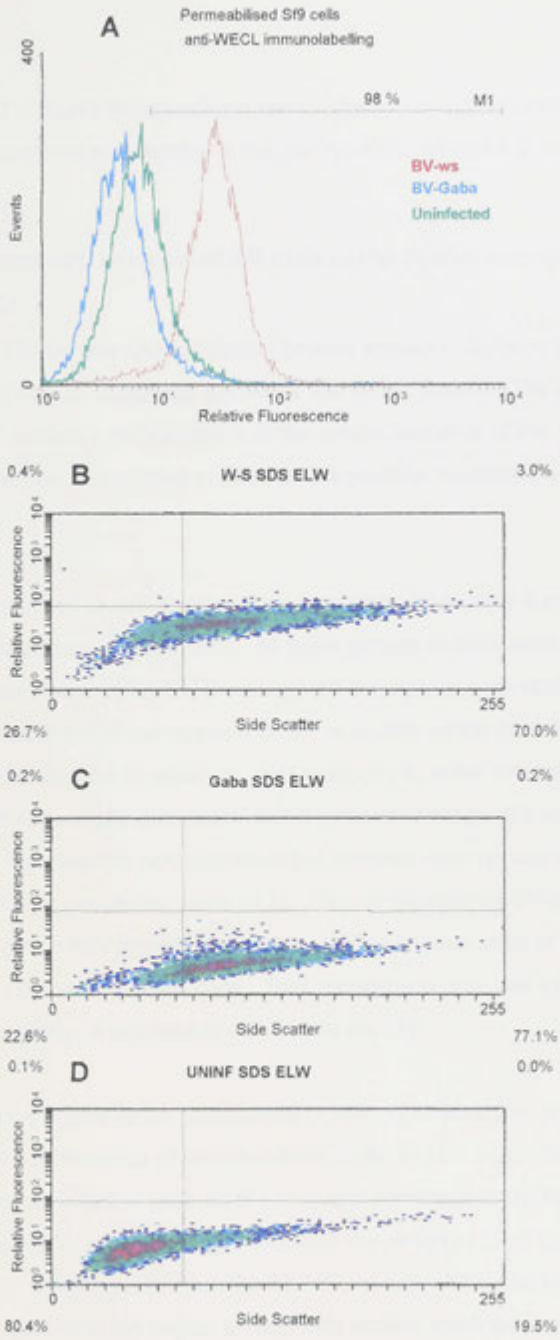
A
Permeabilised Sf9 cells
anti-WECL immunolabelling
98 %
M1
BV-ws
BV-Gaba
Uninfected
Events
400
0
Relative Fluorescence
0.4%
B
W-S SDS ELW
3.0%
Relative Fluorescence
Side Scatter
26.7%
70.0%
0.2%
C
Gaba SDS ELW
0.2%
Relative Fluorescence
Side Scatter
22.6%
77.1%
0.1%
D
UNINF SDS ELW
0.0%
Relative Fluorescence
Side Scatter
80.4%
19.5%

membrane, most is found at intracellular sites. This issue will be further investigated by confocal microscopy in the Sections 5.2.3d and 5.2.3e.

5.2.3.c Flow cytometry analysis of Sf9 cells using Scarlet specific antibody

The anti-stNT antibody was used to detect Scarlet protein in BV-*w,st* insects cells in the same way as described above for the White protein. The protein epitope the stNT antibody recognises is at the amino-terminus of the ATP binding domain which is predicted to have an intracellular localisation (see Chapter 4).

The distribution plot in Fig. 10 illustrates a comparison of relative fluorescence between three populations of Sf9 cells. All three groups of cells were treated with stNT antibody, followed by FITC-conjugated secondary anti-rabbit antibody. The histogram in red represents BV-*w,st* cells which have been permeabilised after fixation to allow the stNT antibody to enter the cell. This population which is normally distributed has a geometric mean of 6 which is 2 fold higher than the cells not permeabilised but infected with the same virus, BV-*w,st* (which had a geometric mean of 3). The permeabilised BV-*gaba* infected control group has a geometric mean relative fluorescence of 2 which is 3 fold lower than BV-*w,st* infected cells. This comparison provides evidence that the Scarlet epitope is accessible only inside the cell.

The density plots of these same populations of cells illustrates the correlation between relative fluorescence of permeabilised cells and BV-*w,st* infection. Comparing the three infected groups, BV-*w,st* non-permeabilised, BV-*w,st* permeabilised and BV-*gaba* permeabilised, with the density plot of the uninfected group, it can be seen that the 80-90% of cells in populations in the infected groups shifted to the region of high side scatter associated with baculovirus infected Sf9 cells, compared to ~20% in the uninfected control group. However the relative fluorescence has increased substantially only in the permeabilised BV-*w,st* infected population and not in the other groups.

Fig. 10 Flow cytometry and immuno-fluorescence analysis of Sf9 cells using anti-stNT antibody

A. The three overlayed distribution plots provide a comparison of relative immuno-fluorescence of cells infected with BV-*w,st* virus and BV-*gaba* virus. Cells were harvested 30 hpi. Permeabilised cells were fixed prior to permeabilisation with 0.01% SDS, incubated with the primary antibody, anti-stNT (1:100) and then labelled with a secondary FITC-conjugated anti-rabbit antibody as described in Chapter 2, Section 2.5.4. Cells which were not permeabilised were treated with primary and secondary antibody prior to fixation. The marker line labelled M1 indicates the number of cells which fall under the horizontal line. The distribution plots are normalised with respect to cell number.

B., C., D. and **E.** Density plots showing side scatter against relative fluorescence as frequency distributions. The colour coding represents an increase in frequency or density where blue is least frequent, green is intermediate and red is the highest frequency. Each plot is separated into four quadrants and the percentage shown in each corner represents the percentage of cells which occur in that quadrant. This allows a direct comparison of the population shift which occurs when side scatter increases due to Baculovirus infection, in addition to the increase in relative fluorescence due to immuno-labelling between cells expressing White or Scarlet protein, and those which do not.

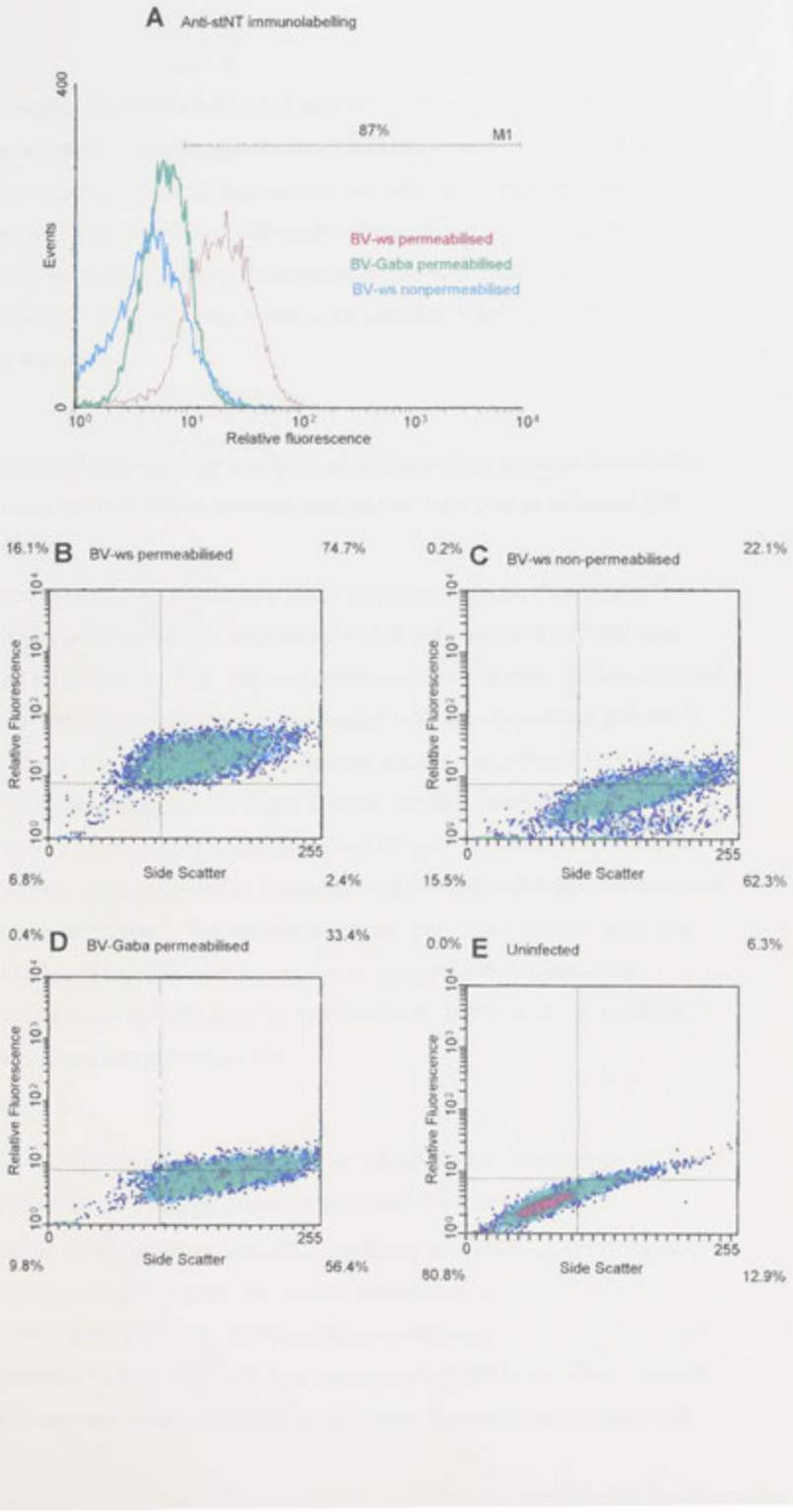
A Anti-stNT immunolabelling
400
Events
0
87%
M1
BV-ws permeabilised
BV-Gaba permeabilised
BV-ws nonpermeabilised
10^0
10^1
10^2
10^3
10^4
Relative fluorescence
16.1%
B BV-ws permeabilised
74.7%
Relative Fluorescence
Side Scatter
6.8%
2.4%
0.2%
C BV-ws non-permeabilised
22.1%
15.5%
62.3%
0.4%
D BV-Gaba permeabilised
33.4%
9.8%
56.4%
0.0%
E Uninfected
6.3%
80.8%
12.9%
0
255

These results provide further evidence that the Scarlet epitope is at an intracellular location. Plasma membrane localisation was investigated by immuno-fluorescence confocal microscopy, as well as cell fractionation, which is described in the next Section. Although differences in test and control cells were detected by flow cytometry, unfortunately due to the low level of fluorescence, stNT antibody was found to be unsuitable for fluorescence microscopy analysis.

5.2.3.d Confocal microscopy analysis of extracellular plasma membrane localisation of White protein expressed by BV-w,st infected Sf9 cells

Laser Scanning confocal microscopy was used to investigate the cellular localisation of the White protein expressed in Sf9 cells infected with BV-*w,st* recombinant baculovirus. Fig. 11A is a micrograph of Sf9 cells, 30 hpi, infected with BV-*w,st* and immuno-fluorescently labelled with affinity purified anti-wECL antibody. The anti-wECL antibody recognises an epitope within a loop region between transmembrane helices 5 and 6 of the White protein and has been predicted to be extracellularly accessible (see Chapter 4). Strong fluorescent immuno-labelling was observed at the surface of the cell and this is represented in Fig. 11A. In comparison, the control BV-*gaba* (Fig. 11B) infected cells and uninfected cells (11C), show some amount of background fluorescence, however do not show specific plasma membrane targeting which is observed for the White/Scarlet expressing cells.

*5.2.3.e Confocal microscopy analysis of intracellular localisation of White protein expressed by BV-*w,st *infected Sf9 cells*

Flow cytometry analysis using anti-wECL antibody provided evidence that the White protein was found in both the plasma membrane (Section 5.2.3a), and intracellularly (Section 5.2.3b). Confocal laser scanning microscopy was used to investigate this further. Fig. 12A is a micrograph of Sf9 cells 30hpi, infected with BV-*w,st* permeabilised with SDS and immuno-fluorescently labelled with

Fig. 11 Confocal microscopy analysis of extracellular plasma membrane localisation of White expressed in Sf9 cells

Cells were infected with either BV-*w,st* or BV-*gaba* as indicated and harvested 30 hpi and were incubated with the primary antibody, anti-wECL (1:100) prior to fixation followed by labelling with secondary FITC-conjugated anti-rabbit antibody as described in Chapter 2, Section 2.5.4. The gain is the same for each group.

A. Cells infected with BV-*w,st*.

B. Cells infected with BV-*gaba*.

C. Uninfected cells

A

BV-ws infected

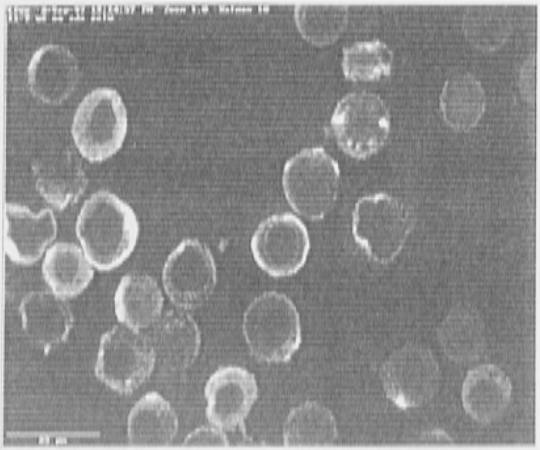

B

BV-Gaba infected

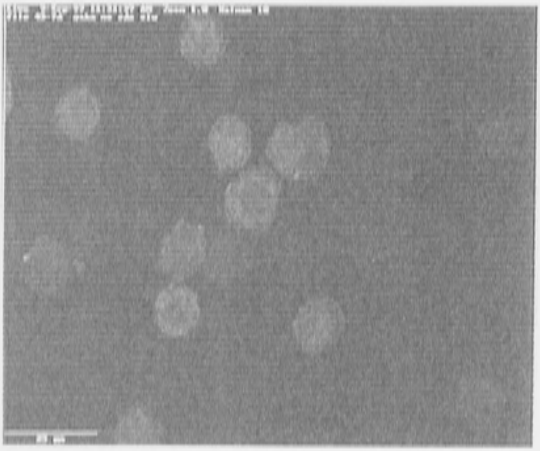

C

Uninfected

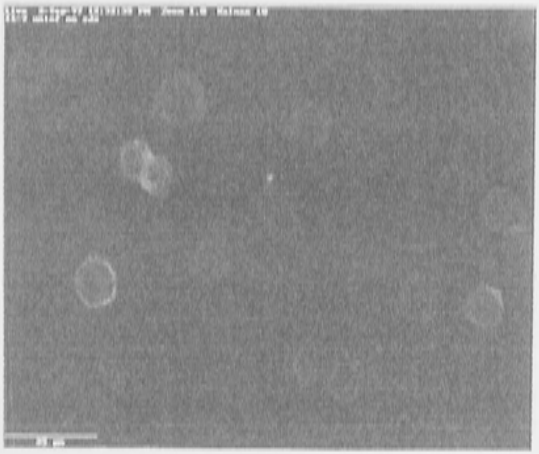

Fig. 12 Confocal microscopy analysis of intracellular localisation of White protein expressed by Sf9 cells

Cells were harvested 30 hpi prior to fixation and permeabilisation with 0.01% SDS before incubation with the primary antibody, anti-wECL (1:100) followed by a secondary FITC-conjugated anti-rabbit antibody as described in Chapter 2, Section 2.5.4.

A. Cells infected with BV-*w,st*.

B. Cells infected with BV-*gaba*.

A

BV-ws infected

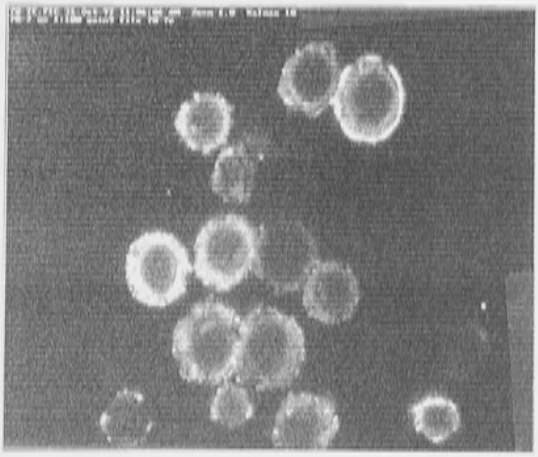

B

BV-Gaba infected

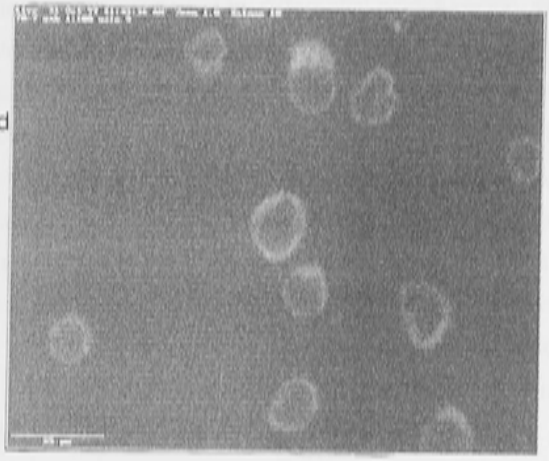

wECL antibody (see Chapter 4). Strong immuno-fluorescent labelling can be seen, appearing as a dense concentration of fluorescent labelling appearing as bright spots. Extensive intracellular labelling was also observed in permeabilised cells immuno-fluorescently stained using the anti-wNT antibody (Fig. 13A). Although there is some cross-reaction in the control infected cells (Fig. 13B), the level of labelling is much greater in the White/Scarlet expressing cells and the punctate labelling observed in Fig. 13A is suggestive of localisation to an intracellular compartment. These results suggest that a large percentage of expressed White protein is not being assembled in the plasma membrane and may be locating to the membrane of an intracellular compartment.

5.2.4 Separation of Sf9 cell fractions by differential centrifugation

In order to investigate further the cellular localisation of the White and Scarlet proteins expressed in insect cells, the crude membranes, cytoplasm and insoluble cell material were separated by differential centrifugation, as described in Section 2.6.5 and analysed by SDS PAGE and Western blotting. Fig. 14 shows the levels of White and Scarlet detected in the different cell fractions. It is clear from Fig. 14B, lane 3 that approximately 95% of the White protein is detected in the insoluble cell material which is separated from the cytoplasm and membrane fractions by low speed centrifugation. A low level of White protein was detected in the crude membrane fraction (Fig. 14B lane 4). On the other hand, 100% of the Scarlet protein was detected in the insoluble cell fraction (Fig. 14C lane 3) and none in the crude membrane fraction (Fig. 14C lane 4). No White or Scarlet protein was detected in the cytoplasmic fraction (Fig. 14B & C lane 5).

The method of percoll gradient centrifugation was also used to separate membrane and other cell fractions (described in Chapter 2, Section 2.6.6). The initial purpose of the percoll gradient was to attempt to isolate White and Scarlet enriched membrane vesicles with a view to functional characterisation of the White/Scarlet transporter complex. This method resulted in the

Fig. 13 Confocal microscopy analysis of intracellular immuno-fluorescent labelling White protein expressed by Sf9 cells

Cells were harvested 30 hpi prior to fixation and permeabilisation with 0.01% SDS before incubation with the primary antibody, anti-wNT (1:10) followed by a secondary FITC-conjugated anti-rabbit antibody as described in Chapter 2, Section 2.5.4.

A. Cells infected with BV-*w,st*.

B. Cells infected with BV-*gaba*.

A

BV-ws infected

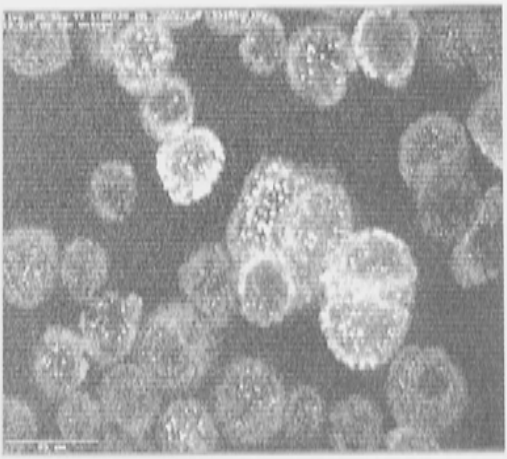

B

BV-Gaba infected

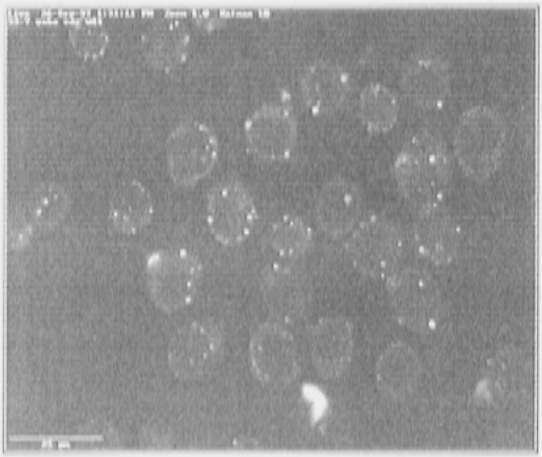

Fig. 14 SDS PAGE and Western blot analysis of cell fractions from Sf9 cells expressing White and Scarlet protein

Cells were infected with either BV-*gaba* control virus or BV-*w,st* virus and were harvested 48 hpi and lysed using a dounce homogeniser. Fractions were separated by differential centrifugation as described in Chapter 2, Section 2.6.5b. The gain is the same for each group.

A. SDS PAGE analysis of proteins.

B. Western blot using wNT primary antibody.

C. Western blot using stNT primary antibody

The labelled wells are representative of samples taken from the following cell fractions:

Lane	Cell fraction
1	Lysed cells, prior to differential centrifugation.
2	Supernatant obtained from low speed centrifugation (121 g).
3	Pellet obtained from low speed centrifugation (121 g). Representative of insoluble proteins.
4	Pellet obtained from high speed centrifugation (100,000 g). Representative of crude cell membranes.
5	Supernatant obtained from high speed centrifugation (100,000 g). Representative of soluble cell cytoplasm.

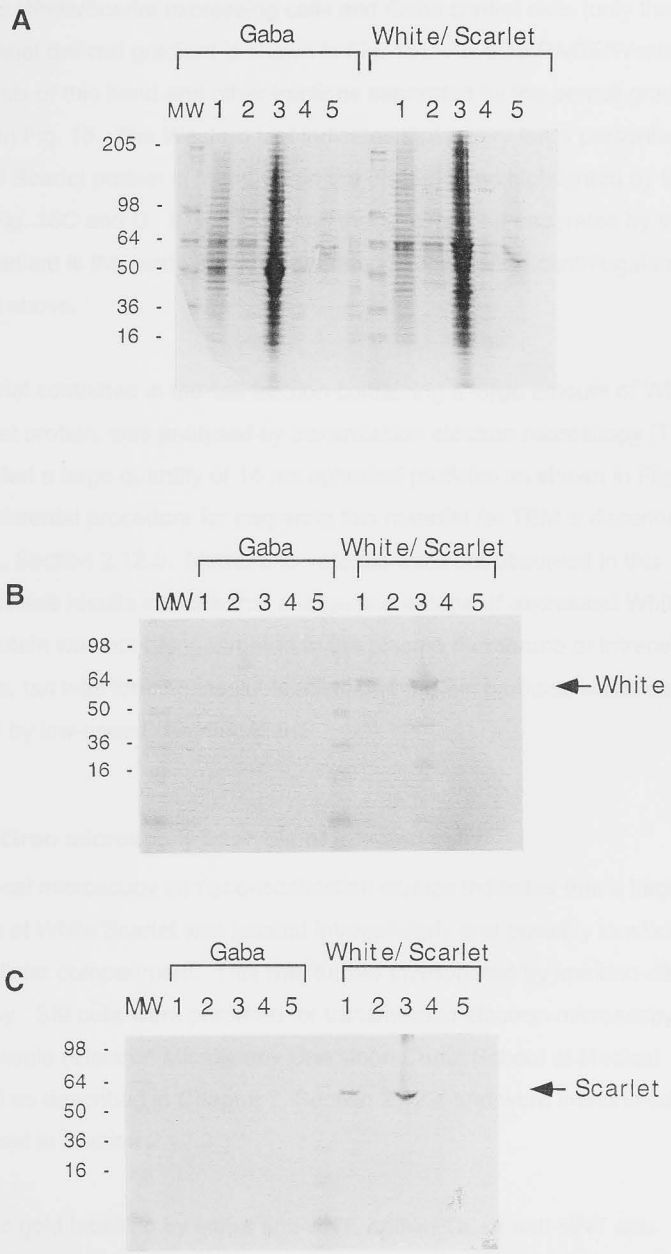
A
Gaba
White/ Scarlet
MW 1 2 3 4 5
1 2 3 4 5
205
98
64
50
36
16
B
Gaba
White/ Scarlet
MW 1 2 3 4 5
1 2 3 4 5
98
64
50
36
16
White
C
Gaba
White/ Scarlet
MW 1 2 3 4 5
1 2 3 4 5
98
64
50
36
16
Scarlet

separation of a very distinct band which is shown in Fig. 15A, which is present in both the White/Scarlet expressing cells and Gaba control cells (only the White/Scarlet derived gradient is shown in Fig. 15). An SDS PAGE/Western blot analysis of this band and other fractions separated by the percoll gradient is shown in Fig. 15. The Western blot indicates that a very large percentage of White and Scarlet protein is found within the distinct band highlighted by the arrow in Fig. 15C and D. It was assumed that this fraction separated by the percoll gradient is the same fraction separated by low speed centrifugation as described above.

The material contained in the cell fraction containing a large amount of White and Scarlet protein, was analysed by transmission electron microscopy (TEM) and revealed a large quantity of 14 nm spherical particles as shown in Fig. 16. The experimental procedure for preparing this material for TEM is described in Chapter 2, Section 2.12.3. Membrane vesicles were not observed in this fraction. These results indicate that a large percentage of expressed White and Scarlet protein was not being targeted to the plasma membrane or intracellular membrane, but was forming insoluble misfolded protein particles which can be separated by low-speed centrifugation.

5.2.5 Electron microscopy analysis of infected cells

The confocal microscopy immuno-localisation studies indicated that a large proportion of White/Scarlet was located intracellularly and possibly localising to an intracellular compartment. This was further investigated by immuno-electron microscopy. Sf9 cells were prepared for transmission electron microscopy by Cathy Gillespie (Electron Microscopy Unit, John Curtin School of Medical Research) as described in Chapter 2, Section 2.12.4 and were immuno-labelled as described in Section 2.12.2.

No specific gold labelling by either anti-wNT, anti-wECL or anti-stNT was observed at the plasma membrane or any other intracellular site, possibly due to the destruction of the antigenic sites by the preparative process required for

Fig. 15 Analysis of cell fractions separated by percoll density gradient

A cell monolayer in a 25cm^2 flask was infected with BV-*w,st* virus, harvested 48 hpi and lysed using a dounce homogeniser. The cell lysate was added to percoll solution to a final percoll concentration of 11.9% prior to centrifugation as described in Chapter 2, Section 2.6.6.

A. Photograph of the tube after percoll gradient was generated by centrifugation. Fractions labelled 1 to 4 were extracted by aspiration with a pasteur pipette and analysed by SDS PAGE and Western blotting shown in B and C.

B. SDS PAGE analysis (12% Tris-glycine gel). Wells labelled 1 to 4 represent samples from fractions 1 to 4 shown in A.

C. Detection of White protein by Western blot analysis of fractions 1 to 4 shown in A.

D. Detection of Scarlet protein by Western blot analysis of fractions 1 to 4 shown in A.

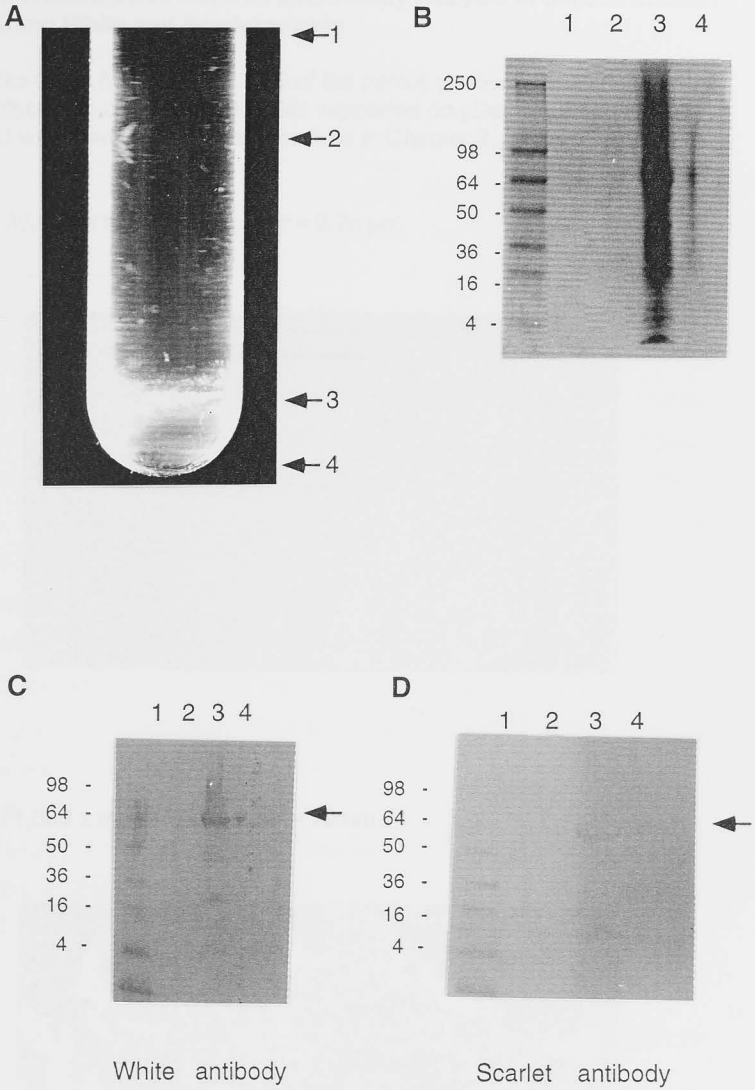
A
1
2
3
4
B
1 2 3 4
250
98
64
50
36
16
4
C
1 2 3 4
98
64
50
36
16
4
White antibody
D
1 2 3 4
98
64
50
36
16
4
Scarlet antibody

Fig. 16 Transmission electron microscopy analysis of the cell fraction containing White and Scarlet protein

Samples taken from the fraction 3 of the percoll gradient shown in Fig. 15 were placed on carbon coated grids supported on plastic and negatively stained with uranyl acetate as described in Chapter 2, Section 2.15.3.

A. 38,000 x magnification, bar = 0.26 μm

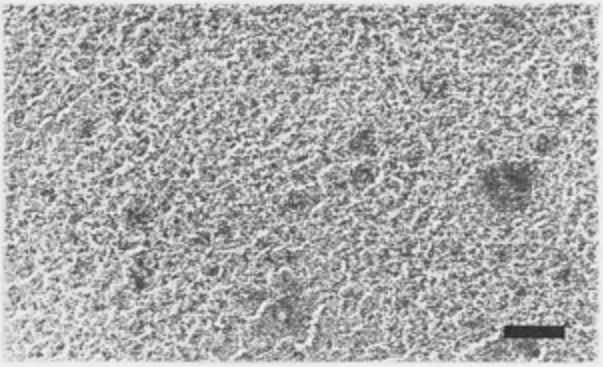

B. 71,000 x magnification, bar = 70 nm

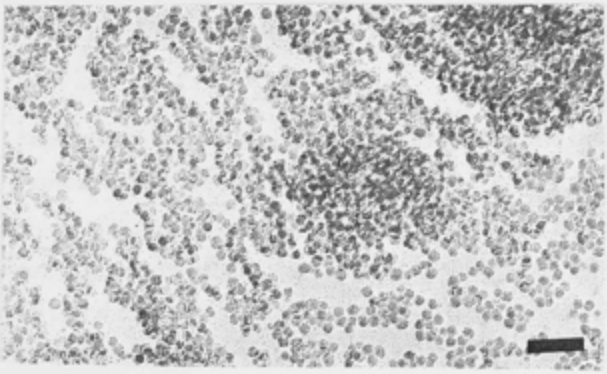

transmission electron microscopy. The internal organisation of BV-*gaba*, BV-*w,st*, and uninfected cells were compared and the following observations were made.

BV-*w,st* infected cells showed typical signs of baculovirus infection (see Fig. 17). The baculovirus genome is associated with a highly basic (arginine-rich) protein of 6.5kDa (Tweeten et al, 1980), within a rod-shaped nucleocapsid which contains a 39 kDa capsid protein (Thiem and Miller, 1989). Several nucleocapsids are packaged within a lipoprotein envelope forming a virus particle or virion and these are easily seen in Fig. 17B and 17C. This type of virion, i.e. harbouring one or more nucleocapsids, are typical of this sub-group of the *Baculoviridae* family, known as nuclear polyhedrosis viruses (NPV) which have been developed as expression vectors in this system. In a wild-type AcNPV infection virions are encapsulated within an electron dense polyhedrin envelope made up of polyhedrin protein, collectively called polyhedra. The polyhedrin gene has been removed in this recombinant expression vector and hence the absence of polyhedra. The nucleus of the infected cells were enlarged compared to uninfected cells which is typical in a baculovirus infection (King and Possee, 1992).

Investigation of the cytoplasm of infected cells (Fig. 17D) revealed a large number of spherical particles, very similar to the particles observed in the percoll fraction containing high levels of White and Scarlet protein (see Fig. 16).

5.2.6 Analysis of tryptophan transport activity of White and Scarlet expressing insect cells

As described in the introductory Chapter 1, the White and Scarlet proteins are postulated to form an ABC transporter specific for tryptophan which is a precursor of the brown pigment, xanthommatin. It was established in the previous sections that the White and Scarlet proteins were being expressed in

Fig. 17 Transmission electron microscopy analysis of Sf9 cells infected with BV-*w,st*

Sf9 cells were harvested 30 hpi from monolayer cultures and prepared for transmission electron microscopy as described in Chapter 2, Section 2.12. Immuno-labelling was attempted using anti-wNT, anti-wECL and anti-stNT as described in Chapter 2, Section 2.12.2 however specific labelling was not observed.

A. Uninfected Sf9 cell, magnification 3,750 x (bar = 5.3 μm)

B. BV-*w,st* infected cell, magnification 2,500 x (bar = 5.3 μm)

C. Higher magnification of cell nucleus of a BV-*w,st* infected cell. Magnification 10,500 x (bar = 2 μm).
N = nucleus, NS = nucleolus, NE = nuclear envelope C = cytoplasm, V = virion

D. Higher magnification of a cytoplasmic region of a BV-*w,st* infected cell. Magnification 255,000 x (bar = 0.08 μm). N = nucleus, NE = nuclear envelope, V = virion, C = cytoplasm.

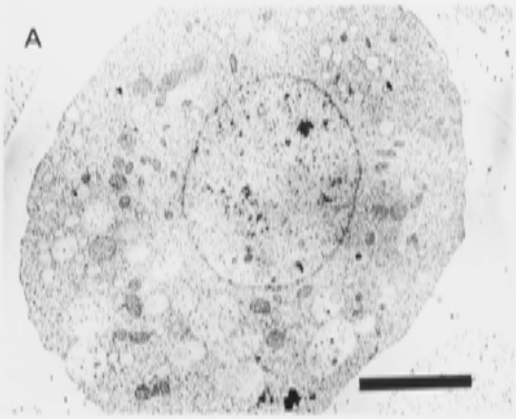
A

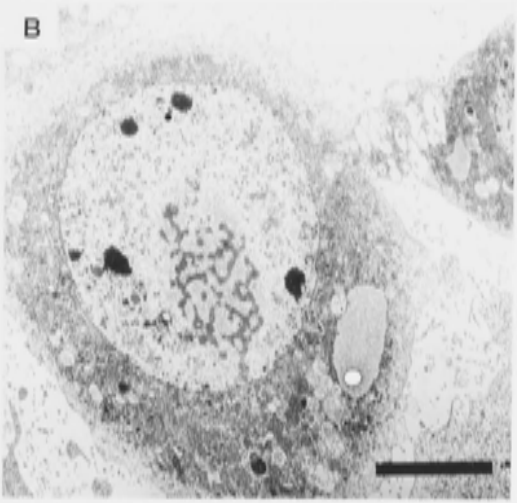
B

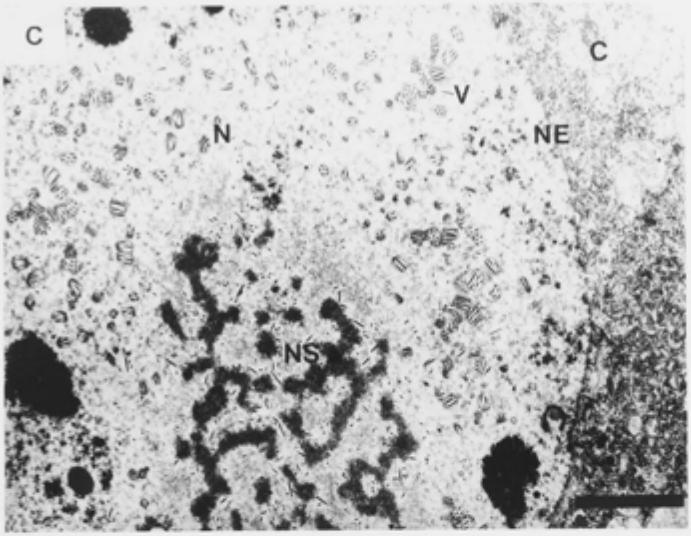
C
C
V
N
NE
NS

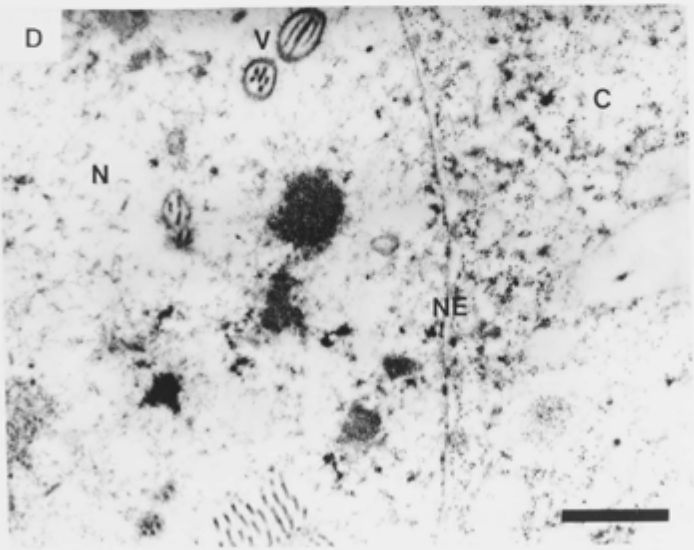
D
V
C
N
NE

insect cells after recombinant baculovirus infection and that some of the White protein was reaching the plasma membrane. The confocal and flow cytometry analysis of the localisation of Scarlet protein indicated Scarlet protein was located intracellularly, however it could not be determined whether Scarlet protein was also assembling in the plasma membrane. Consequently, it seemed appropriate to test White/Scarlet expressing cells for an increase in tryptophan uptake in comparison with uninfected and control virus infected cells. This was carried out by incubating the cells with radiolabelled tryptophan and subsequently harvesting the cells at different times after infection and then quantifying the level of radiolabel uptake of the cell samples by liquid scintillation counting (as described in Section 2.6.4).

Fig. 18 illustrates graphically the counts/min versus the hours post infection of the three experimental groups: A. BV-w/s infected, B. BV-control virus infected, C. uninfected cells. The graphs illustrate that there is no significant difference in level of uptake of radiolabelled tryptophan between uninfected cells, White/Scarlet expressing cells, or control virus infected cells. This experiment was performed on two separate occasions with similar results on each occasion.

5.3 Discussion

The results presented in this chapter describe work directed towards the development of a heterologous insect cell expression system for characterising the structure and function of the White and Scarlet proteins of *D. melanogaster*. As an adjunct to this work, antibodies were raised against synthetic peptides representing protein epitopes of White and Scarlet (described in Chapter 4). The cDNA of both genes were sub-cloned into the baculovirus transfer vector pAcUW31 for the dual expression of both the White and Scarlet proteins under the control of the p10 and polyhedrin baculovirus promoter elements respectively. Recombinant baculovirus BV-*w,st* was produced by co-transfection and homologous recombination between

Fig. 18 Analysis of L-[5-^{3}H]Tryptophan uptake activity of White and Scarlet expressing cells

Sf9 cells growing as a cell monolayer in a microtitre plate were infected with the respective virus as indicated on each graph and L-[5-^{3}H]Tryptophan was added to the cells in growth medium at a concentration of 1 μCi/ml, as described in Chapter 2, Section 2.6.4. Cells were harvested at 6 hpi, 24 hpi, 31 hpi and 48 hpi and counted for radioactivity. Each time course was performed in quadruplicate and the mean plotted on the graph. The error bars represent the standard deviation of the mean.

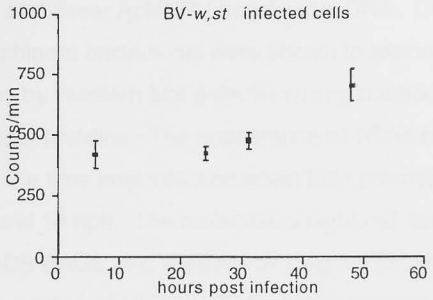
BV-w,st infected cells
Counts/min
1000
750
500
250
0
0
10
20
30
40
50
60
hours post infection

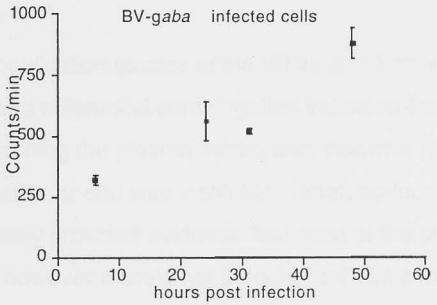
BV-gaba infected cells
Counts/min
1000
750
500
250
0
0
10
20
30
40
50
60
hours post infection

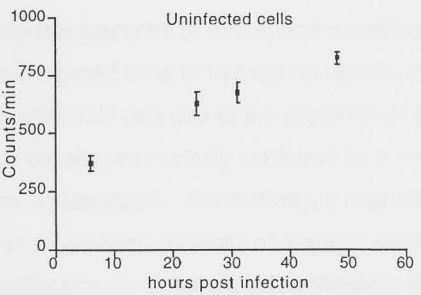
Uninfected cells
Counts/min
1000
750
500
250
0
0
10
20
30
40
50
60
hours post infection

pAcUW31*w,st* and linear AcMNPV baculovirus DNA. Cells infected with the resulting recombinant baculovirus were shown to express both the White and Scarlet proteins by Western blot detection using antibodies specific for the White and Scarlet proteins. The appearance of White and Scarlet protein coincided with the time post infection when both promoter elements were activated (around 18 hpi). The molecular weights of both White and Scarlet observed by SDS PAGE and Western blotting indicated that the proteins were not being glycosylated which was confirmed by addition of tunicamycin (an inhibitor of glycosylation) which did not alter the apparent molecular weight of White or Scarlet.

The immuno-localisation studies of the White and Scarlet protein in BV-*w,st* infected cells and differential centrifugation indicated that some of the White protein was reaching the plasma membrane, however most of the protein remained intracellular and was insoluble. Immuno-localisation of Scarlet using anti-stNT antibody provided evidence that most of the protein was intracellular and insoluble, however it could not be ruled out that a low level - which could not be detected by Western blotting - might be reaching the plasma membrane and assembling with the White protein. A further antibody recognising an extracellular epitope of Scarlet would have been useful to clarify this point. However, despite the presence of White, and possibly a low level of Scarlet, no evidence for an increased level of tryptophan uptake in Sf9 cells was observed. It is not clear whether this was due to the presence of a native tryptophan transport activity causing any activity conferred by a low level of White/Scarlet transporter to be undetectable. Alternatively, it may be that the White/Scarlet transporter is not assembling correctly or requires some form of post-translational modification for function. The Western blot analysis of White and Scarlet protein from *Drosophila* heads suggests that White and Scarlet are glycosylated or post-translationally modified in some way, *in vivo*.

The observation that most of the protein was sedimented by low speed centrifugation, as well as the presence of 14 nm particles in this cell fraction

(observed by transmission electron microscopy) strongly suggests that a large proportion of the expressed White and Scarlet protein was failing to enter the correct folding and targeting pathway resulting in misfolding and precipitation. The presence of some White at the plasma membrane however, suggests that at least some White protein (and possibly also Scarlet) leaks into an appropriate pathway for plasma membrane localisation. The observation that insoluble 14 nm particles were also present in Gaba infected cells suggests that a large proportion of the Gaba protein was also misfolded and forms very similar protein particles. It is possible that this is a common problem with over-expression of membrane proteins late in the Baculovirus infection and this is discussed below.

The possible reasons for the misfolding could be due to a combination of the following:

a) late over-expression of the heterologous proteins, at a time when the cells are under severe metabolic stress;
b) the protein sorting signals of White and Scarlet may not be recognised by the Sf9 protein sorting machinery;
c) and the absence of glycosylated White and Scarlet may contribute to protein instability and misfolding of these proteins.

Each of these factors are discussed below.

Heterologous protein expression during the late stages of baculovirus infection

It has been recently noted that a major disadvantage of the baculovirus based expression system is that the viral infection causes dramatic perturbations of the cellular environment (Lenhard and Reiländer, 1997). As a result, the insect cells may not be able to fulfil the post-translational modification and folding pathways required for the over-expressed foreign protein (Lenhard and Reiländer, 1997). This was thought to be particularly evident for polytopic

membrane proteins where correct folding of the recombinant protein is often the rate limiting step in production of the active protein (Grisshammer and Tate, 1995; Lenhard and Reiländer, 1997). The polyhedron and p10 promoters are designated "very late" promoters and therefore the over-expression of a foreign polytopic membrane protein at this late stage of viral infection - at a time when the cell is under severe metabolic stress - can often result in misfolding (Lenhard and Reiländer, 1997). This problem has been recently addressed by a combination of the use of an earlier promoter, in addition to a modified Sf9 cell line, stably transformed with the *ninaA* gene from *Drosophila* (Lenhard and Reiländer, 1997). The product of the *ninaA*[13] gene has been demonstrated to ensure the correct folding of the membrane protein rhodopsin 1 in the photoreceptor cells of *Drosophila*, as well as playing a role in protein trafficking (Schneuwly et al, 1989; Shieh et al, 1989; Stamnes et al, 1991). The combination of an early promoter element (immediate early 1 (ie1)) and the modified Sf9 cell line (Sfn) was used to express the human dopamine transporter with a five fold increase in activity of the transporter, compared to expression in standard Sf9 cells (Lenhard and Reiländer, 1997).

Protein sorting and trafficking

A possible contributing factor to the misfolding of White and Scarlet may be due to the absence of appropriate protein sorting signal sequences which are recognised by the sorting machinery of Sf9 cells. Protein sorting motifs are generally found at specific regions of the carboxy-terminal or amino-terminal cytoplasmic tails of membrane proteins and a number of examples of membrane protein sorting signals are shown in Table 1. The protein localisation prediction program PSort (Nakai and Horton, 1999) was applied to White, Scarlet and Brown and did not detect any relevant signal sequences. Close inspection of the amino acid sequences of White and Scarlet reveals no obvious sorting signals, however a possible di-leucine motif is evident in the White protein

[13] The NinaA protein is a cyclophilin homolog which are peptidyl-prolyl cis-trans isomerases and has been implicated in catalyzing protein folding (Lang et al, 1987).

Table 1 Consensus sequence motifs for membrane protein localisation

Consensus sequence & type	Protein	Reference
Tyrosine based (NPXY-type)		
FD**NPV**Y	LDL receptor	(Chen et al, 1990)
YE**NPT**Y	β-amyloid precursor protein	(Kang et al, 1987)
FENTLY	mannose receptor	(Taylor et al, 1990)
Tyrosine based (YXX∅-type)		
YK**YSK**V	CD-Mannose-6-phosphate receptor	(Canfield et al, 1991)
YTRF	transferrin receptor	(Collawn et al, 1990)
YQPL	T-cell receptor (CD3)	(Letourneur and Klausner, 1992)
GYQT**I**	lgp-A/lamp-1	(Williams and Fukuda, 1990)
GYRH**V**	lysosomal acid phosphatase	(Trowbridge and Collawn, 1993)
Di-leucine-based		
DKQTLL	CD3-γ	(Letourneur and Klausner, 1992)
ENTITYSLL	IgG Fc receptor	(Hunziker and Fumey, 1994)
LI	MHC class II invariant chain	(Salamero et al, 1996)
DEXXXLI	LIMP-II	(Höning et al, 1998)
EEXXXLL	Tyrosinase	(Höning et al, 1998)

sequence, at the N-terminal domain close to the first predicted transmembrane domain (Fig. 19). This sequence does not appear to be conserved in the Scarlet or Brown protein sequences, although it is conserved in homologs of White in other species (see Fig. 19). This sequence is similar to a di-leucine motif important for protein sorting of membrane proteins to the eucaryotic lysosome and melanosome[14], as well as the yeast vacuole (see Fig. 19). This issue is taken up again in more depth in Chapter 7 which describes the localisation of White and Scarlet in *Drosophila* eye tissue, providing new insights into the specialised nature of targeting of the White and Scarlet proteins.

Role of glycosylation in protein folding

The absence of glycosylated product is another possible contributing factor to the misfolding of White and Scarlet in Sf9 cells. Western blot analysis of White and Scarlet extracted from eye tissue indicated that the protein is glycosylated (or post-translationally modified in some other way) due to the higher molecular weight observed in comparison to the predicted molecular weight. In this study it was clear that White and Scarlet were not glycosylated in Sf9 cells (see Section 5.2.2b). It has been previously observed that membrane proteins containing 10 to 12 transmembrane domains are poorly glycosylated in Sf9 cells when over-expressed (e.g. P-glycoprotein, CFTR and serotonin receptor), particularly during the later stages of Baculovirus infection (Germann et al, 1990; Kartner et al, 1991; Tate and Blakely, 1994). This is in contrast to recombinant membrane proteins with only one or relatively few transmembrane spanning regions which are glycosylated efficiently (Grisshammer and Tate, 1995; Tordo et al, 1993). This indicates that the machinery required for glycosylation is not deficient in insect cells, but is less likely to function efficiently when faced with more complex membrane proteins harbouring multiple transmembrane regions.

---

[14] Melanosomes and pigmented organelles containing melanin and are found in eucaryotic melanocytes.

Fig. 19 Comparison of signal sequences of membrane proteins targeted to lysosomes and melanosomes with a possible signal sequence of White

Illustrated here are similarities between a possible sorting signal identified in the White amino-terminal domain, and dileucine-based sorting signals in a number of membrane proteins targeted to the melanosome and to the lysosome of eucaryotes and vacuole of yeast (the yeast vacuole is considered to be equivalent to the eucaryotic lysosome). This diagram was reproduced in part from a review by (Odorizzi et al, 1998). The dileucine-based sequences are boxed, and the surrounding residues are shown, including conserved glutamic acid residues (bold-face) located upstream of the dileucine. The number of additional residues either side of the motif sequence is indicated over a solid line. The positions of the N- or C-termini and transmembrane domains (TMDs) are also shown.

Abbreviations are as follows: dWhite, *Drosophila melanogaster* White; Lc, *Lucilia Cuprina* (Australian sheep blowfly); Cc, *Ceratitis capitata* (Mediterranean fruit fly); Ag, *Anopheles gambiae* (African malaria mosquito); hWhite, human White homolog*; mWhite, mouse White homolog* .

---

* Homologs of the *Drosophila* White protein have been identified in mouse and humans (Chen et al, 1996; Croop et al, 1997; Savary et al, 1996), however homologs of Brown and Scarlet have not been identified in mammals. The function of mammalian homologs of White has not yet been determined.

White related proteins

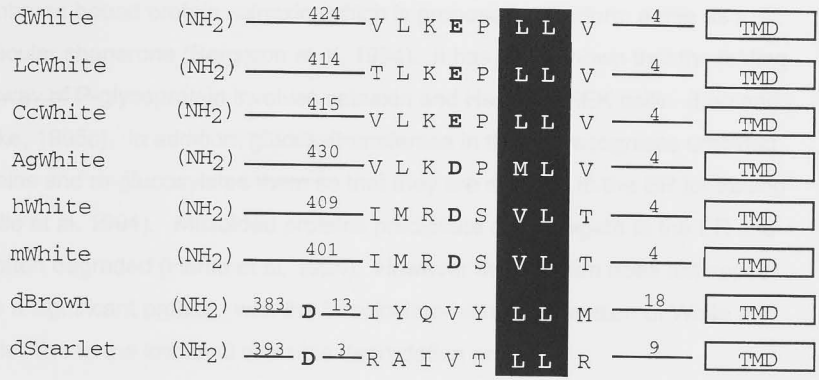

Melanosomal membrane proteins

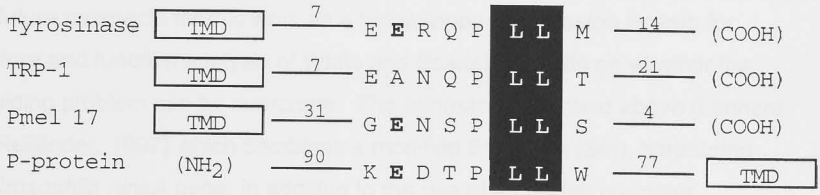

Lysosome and yeast vacuole membrane proteins

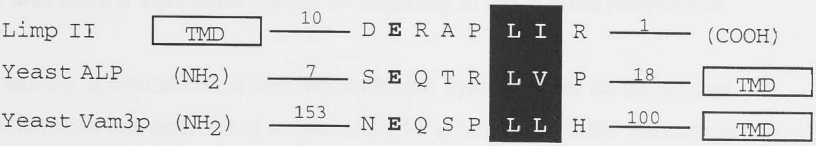

Although glycosylation may not always be required for function, it is often required during the folding pathway and for stabilisation of the protein (reviewed in (Lis and Sharon, 1993)). Glycosylated proteins bind specifically to the membrane bound protein calnexin, which is proposed to perform a role as a molecular chaperone (Bergeron et al, 1994). It has been shown that the folding pathway of P-glycoprotein involves calnexin and Hsc70 in HEK cells (Loo and Clarke, 1995c). In addition, glucosyltransferase in the ER recognises unfolded proteins and re-glucosylates them so that they are retained in the ER for folding (Hartle et al, 1994). Misfolded proteins precipitate or aggregate at the ER and are often degraded (Hartle et al, 1994). However degradation does not appear to be a significant problem with the baculovirus-based expression of White and Scarlet due to the low level of visible degradation products.

Future prospects

The future prospects for this work as a heterologous expression system for structure and function analysis of White and Scarlet depends on whether the misfolding problem can be overcome. The approach described above (Lenhard and Reiländer, 1997) which combines a modified Sf9 strain (Sfn), harbouring the *Drosophila ninaA* gene, in addition to the use of an earlier promoter element, to drive expression, would be a feasible course of action. In addition to this, the introduction of an appropriate plasma membrane signal sequence, could also have a significant impact on targeting to the plasma membrane.

Alternatively, a solubilisation and reconstitution system could be developed. This technique has been used successfully for a number of ABC transporters, including both human P-glycoprotein (Dong et al, 1996; Shapiro and Ling, 1995; Urbatsch et al, 1994), and CFTR, (Bear et al, 1997; Li et al, 1996a; Li et al, 1996b). Chaotropic agents such as urea, guanidine HCl, or SDS are often used to completely denature and solubilise the proteins from protein aggregates or inclusion bodies obtained through *E. coli* based or eucaryotic based expression systems, followed by removal of the denaturant and addition

of membrane phospholipids, resulting in reconstitution of the membrane protein into proteoliposomes. In some cases e.g. P-glycoprotein, the use of denaturants is not required and solubilisation can be achieved using non-denaturing detergents such as octyl-glucoside (Urbatsch et al, 1994). The protein particles observed in this work - believed to be White and Scarlet protein - are not typical of previously described inclusion bodies in Sf9 cells, which form very large, electron dense inclusions within the cytoplasm (Barber et al, 1990; Matsuura et al, 1987). The small size of the White and Scarlet protein particles may allow their solubilisation with non-denaturing detergents.

CHAPTER 6

EXPRESSION OF THE WHITE ATP BINDING DOMAIN IN *E. coli*

6. EXPRESSION OF THE WHITE ATP BINDING DOMAIN IN *E. coli*

6.1 Introduction

The aim of the work described in this chapter was to develop a system for studying the structure and function of the ATP binding domains of the White, Scarlet and Brown proteins of *D. melanogaster*. As a first step towards this goal, attention was focused on the expression and partial purification of the White nucleotide binding domain (NBD), in order to develop a system which could then be applied to the NBDs of Scarlet and Brown. Expression of the full length *white* encoded subunit has been previously attempted in this laboratory, however was unsuccessful largely due to low expression levels and to the insolubility of the protein. For this reason, the expression of the NBD on its own, was thought to provide a much better chance for high expression levels and solubility. The NBD of the White protein, as well as those of other ABC transporters, have a high degree of hydrophilicity as predicted from sequence and hydropathy analysis. In addition, the strategy of expressing and purifying the NBD on its own, has been used successfully in the functional characterisation of both NBD 1 and 2 of CFTR (Gruis and Price, 1997; Ko et al, 1997; Randak et al, 1995), and P-glycoprotein (Dayan et al, 1996), as well as for procaryotic ABC transporters (Koronakis et al, 1993).

The power of the technique of heterologous expression and purification of the NBD alone - for gaining insights into the structure and function - has been elegantly shown in studies of the NBDs of CFTR. It has been shown that NBF 1, in the absence of any CFTR transmembrane domain, was able to conduct anions across a planar lipid bilayer and that the channel activity was modulated by ATP (Arispe et al, 1992). This finding challenged the earlier predicted structural models based on sequence and hydropathy analysis that the NBDs of CFTR and other ABC transporters are intracellular and do not

span the membrane (Higgins et al, 1986). It has also been shown that the CFTR NBDs, by themselves, are capable of spanning the eukaryotic cell plasma membrane and are accessible from the outside of the cell (Gruis and Price, 1997). These findings were in agreement with earlier reports that the bacterial histidine transporter NBD, namely HisP protein, was also surface-accessible (Baichwal et al, 1993). These studies suggest that the NBDs of ABC transporters may form an integral part of the channel or transport lumen. Although the structure of HisP is now known (Hung et al, 1998), the extracellular accessibility could not have been predicted from the structure alone. It is only biochemical and biophysical studies such as those mentioned above, that can provide such insights, particularly in the absence of a crystal structure of the complete transporter in its various conformational states between open and closed.

This work represents the first steps towards the development of a new model system for studying not only ATP binding and hydrolysis activity of this domain of the *Drosophila* transporters, but also for protein-protein interactions. The proposed importance of intracellular loops as an interface between the NBD and TM domains was introduced in Chapter 1, Section 1.4. Work towards the development of an experimental approach to investigate interactions between the predicted intracellular loop between TM 2 and TM 3 (see Fig. 1), and the White NBD, and the effect of the mutation identified in the w^{ET87} allele (Chapter 3), is investigated.

The experimental strategy used in this work, utilises fusion protein technology which is a well established technique used for the over-expression of heterologous proteins in *E. coli* (Uhlen and Moks, 1990). Recombinant DNA technology allows relatively easy construction of gene fusions. There are many specialised plasmid vectors available commercially with convenient multiple cloning sites allowing insertion of the gene of interest, in frame with the fusion partner, for expression in *E. coli*. A number of different proteins have been utilised as fusion partners, and advantage is taken of particular

Fig. 1 Model of the White/Scarlet transport complex

This cartoon illustrates the possible interactions which may occur between the nucleotide binding domains (NBDs) and intra-helical loop regions. Evidence of such interactions in other ABC transporters was discussed in Chapter 1. The position of the mutation identified in the eye colour mutant w^{ET87} (G509D) is highlighted and the sequence representing the wild type and mutant loops is provided. The interaction between the White NBD and the wild type and mutant forms of this loop is investigated in this chapter.

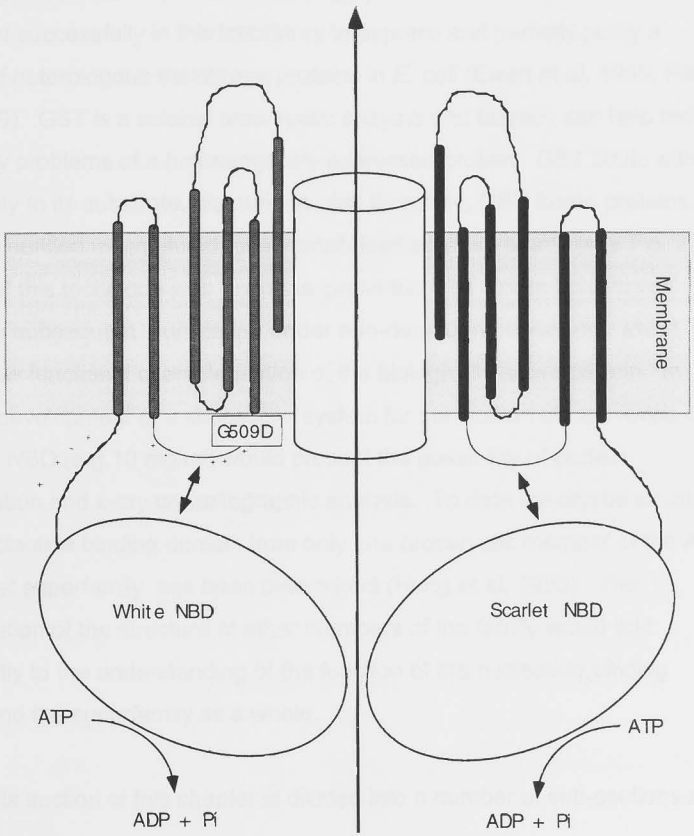

Loop 2-3 peptides:

C M R E A R S R L Y R C D T Y F L G K T I A E wild type

D w^{ET87} G509D mutant

characteristics or properties of the protein (e.g. substrate binding affinity can be used as an affinity tag). Another advantage of expressing heterologous proteins in *E. coli* as fusion proteins, is the increased solubility and decreased proteolytic degradation often observed compared to expression of the foreign protein alone (Uhlen and Moks, 1990).

Glutathione-S-transferase (GST) was chosen as the fusion partner for the White NBD. GST fusion protein technology (Smith and Johnson, 1988) has been used successfully in this laboratory to express and partially purify a number of heterologous membrane proteins in *E. coli* (Ewart et al, 1996; Piller et al, 1999). GST is a soluble procaryotic enzyme and thereby can help reduce insolubility problems of a heterologously expressed protein. GST binds with high affinity to its substrate, glutathione, and therefore, GST fusion proteins can be affinity purified using glutathione-immobilised agarose beads (see Fig. 2). The aim of this technique was to over-express the GST-White NBD fusion protein for subsequent purification under non-denaturing conditions which would allow functional characterisation of the biologically active protein. In addition, development of a successful system for purification of high levels of the White NBD (e.g.10 mg/ml) would present the possibility of protein crystallisation and x-ray crystallographic analysis. To date the crystal structure of the nucleotide binding domain from only one procaryotic member of the ABC transporter superfamily has been determined (Hung et al, 1998). The determination of the structure of other members of the family would add significantly to the understanding of the function of the nucleotide binding domain and the superfamily as a whole.

The results section of this chapter is divided into a number of sub-sections as follows:

* **Construction of expression vectors**. This part describes the *E. coli* plasmid expression vectors used for expression of the *white* NBD. In addition, the site directed mutagenesis of the Walker motif A for subsequent functional studies is described.

* **Purification trials**. A number of difficulties were encountered with the attempted purification of the White NBD and this section summarises the different conditions which were trialed in an attempt to optimise the purity and yield of the White NBD.

* **Functional studies**. ATP binding and hydrolysis studies were performed using partially purified wild-type and mutant White NBD to determine whether the protein was biologically active.

* **Protein-peptide interaction studies**. Interactions between the White NBD and a predicted intracellular loop between TM 2 and 3 of the White transmembrane domain were investigated.

6.2 Results

6.2.1 Construction of *E. coli* plasmid vectors for expression of the White NBD as a GST fusion protein

A number of *E. coli* plasmid expression vectors were constructed in this work and these are described in the first part of the results section. They are based on the plasmid p2GEX (see Chapter 2 Section 2.4 for a full description of this and related plasmids). This vector in turn was based on the commercially available vector pGEX-4T-1 (Pharmacia) which was modified by our laboratory to incorporate an additional GST gene; one which will act as the 5' fusion partner to the *white* NBD; and the other which is expressed as unfused GST. This construct was found in some cases to aid solubility of heterologously over-expressed proteins, as well as decrease degradation of the fusion protein and was the original concept of our Group Leader G Cox. The reasoning for this is due to the high propensity of GST monomers to dimerize (Reinemer et al, 1991), and when a GST fusion protein is expressed without free GST present, some GST fusion proteins may aggregate and become unstable due to the steric hindrance to the dimerization caused by the heterologous protein fused to the GST. The effect of the presence of unfused GST is tested here and was consistent with the above interpretation. The theory behind the purification of GST-fusion protein is shown in Fig. 2.

Fig. 2 Affinity purification by glutathione-agarose chromatography and Ni-NTA affinity chromatography

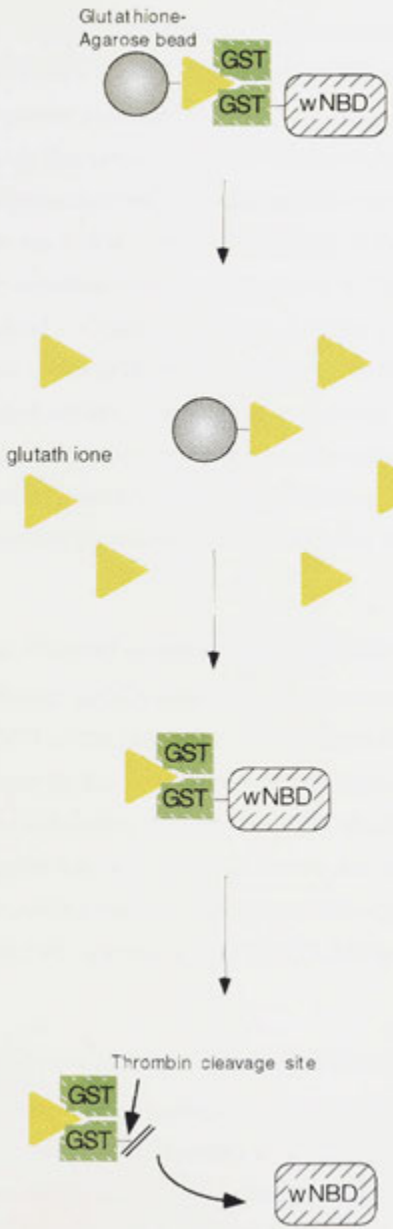

GST fusion protein over-expressed in *E. coli* is partially purified from fractions containing fusion protein by binding to glutathione-agarose beads.

Fusion proteins are eluted from glutathione-agarose by incubation with reduced glutathione.

Partially purified fusion protein

The wNBD is released from its GST fusion partner by digestion with thrombin.

6.2.1.a Plasmid construct pGEX4T1,wNBD

A DNA fragment encoding the White nucleotide binding domain (NBD) (nucleotides 1 to 1293 of the *white* cDNA; amino acids 1 to 431 of White protein) (see Appendix 1) was amplified by PCR using oligonucleotides 94-6 and 94-5 (the sequences of these oligonucleotides are listed in Section 2.14). The oligonucleotides were designed to incorporate *Bam*HI and *Eco*RI restriction sites at the 5' and 3' ends respectively of the amplified DNA fragment. The 1.3 Kb amplified PCR product (shown in Fig. 3A) was purified and then ligated (described in Chapter 2, Section 2.3) into the multiple cloning site of the plasmid vector pGEX41T, resulting in the final construct which was named pGEX41T,*w*NBD. The plasmid map of this construct is illustrated in Fig. 3B. Fig. 3C shows restriction analysis of a sub-clone, where a *Bam*HI and *Eco*RI restriction digest of pGEX41T,*w*NBD resulted in the predicted fragment sizes representing the vector DNA (4.9 Kb) and the *w*NBD DNA (1.3 Kb).

6.2.1.b Plasmid construct p2GEX,wNBD

The plasmid p2GEX,*w*NBD was constructed in the same way as described for pGEX4T1,*w*NDB (Section 6.2.1a), except that the plasmid p2GEX was used as the vector for the *w*NBD cDNA PCR fragment. The plasmid map of this construct is illustrated in Fig. 3D. Fig. 3E shows restriction analysis of a successful sub-clone where a *Bam*HI and *Eco*RI restriction digest of p2GEX,*w*NBD resulted in the predicted fragment sizes representing the vector DNA (6.1 Kb) and the *w*NBD DNA (1.3 Kb).

6.2.1.c Introduction of a hexa-histidine motif into p2GEX,wNBD

A DNA fragment encoding a six-histidine repeat motif was introduced into the plasmid vector p2GEX,*w*NBD at the 5' of the *white* NBD in order to provide a second affinity tag and enhance purification. Two complimentary oligonucleotides (96-61 and 96-62) (sequences provided in Section 2.14) were

Fig. 3 Plasmid maps and restriction analysis of p2GEX,*w*NBD and pGEX4T1,*w*NBD.

A. The 1.3 Kb PCR product of a reaction amplifying the *white* cDNA encoding the nucleotide binding domain (NBD). This product was subcloned into the plasmid vectors shown in B and D.

B. Plasmid map of pGEX4T1,*w*NBD. A full description of the plasmid vector is provided in Chapter 2, Section 2.4. The 1.3 Kb PCR product encoding the White NBD was sub-cloned into the *Bam*HI and *Eco*RI restriction site as a C-terminal fusion to GST.

C. Agarose gel electrophoresis analysis of DNA fragments resulting from a *Bam*HI and *Eco*RI restriction digest of pGEX4T1,*w*NBD. The 4.9 Kb vector, and 1.3 Kb *w*NBD DNA can be seen.

D. Plasmid map of p2GEX,*w*NBD. A full description of the plasmid vector p2GEX is provided in Chapter 2, Section 2.4. This construct harbours an addition, unfused GST gene. The 1.3 Kb PCR product encoding the White NBD was sub-cloned into the *Bam*HI and *Eco*RI restriction site as a C-terminal fusion to GST.

E. Agarose gel electrophoresis analysis of DNA fragments resulting from a *Bam*HI and *Eco*RI restriction digest of p2GEX,*w*NBD. The 6.1 Kb vector, and 1.3 Kb *w*NBD DNA can be seen.

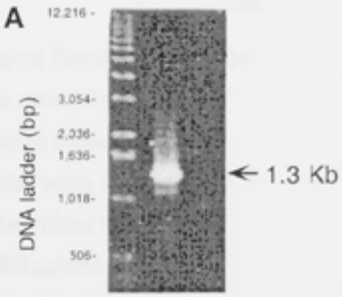
A
12,216 -
3,054-
2,036-
1,636-
1,018-
506-
DNA ladder (bp)
1.3 Kb

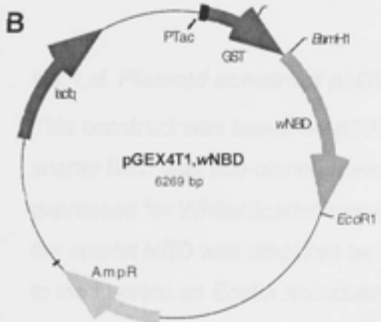
B
PTac
GST
BamHI
lacI
wNBD
pGEX4T1,wNBD
6269 bp
EcoR1
AmpR

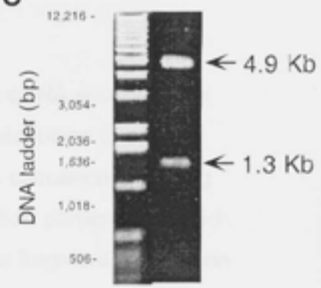
C
12,216 -
3,054-
2,036-
1,636-
1,018-
506-
DNA ladder (bp)
4.9 Kb
1.3 Kb

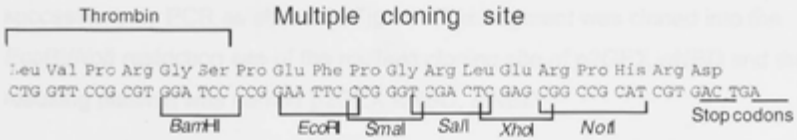
Thrombin
Multiple cloning site
Leu Val Pro Arg Gly Ser Pro Glu Phe Pro Gly Arg Leu Glu Arg Pro His Arg Asp
CTG GTT CCG CGT GGA TCC CCG GAA TTC CCG GGT CGA CTC GAG CGG CCG CAT CGT GAC TGA
BamHI
EcoRI
SmaI
SalI
XhoI
NotI
Stop codons

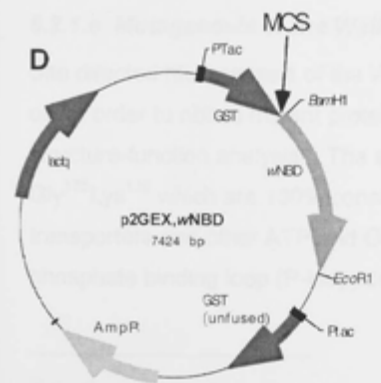
D
MCS
PTac
GST
BamHI
lacI
wNBD
p2GEX,wNBD
7424 bp
EcoR1
GST
(unfused)
Ptac
AmpR

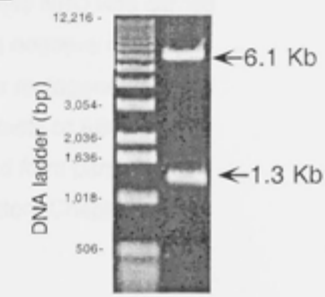
E
12,216 -
3,054-
2,036-
1,636-
1,018-
506-
DNA ladder (bp)
6.1 Kb
1.3 Kb

designed to encode a six histidine repeat, with overhanging *Bam*HI 'sticky ends'. Equal quantities of each oligonucleotide (0.3 μg/μl) were mixed in water and heated to 100°C, then cooled slowly to room temperature to allow the oligonucleotides to anneal. The annealed oligonucleotides were then ligated into the *Bam*HI digested, and phosphatased vector as described in Chapter 2, Section 2.3. The resulting plasmid (named p2GEX,*w*NBD$_{6his}$ was sequenced over the region of the inserted hexa histidine to ensure the insert was correctly oriented and that it was in frame with the *GST* gene and *white* NBD (data not shown).

6.2.1.d Plasmid construct p2GEX,wNBD, stNBD

This construct was based on p2GEX,*w*NBD however the cDNA encoding the *scarlet* NBD was sub-cloned downstream of the GST-*white* fusion to be co-expressed for White/Scarlet interaction tests. The cDNA sequence encoding the *scarlet* NBD was amplified by PCR using oligonucleotide primers designed to incorporate an *Eco*RI restriction site at the 5' end of the fragment, in addition to the UncE pregenic sequence[15] upstream of the start codon, and a *Not*I restriction site at the 3' end. The *scarlet* NBD fragment was amplified successfully by PCR as shown in Fig. 4. This fragment was cloned into the *Eco*RI/*Not*I restriction site of the multiple cloning site of p2GEX,*w*NBD and the resulting plasmid was named p2GEX,*w*NBD, *st*NBD.

6.2.1.e Mutagenesis of the Walker motif A of the white NBD

Site directed mutagenesis of the Walker motif A of the *white* NBD was carried out in order to obtain mutant protein which would act as a negative control for structure-function analysis. The amino acids targeted for mutagenesis were Gly^{135}Lys^{136} which are 100% conserved in the Walker A motif of ABC transporters and other ATP and GTP binding proteins and form part of the phosphate binding loop (P-loop) described in the introductory Chapter 1,

---

[15] *uncE* gene of *E.coli* encodes the c subunit of ATPsynthase and the uncE pregenic sequence contains a ribosome binding site and results in high expression in *E. coli* (Solomon et al, 1989).

Fig. 4 Plasmid construct p2GEX,*w*NBD,*st*NBD

This plasmid vector p2GEX, *w*NBD,*st*NBD was designed for co-expression of the following proteins:

1. GST-wNBD fusion protein
2. Unfused GST
3. stNBD

A. Physical map of the p2GEX,*w*NBD,*st*NBD plasmid.

B. Amplified PCR product representing cDNA encoding the NBD of Scarlet. Plasmid DNA harbouring the *scarlet* cDNA was used as template.

C. Agarose gel electrophoresis analysis of an *Eco*RI/*Not*I restriction digest of p2GEX,*w*NBD,*st*NBD after successful sub-cloning of *st*NBD amplified by PCR. The *st*NBD insert (1,300 bp) and the vector DNA (7,430) are labelled).

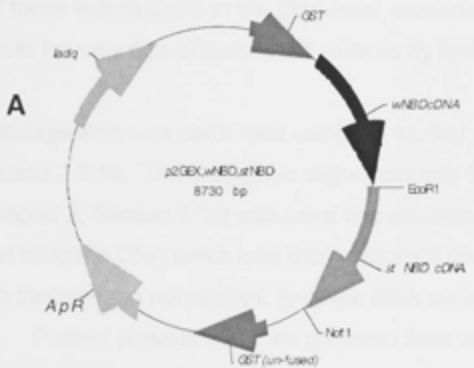

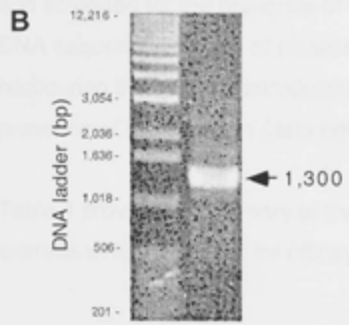

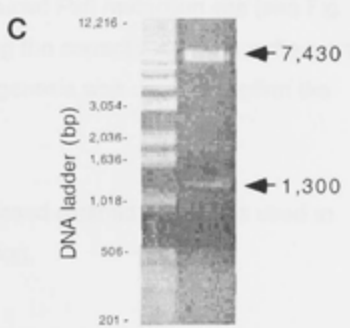

Section 1.5.2a. Mutations of this motif have been shown to completely knock-out function of a number of ABC transporters (Cox et al, 1989; Ewart et al, 1994; Mimura et al, 1991) and reduce ATP binding and hydrolysis activity (Mimura et al, 1991). In this work, $Gly^{135}Lys^{136}$ were mutated to $Leu^{135}Gln^{136}$ which is a non-conservative mutation expected to alter the structure in the vicinity of the P-loop and thereby substantially reduce ATP binding activity. Mutagenesis of this site has been performed previously and the mutant *white* gene was transformed into w^0 flies carrying a large deletion in the endogenous *white* gene (Ewart et al, 1994). The mutant *white* gene carrying the $Leu^{135}Gln^{135}$ substitutions failed to restore eye pigmentation in the transformants which showed that the mutant White protein was unable to support the function of either White/Scarlet, or White/Brown transporters (Ewart et al, 1994). The oligonucleotide used for the introduction of these substitutions at the DNA level, were designed to introduce a unique *Pst*I site for selection of successful mutants by restriction mapping.

Site directed mutagenesis was performed using the Kunkel method described in Chapter 2, Section 2.2.10. The mutagenic oligonucleotide 91-122 (sequence provided in Chapter 2, Section 2.14) was used and annealed to uracil-containing single stranded template DNA which was then passaged through *E. coli* strain XL1Blue which destroys the non-mutant template DNA while replicating the mutant strand. Purified plasmid was then prepared from transformant colonies and screened for the presence of the introduced *Pst*I restriction site (see Fig. 5). DNA sequence analysis of plasmids showing the correct restriction pattern and harbouring the *Pst*I site introduced by mutagenesis was used to confirm the presence of the mutation (data not shown).

Table 1 provides a summary of the pGEX based plasmid constructs used to express wNBD in *E. coli* for affinity purification.

Fig. 5 Site directed mutagenesis of $G^{135}K^{136}$ of the White NBD

The mutation $G^{135}K^{136} \rightarrow LQ$ within the Walker A motif introduces a *Pst*I restriction site. The Kunkel method of mutagenesis was performed (described Chapter 2) using single stranded DNA template prepared using the *E. coli* plasmid vector pBSK$^-$. When mutagenesis was complete, *w*NBD was sub-cloned into p2GEX and named p2GEX,*w*NBDmut 1.

A. Plasmid map of the plasmid construct pBSK$^-$,*w*NBDmut1 showing predicted fragments which would result from a *Pst*I/*Not*I double digest.

B. *Pst*I/*Not*I double digest showing the successful introduction of the *Pst*I restriction site (lane 1). Lane 2 is pBSK$^-$,*w*NBD prior to mutagenisis which results in a single DNA band of around 4,200 bp.

C. Plasmid map of plasmid p2GEX,*w*NBDmut 1 showing predicted fragments which would result from a *Pst*I/*Not*I double digest.

D. *Pst*I/*Not*I double digest showing correct restriction pattern (labelled) as predicted in **C** (lane 1). Lane 2 is p2GEX,*w*NBD prior to mutagenesis which results in the bands 4380, 2145 and 900 bp.

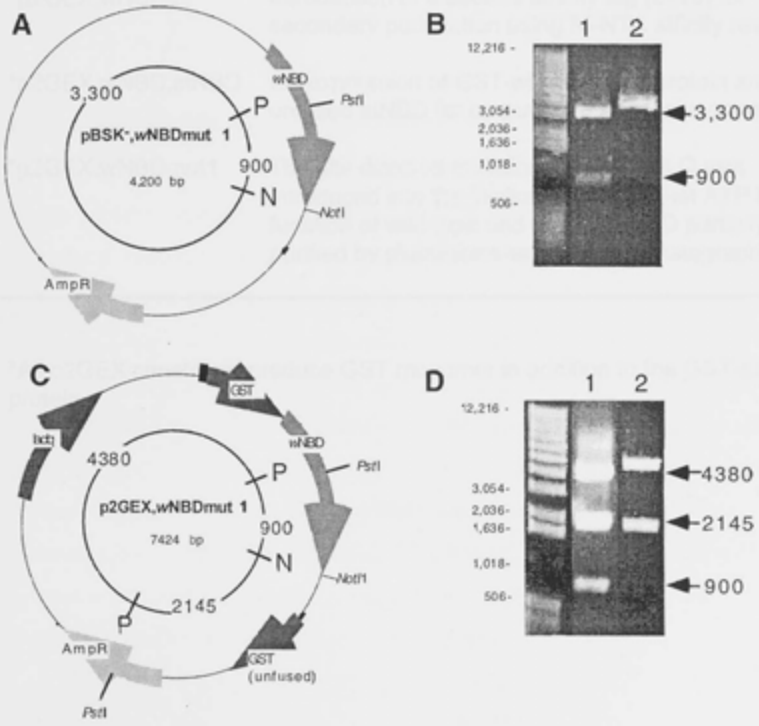

Table 1 Plasmid constructs for over-expression of wNBD in *E. coli* for subsequent affinity purification and functional analysis

Plasmid name	Use
pGEX4T1,wNBD	Over-express GST-wNBD fusion protein for affinity purification using glutathione-agarose chromatography. No unfused GST monomer.
*p2GEX,wNBD	Co over-expression of unfused GST and GST-wNBD to improve yield of fusion protein obtained by affinity purification.
*p2GEX,wNBD$_{6his}$	Introduction of a second affinity tag (6-his) for secondary purification using Ni-NTA affinity resin.
*p2GEX,wNBD,stNBD	Co-expression of GST-wNBD fusion protein and unfused stNBD for co-purification/interaction analysis.
*p2GEX,wNBDmut1	The site directed mutation $G^{135}K^{136} \rightarrow LQ$ was introduced into the Walker A motif to test ATP binding function of wild-type and mutant wNBD partially purified by glutathione-agarose chromatography.

*All p2GEX constructs produce GST monomer in addition to the GST-fusion protein.

6.2.2 Expression and partial purification of the *white* NBD

6.2.2.a Expression of GST,wNBD fusion protein in E. coli

The plasmid p2GEX,*w*NBD was transformed into *E. coli* strain AN3700 and expression of the GST,wNBD was analysed by SDS PAGE and Western blot detection over a time course. Fig. 6A shows the detection of the fusion protein from whole cell samples, and its increase in quantity over a time period between 0 and 3 hours after inducing expression from the pTac promoter by the addition of IPTG. A low level of fusion protein was detected at time 0 indicating that the pTac promoter element is not completely repressed by the Laq I^q represser. This low level of fusion protein did not inhibit growth since high cell densities were obtained prior to induction. After induction rapid cell growth halted due to the over-expression of the heterologous protein.

6.2.2.b Cell fractionation of cells expressing GST-wNBD fusion protein

In order to determine the sub-cellular localisation of the expressed GST-wNBD fusion protein, cells were fractionated by differential centrifugation (described in Chapter 2, Section 2.6.5a). Fig. 6B is an SDS PAGE and Western blot analysis of the cell fractions obtained from the cytoplasm, crude membranes and cell debris[16]. It can be seen from the SDS PAGE and Western analysis shown in Fig. 6A and B that most of the fusion protein was found in the insoluble cell debris fraction and also in the membrane fraction, and essentially no fusion protein was detected in the soluble, cytosolic fraction. This result gave a strong indication that most of the fusion protein was insoluble and that some was associating with the cell membrane. The following sections describe efforts to optimise some of the conditions necessary in order to solubilise the GST-wNBD from the membrane and cell debris fractions.

---

[16] Cell debris is the term given to cellular material which can be separated from the soluble and membrane fractions by low speed centrifugation (10,000 rpm). This includes insoluble proteins and other insoluble cell components such as the cell wall.

Fig. 6 Expression of GST-wNBD fusion protein and its detection in different cell fractions of *E. coli*

1L of *E. coli* strain AN3701, p2GEX,wNBD was grown to late log phase and induced with 0.1 mM IPTG for 3 hrs.

A. 50 μl samples of cell culture were taken at the times (mins) indicated and mixed with 2 x SDS PAGE sample buffer, and analysed by SDS PAGE (Coomassie stained) and Western blotting using anti-wNT antibody.

B. Cell fractions were separated by differential centrifugation (described Chapter 2, Section 2.6.5). Each fraction was resuspended to give a final volume equal to the starting volume when the cells were lysed, so that the levels of protein in each fraction could be directly compared. Samples were then analysed by SDS PAGE and Western Blotting.

Abbreviations: Smash, lysed whole cells; CD, cell debris; cyto, cytoplasm; mem, crude membrane fraction.

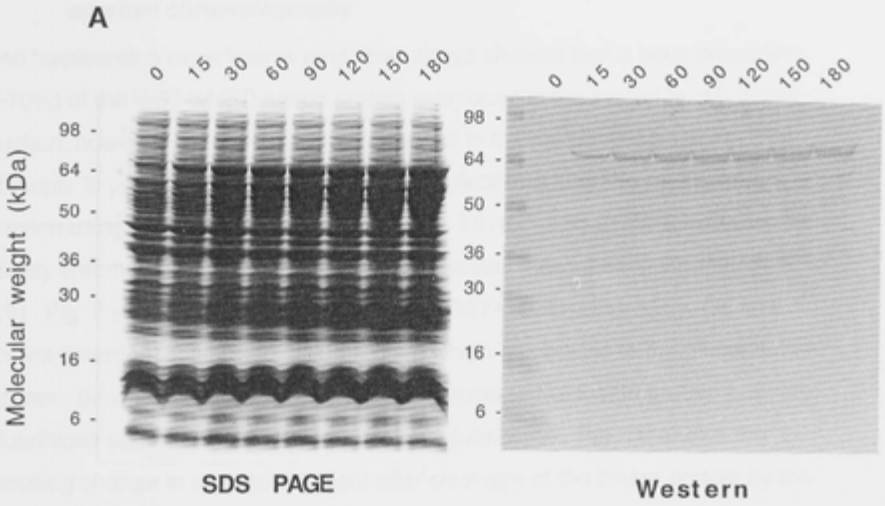
A
0 15 30 60 90 120 150 180
98
64
50
36
30
16
6
Molecular weight (kDa)
SDS PAGE
Western

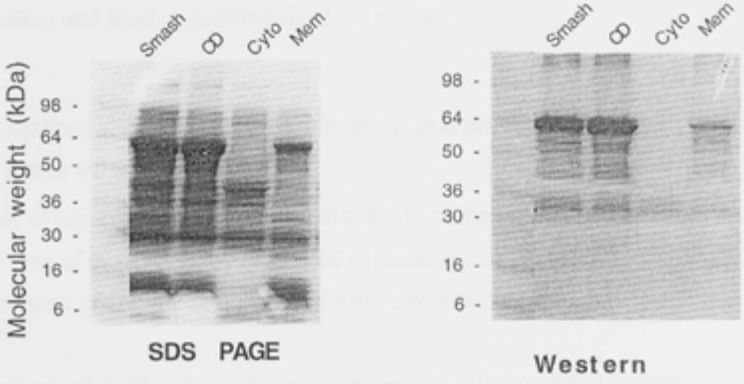
B
Smash
CD
Cyto
Mem
98
64
50
36
30
16
6
Molecular weight (kDa)
SDS PAGE
Western

6.2.2.c Partial purification of GST-wNBD fusion protein by glutathione agarose chromatography

Cell fractionation experiments described above showed that a large proportion (~70%) of the GST-wNBD fusion protein was found in the insoluble cell debris fraction, however some (~30%) was detected in the membrane fraction. First attempts to purify GST-wNBD involved the solubilisation of the membrane fraction using the non-denaturing detergents TX-100, and CHAPS, followed by affinity chromatography using glutathione-agarose (described in Chapter 2, 2.9). Fig. 7 shows the partial purification of GST-wNBD, where Fig. 7A, lane 1 shows detergent solubilised fusion protein which has bound to the glutathione-agarose beads, while lanes 2 to 5 shows removal of the fusion protein from the glutathione agarose by addition of reduced glutathione. Fig. 7B shows the resulting change in molecular weight after cleavage of the fusion protein by the addition of thrombin, from around 72 kDa, to around 47 kDa, which is the predicted molecular weight of the White NBD. This result was encouraging as it showed that the wNBD can be partially purified using this technique, from small scale cultures (1 L) at a level which is easily detectible by Coomassie Blue on an SDS PAGE gel. The following sections summarise work performed in an attempt to optimise the conditions required to obtain the highest yield, solubilisation and level of purification of the wNBD.

6.2.2.d Optimisation of yield, solubilisation and purification of the White NDB

A number of parameters were altered in order to compare different conditions with the view of increasing the final yield of partially purified wNBD. This work is summarised in Table 2 and the results are described below.

Comparison of yields of soluble partially purified GST-wNDB fusion protein using single and double GST expression vectors

As mentioned earlier in the introduction to this chapter, the p2GEX vector was thought to be superior to pGEX4T1 in that the presence of an unfused GST

Fig. 7 Expression of GST-wNBD fusion protein in *E. coli*, and partial purification by glutathione-agarose affinity chromatography

1L of *E. coli* strain AN3701, p2GEX,wNBD was grown at 30°C in LB, Glucose, Amp, Tet medium and induced with 0.1 mM IPTG at late log phase and grown for a further 3 hrs. Cells were harvested, lysed and GST-wNBD fusion protein partially purified from the solubilised membrane cell fraction (with 0.1% TX-100) by glutathione-agarose chromatography using 0.2 ml of beads. Samples for SDS PAGE were diluted 10:1 in SDS PAGE sample buffer. Samples of glutathione agarose were a 50% slurry. The fusion protein was eluted with 1 ml samples of reduced glutathione.

A. SDS PAGE and Western blot analysis of the partial purification of GST-wNBD fusion protein

Lane

1. Protein bound to glutathione-agarose.
2. 1st eluent with 100 mM reduced glutathione
3. 2nd eluent with 100 mM reduced glutathione
4. 3rd eluent with 100 mM reduced glutathione
5. 4th eluent with 100 mM reduced glutathione

B. SDS PAGE and Western blot analysis of cleavage by thrombin of the GST-wNBD fusion protein

Thrombin was added (5 units/2ml) and incubated overnight at 4°C prior to analysis by SDS PAGE.

Lane

1. GST-wNBD fusion protein prior to addition of thrombin.
2. Post thrombin cleavage.

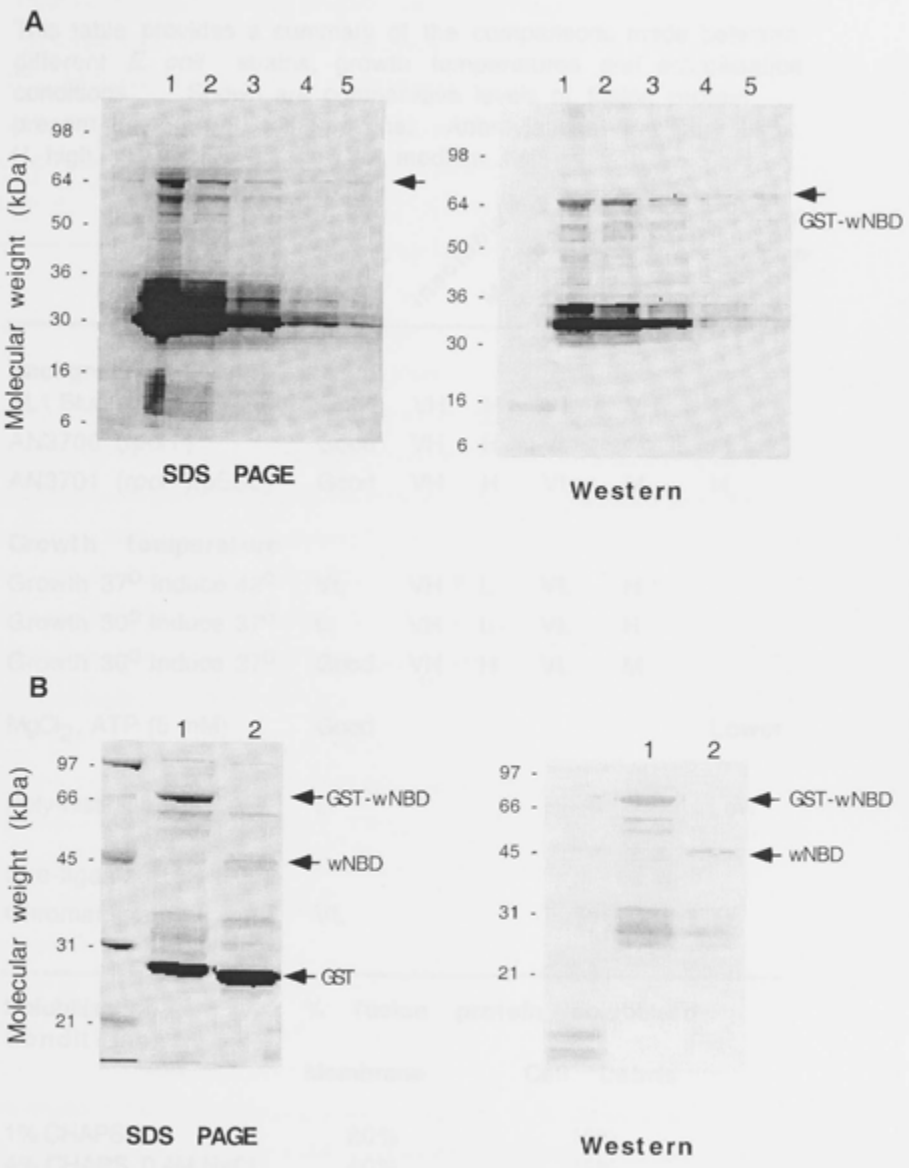
A
1 2 3 4 5
98 -
64 -
50 -
36 -
30 -
16 -
6 -
Molecular weight (kDa)
SDS PAGE
1 2 3 4 5
98 -
64 -
50 -
36 -
30 -
16 -
6 -
GST-wNBD
Western
B
1 2
97 -
66 -
45 -
31 -
21 -
Molecular weight (kDa)
GST-wNBD
wNBD
GST
SDS PAGE
1 2
97 -
66 -
45 -
31 -
21 -
GST-wNBD
wNBD
Western

Table 2 Summary of conditions tested for optimisation of expression, solubilisation and purification of GST-wNBD heterologously expressed in *E. coli*

This table provides a summary of the comparisons made between different *E. coli* strains, growth temperatures and solubilisation conditions. Shown are comparative levels of fusion protein present in different cell fractions. Abbreviations: VH, very high; H, high; VL, very low; L, low; M, medium.

	Yield	Insoluble	Membrane	Cytoplasm	Degradation	Contaminants
Background Strain						
XL1 Blue	Good	VH	H	VL	VH	M
AN3700 (*rpoH*$^-$)	Good	VH	H	VL	M	M
AN3701 (*rpoH*$^-$)(pESL)	Good	VH	H	VL	M	H
Growth temperature						
Growth 37^0 Induce 42^0	VL	VH	L	VL	H	
Growth 30^0 Induce 37^0	L	VH	L	VL	H	
Growth 30^0 Induce 37^0	Good	VH	H	VL	M	
$MgCl_2$, ATP (5 mM)	Good					Lower
Poly-histidine-Ni-NTA	L					Low
Dye-ligand Chromatography	VL					

Solubilisation Conditions	**% fusion protein solubilised**	
	Membrane	**Cell Debris**
1% CHAPS	20%	10%
4% CHAPS, 0.4M NaCl	40%	15%
0.1% TX-100	20%	10%
0.1% TX-100, 0.4M NaCl	40%	15%
DOC, 0.4M Nacl	ND	20%

enables dimerization between free and fused GST resulting in greater solubility of the fusion protein. To test that this was in fact the case with respect to the GST-wNBD fusion protein, a comparison was made of the levels of soluble GST-wNBD fusion which could be partially purified. This comparison is shown in Fig. 8 where it can be seen that a higher yield of partially purified, soluble GST-*w*NBD was obtained using the p2GEX,*w*NBD vector. As a consequence of this result, the p2GEX vector was used for the rest of the work described here.

Protease deficient background strains

The over-expression of a heterologous protein in *E. coli* causes substantial metabolic stress and the level of mis-folded proteins can cause a 'stress response' to be mounted. The *rpoH* gene encodes a sigma factor involved in regulating expression of many of the proteases and chaperones involved in the stress response, resulting in proteolytic degradation of misfolded proteins. The *rpoH* negative *E. coli* strain AN3700 (described in Section 2.13) was shown to result in a lower level of proteolytic degradation in comparison to a non-protease deficient strain XL1Blue (Table 2) and was therefore the strain used for the work described here.

The effect of altering growth and induction temperatures on proteolysis and expression levels was also tested. Levels of soluble fusion protein which could be partially purified by glutathione-agarose chromatography under the same solubilisation conditions were compared. The following experiments were performed:

Growth at 37°C, induction at 42°C

Growth at 30°C, induction at 37°C

Growth at 30°C, induction at 30°C

The results of these experiments are shown in Fig. 9. It can be seen from Fig. 9A and B, that induction at 42°C resulted in no detectible fusion protein bound to the glutathione-agarose beads. In addition induction at 42°C resulted in a decreased level of fusion protein expressed overall as judged by the lower

Fig. 8 Effect on yield of GST-wNBD fusion protein in the presence of an unfused GST

1L of *E. coli* AN3700, p2GEX,*w*NBD and pGEX41T,wNBD respectively were grown to late log phase and induced with 0.1 mM IPTG for 2 hrs. Fusion protein was partially purified from solubilised membrane fraction (0.1% TX-100), (as described in the experimental procedures). Shown is an SDS PAGE analysis of proteins from samples of glutathione-agarose beads with bound fusion protein (50% slurry of beads). The positions of GST-wNBD, groEL and GST are shown at their respective molecular weights.

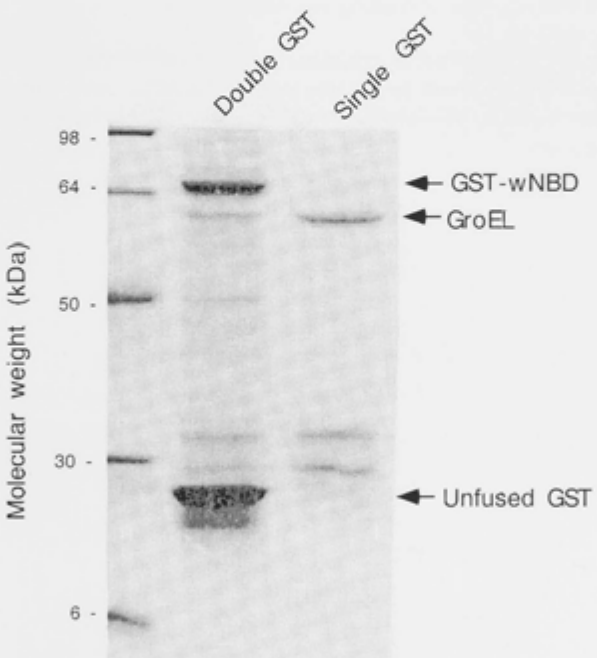

Fig. 9 Effect of growth and induction temperature on degradation and yield of GST-wNBD fusion protein

1L of *E. coli* strain AN3700, p2GEX, wNBD was grown to late log phase and induced with 0.1 mM IPTG for 2 hrs. Fusion protein was partially purified from the solubilised membrane fraction using 0.1% TX-100 (described in Chapter 2, Section 2.9) using 0.2 ml glutathione-agarose beads. Proteins bound to glutathione-agarose beads were separated by SDS PAGE on a 12% polyacrylamide gel using a 50% bead slurry diluted in 2 x SDS PAGE sample buffer. The cell debris fraction was also analysed in A.

A. Comparison of the effect of induction temperatures of 37°C or 42°C after growth at 37°C on levels of partially purified fusion protein. The protein band representing GST-wNBD is highlighted with an arrow.

B. Western blot analysis of A using anti-wNT antibody.

C. Comparison of the effect of induction temperatures of 30°C or 37°C after growth at 30°C on levels fo partially purified fusion protein. The protein band representing GST-wNBD is highlighted with an arrow.

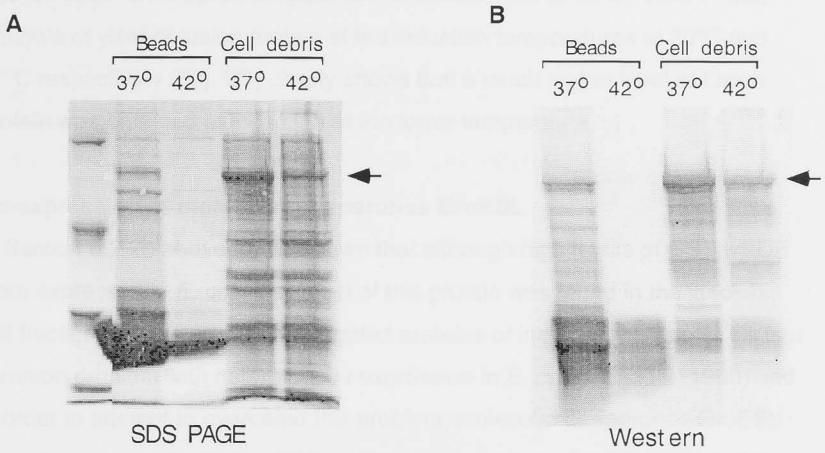
A
Beads
Cell debris
37° 42° 37° 42°
SDS PAGE
B
Beads
Cell debris
37° 42° 37° 42°
Western
C
Beads
30° 37°
SDS PAGE

level found in the cell debris. Induction at 37°C resulted in an easily detectible level of fusion protein, in addition to some degradation products detected by Western blot. A higher level of fusion protein was seen in the cell debris fraction at 37°C induction temperature, in comparison to 42°C. SDS PAGE analysis of yield of fusion protein at the induction temperatures at 30°C and 37°C respectively (Fig. 9C) clearly shows that a much higher level of fusion protein was obtained at induction at the lower temperature.

Co-expression of molecular chaperones GroESL

In Section 6.2.2b above it was shown that although high levels of GST-wNDB were expressed in *E. coli*, that most of this protein was found in the insoluble cell fraction associated with aggregated proteins or inclusion bodies. This is a common problem with heterologous expression in *E. coli* (Goeddel, 1990) and in order to attempt to overcome this problem, molecular chaperones GroESL were co-expressed with the GST-wNBD fusion protein. GroESL is part of the *E. coli* Hsp60 family of proteins expressed during the stress-response. GroESL forms a protein folding machine which binds to unfolded polypeptides and can potentiate correct folding (reviewed in (Braig et al, 1994; Georgopoulos, 1993)). The use of the molecular chaperones GroESL have been previously shown to help the folding and solubility of heterologously expressed proteins in *E. coli* (Goloubinoff et al, 1989; Lee and Olins, 1992).

Yields of soluble fusion protein were compared between strain AN3701 harbouring the plasmid pESL which expresses the GroES and GroEL subunits of GroESL, and the same strain without pESL (AN3700) (a description of these strains is provided in Chapter 2, Section 2.13). It can be seen from Fig. 10 that there was no visible difference between the levels of partially purified fusion protein. It was also noted that a large amount of a 60 kDa contaminant co-purified with the fusion protein which was shown by N-terminal sequence analysis[17] to be groEL (data not shown). The pathway for chaperone-facilitated

---

[17] N-terminal sequence analysis was performed by the Biomolecular Resource Facility of the ANU.

Fig. 10 Effect of levels of contaminating groEL protein in a strain over-expressing groESL proteins

1L of *E. coli* strains AN3700, and AN3701 (harbouring the plasmid pESL for overexpression of GroESL) both harbouring the plasmid pGEX4T1*w*NBD, were grown to late log phase and induced with 0.1 mM IPTG for 2 hrs. Fusion protein was partially purified from solubilised membrane fraction (0.1% TX-100), (as described in the experimental procedures). Shown is an SDS PAGE analysis of proteins from samples of glutathione-agarose beads with bound fusion protein (50% slurry of beads). The positions of GST-wNBD and groEL are shown at their respective molecular weights.

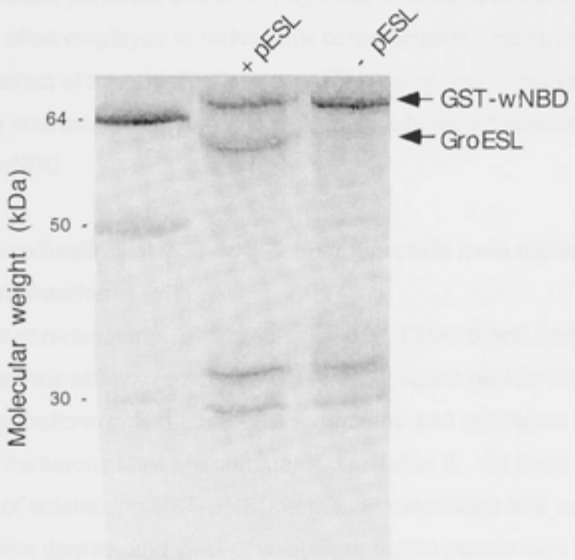

folding of proteins requires firstly that the groES subunit binds to the groEL subunit complex and secondly, ATP hydrolysis brings about the release of the folded protein. It was thought that ATP may be a limiting factor in the groESL folding pathway due to the high levels of the recombinant fusion protein being produced in the cell, in addition to the over-expression of groES and groEL. The effect of the addition of Mg^{+2} and ATP (5 mM) during solubilisation and affinity purification, on the presence of the 60 kDa contaminant, was tested and it can be seen from Fig. 11 that the presence of $MgCl_2$ and ATP reduced this contamination substantially but not completely. As a consequence of these results, the strain AN3700 which does not harbour the pESL plasmid, was routinely used for further studies. However, even with this strain, the 60 Kd GroEL contaminant persisted due to endogenous GroESL and the inclusion of Mg^{2+}ATP was often employed to reduce this contamination. However, due to the unknown effect of this practice on later ATP binding and hydrolysis studies, this procedure was usually omitted and other methods were trialed in attempt to further purify wNBD.

Detergent solubilisation of GST-wNBD fusion protein from membrane and cell debris cell fractions

Three different non-denaturing detergents (TX-100, CHAPS and deoxycholate) were tested for their ability to solubilise GST-wNBD fusion protein under different concentrations of NaCl, from the membrane and cell debris fractions. The results of numerous trials are summarised in Table 2. All three detergents were capable of solubilising GST-wNBD from both membrane and cell debris fractions to some degree, and yield of solubilised fusion protein was increased in the presence of 0.4 M NaCl. It was noted that deoxycholate solubilised a much higher level of fusion protein from the cell debris fraction, compared to TX-100 and CHAPS. However activity tests showed that wNBD partially purified from cell debris using deoxycholate was inactive (data not shown). The levels of solubilisation achieved using CHAPS and TX-100 were not visibly different. As a consequence of these studies TX-100 (0.1%), and 0.4 M NaCl were used for solubilisation and subsequent purification. TX-100 is very cheap

Fig. 11 Effect of ATP, $MgCl_2$ on the level of groEL protein

1L of *E. coli* AN3701, p2GEX, *w*NBD was grown to late log phase and induced with 0.1 mM IPTG for 2 hrs. Fusion protein was partially purified in the presence or absence of 5 mM $MgCl_2$ and 5 mM ATP, from solubilised membrane fraction (0.1% TX-100), (as described in the experimental procedures). Shown is an SDS PAGE analysis of proteins from samples of glutathione- agarose beads with bound fusion protein (50% slurry of beads). The positions of GST-wNBD, groEL and GST are shown at their respective molecular weights.

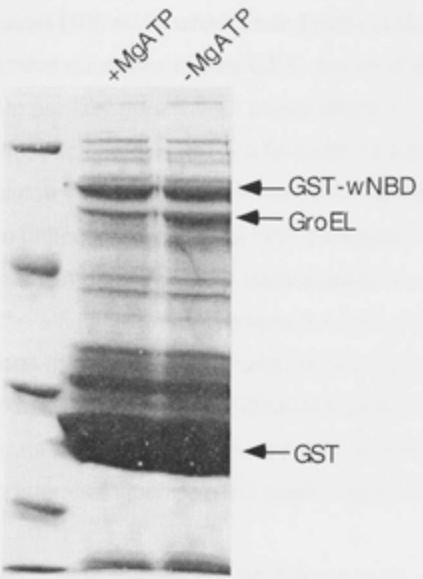

in comparison to CHAPS and does not interfere with subsequent 8-azido-ATP-affinity labelling (unlike CHAPS) (Koronakis et al, 1993) which is described in Section 6.2.3.

Additional affinity-purification utilising the six-his affinity tag, dye-ligand chromatography and HPLC cation exchange

The additional unfused GST expressed using the p2GEX,wNBD construct was shown to have a beneficial effect on the yield of soluble partially pure fusion protein (see Fig. 8), however it also resulted in high levels of contaminating GST. In order to remove GST-wNBD from the affinity resin, high levels of reduced glutathione were used (100 mM), which eluted most of the fusion protein, in addition to excessive quantities of free GST. Some of the unfused GST could be removed from partially pure wNBD preparations by removing the reduced glutathione by buffer exchange or dialysis followed by addition of a small amount of reduced glutathione beads which were then removed by centrifugation. However an unacceptable level of GST persisted. Attempts to elute wNBD alone, after thrombin digestion were unsuccessful due to the wNBD binding strongly to the affinity resin for reasons not understood. A number of different conditions (high salt, low salt and reducing agents), were trialed in an attempt to remove wNBD from the glutathione beads, however these were unsuccessful (data not shown). Additional affinity purification steps were therefore trialed in an attempt to increase the level of purity of the wNBD.

The construct p2GEX,$wNBD_{6his}$ (see Section 6.2.1c) was used to express GST-$wNBD_{6his}$ introducing an additional affinity tag to the N-terminus of the wNBD for purification using Ni-NTA resin (described in Chapter 2, Section 2.9). Fig. 12 shows an additional affinity purification step involving binding $wNBD_{6his}$ to Ni-NTA affinity resin. The $wNBD_{6his}$ protein bound to the affinity resin (Fig. 12 lane 2), and was removed from the resin with the addition of imidazole (lanes 1, 3, 4, 5). This purification trial was performed using DOC for the solubilisation of cell debris material prior to the knowledge that material purified using this detergent (or possibly due to its derivation from the cell debris) was inactive (data not

Fig. 12 Further purification of wNBD by Ni-NTA affinity purification

5L of *E. coli* AN3701, p2GEX,$wNBD_{6his}$ was grown to late log phase and induced with 0.1 mM IPTG for 2 hrs. Fusion protein was partially purified from solubilised membrane fraction usng 0.25% DOC, 0.4 M NaCl, and using 0.2 ml glutathione-agarose beads. Fusion protein was eluted with 100 mM reduced glutathione, and digested with thrombin prior to passing through a Ni-NTA column containing 0.2 ml of resin. Partially purified $wNBD_{6his}$ was eluted in 1 ml fractions from the resin with increasing levels of imidazole as indicated.

SDS PAGE and Western analysis of fractions obtained from Ni-NTA purification of $wNBD_{6his}$

Lane

1 First eluent (10 mM imidazole)
2 Proteins bound to Ni-NTA resin prior to eluting with imidazole
3 Second eluent (50 mM imidazole)
4 Third eluent (100 mM imidazole)
5 Fourth eluent (200 mM imidazole)
6 Fifth eluent (500 mM imidazole)
7 Sixth eluent (1 M imidazole)
8 Seventh eluent (1.3 M imidazole)
9 Proteins remaining bound to the resin

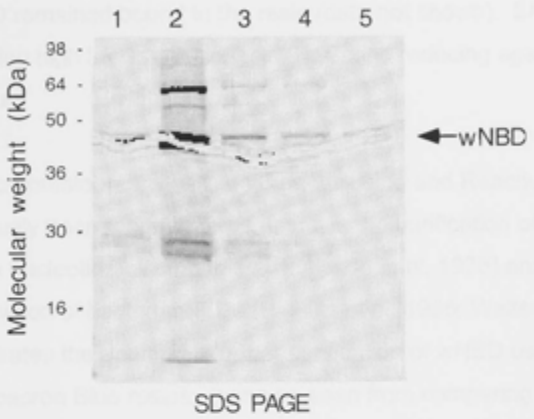

SDS PAGE

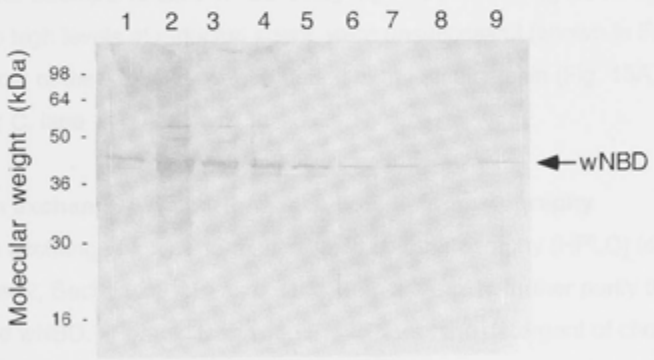

Western

shown). This purification result using the detergent deoxycholate (DOC) was encouraging, however, the yield of wNBD was much lower when TX-100 or CHAPS were tested for solubilisation. When these detergents were used, most of the wNBD remained bound to the resin (data not shown). Efforts to elute $wNBD_{6his}$ using high levels of imidazole, NaCl and reducing agents were unsuccessful.

Dye-ligand chromatography utilising Cibacron Blue and Reactive Red resins have previously been reported to be useful in the purification of many proteins containing a nucleotide binding fold (Thompson et al, 1975) and has been used in the purification of bacterial NBDs (Higgins et al, 1985; Walter et al, 1992). Fig. 13 illustrates the attempted further purification of wNBD using Reactive Red and Cibacron Blue resins. It can be seen from comparing Fig. 13A lanes 1 and 2 which represent samples before and after addition to the resin that the wNBD protein bound to the affinity resin of both Cibacron Blue and Reactive Red (Fig. 13C, lane 4), and that a large proportion of contaminating proteins were removed and found in the flow through (Fig. 13A lane 2, Fig. 13C, lane 3). However attempts to elute wNBD using Mg-ATP, increasing levels of NaCl, as well as high levels of reducing agent, were unsuccessful (shown in Fig. 13B) and most of the wNBD remained bound to the affinity resin (Fig. 13A, lane 7; B, lane 6; C, lane 11).

Cation exchange high performance liquid chromatography

Cation exchange high performance liquid chromatography (HPLC) (described in Chapter 2, Section 2.9.4) was utilised in an attempt to further purify the partially purified wNBD. For this technique CHAPS was the detergent of choice for the solubilisation of wNBD from membrane fractions because TX-100 was unsuitable due its high optical absorbance reading at 278 nm which interferes with protein detection. The iso-electric point predicted from sequence analysis of wNDB is Pi 8.95, which is substantially different to the iso-electric points of both GST (Pi 6.09) and GroEL (Pi 4.65) which are the major contaminants. A strong cation exchange column (Biorad) was chosen in an attempt to separate

Fig. 13 Reactive Red and Cibacron Blue affinity purification trials

1L of *E. coli* strain AN3701, p2GEX,*w*NBD was grown at 30°C in LB, Glucose, Amp, Tet medium and induced with 0.1 mM IPTG at late log phase. Cells were harvested, lysed and GST-wNBD fusion protein partially purified from the solubilised membrane cell fraction by glutathione-agarose chromatography (Chapter 2, Section 2.9). After digesting the GST-wNBD fusion protein with thrombin, samples were added to either 0.2 ml of Reactive Red or Cibacron Blue resin, as indicated, and attempts to elute wNBD from the dye-resin under different conditions of salt are shown. The figures illustrate SDS PAGE (Coomassie stained except where indicated) and Western blot analysis (using anti-wNT antibody).

A. Cibacron Blue

Lane

1 Sample prior to adding to Cibacron Blue
2 Unbound fraction
3 First eluent, 10 mM $MgCl_2$, ATP
4 Second eluent, 20 mM $MgCl_2$, ATP
5 Third eluent, 50 mM $MgCl_2$, ATP
6 Fourth eluent, 50 mM $MgCl_2$, ATP, 10 mM β-mercapto-ethanol
7 Protein remaining bound to resin

B. Cibacron Blue, high salt during elution

Lane

1 Sample prior to adding to Cibacron Blue
2 Unbound fraction
3 First eluent, 10 mM $MgCl_2$, ATP, 100 mM NaCl
4 Second eluent, 10 mM $MgCl_2$, ATP, 200 mM NaCl
5 Third eluent, 10 mM $MgCl_2$, ATP, 400 mM NaCl
6 Fourth eluent, 10 mM $MgCl_2$, ATP, 500 mM NaCl
8 Protein remaining bound to resin

C. Reactive Red

SDS PAGE Gel is silver stained

Lane

1 Sample prior to thrombin digestion
2 Sample post thrombin digestion
3 Unbound fraction
4 Protein bound to resin
5 First eluent, 0.4 M NaCl, 20 mM $MgCl_2$, ATP
6 Second eluent, 0.5 M NaCl, 20 mM $MgCl_2$, ATP
7 Third eluent, 0.6 M NaCl, 20 mM $MgCl_2$, ATP
8 Fourth eluent, 0.7 M NaCl, 20 mM $MgCl_2$, ATP
9 Fifth eluent, 0.8 M NaCl, 20 mM $MgCl_2$, ATP
10 Sixth eluent, 1.0 M NaCl, 20 mM $MgCl_2$, ATP
11 Protein remaining bound to resin

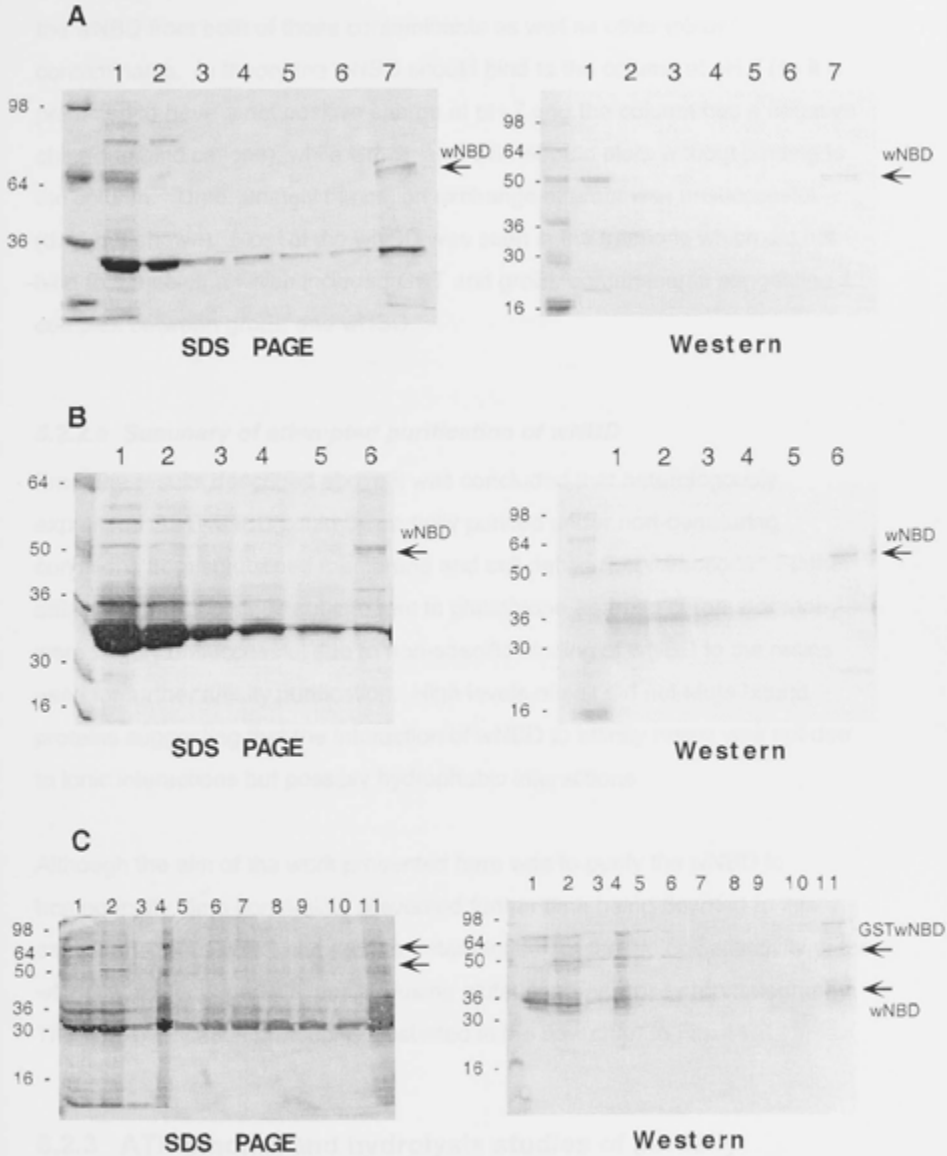
A
1 2 3 4 5 6 7
98 -
64 -
36 -
wNBD
SDS PAGE
1 2 3 4 5 6 7
98 -
64 -
50 -
36 -
30 -
16 -
wNBD
Western
B
1 2 3 4 5 6
64 -
50 -
36 -
30 -
16 -
wNBD
SDS PAGE
1 2 3 4 5 6
98 -
64 -
50 -
36 -
30 -
16 -
wNBD
Western
C
1 2 3 4 5 6 7 8 9 10 11
98 -
64 -
50 -
36 -
30 -
16 -
SDS PAGE
1 2 3 4 5 6 7 8 9 10 11
98 -
64 -
50 -
36 -
30 -
16 -
GSTwNBD
wNBD
Western

the wNBD from both of these contaminants as well as other minor contaminants. In theory the wNBD should bind to the column at pH 7 (as it is predicted to have a net positive charge at pH 7 and the column has a negative charge to bind cations), while GroEL and GST should elute without binding to the column. Unfortunately the cation exchange attempt was unsuccessful (data not shown). Most of the wNBD was seen in the fractions which did not bind to the column which included GST and groEL contaminants suggesting a complex between groEL and wNBD.

6.2.2.e Summary of attempted purification of wNBD

From the results described above it was concluded that heterologously expressed GST-wNBD could be partially purified under non-denaturing conditions from solubilised membrane and cell debris *E.coli* fractions. Further affinity purification steps subsequent to glutathione-agarose chromatography were largely unsuccessful due to non-specific binding of wNBD to the resins used for further affinity purification. High levels of salt did not elute bound proteins suggesting that the interaction of wNBD to affinity resins was not due to ionic interactions but possibly hydrophobic interactions.

Although the aim of the work presented here was to purify the wNBD to homogeneity, time constraints prevented further time being devoted to this cause, and focus was turned to the determination of the biological activity of the wNBD which was partially purified using glutathione-agarose chromatography. The final purification protocol is illustrated in the flow chart in Fig. 14.

6.2.3 ATP binding and hydrolysis studies of partially purified wNBD

In order to detect ATP binding and/or hydrolysis activity of the partially purified wNBD obtained through the work described above, the following three methods were used:

Fig. 14 Final protocol of the partial purification of wNBD

This figure summarises the purification wNBD after *E. coli* expression using strain AN3700, p2GEX,wNBD grown to late log phase at 30°C in LB medium (plus glucose and antibiotics). Cells were induced with 0.1 mM IPTG for 2-3 hrs (30°C). Cells were harvested by centrifugation at 4°C and lysed by french press. Partial purification of wNBD was achieved as follows:

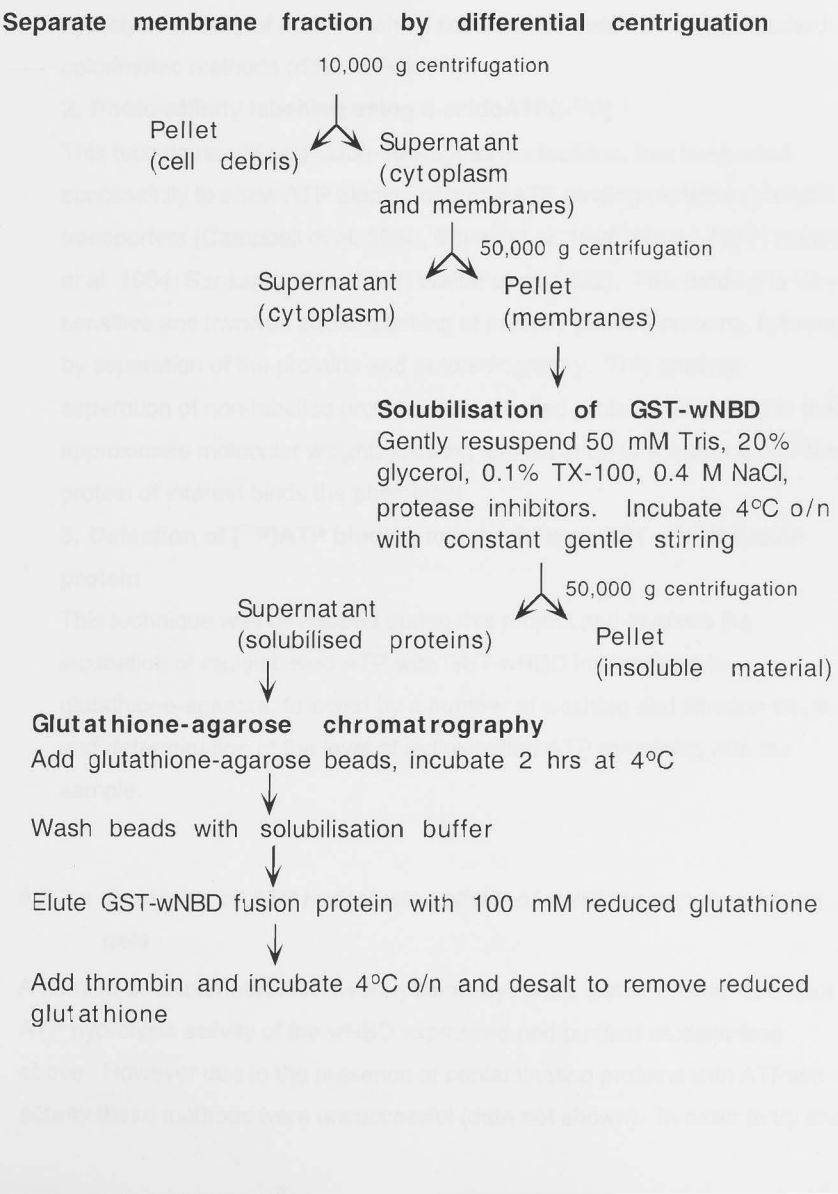

1. Detection of ATP hydrolysis activity in non-denaturing gels

This technique was used both to separate proteins by polyacrylamide gel electrophoresis, followed by staining for ATP hydrolysis by detection of a lead phosphate precipitate concurrent with ATP hydrolysis (Weinbaum and Markman, 1966). This technique was found to detect low levels of ATP hydrolysis activity of proteins which could not be detected using standard colorimetric methods (data not shown).

2. Photo-affinity labelling using 8-azidoATP[α^{32}P]

This technique, utilising azido-derivatised nucleotides, has been used successfully to show ATP binding of many ATP binding proteins and ABC transporters (Campbell et al, 1990; Dayan et al, 1996; Haley, 1977; Hobson et al, 1984; Sankaran et al, 1997; Walter et al, 1992). This method is very sensitive and involves photo-labelling of partially purified proteins, followed by separation of the proteins and autoradiography. This enables separation of non-labelled proteins from labelled proteins according to their approximate molecular weight, allowing identification of whether or not the protein of interest binds the photolabel.

3. Detection of [^{32}P]ATP binding to immobilised GST-wNDB fusion protein

This technique was developed during this project and involves the incubation of radiolabelled ATP with GST-wNBD immobilised to glutathione-agarose, followed by a number of washing and filtration steps and determination of the level of radiolabelled ATP remaining with the sample.

6.2.3.a Detection of ATP hydrolysis activity of wNBD in non-denaturing gels

A number of colorimetric ATP hydrolysis assays were tested in order to detect ATP hydrolysis activity of the wNBD expressed and purified as described above. However due to the presence of contaminating proteins with ATPase activity these methods were unsuccessful (data not shown). In order to try and

overcome this problem, non-denaturing PAGE was used to separate the proteins contained in the partially purified preparations of wNBD and the gel was stained for ATPase activity which was detected by a lead-phosphate precipitate (see Chapter 2, Section 2.6.9). Positive staining for ATPase activity was detected in samples of partially purified wNBD, and these bands aligned with immuno-reactive bands analysed by Western blot (see Fig. 15). However ATP hydrolysis activity was detected both in the wild type lane, and also the lane containing the Walker A mutation. It was subsequently shown in Sections 6.2.3b and 6.2.3c that this mutation should substantially decrease ATP binding activity. The presence of ATP hydrolysis activity is therefore unexpected in the mutant lane and was thought to be due to contaminating groEL protein which is known to have ATP hydrolysis activity. Therefore, it is not possible from these results to conclude whether wNBD has ATPase activity.

6.2.3.b 8-AzidoATP[^{32}P] photo-affinity labelling of wNBD

Partially purified wNBD protein samples were irradiated at 254 nm in the presence of 8-AzidoATP[^{32}P], plus, and minus non-radioactive Mg^{2+} ATP for either 45 seconds or 90 seconds (see Chapter 2, Section 2.6.8). The proteins were then TCA precipitated and separated by SDS PAGE. Fig. 16A is an autoradiograph of the Coomassie stained gel and it can be seen that a band corresponding to the wNBD was strongly labelled (Fig. 16A lane3). Interestingly, the GST-wNBD fusion protein (i.e. sample prior to thrombin digestion - lane 1) was only weakly labelled compared to the liberated wNBD[18].

This experiment was repeated in order to determine the effect of the Walker A mutation $Gly^{135}Lys^{136} \rightarrow Leu^{135}Gln^{136}$ which is harboured by wNDBmut1 (Section 6.2.1e). Fig. 16B is an autoradiograph and corresponding Coomassie stained gel of proteins separated by SDS PAGE after photo-affinity labelling as described above. A comparison of Lanes 2 (wild-type) and lane 3 (mut1)

---

[18] The weak labelling of the GST-wNBD fusion protein is difficult to see in the reproduction of the autoradiograph shown in Fig. 16A, however was clearly identifiable in the original.

Fig. 15 Detection of ATPase activity by non-denaturing PAGE

Protein samples containing partially purified GST-wNBD fusion protein and fusion protein digested with thrombin (Tn) were separated by non-denaturing PAGE (see experimental procedures). Gels were then either stained for ATPase activity, stained with Coomassie blue, or analysed by Western blotting using anti-White (wNT) antibody. The gels shown below show a comparison between wild type and mutant ($G^{135}K^{136}$ → LQ) forms of wNBD

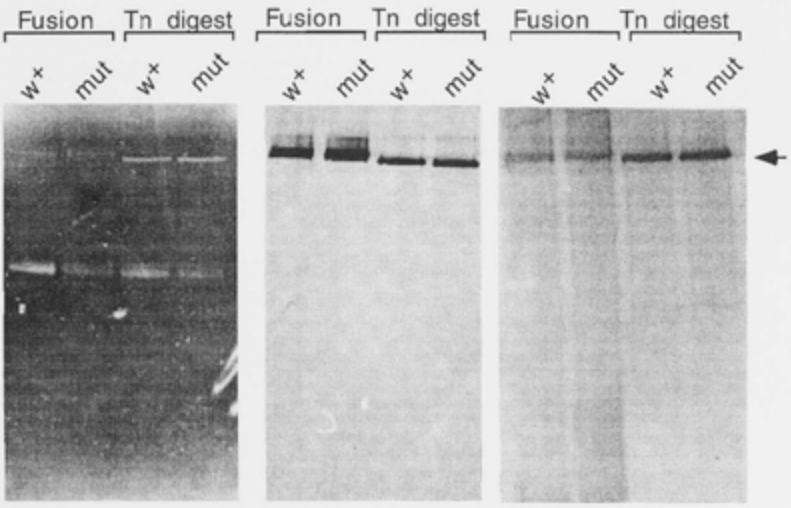

Activity gel

Coomassie

anti-White Western

Fig. 16 Azido-ATP photo-crosslinking to wNBD

GST-wNBD fusion protein was in expressed *E. coli* and partially purified from solubilised membrane fraction (0.1% TX-100) by glutathione-agarose chromatography. Fusion protein was eluted with 100 mM reduced glutathione and a sample of eluted fusion protein was digested with thrombin resulting in unfused wNBD. Protein samples were desalted using a PD-10 column (Pharmacia) prior to the photo-crosslinking experiment. 50 μl samples containing either GST-wNBD or wNBD were irradiated with UV light (254 nm) in the presence of [α^{32}-P]-Azido-ATP as described in Chapter 2, Section 2.6.8. The proteins were TCA precipitated prior to separating by SDS PAGE followed by autoradiography of the dried gel.

A. Photocrosslinking [α^{32}-P]-Azido-ATP to the wNBD
Samples used in this experiment were partially purified from a large scale (40 L) *E.coli* culture.

Lane
1. GST-wNBD fusion protein
2. wNBD + 1 mM non-radioactive ATP
3. wNBD

B. Comparison of photocrosslinking to wild-type and mutant forms of wNBD
Samples used in this experiment were partially purified from a 20 L *E.coli* culture.

Lane
1. Wild-type wNBD + non-radioactive azido-ATP (1 mM)
2. Wild-type wNBD
3. wNBD mut 1

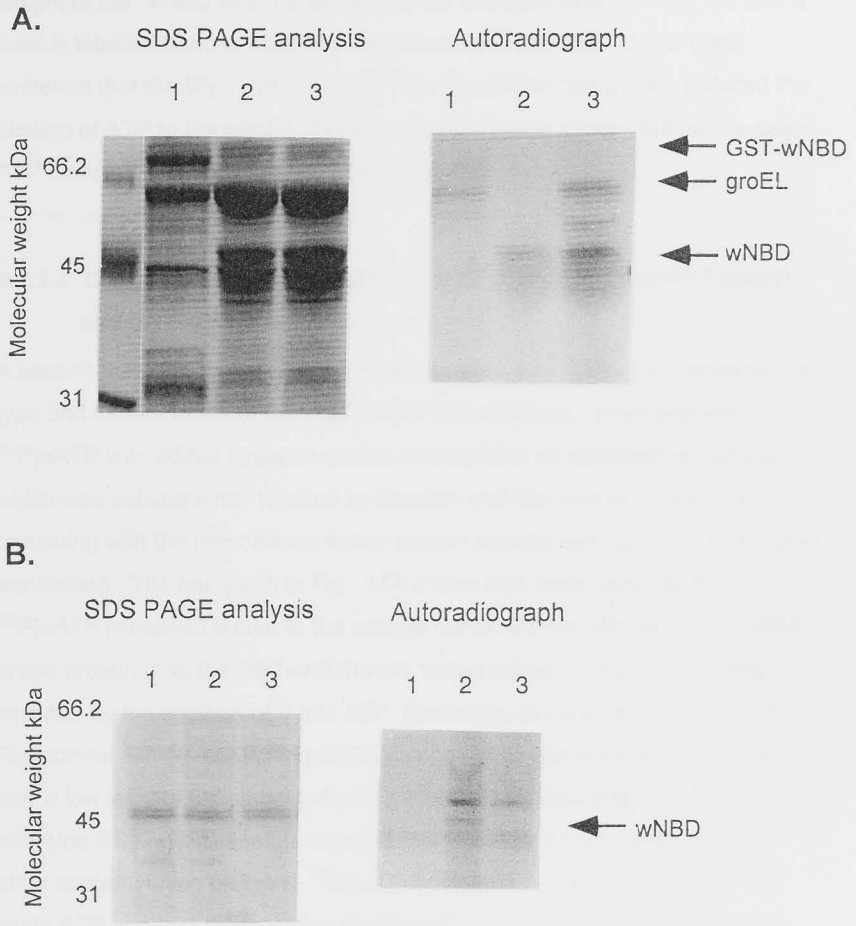
A.
SDS PAGE analysis
Autoradiograph
1 2 3
1 2 3
Molecular weight kDa
66.2
45
31
GST-wNBD
groEL
wNBD
B.
SDS PAGE analysis
Autoradiograph
1 2 3
1 2 3
Molecular weight kDa
66.2
45
31
wNBD

reveals that there is a labelled band corresponding to the predicted molecular weight of the wNBD which is present in the wild-type lane (lane 2), but only a weakly labelled band is visible in the mutant lane (lane 3). This is good evidence that the $Gly^{135}Lys^{136} \rightarrow Leu^{135}Gln^{136}$ mutation has greatly reduced the binding of ATP to the wNBD. Note that the presence of non-radioactive azido-ATP completely inhibits radiolabelling (Fig. 16B, lane 1).

6.2.3.c Comparison of ATP binding activity of immobilised GST-wNBD and GST-wNBDmut 1 fusion protein

A second method for detecting ATP binding activity was used to compare wild-type and mutant forms of the GST-wNBD fusion protein. Radiolabelled [^{32}P]αATP was added to fusion protein immobilised on glutathione-agarose, which was subsequently washed by filtration and the level of radioactivity remaining with the immobilised fusion protein sample was determined by liquid scintillation. The bar graph in Fig. 17A shows that more radiolabelled [^{32}P]αATP remained bound to the sample containing the wild-type GST-wNBD fusion protein than the GST-wNDBmut1 fusion protein. This radiolabelling is inhibited by the addition of 5 mM ATP illustrating the specificity of the binding. The control sample containing GST immobilised to glutathione-agarose bound only a low level of radiolabel indicating that the radiolabelling observed in the wild-type GST-wNBD sample was due to the wNBD protein rather than GST or other contaminating proteins. This result provides evidence that the wNBD binds ATP and that the mutation $Gly^{135}Lys^{136} \rightarrow Leu^{135}Gln^{136}$, decreases this activity at least three fold.

A further experiment was performed to test the ATP binding activity of fusion protein samples with high and low levels of groEL contamination. Wild-type GST-wNBD was partially purified as described above, from two different strains:

1) harbouring the pESL plasmid which over-expresses groES and groEL (strain AN3701); and

Fig. 17 ATP binding activity of immobilised GST-wNBD fusion protein

The GST fusion proteins were partially purified by glutathione-agarose chromatography (Chapter 2, Section 2.9) however were not eluted from the affinity beads but remained immobilised to the glutathione-agarose. Radiolabelled ATP ([^{32}P]αATP) was added to samples of the immobilised fusion protein for 30 seconds (and pre-incubated with non-radioactive ATP where indicated), prior to washing by filtration and subsequent scintillation counting (described in Chapter 2, Section 2.6.7). The samples labelled 'control' were samples of immobilised GST (no wNBD present) which was prepared in the same manner as the immobilised GST-wNBD, however using the plasmid vector pGEX4T1. GST was purified from the cell lysate under the same buffer conditions used in purification of GST-wNBD.

A. Bar graph comparing radiolabelled ATP binding activity of wild type GST-wNBD and GST-wNBDmut1 which harbours the mutation $G_{135}K_{136}$ to LQ. The same amount of immobilised fusion protein were used for both the wild type and mutant experiments.

B. SDS PAGE analysis (Coomassie stained) of samples used in experiment shown in A.

C. Bar graph comparing ATP binding activity of GST-wNBD fusion protein samples either containing a high or low level of groEL contamination (indicated by + pESL, or -pESL respectively) in order to rule out the possibility that the ATP binding observed in A was due to this contaminant.

D. SDS PAGE analysis (Coomassie stained) of samples used in experiment shown in C.

A [^{32}P]ATP binding comparison between wild type and mutant GST-wNBD

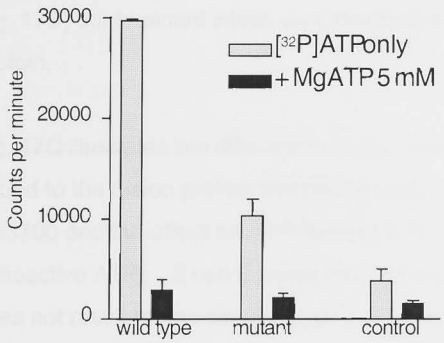

B

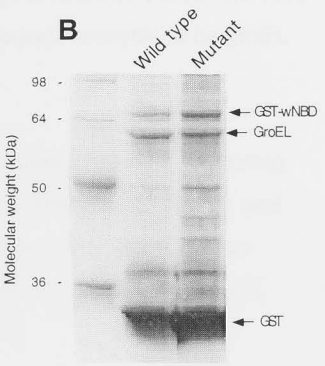

C GST-wNBD [^{32}P]ATP binding + and - groEL contamination

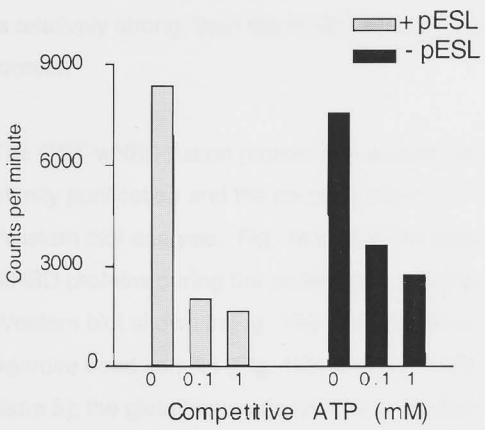

D

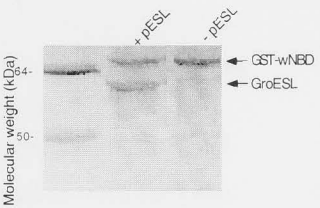

2) the same strain as above but without pESL (AN3700).

The presence of the plasmid pESL results in a large amount of the 60 kDa (see Fig. 17D) contaminant which was identified by sequence analysis to be groEL protein.

Fig. 17C illustrates the differences in the level of radiolabelled ATP remaining bound to the fusion protein samples partially purified from either AN3701 and AN3700 and the effect on ATP binding in the presence of competitive non-radioactive ATP. It can be seen that the presence of contaminating groEL does not result in an increase in ATP binding activity.

6.2.4 Co-purification of wNBD and stNBD

In order to investigate whether the White and Scarlet NBDs physically interact, these two proteins were co-expressed in *E. coli* using the plasmid construct p2GEX,*w*NBD, *st*NBD (see Section 6.2.1d), in which the stNBD is expressed on its own i.e. not fused to GST. The aim of this experiment was to determine whether the wNBD and stNBD interact (e.g. form a dimer), and if this interaction is relatively strong, then the stNBD should co-purify with the GST-wNBD fusion protein.

The GST-wNBD fusion protein was partially purified by glutathione-agarose affinity purification and the co-purification of the stNBD was detected by Western blot analysis. Fig. 18 shows the detection of both the wNBD and stNBD proteins during the purification procedure. It can be seen from the Western blot shown in Fig. 18B, that stNBD is present in: the glutathione-agarose bead sample (Fig. 18B lane 4); the first eluent with reduced glutathione (lane 5); the glutathione-agarose bead fraction with proteins which remain bound (lane 11). This result indicates that the stNBD protein co-purifies with the GST-wNBD. However due to the possibility that the stNBD may interact non-specifically with the glutathione-agarose beads, a further control

Fig. 18 Co-expression and co-purification of GST-wNBD fusion protein and stNBD

1L of *E. coli* AN3700, p2GEX,*w*NBD, *st*NBD was grown to late log phase and induced with 0.1 mM IPTG for 2 hrs. Fusion protein was partially purified from solubilised membrane fraction (0.1% TX-100) using 0.2 ml glutathione-agarose beads and analysed by SDS PAGE and Western blot.

A. Detection of wNBD by SDS PAGE and Western blot.

Lane
1. Supernatant and membrane fractions.
2. Cell debris.
3. Proteins which did not bind to the glutathione agarose
4. Proteins bound to glutathione-agarose beads
5. First eluent (100 mM reduced glutathione) digested with thrombin
6. Second eluent (100 mM reduced glutathione)
7. Third eluent (100 mM reduced glutathione)
8. Fourth eluent (100 mM reduced glutathione)
9. Fifth eluent (100 mM reduced glutathione)
10. Protein remaining bound to glutathione-agarose.

B. Detection of stNBD by SDS PAGE and Western blot

Lane
1. Supernatant and membrane fractions.
2. Cell debris.
3. Proteins which did not bind to the glutathione agarose
4. Proteins bound to glutathione-agarose beads
5. First eluent (100 mM reduced glutathione) digested with thrombin
6. Second eluent (100 mM reduced glutathione)
7. Third eluent (100 mM reduced glutathione)
8. Fourth eluent (100 mM reduced glutathione)
9. Fifth eluent (100 mM reduced glutathione)
10. Protein remaining bound to glutathione-agarose.
11 No Scarlet NBD control.
12. Sample containing wNBD but no stNBD
13. Background strain, no wNBD or stNBD

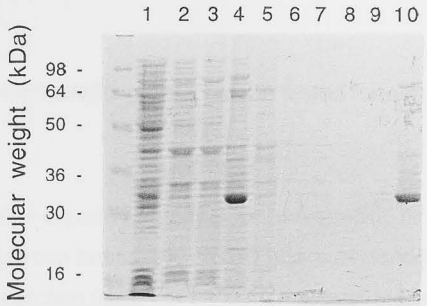

SDS PAGE

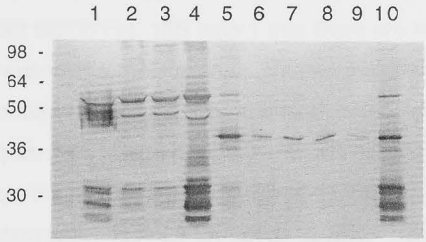

anti-wNT Western

A

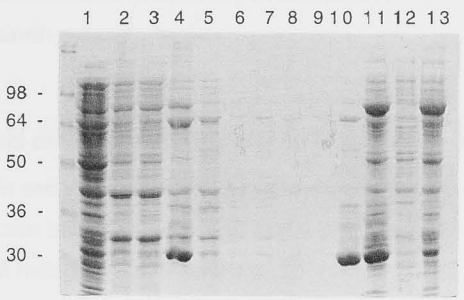

SDS PAGE

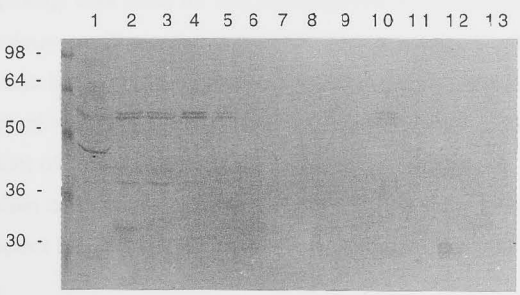

anti-stNT Western

B

experiment is required in which stNBD protein can be tested for non-specific binding.

In an attempt to do the control experiment to test for non-specific binding of stNBD to the glutathione-agarose beads, the stNBD was sub-cloned and expressed as a GST fusion protein (data not shown), however the resultant protein detected by Western blot was a much lower apparent molecular weight than predicted (data not shown) which is suggestive of proteolytic degradation. It can be seen from the Western blot in Fig. 18B lane 1 that there are two anti-stNT immuno-reactive bands, one with a molecular weight much higher than that predicted (~70 kDa) and another at around the predicted molecular weight predicted from sequence analysis (~45 kDa). It is possible that co-expression of GST-wNBD and stNBD protects the stNBD from proteolytic degradation, and also results in a strong interaction which is not interrupted by SDS PAGE resulting in the high apparent molecular weight. Since a number of such issues remain unanswered at this stage, the observation that stNBD co-purifies with GST-wNBD should be considered as preliminary evidence only. However, this is an encouraging result worth pursuing further.

6.2.5 Interaction analysis of the White NBD and an intracellular loop

The work described in this section is a preliminary investigation into possible interactions which may occur between the wNBD and a predicted intracellular loop between putative TM helices 2 and 3 (see Fig. 1).

IAsys Biosensor technology was used for this investigation and the basic principles of this technique are illustrated in Fig. 19. This system has the sensitivity to detect weak inter-molecular interactions and has many advantages over the yeast two-hybrid interaction analysis system in that it is quantitative and provides a large amount of flexibility with respect to solution conditions. In addition, different protein concentrations can be tested and direct comparisons can be made with respect to the level of protein interaction between different controls and mutants.

Fig. 19 IAsys Biosensor - general principles

The components of the IAsys Biosensor are illustrated in this Figure. The cuvette carboxy methyl dextran (CMD) surface is designed to acts as a resonant mirror comprised of a thin, monomode waveguide which is highly sensitive to changes in the surface refractive index. The optical components of the instrument are suitably arranged so that a sharp peak of intensity is seen at a discreet angle of interest and this is extremely sensitive to the surface binding reactions which are subsequently detected by the instrument. A typical surface binding event is illustrated in B, where the binding event is revealed as an increase in arc seconds (i.e. changes in the angle of reflectance) over time. The graph shown in B illustrates a text book profile of a molecule binding to an immobilised ligand at the cuvette surface, followed by dissociation and regeneration of the cuvette by washing. This figure was taken from an IAsys publication entitled "How IAsys Works".

A

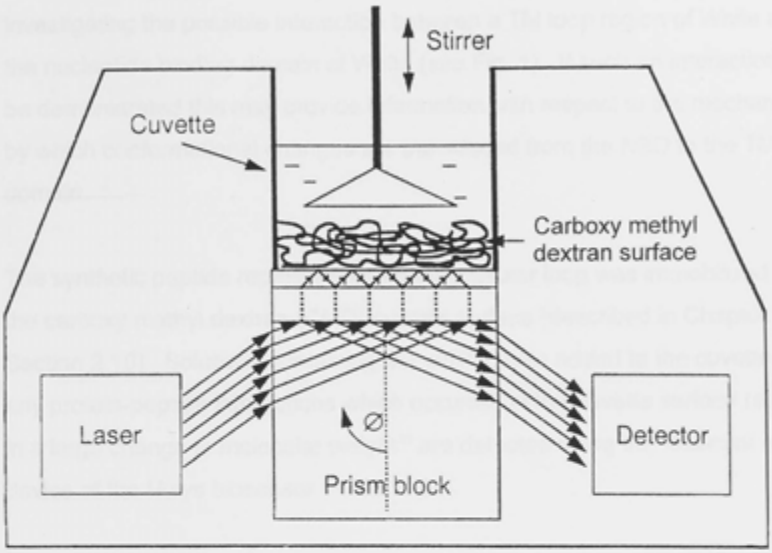
Stirrer
Cuvette
Carboxy methyl
dextran surface
Laser
Detector
Prism block

B

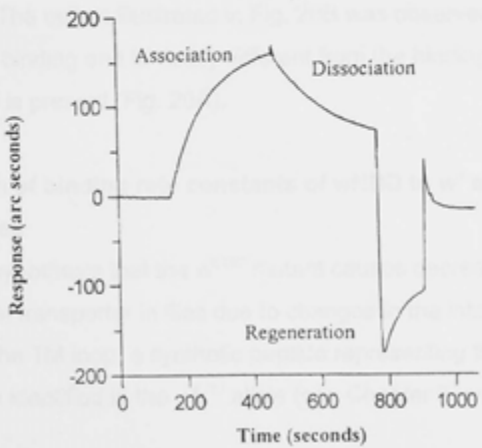
200
100
0
-100
-200
Association
Dissociation
Regeneration
Response (arc seconds)
0
200
400
600
800
1000
Time (seconds)

The interaction analysis experiments performed herein were aimed at investigating the possible interaction between a TM loop region of White and the nucleotide binding domain of White (see Fig. 1). If such an interaction can be demonstrated this may provide information with respect to the mechanism by which conformational changes are transduced from the NBD to the TM domain.

The synthetic peptide representing the intracellular loop was immobilised onto the carboxy methyl dextran (CMD) cuvette surface (described in Chapter 2, Section 2.10). Solutions containing the wNBD were added to the cuvette and any protein-peptide interactions which occurred at the cuvette surface resulting in a large change in molecular weight[19] are detected using the resonant mirror device of the IAsys biosensor.

Fig. 20A illustrates the IAsys biosensor output obtained when partially purified wNBD was added to the cuvette with immobilised loop peptide. The curve shown in Fig. 20A is typical of a specific binding event. The major contaminant of this partially purified wNBD preparation was GST (Fig. 20C, lane 1), so a control reaction containing a high level GST protein but no wNDB was performed. The output illustrated in Fig. 20B was observed, which is typical of non-specific binding and is visibly different from the binding curve observed when wNBD is present (Fig. 20A).

Comparison of binding rate constants of wNBD to w^+ and w^{ET87} mutant loop peptides

To test the hypothesis that the w^{ET87} mutant causes decreased function of the White/Scarlet transporter in flies due to changes in the interaction between the wNBD and the TM loop, a synthetic peptide representing this loop harbouring the mutation identified in the w^{ET87} allele (see Chapter 3) was immobilised onto

Fig. 20 wNBD interacts with peptide corresponding to the loop between TM 2 and 3 of the White protein

The graphs shown in this figure illustrate binding profiles obtained using the IAsys biosensor machine where binding of wNBD and GST was tested respectively, to an immobilised peptide representing the loop between TM helices 2 and 3 of the White protein. Samples of wNBD used in these experiments was partially purified using the *E. coli* expression, and glutathione-agarose affinity purification system described in Section 6.2.2e. The control sample containing no wNBD but a high level of GST was obtained by expression of GST in *E. coli* using the plasmid p2GEX4T1 (Chapter 2, Section 0) and affinity purification using glutathione-agarose chromatography from cell lysates under the same detergent and buffer conditions used for purification of the wNBD.

A. Graph of binding response recorded when partially purified wNBD was added to an IAsys cuvette containing immobilised wild type loop peptide.

B. Graph of binding response when GST was added to an IAsys cuvette containing immobilised wild type loop peptide.

C. SDS PAGE and Western blot analysis of samples used in binding experiments.

Lane
1 Partially purified wNBD (diluted 10:1 in SDS PAGE sample buffer)
2 GST control (diluted 10:1 in SDS PAGE sample buffer)

A

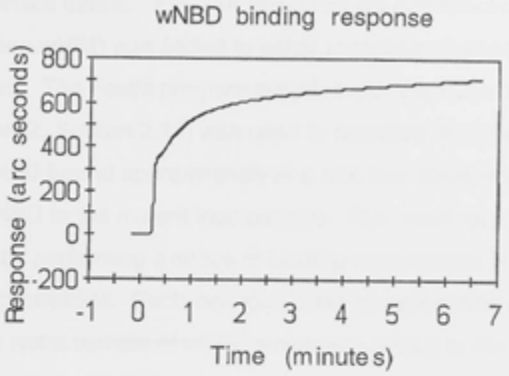
wNBD binding response
Response (arc seconds)
800
600
400
200
0
-200
-1 0 1 2 3 4 5 6 7
Time (minutes)

B

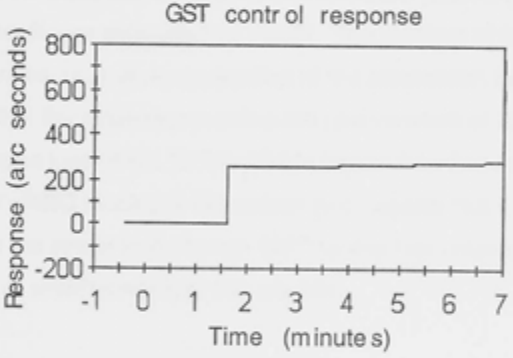
GST control response
Response (arc seconds)
800
600
400
200
0
-200
-1 0 1 2 3 4 5 6 7
Time (minutes)

C

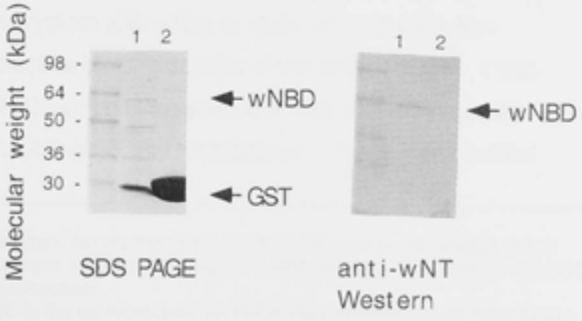
Molecular weight (kDa)
98
64
50
36
30
1 2
wNBD
GST
SDS PAGE
1 2
wNBD
anti-wNT
Western

the cuvette CMD surface matrix. Fig. 21A illustrates the differences in binding curves observed when wNBD was added to either immobilised wild-type and mutant loop peptides. The Fastfit program supplied with the IAsys machine (described in Chapter 2, Section 2.10) was used to calculate the binding rates and showed that wNBD bound approximately at a rate four times that of the rate of binding of wNBD to the mutant loop peptide. This result was investigated further by performing a series of binding experiments at four different wNBD concentrations. Each individual binding experiment was performed using the same sample of wNBD which was added to the cell containing either immobilised wild-type loop peptide, or mutant loop peptide respectively. Rate constants were calculated at each concentration using the Fastfit program. Fig. 21B illustrates the individual rate constants obtained at each concentration of wNBD plotted against concentration (arbitrary units[20]) and a the line of best fit was calculated by Fastfit. The gradient of the line fitted to these individual rates (k_{on}) is representative of the association rate constant. Fig 21B illustrates that the slope representing the rate constant of wNBD binding to the wild-type loop (4.9×10^{-4}) is 10 fold higher than that calculated for the rate constant of wNBD binding to the mutant loop peptide (3.8×10^{-5}). This result indicates that the amino acid change Gly^{509} to Asp has substantially decreased the rate of wNBD binding to this peptide.

6.3 Discussion

The results presented in this chapter described work directed towards the development of a model system with which to study structure-function relationships of the nucleotide binding domain of the White protein. It was shown that the White NBD can be expressed in *E. coli* and subsequently partially purified from solubilised *E. coli* membranes. The partially purified

---

[19] The 23 residue immobilised peptide has a very low molecular weight in comparison to the wNBD resulting in a large increase in molecular weight if a binding event occurs which should be easily detected by the IAsys Biosensor.

[20] The concentration of wNBD in the samples used for these experiments was not determined. Samples of wNBD were diluted in sample buffer by 90%, 80%, 50% and an undiluted sample was also tested.

Fig. 21 Comparison of association rate constants of wNBD binding to wild-type and mutant loop peptides

The IAsys biosensor machine was used to detect differences in binding of wNBD to the wild-type loop peptide, and a mutant loop peptide containing a mutation identified in w^{ET87} (G509D). Samples of wNBD used in these experiments were partially purified using the *E. coli* expression, and glutathione-agarose affinity purification system described in Section 6.2.2e.

A. Comparison of binding curves obtained from the IAsys biosensor machine when the identical samples of wNBD was added to an IAsys cuvette with immobilised wild-type peptide and mutant peptide respectively.

B. This graph shows plots of the first apparent association rate constants for four concentrations of wNBD for both the wild-type loop and the mutant loop peptide. Identical samples of wNBD were added to the cuvette with immobilised wild type and mutant peptide. The gradient of the fitted line (calculated by the Fastfit program) is the theoretical association rate constant.

C. Sequences of amino-terminally biotinylated peptides (biotin not shown) immobilised via avidin to the CMD surface of the IAsys cuvette. Equivalent amounts of each the wild type and mutant loop peptides respectively were immobilised to separate wells (as described in Chapter 2, Section 2.10.1) of an IAsys 2 well cuvette. Nevertheless, minor differences in levels of immobilised peptide would alter individual k_{on} values, however the overall binding rate constant represented by the line of best fit would not alter appreciably.

A Comparison of wNBD binding to mutant and wild type loop peptides

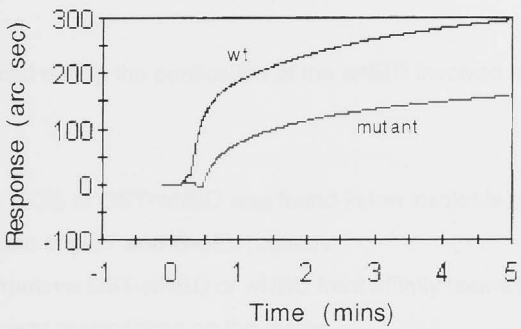

B Binding rates of wNBD to wild type and mutant loop peptides

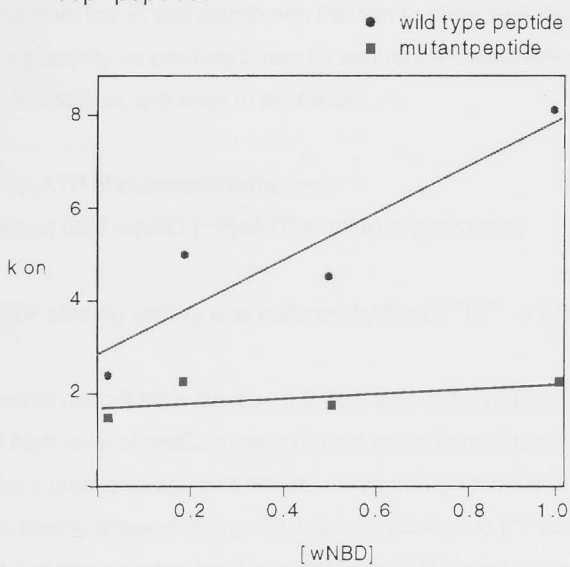

C Immobilised Peptides:

C M R̄ E A R̄ S R̄ L Y R̄ C D̄ T Y F L G K̄ T I A Ē wild type

D̄ mutant

wNBD was shown to have ATP binding activity, as well as being able to interact with an intracellular loop predicted to form an interface between the NBD and TM domains.

The difficulties faced during the purification of the wNBD involved a number of factors including:

- insolubility (90% of GST-wNBD was found in the insoluble cell fraction);
- co-purification of GST and GroEL proteins;
- inability to remove GST-wNBD or wNBD from affinity resins suggesting the protein was precipitating on the resins.

Despite the abovementioned difficulties, sufficient wNBD was solubilised and partially purified from the *E. coli* membrane fraction to show that the domain has ATP binding activity as predicted from its sequence conservation with ABC transporters. In addition, two lines of evidence:

(i) [^{32}P]azido-ATP photocrosslinking; and
(ii) immobilised GST-wNBD [^{32}P]αATP binding experiments;

showed that ATP binding activity was reduced by the $G^{135}K^{136} \rightarrow$ LQ mutant.

In the experiments described in Section 6.2.3c it was observed that the presence of a high level of groEL protein did not result in additional retention of [^{32}P]ATP on the glutathione-agarose beads - even though the experiments in Section 6.2.3b clearly showed that groEL was crosslinked to [^{32}P]azido-ATP. This apparent discrepancy may be due to groEL's ATP hydrolysis activity, whereby ATP does not remain bound to the protein, but is removed easily once it is hydrolysed, by the washing steps. On the other hand, the GST-wNBD may have ATP binding activity, but if ATP hydrolysis activity is absent, ATP may remain tightly bound to the protein. Although effort was devoted to determining whether this domain had ATP hydrolysis activity, this was not shown

conclusively. The ATP hydrolysis activity observed in activity stained gels may reflect the hydrolysis activity of groEL. Although a number of procaryotic NBDs purified in this way have been shown to hydrolyse ATP, these systems are different to the *D. melanogaster* transporters in that the two NBDs of the transporter are identical (e.g. HisP, HlyB) and there is evidence that they interact and function as dimers (Koronakis et al, 1993; Nikaido et al, 1997). In particular, positive cooperativity has been demonstrated for the maltose transporter of *E. coli* indicating that the two NBDs interact (Davidson et al, 1996). In eucaryotic systems there is also an increasing body of evidence suggesting the NBDs interact and function cooperatively. A model has been postulated for the P-glycoprotein system, which predicts that the two NBDs interact in alternating cycles of ATP binding and hydrolysis, and that loss of function of one NBD results in loss of function of the other NBD (Azzaria et al, 1989; Loo and Clarke, 1995a; Senior et al, 1995; Urbatsch et al, 1995a). Although it has been reported that purified CFTR NBD-1 has ATP hydrolysis activity (Ko and Pedersen, 1995), the CFTR second NBD-2 does not hydrolyse ATP when expressed and purified in isolation (Randak et al, 1995). It is possible that the White NBD may not dimerize and interact appropriately as a homodimer but instead may require either the Scarlet or Brown NBD to exhibit ATP hydrolysis activity. This would be an interesting issue to pursue using the model system developed here.

The insolubility problems experienced in this work suggests that the wNBD is not the soluble protein domain predicted from sequence analysis. The finding that some of the GST-wNBD fusion protein was associating with the membrane fraction of the cell suggests the wNBD harbours protein determinants enabling membrane interactions. The interaction of the NBD of other ABC transporters with membranes has been described previously, and has subsequently been shown to be functionally important (Gruis and Price, 1997; Kerppola et al, 1991; Ko et al, 1997). As mentioned earlier in the introduction to this chapter, NBD-1 of CFTR interacts with lipid bilayers to such an extent as to allow formation of an ion channel (Arispe et al, 1992). Membrane association characteristics

have also been reported for the NBD component of the *S. typhimurium* histidine transporter (HisP) which was shown to be tightly membrane bound despite its hydrophilic sequence (Baichwal et al, 1993; Kerppola et al, 1991) and has been described as being intermediate between a peripheral and integral membrane protein (Kerppola et al, 1991).

Intracellular loop regions of the transmembrane domains of ABC transporters have previously been implicated to be an important functional link between the NBDs and transmembrane domains. The interaction analysis described in Section 6.2.5 represents the early stages of development of a model system which may be used to pursue this important issue. The results obtained so far, indicate that the White NBD interacts with the loop 2-3 peptide (see Fig. 1), and that the mutation present in this loop encoded by the w^{ET87} eye-colour mutant reduces this binding. The w^{ET87} mutation (Gly^{509} to Asp) introduces an acidic residue adjacent to Lys^{510} (which would neutralise the positive charge of this residue) and flies homozygous for this mutation have very low levels of pigments (2% drosopterins, 0% xanthommatin) (described in Chapter 3, Section 3.2.1). The decreased binding observed, as analysed by the IAsys Biosensor, is consistent with current models of a number of ABC transporters, based on genetic and mutational analysis that NBDs and specific loops of the TM domain interact (Cotten et al, 1996; Kerppola and Ames, 1992; Mourez et al, 1997; Saurin et al, 1994a; Seibert et al, 1997; Shani et al, 1996). In addition, the results reported herein are also consistent with the observed phenotypic effect of the w^{ET87} mutation and indicates that the positive charge of Lys^{510} is important in the interaction between the loop 2-3 peptide and the White NBD.

The importance of the intracellular loop region harbouring the EAA motif of procaryotes and the EAA-like motif of eucaryotes was discussed earlier (see Chapter 3). In the bacterial maltose transporter, it has been shown that particular mutations in this motif result in the nucleotide binding domain (MalK) failing to assemble with the transmembrane domains (MalF and MalG) (Mourez

et al, 1997). Two of these mutations affect charged residues, one involves the replacement of the conserved glutamic acid with a hydrophobic amino acid; and the other with the introduction of an aspartic acid residue at a position normally held by an alanine (Mourez et al, 1997). This indicates the importance of charge in the interaction between MalK and the EAA motif, which is consistent with the introduction of the charged aspartic acid residue found in w^{ET87}. Also of interest are MalK suppressor mutations which compensate for mutations within the EAA motif (Mourez et al, 1997). According to sequence alignment information and inferences from the recent crystal structure of HisP (Hung et al, 1998) these mutations occur within regions which could potentially be important for transmission of signals from Arm I (site of ATP binding/hydrolysis) to Arm II (region which interacts with the TM domain), or which may alter slightly the structure of the helical domain in Arm II (see Fig. 22). It is noteworthy that signal-independent mutants (mutations which release HisP from the regulatory control of HisQ/HisM and result in constitutive ATPase activity in the absence of HisJ) occur in similar positions to two MalF suppressor mutants. These HisP mutations occur within a loop which connects α5 with β9 (see Fig. 22) which is close to the ABC signature sequence. These studies therefore strongly suggest that arm II and the EAA motif are involved both with protein-protein interactions and with signal transduction between the NBDs and TM domains.

Future directions

This system can be applied to the expression and partial purification of the Scarlet and Brown NBDs in order to investigate predicted interactions between the NBDs of White/Scarlet, and White/Brown and to characterise the ATP binding and hydrolysis activity which is predicted from such interactions.

The results obtained from the IAsys experiments analysing the interaction between the intracellular loop and the wNBD indicate that this is a feasible and potentially very powerful technique for analysis of protein-peptide interactions. This system allows analysis of interaction under different conditions which

Fig. 22 Crystal structure of the nucleotide binding domain of HisP

The crystal structure of HisP dimer (Hung et al, 1998) shows that the HisP monomer is roughly "L" shaped with two arms as indicated in this figure. Arm II is predicted to be the region of HisP which interacts with the membrane bound domains. Mutant data (discussed in the text) of HisP and other ABC transporters suggests that the loop connection between β-9 and α-5 is important for the structure-function of arm II with respect to interactions with the membrane domain and loop regions of this domain.

A

B

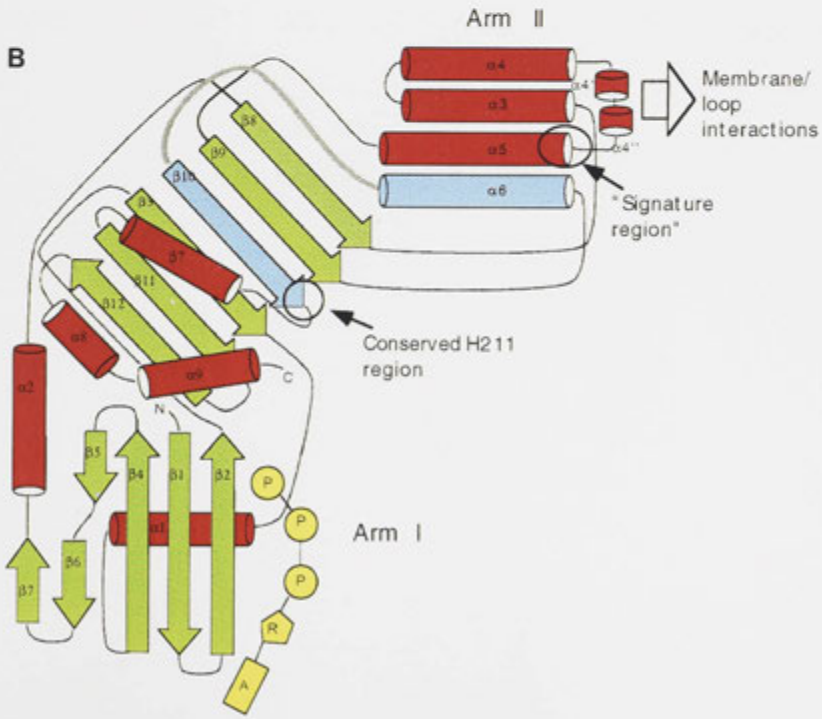
Arm II
α4
α3
α5
α6
α4'
α4''
Membrane/
loop
interactions
"Signature
region"
Conserved H2 11
region
β8
β9
β10
β7
β11
β12
α2
α6
N
C
β5
β4
β1
β2
α1
β7
β6
P
P
P
R
A
Arm I

would enable the effects on interactions in the presence or absence of ATP to be determined. In addition, analysis of mutant wNBDs with an aim of identifying the region which interacts with the loop peptide could be pursued. This system could also be used to further characterise the interaction of the wNBD and stNBD for which co-purification provides the first preliminary biochemical evidence that these domains interact. The tethering of either the White or Scarlet NBD to the matrix surface would allow the analysis the interaction between the domains. An interaction study such as the one suggested here has not been reported for any ABC transporter.

CHAPTER 7

IMMUNO-LOCALISATION OF WHITE AND SCARLET PROTEINS IN *Drosophila* EYE TISSUE

7. IMMUNO-LOCALISATION OF WHITE AND SCARLET PROTEINS IN DROSOPHILA EYE TISSUE

7.1 Introduction

The aim of the work described in this chapter is to determine the localisation of White and Scarlet protein within the compound eye of *D. melanogaster*. Biochemical analysis of mutant tissues as discussed in Chapter 1, Section 1.6.2 imply a plasma membrane location of White and Scarlet, where the heterodimeric complex transports tryptophan into the cell. However direct evidence is lacking, and such information is fundamental to the understanding of the biology of the xanthommatin biosynthetic pathway and the major question addressed in this chapter is whether the proteins localise to the plasma membrane of pigment cells, or a subcellular membrane, such as the pigment granule membrane.

The localisation studies described in this chapter were performed using transmission electron microscopy, and in order to provide a perspective of the cellular structure of the compound eye an overview is provided below.

Ultra-structure of the compound eye of *D. melanogaster*

The structure of the compound eye of *D. melanogaster* has been studied previously by electron microscopy (Cagan and Ready, 1989; Carlson and Chi, 1979; Shoup, 1966) and is illustrated diagrammatically in Fig. 1. An overall view of the whole *Drosophila* eye is shown in the scanning electron micrograph in Fig. 2.

The peripheral retina of the compound eye is made up of a repetitive array of ommatidia or facets and a diagrammatic structure of a single ommatidia is illustrated in Fig. 3. Each ommatidium is a stereotyped assembly of 14 cells including 8 photoreceptor cells, 4 cone cells and 2 primary pigment cells.

Fig. 1 Components of the dipteran compound eye

This figure was taken from (Summers et al, 1982). There are two major components which make up the dipteran compound eye. The first component, the peripheral retina (PR) is made up primarily of non-nervous tissue and includes many hundred ommatidia. The peripheral retina receives optical information (e.g. light, movement, contrast) and electrically transmits this information to the second component of the retina which is made up mainly of nerve fibres and is collectively termed the optic neuropile masses. This component of the retina integrates information received from the peripheral retina and transmits it to the protocerebrum of the brain for analysis (Bullock and Horridge, 1965; Laughlin, 1975). The peripheral retina and the optic neuropile masses are separated by a basal lamina.

Abbreviations: PR peripheral retina; IC, intermediate chiasma; M, medulla; lamina (L); medulla (M); the optic lobe (OL).

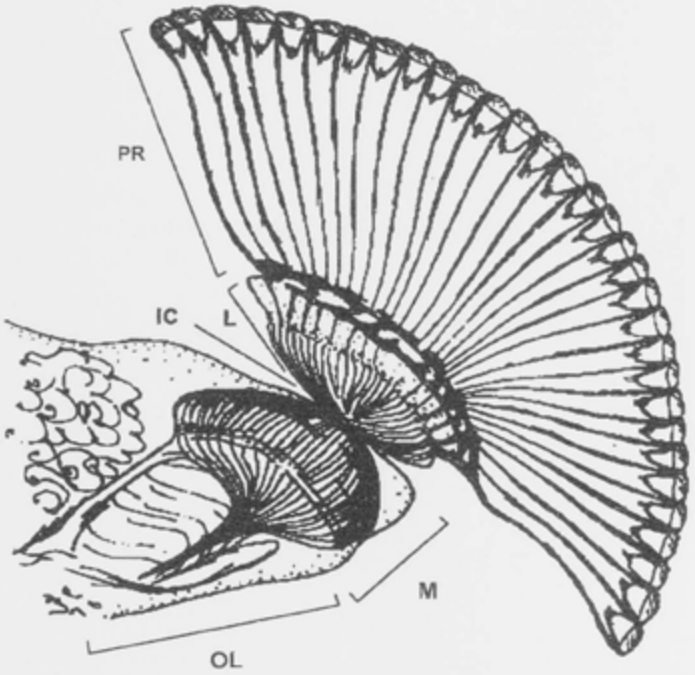

Fig. 2 Surface structure of the *D. melanogaster* compound eye

This scanning electron micrograph was taken from (Renfranz and Benzer, 1989) and shows the wild-type adult eye made up of around 800 ommatidia or facets. Bristle processes which intervene between each facet and which perform a mechano-sensory function can be seen. Bar = 50 μm.

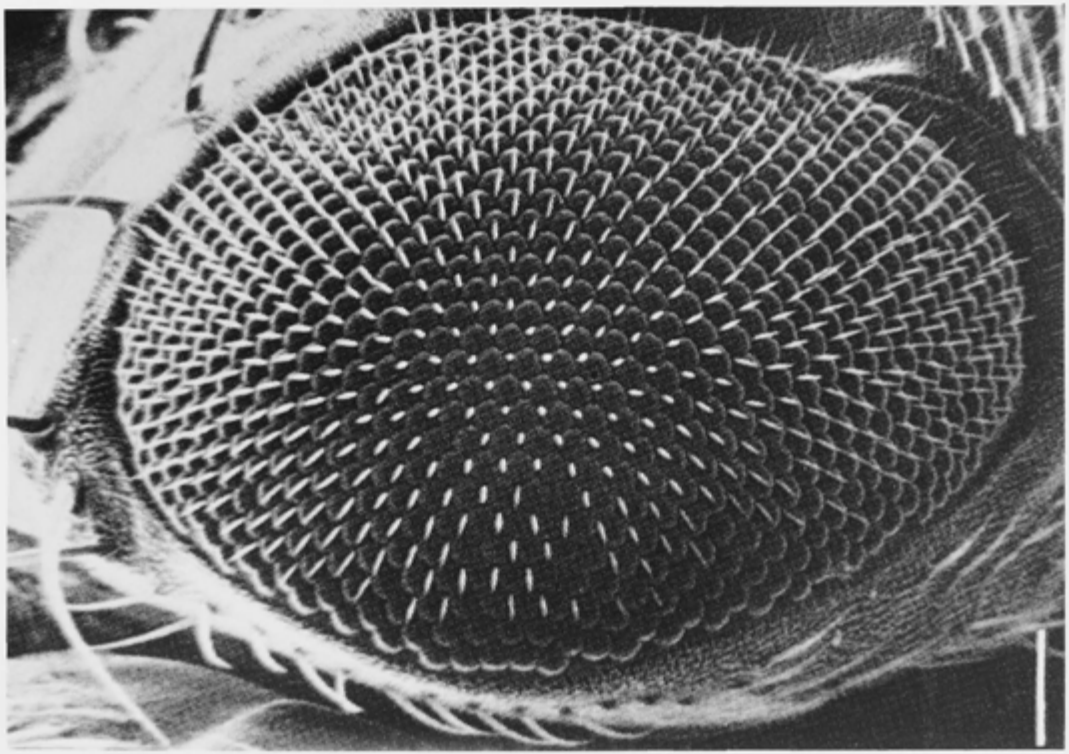

Fig. 3 The structure of the ommatidium of the adult retina of *D. melanogaster*

This figure was reproduced from (Cagan and Ready, 1989).

"**A.** A schematic longitudinal view of a single ommatidium, drawn to scale.

B. Five micrometers below the lens. The secondary and tertiary pigment cells and bristles, which form the hexagonal lattice, are the most apical cells. At this level, the lattice surrounds the pseudocone.

C. Twelve micrometers below the lens. The anterior and posterior cone cells are separated by the equatorial and polar cones. They are enwrapped by two primary pigment cells and the surrounding hexagonal lattice of the secondary and tertiary pigment cells.

D. Twenty to eighty micrometers below the lens. Seven photoreceptors can be seen. They are surrounded by the hexagonal lattice. The cone cells are thin threads, and the primary pigment cells do not extend to this depth.

E. Eighty to one hundred fifteen micrometers below the lens. Photoreceptor R8 is visible at this depth, its rhabdomere replacing R7's in the center.

F. One hundred twenty micrometers below the lens. The feet of the secondary and tertiary pigment cells widen into the filamentous fenestrated membrane. At the centre, the cone cells have enlarged into pigment-containing sacs; the anterior and posterior cone cells contact each other (compare with C).

Abbreviations: 1° pig. cell, primary pigment cell; 2° pig. cell, secondary pigment cell; 3° pig. cell, tertiary pigment cell; ac, anterior cone cell; eqc, equatorial cone cell; pc, posterior cone cell; plc, polar cone cell. Anterior is to the right." (Cagan and Ready, 1989)

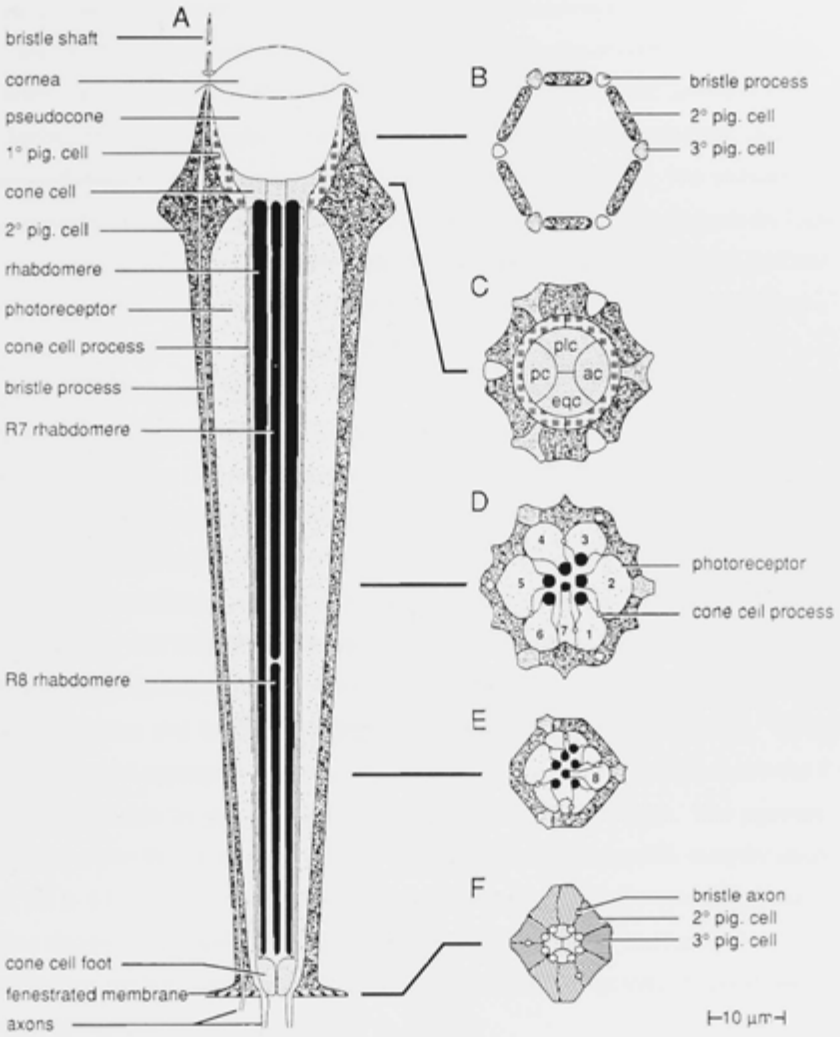
A
bristle shaft
cornea
pseudocone
1° pig. cell
cone cell
2° pig. cell
rhabdomere
photoreceptor
cone cell process
bristle process
R7 rhabdomere
R8 rhabdomere
cone cell foot
fenestrated membrane
axons
B
bristle process
2° pig. cell
3° pig. cell
C
plc
pc
ac
eqc
D
4
3
5
2
6
7
1
photoreceptor
cone cell process
E
8
F
bristle axon
2° pig. cell
3° pig. cell
10 µm

Secondary pigment cells are shared between neighbouring ommatidia. The bristle process has a mechanosensory function and projects out from the pigment cell lattice. The photoreceptor cells possess a unique microvillar arrangement of the plasma membrane forming a structure called the rhabdomere and is the photosensitive component of the cell and harbours the visual pigment rhodopsin (Carlson and Chi, 1979; Eakin, 1972). The primary pigment cells surround the pseudocone and cone cells of the ommatidium. The secondary pigment cells surround both the primary pigment cells and photoreceptor cells. The primary pigment cells harbour pigment granules containing xanthommatin (known as Type I pigment granules (Shoup, 1966), while the secondary pigment granules harbour both xanthommatin Type I granules and drosopterin containing granules (called Type II pigment granules (Shoup, 1966)).

Fig. 4 is a low magnification transmission electron micrograph montage illustrating the structure of the *Drosophila* eye tissue section which provides an overall view of the sections studied in this work. Ultra-structural components are illustrated at higher magnification in Fig. 5. In the longitudinal section (Fig. 5A) the cornea, psuedocone and photoreceptor cells (retinula cells) can be easily seen, in addition to the primary and secondary pigment cells which harbour pigment granules. While some of the retinula cells are cut longitudinally, most are cut tangentially or in cross-section and the rhabdomeres appear as bundles of seven circles. This cross sectional appearance of the rhabdomeres is shown in (Fig. 5B) where the 7 rhabdomeres can be seen surrounded by secondary pigment cells. The pigment granules within the secondary pigment cells are clearly seen at this magnification. Fig. 5C is a low magnification electron micrograph of a section of the peripheral retina showing the repetitive array of ommatidia in both cross section and longitudinal section, and provides a perspective of the higher magnification view shown in Fig. 5B.

Fig. 4 Cross section of the *Drosophila* compound eye viewed by transmission electron microscopy

This figure was produced during the course of the work described herein and is a montage of many low magnification (1,000 x) transmission electron micrographs taken of a section of eye tissue from the wild-type Canton-S strain of *D. melanogaster*. The tissue was prepared for transmission electron microscopy (TEM) by Cathy Gillespie (EM unit, JCSMR, ANU) as described in Chapter 2, Section 2.12.1. This montage provides an overall perspective of the compound eye and some of the structures are labelled as follows:

C, cornea; PR, peripheral retina; BM, basement or fenestrated membrane; NS, neural sheath.

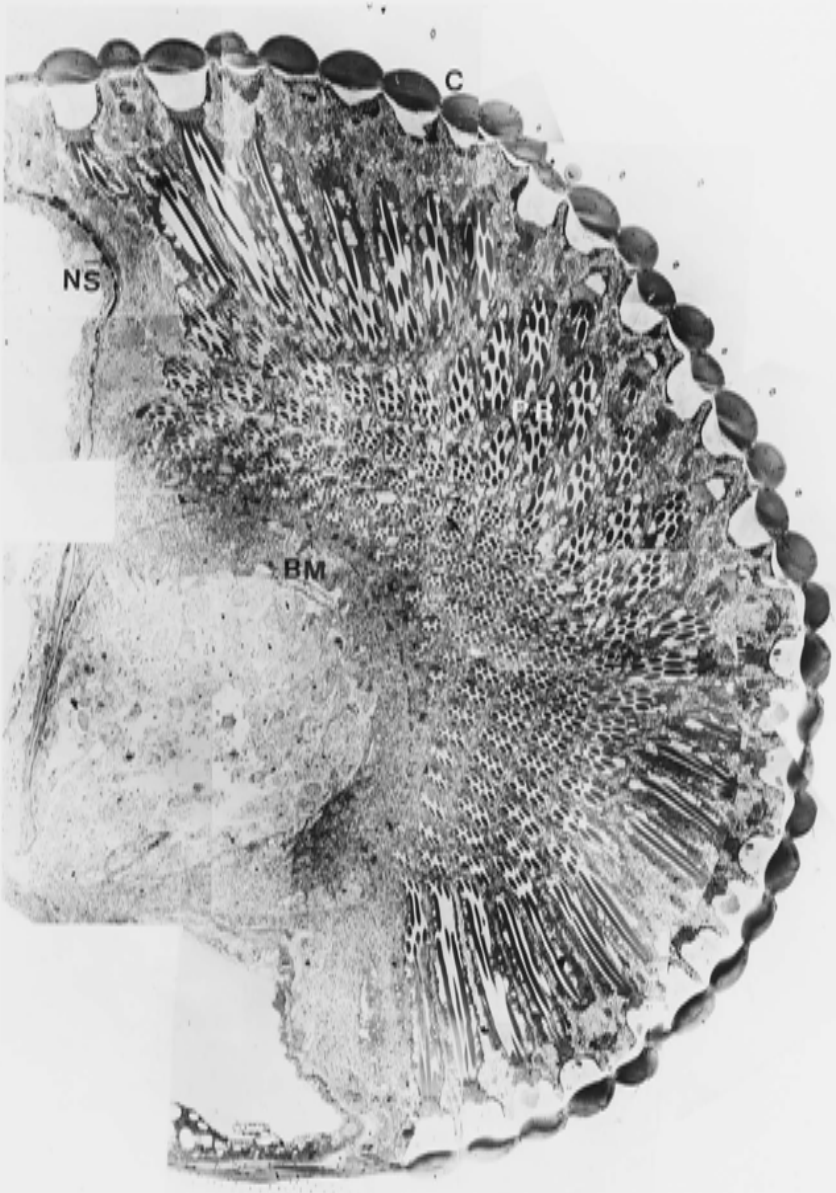
C
NS
BM

Fig. 5 Transmission electron microscopy analysis of the ultrastructure of the compound eye of *D. melanogaster*

Thin sections of adult eyes were prepared for TEM as described in Chapter 2, Section 2.12.

A. Longitudinal section of the anteria portion of the peripheral retina. The primary pigment cells can be distinguished from secondary pigment cells by the darker staining of the cytoplasm of the primary pigment cells which are adjacent the psuedocone. The cellular components are labelled as follows: C, cornea; PC, pseudocone; RC, retinula cells; R, rhabdomere; P, primary pigment cells; S, secondary pigment cells; B, bristle.
Magnification 3,000, Bar = 6.5 μm.

B. Cross section showing a set of seven rhabdomeres within their respective retinula cells of an ommatidium and the surrounding pigment cells which harbour pigment granules.
RC, retinula cell; R, rhabdomere; S, secondary pigment cell; pg pigment granule.
Magnification 105,000 x, bar = 2 μm

C. Lower magnification view of B, showing the repetitive array of ommatidia which make up the peripheral retina. The retinula cells of ommatidia can be seen both in cross section (lower half of the page) as well as longitudinal section (top of figure).
Magnification 1,500 x, bar = 13 μm.

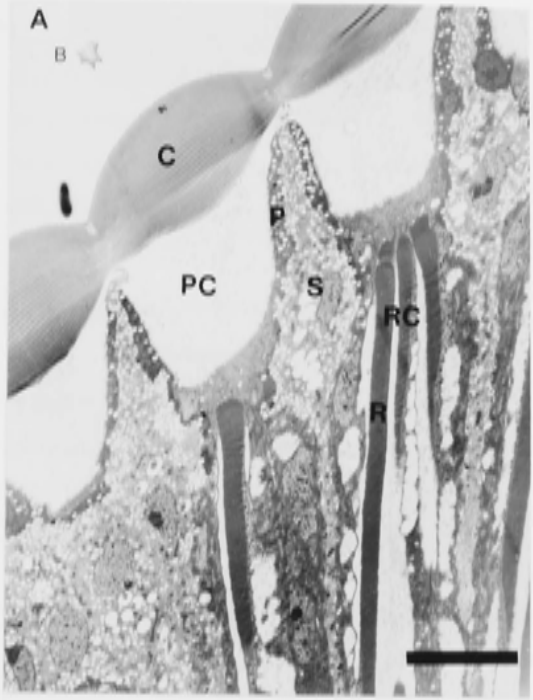
A
B
C
P
PC
S
RC
R

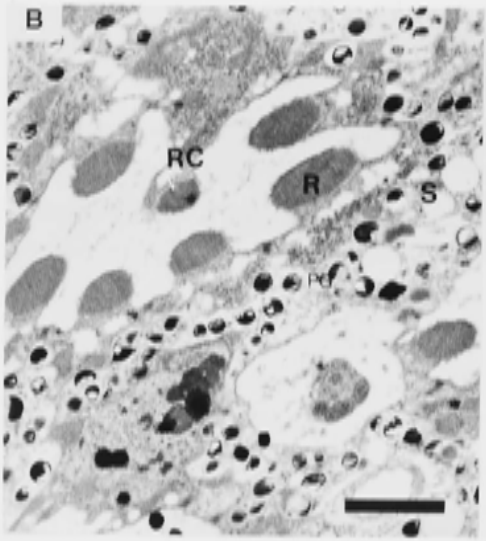
B
RC
R
S


C
RC
RC

7.2 Results

The preparation of *D. melanogaster* eye tissue for electron microscopy studies described herein (described in Chapter 2, Section 2.12.1) (i.e. fixation, dehydration, embeding in resin and sectioning) was performed by Cathy Gillespie (EM Unit, JCSMR, ANU).

7.2.1 Immuno-Localisation of the White protein to pigment granules

The preparation of eye tissue and immuno-gold labelling for transmission electron microscopy was performed as described in Chapter 2, Section 2.12. Immuno-gold labelling using purified anti-White antibody raised against a predicted extracellular loop of the White protein (described in Chapter 4) was observed strongly associating with pigment granules of both the primary (Fig. 6A) and secondary pigment cells (Fig. 6B and C) as well as to the small pigment granules within retinula cells (Fig. 6E and F). Some of the pigment granules in the primary pigment cells (Fig. 6A) appear electron lucent (or pale but not transparent) which is consistent with previously reported findings in newly emerged flies (Stark and Sapp, 1988). Newly emerged flies were selected for this work as the cuticle covering the eye hardens with age making it increasingly difficult to obtain cleanly cut sections. It has been shown by freeze fracture and platinum replicas that these granules are membrane bounded, although the membrane is usually difficult to see in micrographs of sectioned material (Stark and Sapp, 1988). Difficulty in preservation of pigment granules of eclosed flies for electron microscopy analysis has been noted previously and attributed to their increased solubility in alcohol and water (Cagan and Ready, 1989; Forrest, 1957; Shoup, 1966; Stark and Sapp, 1988). This problem was partially overcome in this work by reducing the level of alcohol during the dehydration process, resulting in increased preservation of intact pigment granules. Also shown in Fig. 6F and G are immuno-labelled pigment granules at the posterior region of secondary pigment cells close to the basement or fenestrated membrane of the secondary pigment cell, as well as pigment granules of the sub-retinal cells which lie beneath the fenestrated

Fig. 6 Immuno-labelling of White protein at pigment granules of primary, secondary pigment cells, retinula cells and sub-retinal cells

Thin sections of adult eyes were immuno-labelled using the procedure described in the experimental procedures Section 2.12. The anti-White antibody (raised against the wECL peptide, Section 2.11.1) was used for the primary antibody incubation, followed by a secondary anti-rabbit 10nm colloidal gold conjugated antibody which are visualised as very electron dense (black) particles easily seen at a magnification of 17,000 x.

A. Longitudinal section of the peripheral retina where a large amount of gold label is seen associated with intact pigment granules within a primary pigment cell. The primary pigment cell can be identified due to its darker appearance compared to the neighbouring secondary pigment cell, as well as its proximity to the cornea. P, primary pigment cell; PG, pigment granule; C, cornea; S secondary pigment cell.
Magnification 22,500x, bar = 0.8 μm.

B. Longitudinal section of the peripheral retina, where gold label is seen associated with pigment granules within a secondary pigment cell.
PG, pigment granule; S, secondary pigment cell. Magnification 22,500x , bar = 0.8 μm.

C. A lower magnification view showing the general area seen in B. PG, pigment granule; S, secondary pigment cell; R, rhabdomere.
Magnification, 13,500 x, bar = 1.5 μm.

D. Gold label can be seen associating with small pigment granules within a retinula cell. R, rhabdomere; PG, pigment granule. Magnification, 60,000 x, bar = 0.3 μm.

E. Lower magnification where the area shown in C. is boxed.
PG, pigment granule; R, rhabdomere; D, desmosome; RC, retinula cell.
Magnification 12,000 x, bar = 1.6 μm.

F. Immuno-labelling of pigment granules of both secondary pigment cells near the basement or fenestrated membrane of the secondary pigment cell, in addition to pigment granules of the sub-retinal cells below the basement membrane. S, secondary pigment cell; PG, pigment granule; BM, basement membrane; SR, sub-retinal cell.
Magnification 255,000 x, bar = 0.8 μm.

G. Lower magnification view where the area shown in F is boxed.
Magnification 6,000 x, bar = 3 μm.

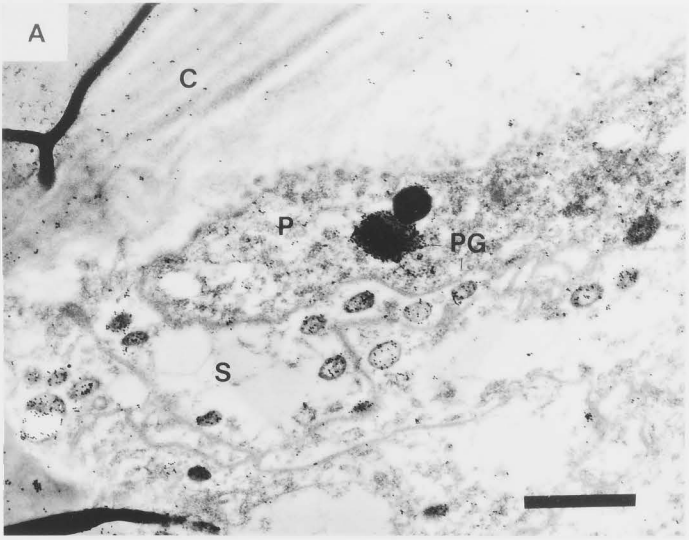
A
C
P
PG
S

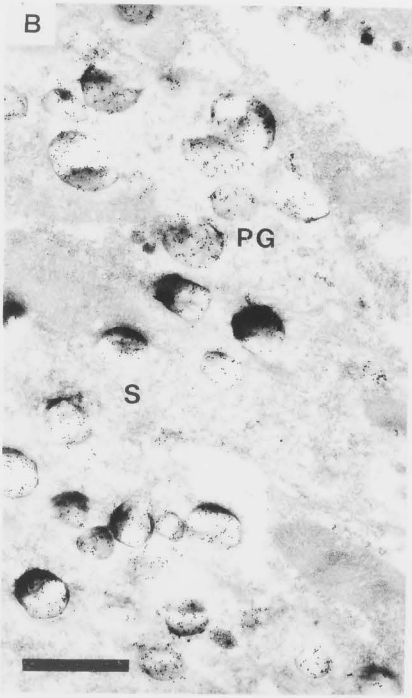
B
PG
S

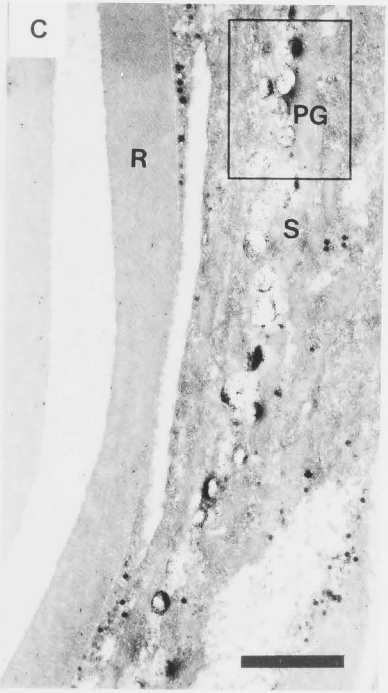
C
PG
R
S

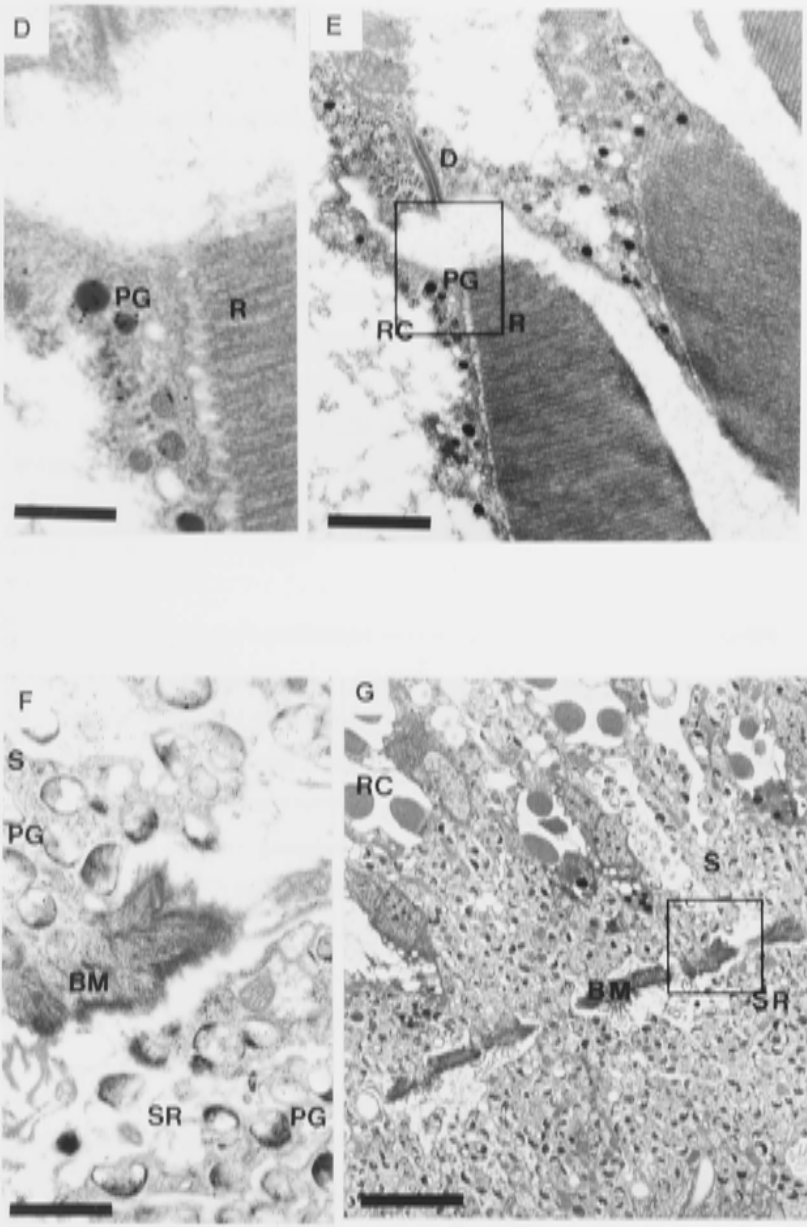
D
PG
R
E
D
PG
RC
R
F
S
PG
BM
SR
PG
G
RC
S
BM
SR

membrane. Although there is some background gold labelling, it is highly concentrated at the pigment granule. Labelling of the pigment cell plasma membranes was not observed.

7.2.2 Immuno-gold localisation of Scarlet protein to pigment granules

Immuno-localisation of the Scarlet protein was carried out as described for the localisation of the White protein, using purified anti-Scarlet antibody which was raised against a peptide representative of the amino-terminus of the Scarlet protein (see Chapter 4). Fig. 7 shows transmission electron micrographs of eye sections immuno-gold labelled using anti-Scarlet antibody. Again, labelling is concentrated on pigment granules within both primary pigment cells (Fig.7A and B) and secondary pigment cells (Fig. 7C and D), in addition to the small pigment granules of retinula cells (Fig. 7E and F). Pigment granules of sub-retinal cells were also immuno-labelled (Fig. 7G and H). Labelling of the pigment cell plasma membranes was not observed.

Control experiments were performed where the secondary gold-conjugated antibody alone was tested for non-specific labelling. Tissue sections cut from the same blocks as used for staining with anti-White and anti-Scarlet antibodies, were stained as described in Section 2.12 with the omission of the primary antibody incubation. Electron micrographs shown in Fig. 8 show that there is no gold labelling around pigment granules in primary (Fig. 8A and B) or secondary pigment cells (Fig. 8C) which provides good evidence that gold labelling of pigment granules described above is not due to non-specific labelling by the secondary antibody, but is due to specific labelling of the White and Scarlet proteins by anti-White and anti-Scarlet antibodies respectively.

In order to further rule out the possibility that the antibody labelling observed at pigment granules using either anti-White or anti-Scarlet was non-specific, eye tissue sections using material from the strain harbouring the mutation w^{1118} was

Fig. 7 Immuno-labelling of Scarlet protein at pigment granules of primary and secondary pigment cells, retinula cells, and sub-retinal cells.

Thin sections of adult eyes were immuno-labelled using the procedure described in the Section 2.12. Anti-Scarlet, antibody (raised against the stNT peptide, Section 2.11.1) was used for the primary antibody incubation, followed by a secondary anti-rabbit 10nm colloidal gold conjugated antibody which are visualised as very electron dense particles easily seen at a magnification of 17,000 x.

A. Longitudinal section of the peripheral retina where gold label is seen associated with pigment granule membranes within a primary pigment cell. The primary pigment cell can be identified due to its darker appearance compared to the neighbouring secondary pigment cell, as well as its proximity to the cornea. P, primary pigment cell; PG, pigment granule; S secondary pigment cell. Magnification 22,500 x, bar = 0.8 μm.

B. A lower magnification view of the area shown in A (boxed). PG, pigment granule; S, secondary pigment cell; C, cornea.
Magnification, (10,500 x), bar = 2 μm.

C. Cross section of the peripheral retina where gold label is seen associated with pigment granules within a secondary pigment cell. PG, pigment granule; S secondary pigment cell, R, rhabdomere.
Magnification 22,500 x , bar = 0.8 μm.

D. A lower magnification view of the area shown in C (boxed). PG, pigment granule; R, rhabdomere; S, secondary pigment cell.
Magnification, (13,500 x). Bar = 1.5 μm.

E. Gold label can be seen associating with small pigment granules within a retinula cell. PG, pigment granule; R, rhabdomere.
Magnification 60,000 x, bar = 0.3 μm.

F. Lower magnification where the area shown in C. is boxed.
PG, pigment granule; RC, retinula cell.
Magnification 7,500 x, bar = 2.6 μm.

G. Immuno-labelling of pigment granules of both secondary pigment cells near the basement or fenestrated membrane of the secondary pigment cell, in addition to pigment granules of the sub-retinal cells below the basement membrane. S, secondary pigment cell; PG, pigment granule; BM, basement membrane; SR, sub-retinal cell.
Magnification 255,000 x, bar = 0.8 μm.

H. Lower magnification view where the area shown in F is boxed.
Magnification 3,750 x, bar = 5 μm.

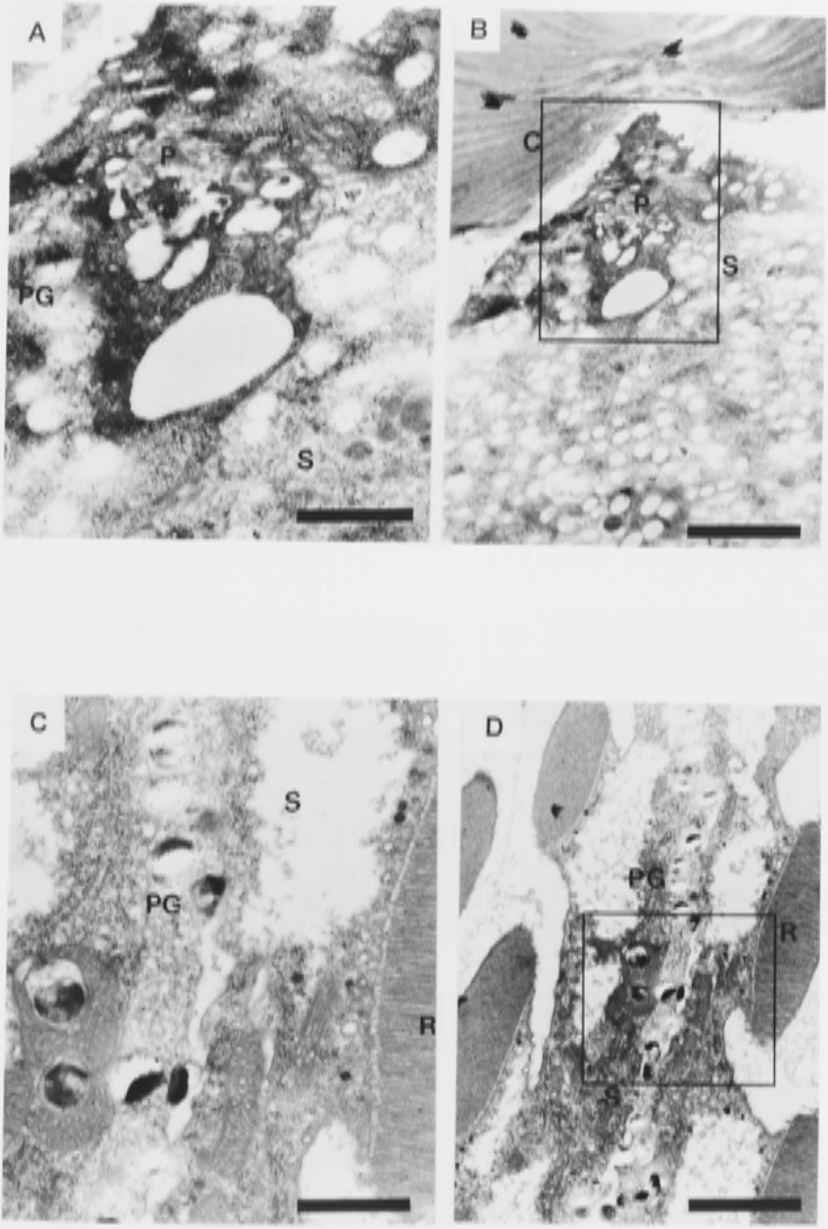
A
P
PG
S
B
C
P
S
C
S
PG
R
D
PG
R

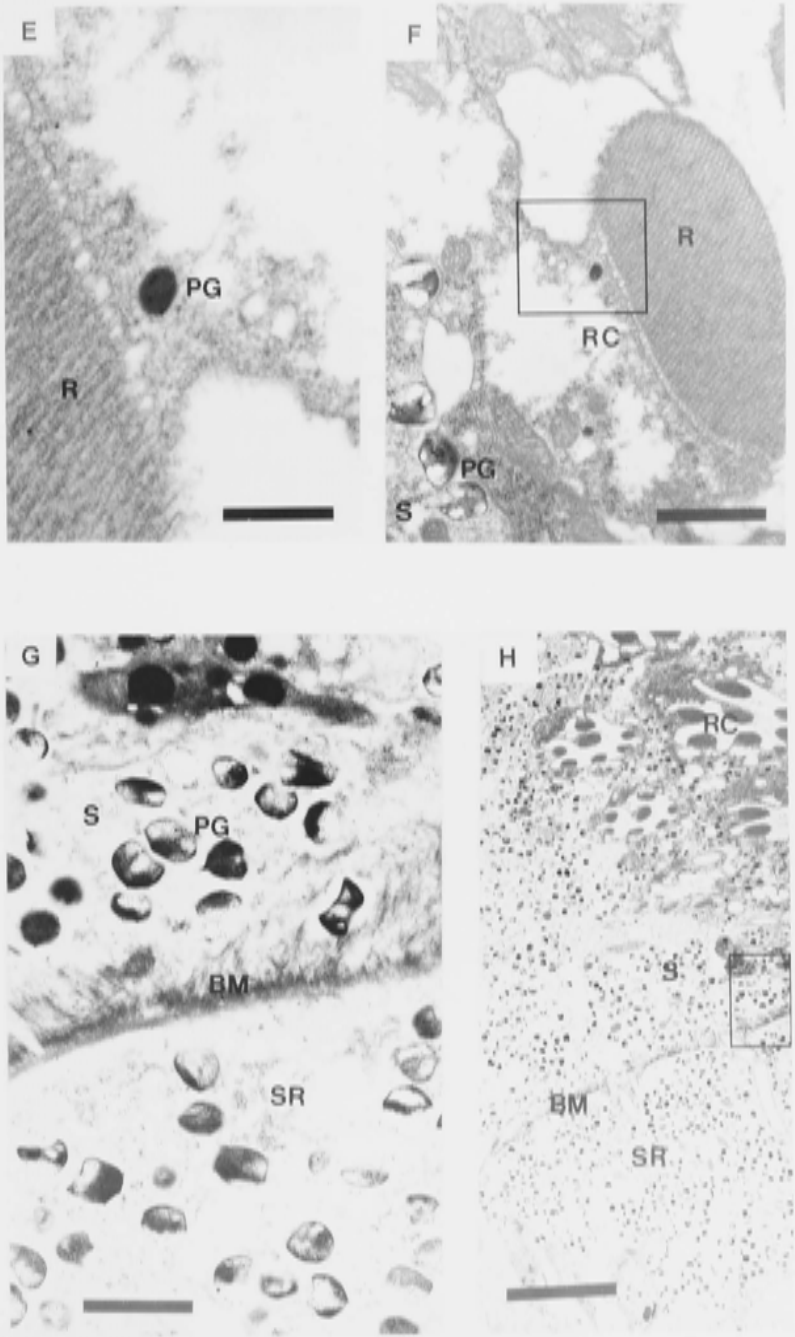
E
PG
R
F
R
RC
PG
S
G
S
PG
BM
SR
H
RC
S
BM
SR

Fig. 8 Secondary antibody control immuno-labelling of pigment cells

Thin sections of adult eyes were immuno-labelled using the procedure described Chapter 2, Section 2.12, however primary antibody incubation was omitted followed by incubation with the secondary anti-rabbit 10nm colloidal gold conjugated antibody.

A. Longitudinal section of the peripheral retina where no gold labelling can be seen associating with pigment granules of the primary pigment cells. Primary pigment cells can be identified as staining darker than the adjacent secondary pigment cells. Labelling is also absent from pigment granules within secondary pigment cells. S, secondary pigment cell; P, primary pigment cell; PG, pigment granule. Magnification 22,500 x, bar = 0.8 μm.

B. Lower magnification micrograph illustrating the general area shown in A (boxed). C, cornea; P, primary pigment cell; S, secondary pigment cell. Magnification 6,000 x, bar = 3 μm.

C. Cross section of the peripheral retina showing the absence of gold-labelling associated with pigment granules of secondary pigment cells. R, rhabdomere; S, secondary pigment cell; PG, pigment granules. Magnification, 22,500 x, bar = 0.8 μm.

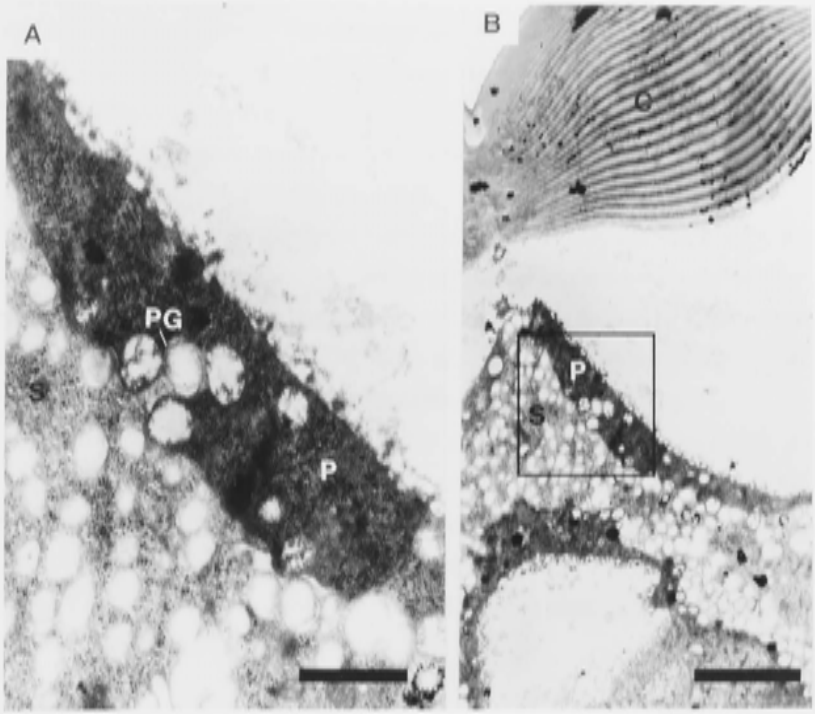
A
PG
S
P
B
C
P
S

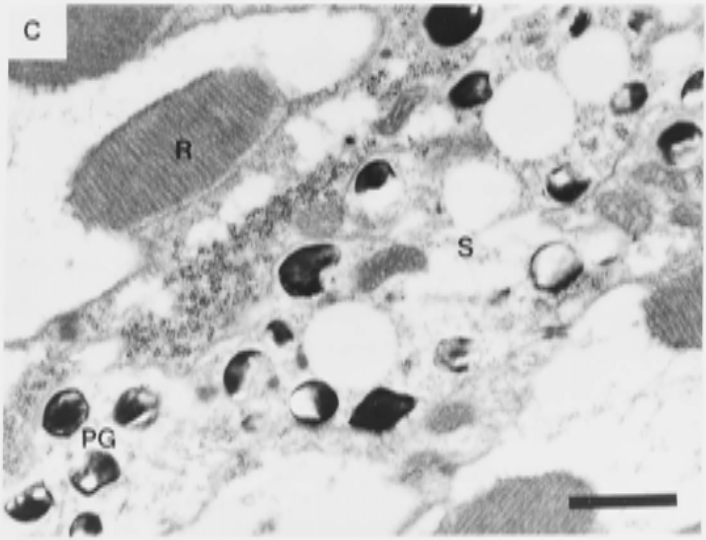
C
R
S
PG

used as a negative control. The mutation associated with w^{1118} is due to a deletion of the 5' region of *white* including all of exon I (Kurkulos et al, 1991; Levis et al, 1985) resulting in loss of function and a white-eyed phenotype. Ultrastructure of white-eyed mutants have been described previously (Schraermeyer and Dohms, 1993; Shoup, 1966; Stark and Sapp, 1988). These mutants lack pigment granules, however in their place are numerous electron dense granules of varying morphology, which are peculiar to the loss of function of the *white* gene product and were named type IV granules (Shoup, 1966). These type IV granules were observed in secondary pigment cells in the w^{1118} tissue, as shown in Fig. 9. No immuno-labelling was observed by anti-White, or anti-Scarlet antibodies respectively at type IV granules or any other cellular location in primary (Fig. 9A and B) or secondary pigment cells (Fig. 9C and D). This result provides strong evidence that the labelling observed in wild-type tissue was specific for White and Scarlet protein. The absence of Scarlet immuno-labelling suggests that Scarlet protein is not stably incorporated into pigment granule membranes (or type IV granules) in the absence of the White protein.

7.3 Discussion

The immuno-electron microscopy localisation studies described in this report provide the first experimental evidence that both White and Scarlet proteins co-localise to the membrane of pigment granules of primary and secondary pigment cells as well as pigment granules of retinula cells of the *D. melanogaster* compound eye. No evidence of plasma membrane localisation was observed, suggesting that White and Scarlet are not located in the pigment cell plasma membrane. Therefore, these findings do not support the traditional model for the involvement of these proteins in pigmentation (see Chapter 1, Section 1.6.2). Instead they suggest the model depicted in Fig. 10 for the involvement of White and Scarlet in the xanthommatin biosynthetic pathway. Entry of tryptophan into the pigment cells is not facilitated by the White/Scarlet transporter, but is presumably mediated by another transporter localised in the plasma membrane.

Fig. 9 Immuno-labelling with anti-White and anti-Scarlet antibodies respectively of eye tissue from a *white* mutant (w^{1118})

Tissue was prepared eyes of adult w^{1118} flies and immuno-labelled in the same way as for wild-type. Results of immuno-labelling with both anti-White and anti-Scarlet antibodies respectively were the same and TEMs shown here are representative of both immuno-labelling experiments.

A. Longitudinal section of the peripheral retina showing the absence of gold-labelling associated with electron dense type IV granules within primary pigment cells; these granules are peculiar to the *white* loss of function mutants, as described in the text. PC, psuedocone; S, secondary pigment cell; P, primary pigment cell; T, type IV granule. Magnification, 22,500 x, bar = 0.8 μm.

B. A lower magnification view showing the general area seen in A (boxed). C, cornea; PC, psuedocone; S, secondary pigment cell; P, primary pigment cell; T, type IV granule. Magnification, (4,500 x). Bar = 4.5 μm.

C. Cross section of the peripheral retina showing the absence of gold-labelling associated with electron dense type IV granules within secondary pigment cells. S, secondary pigment cell; T, type IV granule. Magnification, 22,500 x, bar = 0.8 μm.

D. A lower magnification view showing the general area seen in C (boxed). RC, retinula cell; S, secondary pigment cell; T, type IV granule; R, rhabdomere. Magnification, (4,500 x). Bar = 4.5 μm.

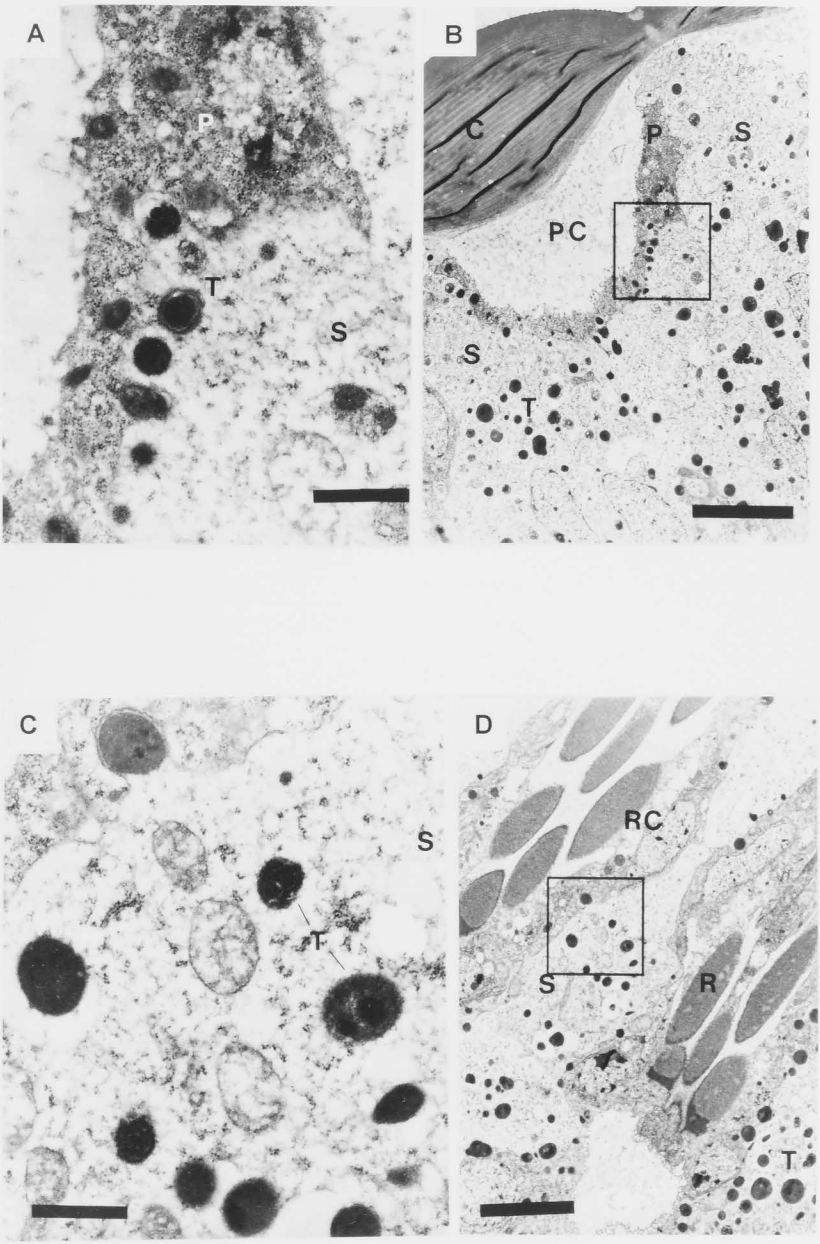
A
P
T
S
B
C
P
S
PC
S
T
C
S
T
D
RC
S
R
T

Fig. 10 Model of the involvement of White and Scarlet proteins in the biosynthetic pathway of xanthommatin

The steps involved in the biosynthesis of xanthommatin within pigment cells of the compound eye, from its precursor tryptophan are outlined here (reviewed in (Summers et al, 1982)) and illustrates how the White and Scarlet proteins fit into this pathway. Enzymes involved at different steps of the pathway are boxed and are shown at their respective sub-cellular locations. Our results show that the White and Scarlet proteins are not located in the plasma membrane but are located in the membrane surrounding the pigment granules. The predicted orientation of the White/Scarlet transporter is also indicated where the nucleotide binding domains are exposed on the cytoplasmic face of the pigment granule membrane. Putative sites of glycosylation (evidence for which is presented in Chapter 5, Section b) are shown as asterisks.

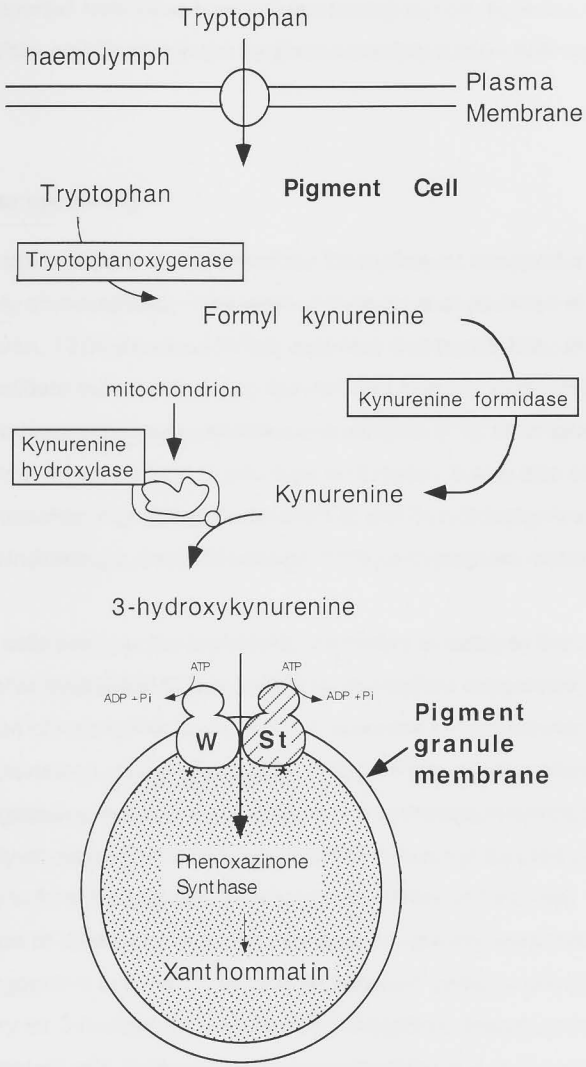
Tryptophan
haemolymph
Plasma
Membrane
Pigment Cell
Tryptophan
Tryptophanoxygenase
Formyl kynurenine
mitochondrion
Kynurenine formidase
Kynurenine
hydroxylase
Kynurenine
3-hydroxykynurenine
ATP
ATP
ADP +Pi
ADP +Pi
W
St
Pigment
granule
membrane
Phenoxazinone
Synthase
Xanthommatin

Instead, the White/Scarlet transporter is located in the membrane of the pigment granules and is probably involved in the transport of 3-hydroxykynurenine. The results reported here raise new and interesting issues regarding the fundamental role of White and Scarlet in the xanthommatin production pathway, as discussed below.

Substrate specificity

To date, the substrate specificity of the White/Scarlet transporter has not been definitively characterised. The work of Sullivan et al (Sullivan et al, 1980; Sullivan and Sullivan, 1975) provided strong evidence that tryptophan, and kynurenine were candidate substrates due to the reduced ability of explanted developing eyes or larval malpighian tubules from the null mutants w^{o} or st^{o} to take up these compounds, in comparison to wild-type w^{+} tissues. It was also shown that these mutants excreted high levels of kynurenine and 3-hydroxykynurenine (Howells et al, 1977) indicating a defect in storage of these tryptophan metabolites.

Pigment cells possess the enzymatic machinery to catalyse the conversion of intra-cellular tryptophan to kynurenine by tryptophan oxygenase, as well as the conversion of kynurenine to 3-hydroxykynurenine by kynurenine hydroxylase (see Fig. 10) (reviewed in (Summers et al, 1982)). Pigment deposition within the pigment granules requires the oxidation of 3-hydroxykynurenine involving both autocatalysis, as well as an enzyme mediated reaction by phenoxazinone synthase to form the pigment xanthommatin (Wiley and Forrest, 1981). The localisation of White and Scarlet to the pigment granule membrane is therefore highly suggestive that the White/Scarlet transport complex provides the import machinery for 3-hydroxykynurenine into the pigment granule (see Fig. 10). It is also consistent with Sullivan's uptake observations in null mutants if it is assumed that tryptophan and kynurenine enter the cells of the eyes or malphigian tubules, are converted to 3-hydroxykynurenine which is then imported into the granules. The observation reported herein for the compound eye may also apply to sub-

cellular compartments of malpighian tubules. Although wild-type malpighian tubules do not contain pigment granules, fluorescent sub-cellular granules have been implicated to be a site for storage of xanthommatin precursors, and these fluorescent granules are absent in null mutants of *white* and in the double *brown/scarlet* mutant (Yagi and Ogawa, 1996).

Another important observation made by Sullivan's group, with respect to *white* and *scarlet* mutants, was that although the tissues of the null mutants w^{o} and st^{o} showed reduced tryptophan uptake, tryptophan was nevertheless available for protein synthesis (Sullivan et al, 1980). In addition there are no known mutations of *white* which are lethal - lethality would be expected from a defect that prevented transport of an essential amino acid into cells - suggesting that tryptophan is transported into cells by another transport mechanism. Evidence for this has been provided by experiments showing that uptake of tryptophan by the w^{+} system of wild-type malpighian tubules was inhibited by the analogue 5-methyl-tryptophan, however, incorporation of radioactive tryptophan into protein in malpighian tubules from wild-type as well as the null mutant w^{o} occurred at the same rates and was not affected by 5-methyl-tryptophan (Sullivan et al, 1980). It was concluded that 'Malpighian tubules have a transport system that enables entry of tryptophan into a cellular pool and that this cellular pool is initially independent of the tryptophan pool used for protein synthesis' (Sullivan et al, 1980). If this proposal also applies to the pigment cells of the compound eye, the immuno-localisation studies reported herein are consistent with this hypothesis. It is probable that tryptophan is imported into pigment cells via amino acid transporters such as those described in other eucaryotic cells (Castagna et al, 1997; McGivan and Pastor-Anglada, 1994; Shotwell and Oxender, 1983). This may be a system of uptake which is common to most cell types and provide a means for uptake of tryptophan necessary for protein synthesis. However in pigment cells, deposition of xanthommatin within pigment granules would cause a metabolic sink for 3-hydroxykynurenine, thereby dictating a higher rate of uptake of xanthommatin precursors in these cells. In this respect, uptake of 3-

similar to the uptake of tyrosine by melanosomes in mammalian melanocytes (Potterf et al, 1996).

The xanthommatin pathway has been recognised as a major pathway for the removal of free tryptophan (Linzen, 1974). The glutarate pathway - the pathway which removes tryptophan in mammalian cells - is absent in insects (Linzen, 1974). The expression of the *white* gene (and presumably also *scarlet*) is largely restricted to tissues which are associated with storage of tryptophan metabolites or pigmentation (Fjose et al, 1984; Summers et al, 1982). It has been reported that 30% of the total tryptophan content of early pupae is channelled into pigment (Ryall and Howells, 1974). During metamorphosis large amounts of tryptophan are released from the fat body and it is thought that expression of *white* and *scarlet* in the pigment cells of the developing eye enables these cells to take up tryptophan, kynurenine and 3-hydroxykynurenine at much higher rates than is required for protein synthesis (Howells and Ryall, 1975; Howells et al, 1977).

Orientation in the membrane

There are two possible orientations for the White and Scarlet proteins in the pigment cell membrane: either the nucleotide binding domains are located in the cytoplasm, or within the lumen of the pigment granule. Unfortunately from the immuno-labelling described here, it is impossible to distinguish the sidedness of the labelling. This issue might best be addressed using a double labelling technique where epitopes on opposite sides would be labelled with different sized gold particles. The molecular weights of White and Scarlet proteins extracted from fly heads and analysed by SDS PAGE and Western blotting, suggests that these proteins may be glycosylated in vivo (described in Chapter 5 Section b). Possible N-linked glycosylation signals are present within a large loop between putative transmembrane helices 5 and 6 of both White and Scarlet. This loop is predicted to be on the opposite side of the membrane to the nucleotide binding domains (Ewart et al, 1994). If White and Scarlet are N-glycosylated in the golgi

and endoplasmic reticulum as suggested by Western analysis - where sugar groups are added to the luminal side of the golgi-ER membrane - then the loop between transmembrane helix 5 and 6 would be located in the lumen of the pigment granule, (and the nucleotide binding domains in the cytoplasm) giving the orientation for the transporter shown in Fig. 10.

Protein targeting of White and Scarlet

It has recently been reported that the protein targeting machinery involved in biogenesis of the eye pigment granules, is similar to pathways involved in protein sorting to melanosomes and lysosomes (reviewed in (Lloyd et al, 1998)). The recent cloning and sequencing of the *Drosophila* eye-colour gene *garnet*, reveals that the product of this gene shows strong sequence homology to a subunit of the human AP-3 complex (Ooi et al, 1997; Simpson et al, 1997), which is involved in protein trafficking to lysosomes as well as specialised endosomal-lysosomal organelles (Simpson et al, 1997). The *garnet* gene product is necessary for biogenesis of eye pigment granules in *Drosophila* and it has been postulated that the Garnet protein is involved in the protein sorting events leading to the granules (Ooi et al, 1997; Simpson et al, 1997). It was suggested that Garnet-containing coat complex may be involved in targeting pigment biosynthetic enzymes and pigment precursor transporters to the pigment granule membrane (Ooi et al, 1997; Simpson et al, 1997).

The relationships between the protein sorting machinery of pigment granules, melanosomes and lysosomes leads to the possibility that membrane proteins targeted to these organelles harbour similar sorting signals. It has been noted that some lysosomal and melanosomal membrane proteins harbour similar di-leucine motifs, which are recognised by AP-3 (Höning et al, 1998; Lloyd et al, 1998; Odorizzi et al, 1998). Inspection of the amino-terminal region of White, Brown and Scarlet from *Drosophila* and White homologs of other species reveals a putative di-leucine motif similar to those reported in membrane proteins of melanosomes, lysosomes and the yeast vacuole (reviewed in (Lloyd et al, 1998)) and this is

melanosomes, lysosomes and the yeast vacuole (reviewed in (Lloyd et al, 1998)) and this is illustrated in Fig. 11. The White homologs which occur in other insect species are related in function to the *D. melanogaster* White protein (Zwiebel et al, 1995). The function of the White homologs identified in humans (which shares 33% identity (56% similarity)) (Chen et al, 1996; Croop et al, 1997) and mouse (which shared 34% identity with *D. melanogaster* White) (Croop et al, 1997; Savary et al, 1996), are unknown. However the mammalian homologs of *white* have been shown to be highly expressed in brain and other tissues, and it has been postulated that the gene product may perform a role in the tryptophan → serotonin biosynthetic pathway (Croop et al, 1997). It is tempting to speculate on the possible location of human White to synaptic vesicles involved in serotonin storage in nerve cells.

It is interesting to note that the amino acid region containing the di-leucine in White is not conserved in Scarlet and Brown (not shown), however there is a sequence further upstream resembling a di-leucine motif in these proteins (see Fig. 11). The observation that no Scarlet labelling was detected in the w^{1118} tissue, even though the wild-type *scarlet* gene is present, raises the possibility that the White subunit interacts with AP-3 and this interaction is required for the assembly of the Scarlet, and also possibly the Brown subunit.

7.4 Summary

The localisation studies described in this chapter has provided new insights into the role of the White and Scarlet proteins in the eye pigmentation. The localisation to the pigment granule membrane rather than the plasma membrane provides fundamental new information with respect substrate specificity, now proposed to be 3-hydroxykynurenine rather than tryptophan, in addition to the likely orientation of the transporter in the membrane and to the direction in which substrate molecules move, relation to the transporter during transport.

Fig. 11 Alignment of putative pigment granule targeting signals of White of *D. melanogaster* and related proteins

A sequence alignment (ClustalW) - performed as described in Section 2.6.10 - reveals a conserved region near the first predicted transmembrane spanning region, which is similar to di-leucine-based signal sequences identified and experimentally characterised in a number of membrane proteins targeted to melanosomes, and lysosomes respectively (Odorizzi et al, 1998). The putative di-leucine-based sequences are boxed, and conserved acidic residues located upstream of the di-leucine are shown in bold face. The positions of the N- or C-termini and transmembrane domains (TMDs) are indicated. Protein sequences were obtained from the Swiss Prot data base.

Abbreviations and Swiss Prot accession numbers are as follows:
dWhite, *D. melanogaster* White, P10090; Lc, *Lucilia cuprina* (Australian sheep blowfly), Q05360; Cc, *Ceratitis capitata* (Mediterranean fruit fly), Q17320; Ag, *Anopheles gambiae* (African malaria mosquito), Q27256; hWhite, human White homolog P45844; mWhite, mouse White homolog Q64343; dBrown, *D. melanogaster* Brown, P12428; dScarlet, *D. melanogaster* Scarlet, P45843.

White related proteins

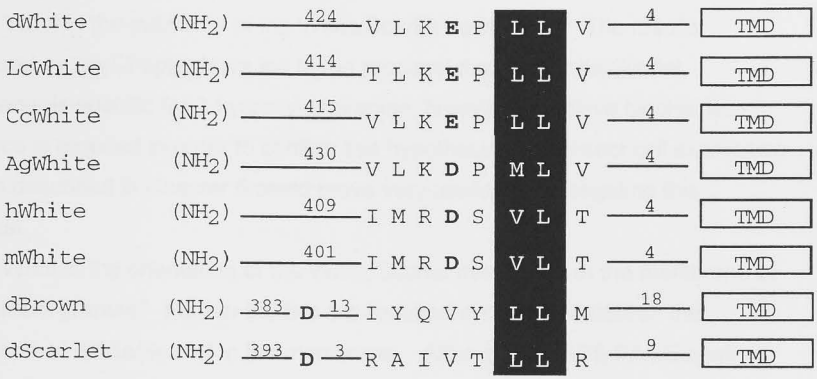

Melanosomal membrane proteins

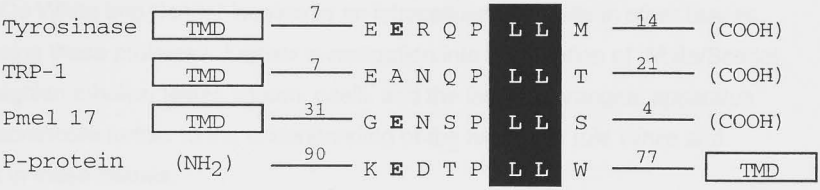

Lysosome and yeast vacuole membrane proteins

* How are White and Scarlet targeted to the pigment granule? The characterisation of the role of the dileucine signal sequence in targeting the White protein would be a good starting point for investigation of this question. In addition, this system could potentially be used as a new model system for the study of protein targeting by the AP-3 adaptor proteins.

* What is the substrate of the White/Scarlet transporter? The results discussed in this Chapter have led to the proposal that the White/Scarlet transporter is specific for 3-hydroxykynurenine, however, definitive biochemical evidence is required in order to confirm this hypothesis. The insect cell expression system described in Chapter 5 could prove very useful in investigating this proposal.

* What is the orientation of the White/Scarlet transporter in the membrane of the pigment granule? Further studies are required in order to establish the orientation of White/Scarlet in the membrane. Although the SDS PAGE analysis of White Scarlet suggests it may be glycosylated, further evidence is required to confirm this possibility.

* Do White and Scarlet localise to an intracellular organelle in other tissues expressing these proteins? Further investigation into the location of White/Scarlet in malpighian tubules, testes sheath, ocelli, and the larval pharangeal apparatus would contribute further to the understanding of the functional role White and Scarlet in these tissues.

CHAPTER 8

FINAL DISCUSSION

8. FINAL DISCUSSION

This final chapter will briefly compare and contrast the aims of the research described in this thesis at its outset, with the experimental systems which were developed in order to achieve these aims. A summary of the experimental results and how they contribute to the understanding of the White/Scarlet and White/Brown ABC transporters will be provided. Potential courses of action to extend the achievements described here will also be discussed.

The major aim of this thesis was to develop a number of experimental systems with which to investigate the structure, function and biology of the pigment precursor ABC transporters of *D. melanogaster*. Methods for the *in vivo* localisation, heterologous expression, isolation and characterisation of White and Scarlet proteins were investigated (summarised in Fig. 1). An important goal of setting up the heterologous expression systems was to facilitate the use of site directed mutagenesis of White and Scarlet in order to determine specifically the effects of certain mutations on various measurable functions such as ATP binding and hydrolysis, substrate transport and inter-subunit interactions. In addition, sequence analysis of *white* alleles from partially pigmented flies was used to identify a number of specific point mutations responsible for the mutant phenotypes (Ewart et al, 1994). This approach has been used previously by the group to identify residues important for functional interactions between the White and Brown subunits (Ewart et al, 1994; Ewart and Howells, 1998).

A summary of the results obtained from each of the experimental systems developed herein is provided below. The contribution these results make to the understanding of the White/Scarlet and White/Brown transporters, as well as the field of ABC transporters is discussed.

Fig. 1 Fundamental concepts and aims of the thesis

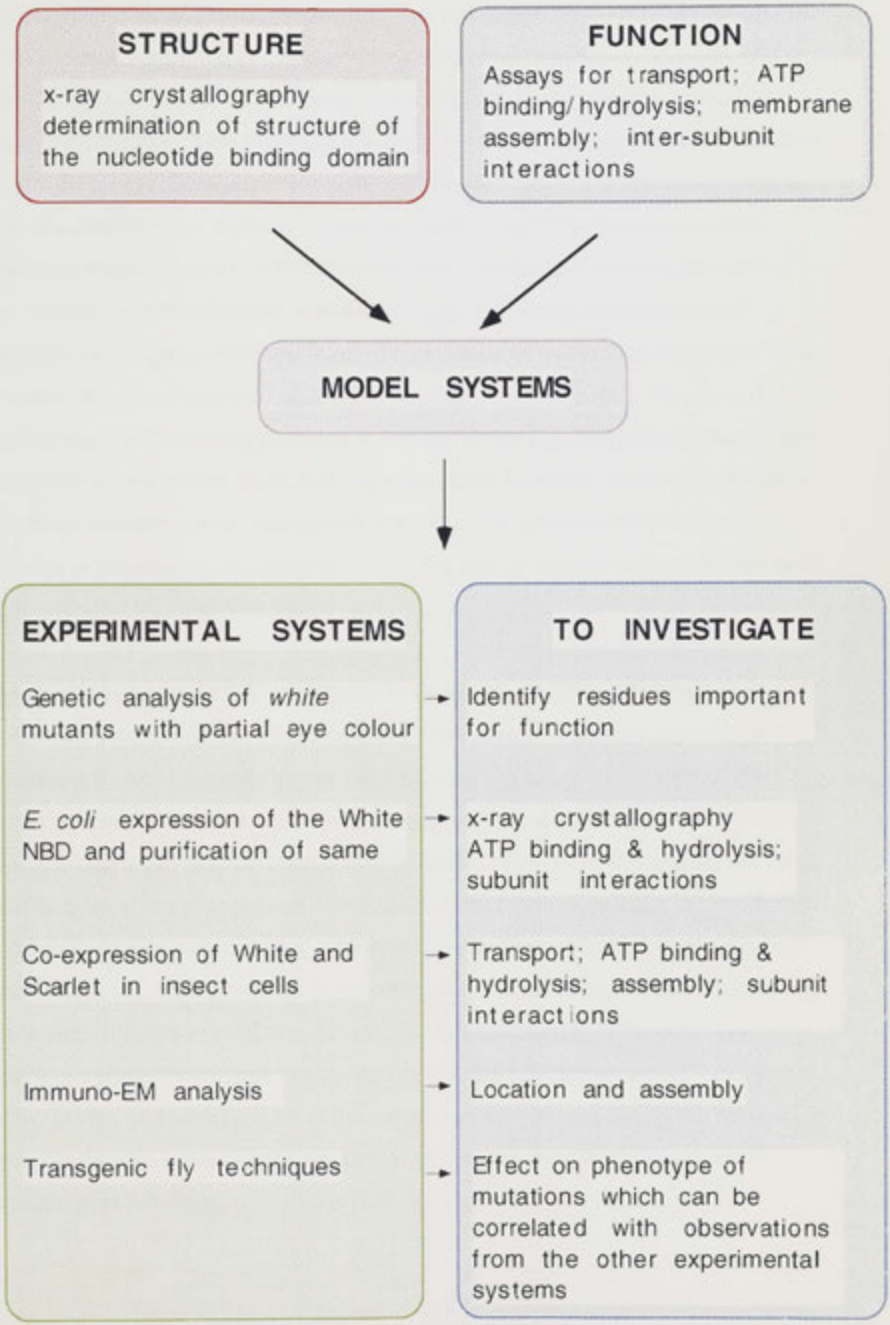

Localisation of White and Scarlet in the compound eye of *D. melanogaster*

The findings presented in Chapter 7 described the localisation of White and Scarlet proteins to the membranes of the sub-cellular organelles known as pigment granules. This finding is significant in that it provides the first definitive evidence for the localisation of White and Scarlet, which provides new insights into the role of these proteins in the transport of xanthommatin precursors. Previous models based on biochemical data, predicted a plasma membrane localisation of White/Scarlet, thereby situating the transporter in an ideal position for tissue specific transport of high levels of tryptophan into those cells involved in pigmentation or storage of tryptophan metabolites. However, the finding that White/Scarlet complex is located at the pigment granule membrane suggests a new model, such that the transporter functions as an importer of 3-hydroxykynurenine into the pigment granule. The absence of White and Scarlet at the plasma membrane implies the use of another transporter for entry of tryptophan into the cells (see Fig. 2).

Another implication of the new model involves the direction of transport of substrate with respect to the transporter orientation. A plasma membrane localisation would logically locate the NBDs on the cytoplasmic side of the plasma membrane and hence, extracellular substrate would first interact with extracellular loops and be transported inwards. However, the location of White and Scarlet at the intracellular membrane of the pigment granule in combination with evidence of glycosylation, indicates the direction of transport of substrate with respect to the transporter is reversed and therefore initial substrate binding sites would reside at locations exposed to the cytoplasm. If the orientation predicted herein is correct, the transporter would function as an ATP-driven efflux pump, hydrolysing ATP in the cytoplasm and linking this to the removal of its substrate from the cytoplasm, similar to the way the drug-efflux pump P-glycoprotein functions.

Fig. 2 Comparison of the previous and new model for the location and transport function of the White/Scarlet transporter.

A. This figure is a simple cartoon illustrating the previously published model for White/Scarlet. In this model White/Scarlet was located in the plasma membrane where it functioned in the uptake of tryptophan into pigment cells of the eye and cells of the malpighian tubules.

B. This figure is a simple cartoon illustration of the new model based on the findings presented in Chapter 7. In this model the White/Scarlet transporter is located in the membrane of pigment granules within pigment cells of the eye and transports 3-hydroxykynurenine into the pigment granule for subsequent conversion into xanthommatin. Asterisks indicate potential glycosylation sites on intra-granular loops which connect transmembrane helices 5 and 6 of both White and Scarlet.

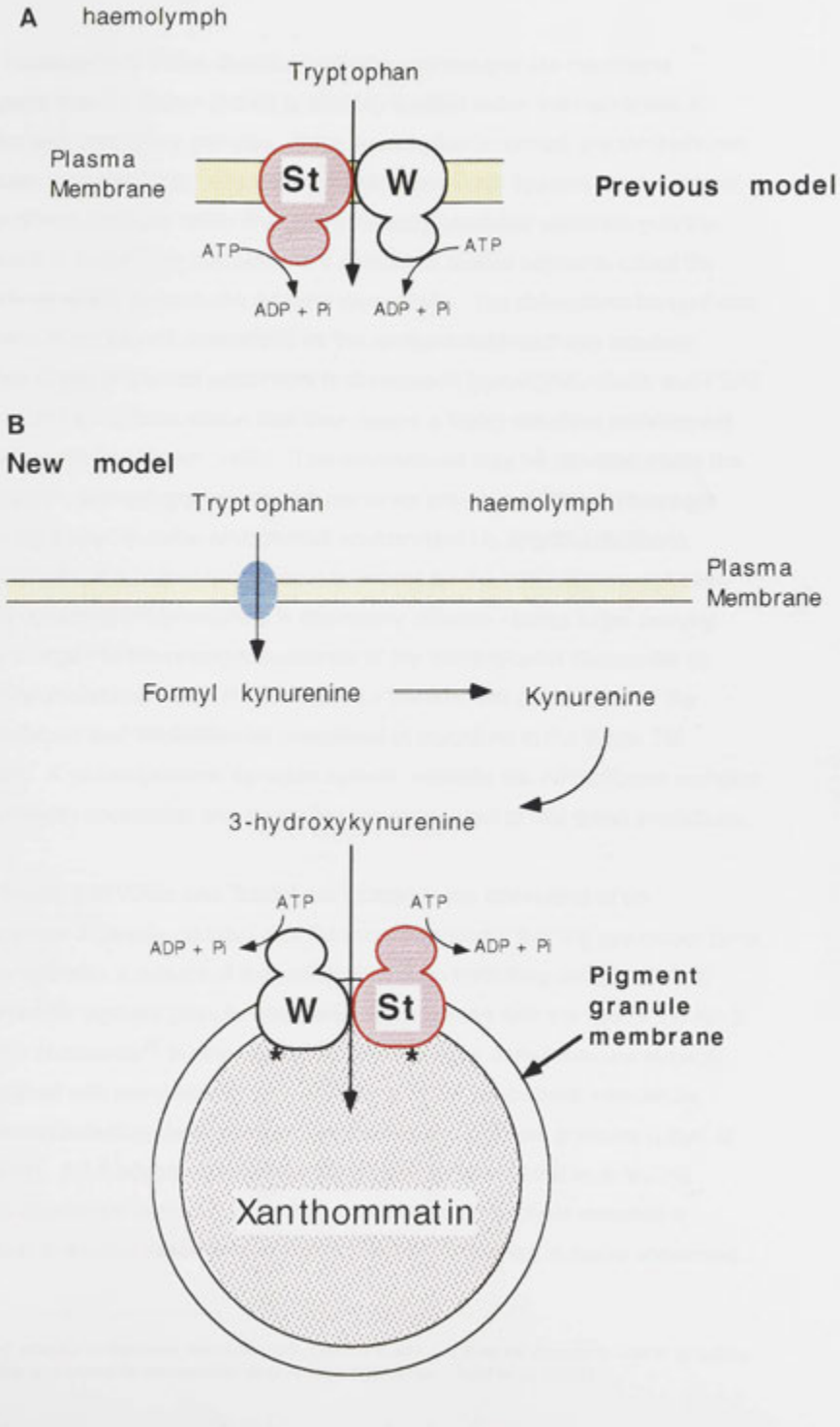
A haemolymph
Tryptophan
Plasma Membrane
St
W
ATP
ATP
ADP + Pi
ADP + Pi
Previous model
B
New model
Tryptophan
haemolymph
Plasma Membrane
Formyl kynurenine
Kynurenine
3-hydroxykynurenine
ATP
ATP
ADP + Pi
ADP + Pi
W
St
Pigment granule membrane
Xanthommatin

The localisation of White and Scarlet to the pigment granule membrane suggests that the Brown protein is similarly located within the membrane of drosopterin containing granules. If this assumption is correct, the White/Brown complex is predicted to transport drosopterin precursor towards the end of the biosynthesis pathway rather than the previously predicted substrate guanine. Guanine is the primary precursor to a number of related pigments called the pteridines which includes the pigment drosopterin. The drosopterin biosynthetic pathway is not as well understood as the xanthommatin pathway however studies of two of the late precursors to drosopterin (pyruvoyl-H_4-pterin and PDA) (shown in Fig. 3) have shown that they require a highly reductive environment (Wiederrecht and Brown, 1984). This environment may be provided inside the drosopterin pigment granule and the precursor previous to those precursors requiring a special redox environment environment i.e. dihydropneopterin triphosphate, is a potential candidate substrate for the White/Brown complex. Dihydropneopterin triphosphate is chemically different - being larger carrying more charge - to the predicted substrate of the White/Scarlet transporter (3-hydroxykynurenine) which may account for the different sensitivities of the White/Brown and White/Scarlet complexes to mutations in the White TM domain. A proteoliposome transport system whereby the White/Brown complex are correctly assembled and orientated, could be used to test these predictions.

The finding that White and Scarlet are located in the membrane of an intracellular organelle coupled with the recent discovery that the eye-colour gene *garnet* encodes a subunit of a specialised protein trafficking complex (AP-3) essential for pigment granule biogenesis, is consistent with the role of the AP-3 adaptor complexes[21] in other systems. AP-3 adaptor complexes are strongly associated with membrane protein trafficking to the specialised intracellular organelles including melanosomes, lysosomes and pigment granules (Lloyd et al, 1998). AP-3 adaptor complexes have been shown to bind to di-leucine signal sequences of the target protein, and sequence analysis revealed a putative di-leucine based sorting signal (Section 7.3) which is highly conserved

[21] AP-3 adaptor complexes associate with clathrin coats and play an important role in targeting membrane proteins to intracellular specialised organelles (Lloyd et al, 1998).

Fig. 3 Drosopterin biosynthetic pathway

This figure is derived from (Summers et al, 1982; and Wiederrecht and Brown, 1984) and shows the chemical structures of precursors to drosopterin and possible sub-cellular locations of the precursors.

Abbreviations:

H_2-NTP, dihydroneopterin triphosphate;

GTP, guanosine triphosphate;

PDA, 2-amino-4-oxo-6-acetyl-7,8-dihydro-3H,9H-pyrimido{4,5-b]-1,4]diazepine;

pyruvoyl-H_4-pterin, pyruvoyltetrahydropterin.

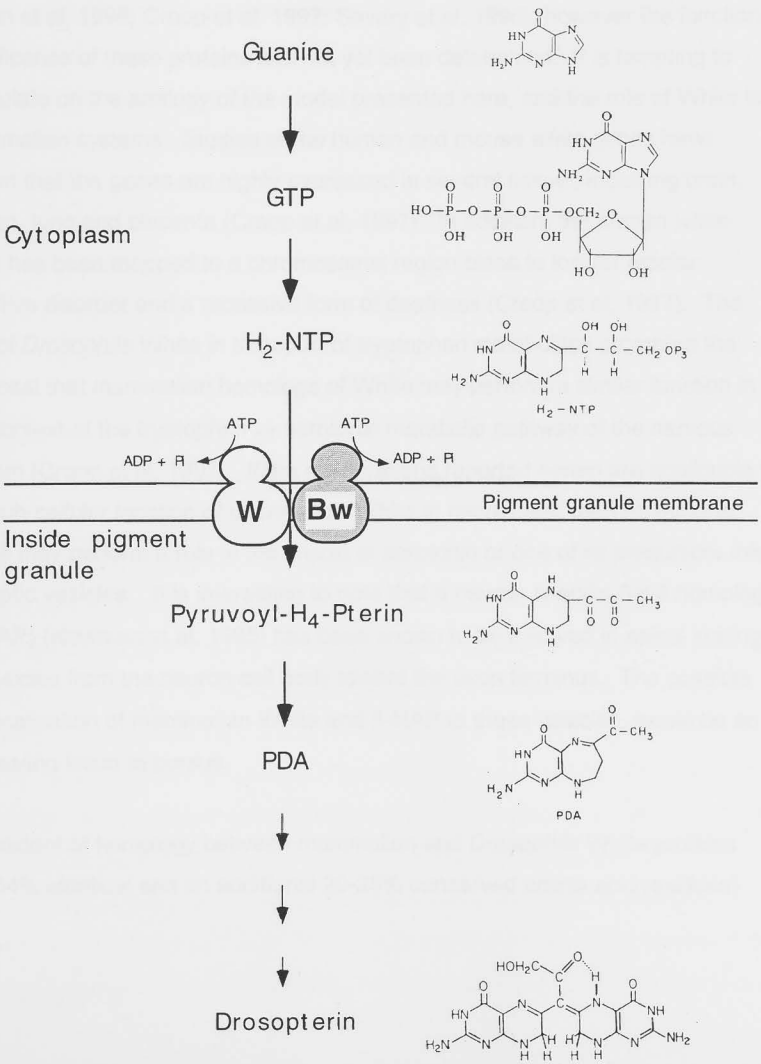

not only in insect homologs of White, but also the mammalian homologs. Construction of transgenic flies with mutations in the putative di-leucine motif could be used to investigate the role of these residues on the sub-cellular location of White and Scarlet which could be assayed by immuno-EM localisation.

Implications for the roles of mammalian homologs of *Drosophila* White

Two mammalian homologs of *Drosophila white* gene have been cloned recently (Chen et al, 1996; Croop et al, 1997; Savary et al, 1996), however the functional significance of these proteins has not yet been determined. It is tempting to speculate on the analogy of the model presented here, and the role of White in mammalian systems. Studies of the human and mouse *white* genes have shown that the genes are highly expressed in several tissues including brain, spleen, lung and placenta (Croop et al, 1997). In addition, the human *white* gene has been mapped to a chromosomal region close to loci for bipolar affective disorder and a recessive form of deafness (Croop et al, 1997). The role of *Drosophila* White in transport of tryptophan metabolites prompted the proposal that mammalian homologs of White may perform a similar function in the context of the tryptophan → serotonin metabolic pathway of the nervous system (Croop et al, 1997). If the observations reported herein are applicable to the sub-cellular location of mammalian White in nerve cells, then mammalian White may perform a role in the import of serotonin or one of its precursors into synaptic vesicles. It is interesting to note that a neuron specific AP-3 homolog (β-NAP) (Newman et al, 1995) has been shown to be involved in apical sorting of vesicles from the neuron cell body toward the axon terminus. The possible co-localisation of mammalian White and β-NAP to these vesicles, would be an interesting issue to pursue.

The extent of homology between mammalian and *Drosophila* White proteins (26-34% identical and an additional 20-25% conserved amino-acid residues)

(Croop et al, 1997) presents the exciting possibility that information gained from the study of the related *Drosophila* proteins may contribute to the understanding of fundamental neurological processes which occur in the mammalian nervous system.

It is interesting to note that over-expression of White in *Drosophila* was reported to cause male-male courtship in *Drosophila* suggesting that White plays a role in the nervous system (Zhang and Odenwald, 1995). Although this effect might be explained by an imbalance of tryptophan metabolites which may alter brain function, further investigation into the possible expression and localisation of White in brain tissue would be worthwhile pursuing. Northern analysis and in situ hybridisation analysis has been reported indicating expression is mainly restricted to tissues known to be involved in pigmentation, however expression was also found in a group of cells associated with the larval photoreceptor organ (Fjose et al, 1984). A thorough immuno-EM study of this tissue and other nervous tissue is required in order to investigate the localisation of White in these tissues.

Heterologous expression of White and Scarlet in insect cells

The main aim of this work was to provide a system whereby White and Scarlet would be co-expressed and subsequently assemble as a biologically active transporter in the plasma membrane, allowing transport function to be characterised by uptake assays. The results presented in Chapter 5 showed that high levels of expression of White and Scarlet protein could be achieved using the Baculovirus-mediated approach, and that some of this protein was located in the plasma membrane. At the time this work was performed, tryptophan was a strong candidate substrate for the White/Scarlet transporter based on previous biochemical uptake studies (Howells et al, 1977; Sullivan et al, 1980; Sullivan and Sullivan, 1975). However uptake assays using [^{3}H]tryptophan provided no evidence of a novel tryptophan transporter in the insect cell plasma membrane. The lack of tryptophan transport function may be due to a number of factors including assembly failure, or the presence of a

native transport activity which masks any small amount of uptake activity which might be due to the White/Scarlet complex. However the immuno-localisation studies described in Chapter 7 suggest that the assumption made at the commencement of this work (that White/Scarlet transported tryptophan at the plasma membrane) was incorrect. In addition, the location and orientation of the White/Scarlet complex as described above not only indicates that the substrate is not tryptophan, but also indicates that even if White/Scarlet did assemble in the Sf9 cell plasma membrane with retention of its function, it would act as an efflux pump or exporter, rather than an importer of substrate. These concepts are highly significant with respect to the design of further experimental work with this system.

A major problem encountered in the insect cell expression system was that a large amount of the White and Scarlet protein was not assembling in the membrane, instead, was found intracellularly and was associated with the insoluble fraction of the cell. Intracellular immuno-localisation studies performed by confocal microscopy - using the anti-White antibody specific for the N-terminus of White - indicated punctate labelling reminiscent of localisation to an intracellular organellar membrane. This observation was consistent with the immuno-EM localisation studies where White and Scarlet locate to the pigment granule membrane. Nevertheless it was evident that much of the protein was not assembling in a cell membrane possibly due to the specialised nature of the sorting requirements of White and Scarlet which are not fulfilled in the Sf9 insect cell line. The over-expression of these polytopic membrane proteins late in viral infection was also deemed to be a contributing factor to the insolubility of White and Scarlet.

Further experimentation is required in order to find an approach which will enable White/Scarlet to assemble efficiently within a membrane bilayer whereby a transport assay could be performed. Two feasible approaches were described:

i) utilising an earlier promoter element to drive expression, in addition to the use of a cell line which stably expresses an additional molecular chaperone; and
ii) solubilisation of White and Scarlet and subsequent reconstitution of the proteins into proteoliposomes.

If approach (i) enabled efficient membrane assembly of White/Scarlet complex, the membranes enriched with these proteins could be isolated by percoll gradient or differential centrifugation and the membrane vesicles obtained could be used for uptake assays. Approach (ii) is also feasible since the technique of reconstituting membrane proteins into proteolipisomes has been shown to be successful for a number of complex membrane transport or channel proteins. In this system, high levels of White and Scarlet protein would be obtained by Baculovirus-mediated expression as described herein, and subsequent solubilisation of the White/Scarlet enriched cell fraction, and reconstitution into lipid vesicles would provide a means of producing vesicles where a proportion of White/Scarlet would be correctly orientated to enable uptake of labelled substrate into proteolipisomes to be assayed.

This system is well worth pursuing, in that if successful, it could provide the basis for a potentially very powerful model system for studying the structure and function of the White/Scarlet transporter. Such a system could be used to test the proposal that White/Scarlet forms a transporter for 3-hydroxykynurenine, and to allow the kinetics of such transport to be determined, as well as a system for studying the effects of site directed mutations such as those identified in partially pigmented *white* mutants described in Chapter 3.

Expression of the nucleotide binding domain of White in *E. coli*

The findings presented in Chapter 6 showed that the White NBD could be expressed at relatively high levels in *E. coli*, as a C-terminal fusion to the enzyme GST. Some of this protein was located in the *E. coli* membrane fraction and was subsequently partially purified and shown to bind ATP as

predicted by the published model (Ewart et al, 1994). Introduction of a mutation within the highly conserved Walker A motif of the wNBD, substantially reduced the ATP binding function. This functional data provided good evidence that the heterologous expression and purification system developed herein resulted in correctly folded wNBD.

The finding that separately expressed White and Scarlet NBDs in this system (Chapter 6, Section 6.2.4) co-purified is the first preliminary experimental evidence for possible protein-protein interactions between these two domains. This finding provides a basis for experimentation in order to characterise this interaction, in addition to investigating the consequences of those interactions on the functional activity of the protein. For example, does the wNBD-stNBD have ATP hydrolysis activity?; and how might the interaction affect ATP binding affinity? The results of co-expression of GST-wNBD and stNBD, indicated that the NBDs form a complex and that the formation of this complex had a stabilising effect on the Scarlet NBD which was degraded to a large extent when expressed as a GST fusion protein without the presence of the wNBD.

Protein-peptide interaction analysis of the nucleotide binding domain of White and an intra-helical loop

The experiments described in Chapter 6, Section 6.2.5 tested the hypothesis that the wNBD interacted with the TM domain via the loop between putative TM α helices 2 and 3. Experiments using an IAsys biosensor, showed that the wNBD binds to a synthetic equivalent of this peptide and that this binding was greatly decreased by a single amino acid change in the peptide representative of the w^{ET87} mutation (G509D) described in Chapter 3. These findings provide the first direct evidence that the NBD of White binds to this loop and thereby represents an important starting point for further experiments to investigate the link between the NDB and conformational changes in the TM domain important for the mechanism of transport. Future issues that may be addressed using the IAsys system include:

i) do conformational changes in the NBD brought about by ATP binding affect the binding affinity between the NBD and the peptide?;

ii) the effects of other mutations in the wNBD - the mutation $G^{135}K^{136} \rightarrow LQ$ which was shown to substantially reduce ATP binding activity by wNBD; does this affect binding between the NBD and the loop peptide?. In addition, the mutations identified in the *white* alleles w^{101} and w^{crr} described in Chapter 3 should be tested. Both are predicted to be located in regions of the wNBD important for conformational signal transduction between the NBD and TM domain. Information about the effects of these mutations on binding could potentially be highly informative with respect to the roles of the ABC signature motif (G243S: w^{101}) as well as the highly conserved histidine residue (H298N: w^{crr});

iii) the effect of the presence of both the wNBD and stNBD;

iv) the use of site directed mutagenesis to locate the region of the wNBD which interacts with the loop peptide, and also the residues in the loop peptide critical for binding; and

v) analysis of interactions of analogous loops linking TM helices of the Scarlet and Brown TM domains.

Such studies could provide a wealth of information with respect to this fundamental aspect of ABC transporter function which to date, has been addressed in an indirect way through mutant and reversion analysis (Mourez et al, 1997; Shyamala et al, 1991).

Genetic analysis of partially pigmented *white* mutants

In Chapter 3 sequences were determined for five *white* alleles which produce partial loss of eye pigmentation phenotype. Most of these turn out to have point mutations in the *white* gene, altering single amino acid residues in critical regions of structure. This study has added further weight to a previous proposal that TM helix 5 of White is essential for substrate specificity for drosopterin precursors. The new data has allowed development of a more detailed (somewhat speculative) model of the transport pore, involving TMs 5

and 6 of both White and Brown, and the roles of residues predicted to line the pore. This is described below.

Figure 4A illustrates the potential interactions of TM 5 and 6 of Brown with TM 6 of White brought about by a salt bridge between Asp^{570} of TM5 of Brown or Asp^{646} of TM 6 of Brown alternating with Arg^{672} of TM 6 of White. These residues all lie within a similar plane of the predicted α-helices around the TM helix mid-point, and this is shown in the net diagrams in Fig 5. The cause of these conformational changes could be brought about in part by the proline residue in TM 5 of Brown which is predicted to be on the other side of the α-helix to Asp^{570}. The two prolines in TM 5 of White would very likely also perform an important structure/function role in the regulation of the structural changes required for the opening and closing of the transport route. Proline has been found to occur in TM domains of transport proteins with a much higher frequency than in TM domains of non-transport proteins (Brandl and Deber, 1986), even though proline is the least likely amino acid to occur in an α-helix[22] (Chou and Fasman, 1978). This gave rise to the notion that functional membrane-buried proline residues are selectively included in transport proteins (Brandl and Deber, 1986). It was postulated that "... the *cis-trans* isomerization of an Xaa-Pro peptide bond (Xaa = unspecified amino acid) buried within the membrane - and the resulting redirection of the protein chain - is proposed to provide the reversible conformational change requisite for regulation (opening/closing) of a transport channel." (Brandl and Deber, 1986). The importance of proline residues has been shown in a number of ABC transporters ((Sheppard et al, 1996; Webb et al, 1992). In particular, in the phosphate transport system (Pst) double mutations P123L, P183L as well as P123A, P183A, resulted in the transporter being locked into an "open" configuration, highlighting a functional role in gating (Webb et al, 1992).

Also shown in Fig. 4A are putative TM helices 3 of White and 2 of Brown. These two helices are the only other TM helices (other than TMs 5 and 6 of

Fig. 4 Putative model of the gating mechanism for transport of drosopterin precursors

A. This figure illustrates diagrammatically the possible conformational changes which may occur in order to open and close the transport channel specific for guanine. The closed conformation results when TM 6 of White and TM 6 of Brown interact by way of electrostatic interaction between R^{672} of White and D^{646} of Brown. The open conformation results when this charge pair between TM 6 of White and Brown breaks and reforms with D^{570} of TM 5 of Brown. The relative position of the proline residues are indicated and may act as "hinge" regions contributing to the gating of the pore. The dashed ellipses give an indication of the change in diameter of the pore in the open and closed conformations. TM 3 of White and TM 2 of Brown are also shown and may play an important role in transmission of conformational changes of the pore region via signals transduced from the NBD → loop 2 → TM. Both TM 2 and 3 of Brown and White harbour glutamic acid residues which may play a role in structure and function of the pore by either attractive forces with R^{672} of White TM 6 or repulsive forces with other negatively charged residues in the helices proposed to line the pore. For example E^{461} of TM2 of Brown is appropriately positioned to interact with R^{672} and may play a role in breaking of the salt bridge between R^{672} and D^{646} by the introduction of a second negative residue.

B. A simplified cartoon illustration which takes into account the localisation data obtained in Chapter 7, where it was shown that White and Scarlet are located in the pigment granule membrane and that the NBDs are located in the cytoplasm. It is assumed that the Brown subunit is similarly orientated within the membrane of drosopterin containing granules. This figure illustrates that the major restriction of the transport route in the closed state is located near the intra-granular face of the membrane. This illustration also takes into account information gained from the crystal structure of HisP (Hung et al, 1998) illustrating the interactions between the two NBDs of White and Scarlet and the interaction of arm II with the loop between TMs 2 and 3 thought to play an important role in transducing conformational changes between the NBDs and the TM domains. This figure was adapted from (Welsh et al, 1998).

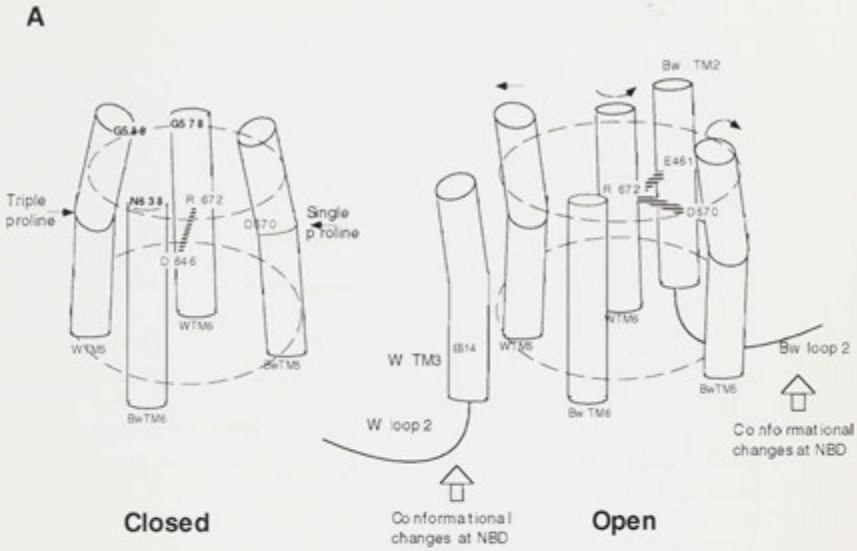
A
Triple proline
N638
G644
G578
R 672
D 646
D570
Single proline
WTM5
WTM6
BwTM5
BwTM6
Bw TM2
E461
W TM3
I514
W loop 2
Bw loop 2
Conformational changes at NBD
Closed
Open

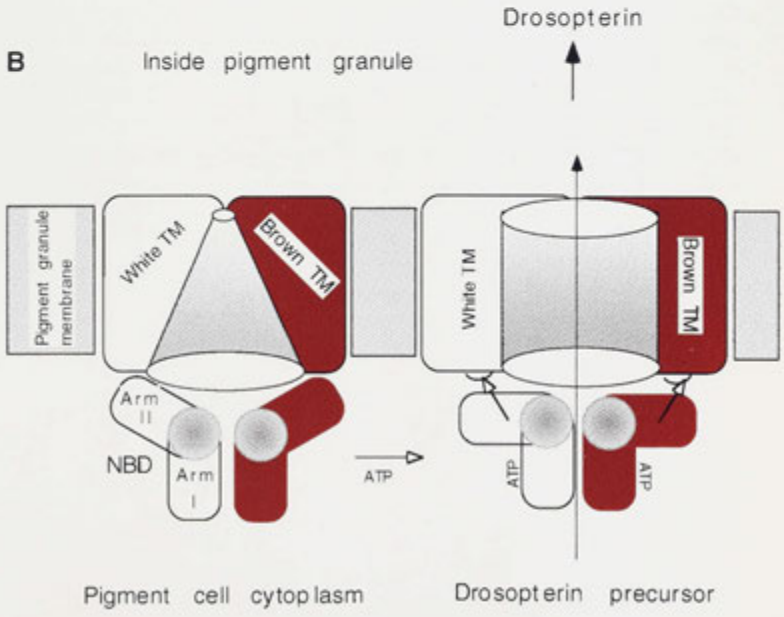
B
Drosopterin
Inside pigment granule
Pigment granule membrane
White TM
Brown TM
Arm II
Arm I
NBD
ATP
Pigment cell cytoplasm
Drosopterin precursor

Fig. 5 Helical net diagram of residues in the putative transmembrane helices 5 and 6 of both the White and Brown subunits.

In the helical net diagrams the intracellular end is at the bottom. The x-axis represents the position on the circumference of the helix. Residues that align vertically are on the same face of the helix. This figure illustrates that R^{672} (TM 6 White), D^{570} (TM 5 Brown), D^{646} (TM 6 Brown) and E^{461} (TM2 Brown) are at positions on the helix appropriate for electrostatic interactions proposed in the text and illustrated in Fig. 2.

Fig. 5 Helical net diagrams of residues in the putative transmembrane helices 5 and 6 of both the White and Brown subunits

In these helical net diagrams the intra-cellular end is at the bottom. The x-axis represents the position on the circumference of the helix. Residues that align vertically are on the same face of the helix. This figure illustrates that R672 (TM 6 White), D570 (TM5 Brown), D646 (TM 6 Brown) and E461 (TM 2 Brown) are at positions on the helix appropriate for electrostatic interactions proposed in the text and illustrated in Fig. 2.

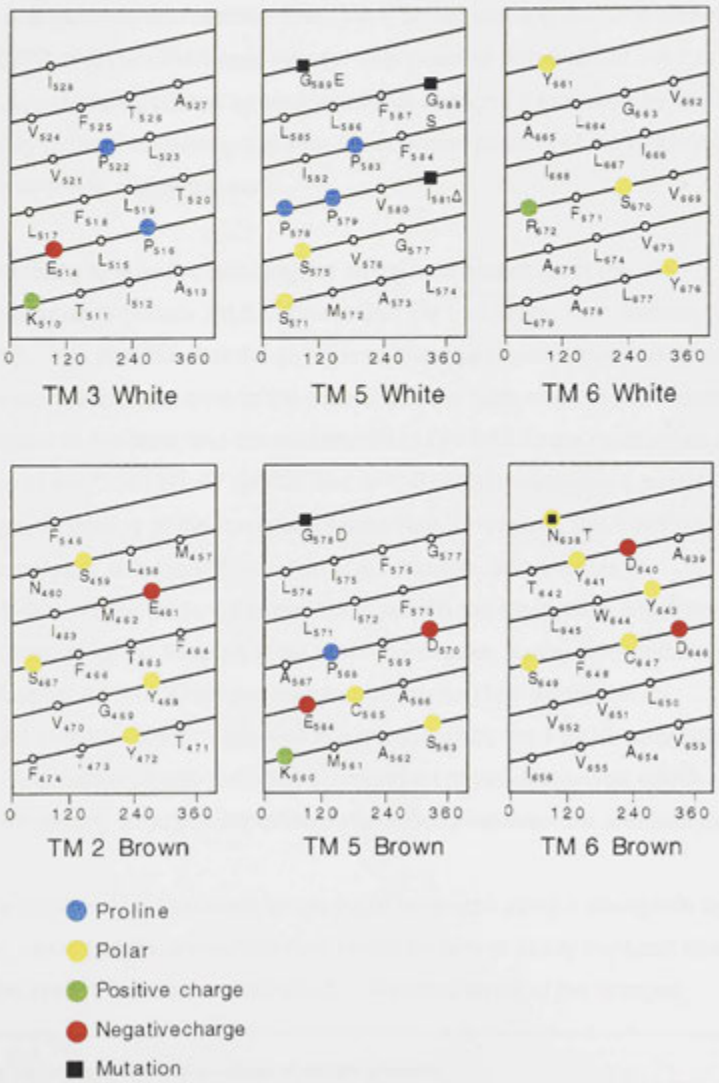

both White and Brown) which contain charged residues. Both TM 2 and TM 3 of Brown and White respectively are linked to the loop 2 region of the TM domain, proposed to form an interface between the NBD and TM region as discussed above. Thus, these helices are predicted to be affected by conformational signals from the NBD. Although there is no evidence of these helices involvement in the transport mechanism, it is predicted that they play a role in the conformational changes proposed in Fig. 4A. TM 2 of Brown harbours a glutamic acid residue (E461) in a similar plane to R672 of White TM 6 and D570 of Brown TM 5 (see Fig. 4). It is possible that E461 of TM 2 of Brown, appropriately placed by conformational changes transduced by the NBD, may provide the driving force for the changed position of the salt bridge which opens and closes the pore.

It is interesting to note the homology of amino acid sequence at the extracellular ends of both TM 5 of Brown and TM 5 of White, both harbouring GGF[I/L]L. It is possible that the glycines at these positions, when positioned appropriately, also contribute to the widening of the pore when facing inwards with respect to the pore, and the substitution of Gly for a larger residue (as is the case in bw^{T50} G578D, w^{cf} G589E and w^{CO2} G588S) may cause a partial blockage, or slowing of the transport of substrate. However, this interpretation is not consistent with the w^{sat} mutation which has the lowest levels of drosopterins. In this mutant a large Phe is substituted for glycine, which could be imagined to cause the pore to be wider than usual. It may be that the loop which follows TM 5 of White and which connects to TM 6 also plays an important structure/function role which is abrogated by the F590G substitution of w^{sat}. Alternatively F590 may play an important physical/chemical role in substrate binding through hydrophobic interactions between the aromatic rings.

The predicted model discussed above could be tested using a transgenic fly system, as well as the proteoliposome model system to assay transport directly, once the system has been established. The importance of the charged

---

[22] This is based on analysis of α-helices of soluble proteins.

residues predicted to form structurally and functionally important salt bridges could be investigated by mutagenesis in addition to the substitution of residues of specific sizes which could be used to study the effects on transport at each end of the proposed pore illustrated in Fig. 4. For example, it is predicted that substitutions for alanine may have little effect at the putative wide end of the pore, while having an increasingly significant effect towards the region of the pore predicted to form a constriction of the pore when in the closed state. If this model is correct, it may be possible to engineer a permanently open transporter by appropriate mutagenesis of the proline residues and other residues proposed to perform a role in closing the pore, analogous to mutagenic studies performed on the Pst phosphate transport system of *E. coli* (Webb et al, 1992). Although insights into regions of the White/Brown complex important for transport of drosopterin precursors have been discussed, little is known with respect to residues within the TM regions of White/Scarlet important for the transport of xanthommatin precursors. Mutagenesis utilizing the model systems mentioned above could be used to investigate this issue.

Conclusion

This thesis has described efforts towards the development of a variety of experimental model systems to investigate various aspects of structure and function of both the transmembrane domains and nucleotide binding domains of the *Drosophila* ABC transporters involved in eye pigmentation. While further work is required to perfect these systems, results have been obtained which contribute to the overall understanding of structure and function of the White, Brown and Scarlet proteins and their roles in the eye pigmentation pathway of *Drosophila*. In addition, information gained through this study is inherently relevant to the ABC transporter superfamily as a whole.

APPENDIX 1

Protein and cDNA sequence of *Drosophila melanogster white*

The genomic *white* was sequenced by (O'Hare et al, 1984) and the intron-exon junctions were deduced with only minor modifications being required when a cDNA clone was subsequently isolated (Pepling and Mount 1990). The cDNA (bases are numbered) and protein sequence is shown here. Motifs characteristic of ABC transporters are highlighted in bold; positions of mutations identified from mutant white alleles which result in partial decreases in eye colouration described in Chapter 3 are shown above the DNA sequence; putative transmembrane domains predicted from hydropathy analysis are shown in bold and underlined.

```
          10          20          30          40          50
ATG GGC CAA GAG GAT CAG GAG CTA TTA ATT CGC GGA GGC AGC AAA CAC CCA TCT
TAC CCG GTT CTC CTA GTC CTC GAT AAT TAA GCG CCT CCG TCG TTT GTG GGT AGA
Met Gly Gln Glu Asp Gln Glu Leu Leu Ile Arg Gly Gly Ser Lys His Pro Ser>

     60          70          80          90          100
GCC GAG CAT CTG AAC AAT GGT GAC AGC GGA GCG GCT TCG CAG AGC TGC ATT AAC
CGG CTC GTA GAC TTG TTA CCA CTG TCG CCT CGC CGA AGC GTC TCG ACG TAA TTG
Ala Glu His Leu Asn Asn Gly Asp Ser Gly Ala Ala Ser Gln Ser Cys Ile Asn>

110         120         130         140         150         160
CAG GGC TTC GGG CAG GCC AAA AAC TAC GGC ACG CTC CTG CCA CCC AGT CCG CCG
GTC CCG AAG CCC GTC CGG TTT TTG ATG CCG TGC GAG GAC GGT GGG TCA GGC GGC
Gln Gly Phe Gly Gln Ala Lys Asn Tyr Gly Thr Leu Leu Pro Pro Ser Pro Pro>

       170         180         190         200         210
GAG GAC TCC GGT TCA GGG AGC GGC CAA CTA GCC GAG AAC CTC ACC TAT GCC TGG
CTC CTG AGG CCA AGT CCC TCG CCG GTT GAT CGG CTC TTG GAG TGG ATA CGG ACC
Glu Asp Ser Gly Ser Gly Ser Gly Gln Leu Ala Glu Asn Leu Thr Tyr Ala Trp>

  220         230         240         250         260         270
CAC AAT ATG GAC ATC TTT GGG GCG GTC AAT CAG CCG GGC TCC GGA TGG CGG CAG
GTG TTA TAC CTG TAG AAA CCC CGC CAG TTA GTC GGC CCG AGG CCT ACC GCC GTC
His Asn Met Asp Ile Phe Gly Ala Val Asn Gln Pro Gly Ser Gly Trp Arg Gln>

          280         290         300         310         320
CTG GTC AAC CGG ACA CGC GGA CTA TTC TGC AAC GAG CGA CAC ATA CCG GCG CCC
GAC CAG TTG GCC TGT GCG CCT GAT AAG ACG TTG CTC GCT GTG TAT GGC CGC GGG
Leu Val Asn Arg Thr Arg Gly Leu Phe Cys Asn Glu Arg His Ile Pro Ala Pro>

    330         340         350         360         370
AGG AAA CAT TTG CTC AAG AAC GTT TGC GGC GTG GCC TAT CCG GGC GAA CTT TTG
TCC TTT GTA AAC GAG TTC TTG CAA ACG CCG CAC CGG ATA GGC CCG CTT GAA AAC
Arg Lys His Leu Leu Lys Asn Val Cys Gly Val Ala Tyr Pro Gly Glu Leu Leu>

380         390         400         410         420         430
GCC GTG ATG GGC AGT TCC GGT GCC GGA AAG ACG ACC CTG CTG AAT GCC CTT GCC
CGG CAC TAC CCG TCA AGG CCA CGG CCT TTC TGC TGG GAC GAC TTA CGG GAA CGG
Ala Val Met Gly Ser Ser Gly Ala Gly Lys Thr Thr Leu Leu Asn Ala Leu Ala>
                        Walker A
```

```
       440          450          460          470          480
TTT CGA TCG CCG CAG GGC ATC CAA GTA TCG CCA TCC GGG ATG CGA CTG CTC AAT
AAA GCT AGC GGC GTC CCG TAG GTT CAT AGC GGT AGG CCC TAC GCT GAC GAG TTA
Phe Arg Ser Pro Gln Gly Ile Gln Val Ser Pro Ser Gly Met Arg Leu Leu Asn>

  490          500          510          520          530          540
GGC CAA CCT GTG GAC GCC AAG GAG ATG CAG GCC AGG TGC GCC TAT GTC CAG CAG
CCG GTT GGA CAC CTG CGG TTC CTC TAC GTC CGG TCC ACG CGG ATA CAG GTC GTC
Gly Gln Pro Val Asp Ala Lys Glu Met Gln Ala Arg Cys Ala Tyr Val Gln Gln>

          550          560          570          580          590
GAT GAC CTC TTT ATC GGC TCC CTA ACG GCC AGG GAA CAC CTG ATT TTC CAG GCC
CTA CTG GAG AAA TAG CCG AGG GAT TGC CGG TCC CTT GTG GAC TAA AAG GTC CGG
Asp Asp Leu Phe Ile Gly Ser Leu Thr Ala Arg Glu His Leu Ile Phe Gln Ala>

    600          610          620          630          640
ATG GTG CGG ATG CCA CGA CAT CTG ACC TAT CGG CAG CGA GTG GCC CGC GTG GAT
TAC CAC GCC TAC GGT GCT GTA GAC TGG ATA GCC GTC GCT CAC CGG GCG CAC CTA
Met Val Arg Met Pro Arg His Leu Thr Tyr Arg Gln Arg Val Ala Arg Val Asp>

650          660          670          680          690          700
CAG GTG ATC CAG GAG CTT TCG CTC AGC AAA TGT CAG CAC ACG ATC ATC GGT GTG
GTC CAC TAG GTC CTC GAA AGC GAG TCG TTT ACA GTC GTG TGC TAG TAG CCA CAC
Gln Val Ile Gln Glu Leu Ser Leu Ser Lys Cys Gln His Thr Ile Ile Gly Val>

       710          720          101          740          750
CCC GGC AGG GTG AAA GGT CTG TCC GGC GGA GAA AGG AAG CGT CTG GCA TTC GCC
GGG CCG TCC CAC TTT CCA GAC AGG CCG CCT CTT TCC TTC GCA GAC CGT AAG CGG
Pro Gly Arg Val Lys Gly Leu Ser Gly Gly Glu Arg Lys Arg Leu Ala Phe Ala>
                                ABC Signature
  760          770          780          790          800          810
TCC GAG GCA CTA ACC GAT CCG CCG CTT CTG ATC TGC GAT GAG CCC ACC TCC GGA
AGG CTC CGT GAT TGG CTA GGC GGC GAA GAC TAG ACG CTA CTC GGG TGG AGG CCT
Ser Glu Ala Leu Thr Asp Pro Pro Leu Leu Ile Cys Asp Glu Pro Thr Ser Gly>
                                Walker B
          820          830          840          850          860
CTG GAC TCA TTT ACC GCC CAC AGC GTC GTC CAG GTG CTG AAG AAG CTG TCG CAG
GAC CTG AGT AAA TGG CGG GTG TCG CAG CAG GTC CAC GAC TTC TTC GAC AGC GTC
Leu Asp Ser Phe Thr Ala His Ser Val Val Gln Val Leu Lys Lys Leu Ser Gln>

    870          880          890          900          910
AAG GGC AAG ACC GTC ATC CTG ACC ATT CAT CAG CCG TCT TCC GAG CTG TTT GAG
TTC CCG TTC TGG CAG TAG GAC TGG TAA GTA GTC GGC AGA AGG CTC GAC AAA CTC
Lys Gly Lys Thr Val Ile Leu Thr Ile His Gln Pro Ser Ser Glu Leu Phe Glu>

920          930          940          950          960          970
CTC TTT GAC AAG ATC CTT CTG ATG GCC GAG GGC AGG GTA GCT TTC TTG GGC ACT
GAG AAA CTG TTC TAG GAA GAC TAC CGG CTC CCG TCC CAT CGA AAG AAC CCG TGA
Leu Phe Asp Lys Ile Leu Leu Met Ala Glu Gly Arg Val Ala Phe Leu Gly Thr>

       980          990         1000         1010         1020
CCC AGC GAA GCC GTC GAC TTC TTT TCC TAC GTG GGT GCC CAG TGT CCT ACC AAC
GGG TCG CTT CGG CAG CTG AAG AAA AGG ATG CAC CCA CGG GTC ACA GGA TGG TTG
Pro Ser Glu Ala Val Asp Phe Phe Ser Tyr Val Gly Ala Gln Cys Pro Thr Asn>

  1030         1040         1050         1060         1070         1080
TAC AAT CCG GCG GAC TTT TAC GTA CAG GTG TTG GCC GTT GTG CCC GGA CGG GAG
ATG TTA GGC CGC CTG AAA ATG CAT GTC CAC AAC CGG CAA CAC GGG CCT GCC CTC
Tyr Asn Pro Ala Asp Phe Tyr Val Gln Val Leu Ala Val Val Pro Gly Arg Glu>

         1090         1100         1110         1120         1130
ATC GAG TCC CGT GAT CGG ATC GCC AAG ATA TGC GAC AAT TTT GCC ATT AGC AAA
TAG CTC AGG GCA CTA GCC TAG CGG TTC TAT ACG CTG TTA AAA CGG TAA TCG TTT
Ile Glu Ser Arg Asp Arg Ile Ala Lys Ile Cys Asp Asn Phe Ala Ile Ser Lys>

    1140         1150         1160         1170         1180
GTA GCC CGG GAT ATG GAG CAG TTG TTG GCC ACC AAA AAT TTG GAG AAG CCA CTG
CAT CGG GCC CTA TAC CTC GTC AAC AAC CGG TGG TTT TTA AAC CTC TTC GGT GAC
Val Ala Arg Asp Met Glu Gln Leu Leu Ala Thr Lys Asn Leu Glu Lys Pro Leu>
```

```
1190          1200          1210          1220          1230          1240
  GAG CAG CCG GAG AAT GGG TAC ACC TAC AAG GCC ACC TGG TTC ATG CAG TTC CGG
  CTC GTC GGC CTC TTA CCC ATG TGG ATG TTC CGG TGG ACC AAG TAC GTC AAG GCC
  Glu Gln Pro Glu Asn Gly Tyr Thr Tyr Lys Ala Thr Trp Phe Met Gln Phe Arg>

       1250          1260          1270          1280          1290
  GCG GTC CTG TGG CGA TCC TGG CTG TCG GTG CTC AAG GAA CCA CTC CTC GTA AAA
  CGC CAG GAC ACC GCT AGG ACC GAC AGC CAC GAG TTC CTT GGT GAG GAG CAT TTT
  Ala Val Leu Trp Arg Ser Trp Leu Ser Val Leu Lys Glu Pro Leu Leu Val Lys>

  1300          1310          1320          1330          1340          1350
  GTG CGA CTT ATT CAG ACA ACG ATG GTT GCC ATC TTG ATT GGC CTC ATC TTT TTG
  CAC GCT GAA TAA GTC TGT TGC TAC CAA CGG TAG AAC TAA CCG GAG TAG AAA AAC
  Val Arg Leu Ile Gln Thr Thr Met Val Ala Ile Leu Ile Gly Leu Ile Phe Leu>
                                    TM 1
            1360          1370          1380          1390          1400
  GGC CAA CAA CTC ACG CAA GTG GGC GTG ATG AAT ATC AAC GGA GCC ATC TTC CTC
  CCG GTT GTT GAG TGC GTT CAC CCG CAC TAC TTA TAG TTG CCT CGG TAG AAG GAG
  Gly Gln Gln Leu Thr Gln Val Gly Val Met Asn Ile Asn Gly Ala Ile Phe Leu>

     1410          1420          1430          1440          1450
  TTC CTG ACC AAC ATG ACC TTT CAA AAC GTC TTT GCC ACG ATA AAT GTG TTC ACC
  AAG GAC TGG TTG TAC TGG AAA GTT TTG CAG AAA CGG TGC TAT TTA CAC AAG TGG
  Phe Leu Thr Asn Met Thr Phe Gln Asn Val Phe Ala Thr Ile Asn Val Phe Thr>
               TM 2
1460          1470          1480          1490          1500          1510
  TCA GAG CTG CCA GTT TTT ATG AGG GAG GCC CGA AGT CGA CTT TAT CGC TGT GAC
  AGT CTC GAC GGT CAA AAA TAC TCC CTC CGG GCT TCA GCT GAA ATA GCG ACA CTG
  Ser Glu Leu Pro Val Phe Met Arg Glu Ala Arg Ser Arg Leu Tyr Arg Cys Asp>

       1520          1530          1540          1550          1560
  ACA TAC TTT CTG GGC AAA ACG ATT GCC GAA TTG CCG CTT TTT CTC ACA GTG CCA
  TGT ATG AAA GAC CCG TTT TGC TAA CGG CTT AAC GGC GAA AAA GAG TGT CAC GGT
  Thr Tyr Phe Leu Gly Lys Thr Ile Ala Glu Leu Pro Leu Phe Leu Thr Val Pro>
                                    TM 3
  1570          1580          1590          1600          1610          1620
  CTG GTC TTC ACG GCG ATT GCC TAT CCG ATG ATC GGA CTG CGG GCC GGA GTG CTG
  GAC CAG AAG TGC CGC TAA CGG ATA GGC TAC TAG CCT GAC GCC CGG CCT CAC GAC
  Leu Val Phe Thr Ala Ile Ala Tyr Pro Met Ile Gly Leu Arg Ala Gly Val Leu>

            1630          1640          1650          1660          1670
  CAC TTC TTC AAC TGC CTG GCG CTG GTC ACT CTG GTG GCC AAT GTG TCA ACG TCC
  GTG AAG AAG TTG ACG GAC CGC GAC CAG TGA GAC CAC CGG TTA CAC AGT TGC AGG
  His Phe Phe Asn Cys Leu Ala Leu Val Thr Leu Val Ala Asn Val Ser Thr Ser>
                                    TM 4
     1680          1690          1700          1710          1720
  TTC GGA TAT CTA ATA TCC TGC GCC AGC TCC TCG ACC TCG ATG GCG CTG TCT GTG
  AAG CCT ATA GAT TAT AGG ACG CGG TCG AGG AGC TGG AGC TAC CGC GAC AGA CAC
  Phe Gly Tyr Leu Ile Ser Cys Ala Ser Ser Ser Thr Ser Met Ala Leu Ser Val>

1730          1740          1750          1760          1770          1780
  GGT CCG CCG GTT ATC ATA CCA TTC CTG CTC TTT GGC GGC TTC TTC TTG AAC TCG
  CCA GGC GGC CAA TAG TAT GGT AAG GAC GAG AAA CCG CCG AAG AAG AAC TTG AGC
  Gly Pro Pro Val Ile Ile Pro Phe Leu Leu Phe Gly Gly Phe Phe Leu Asn Ser>
       TM 5
       1790          1800          1810          1820          1830
  GGC TCG GTG CCA GTA TAC CTC AAA TGG TTG TCG TAC CTC TCA TGG TTC CGT TAC
  CCG AGC CAC GGT CAT ATG GAG TTT ACC AAC AGC ATG GAG AGT ACC AAG GCA ATG
  Gly Ser Val Pro Val Tyr Leu Lys Trp Leu Ser Tyr Leu Ser Trp Phe Arg Tyr>

  1840          1850          1860          1870          1880          1890
  GCC AAC GAG GGT CTG CTG ATT AAC CAA TGG GCG GAC GTG GAG CCG GGC GAA ATT
  CGG TTG CTC CCA GAC GAC TAA TTG GTT ACC CGC CTG CAC CTC GGC CCG CTT TAA
  Ala Asn Glu Gly Leu Leu Ile Asn Gln Trp Ala Asp Val Glu Pro Gly Glu Ile>
```

```
          1900         1910         1920         1930         1940
AGC TGC ACA TCG TCG AAC ACC ACG TGC CCC AGT TCG GGC AAG GTC ATC CTG GAG
TCG ACG TGT AGC AGC TTG TGG TGC ACG GGG TCA AGC CCG TTC CAG TAG GAC CTC
Ser Cys Thr Ser Ser Asn Thr Thr Cys Pro Ser Ser Gly Lys Val Ile Leu Glu>

    1950         1960         1970         1980         1990
ACG CTT AAC TTC TCC GCC GCC GAT CTG CCG CTG GAC TAC GTG GGT CTG GCC ATT
TGC GAA TTG AAG AGG CGG CGG CTA GAC GGC GAC CTG ATG CAC CCA GAC CGG TAA
Thr Leu Asn Phe Ser Ala Ala Asp Leu Pro Leu Asp Tyr Val Gly Leu Ala Ile>

2000         2010         2020         2030         2040         2050
CTC ATC GTG AGC TTC CGG GTG CTC GCA TAT CTG GCT CTA AGA CTT CGG GCC CGA
GAG TAG CAC TCG AAG GCC CAC GAG CGT ATA GAC CGA GAT TCT GAA GCC CGG GCT
Leu Ile Val Ser Phe Arg Val Leu Ala Tyr Leu Ala Leu Arg Leu Arg Ala Arg>
                TM 6
      2060
CGC AAG GAG TAG
GCG TTC CTC ATC
Arg Lys Glu *** >
```

Bibliography

Abrahams JP, Leslie AGW, Lutter R and Walker JE (1994) Structure at 2.8 angstrom resolution of F_1ATPase from bovine heart mitochondria. *Nature* 370: 621-628

Akabas MH, Cheung M and Guinamard R (1997) Probing the structural and functional domains of the CFTR chloride channel. *Journal of Bioenergetics and Biomembranes* 29: 453-463

Akabas MH, Kaufmann C, Cook TA and Archdeacon P (1994) Amino acid residues lining the chloride channel of the cystic fibrosis transmembrane conductance regulator. *Journal of General Physiology* 109: 289-299

Akabas MH, Stauffer DA, Xu M and Karlin A (1992) Acetylcholine receptor channel structure probed in cysteine-substitution mutants. *Science* 258: 307-310

Alberts B, Bray D, Lewis J, Raff M, Roberts K and Watson JD (1989) Molecular Biology of the Cell. Garland Publishing Inc., New York.

Allikmets R, Shroyer NF, Singh N, Seddon JM, Lewis RA, Bernstein PS, Peiffer A, Zabriskie NA, Li Y, Hutchinson A, Dean M, Lupski JR and Leppert M (1997) Mutation of the Stargardt disease gene (ABCR) in age-related macular degeneration. *Science* 277: 1805-1807

Ames GF-L and Lecar H (1992) ATP-dependent bacerial transporters and cystic fibrosis: analogy between channels and transporters. *FASEB Journal* 6: 2660-2666

Ames GF-L, Mimura C, Holbrook S and Shyamala V (1992) Traffic ATPases: a superfamily of transport proteins operating from *Escherichia coli* to humans. *Advances in Enzymology* 65: 1-47

Anderson MP, Gregory RJ, Thompson S, Souza DW, Paul S, Mulligan RC, Smith AE and Welsh MJ (1991) Demonstration that CFTR is a chloride channel by alteration of its anion selectivity. *Science* 253: 202-205

Annereau J-P, Wulbrand U, Vankeerberghen A, Cuppens H, Bontems F, Tümmler B, Cassiman J-J and Stoven V (1997) A novel model for the first nucleotide binding domain of the cystic fibrosis transmembrane conductance regulator. *FEBS Letters* 407: 303-308

Arispe N, Rojas E, Hartman J, Sorcher EJ and Pollard HB (1992) Intrinsic anion channel activity of the recombinant first nucleotide binding fold domain of the cystic fibrosis transmembrane regulator protein. *Proceedings of the National Academy of Science USA* 89: 1539-1543

Azzaria M, Schurr E and Gros P (1989) Discrete mutations introduced in the predicted nucleotide-binding sites of the mdr1 gene abolish its ability to confer multidrug resistance. *Molecular and Cellular Biology* 9: 5289-5297

Baichwal V, Liu D and Ames GF-L (1993) The ATP-binding component of a prokaryotic traffic ATPase is exposed to the periplasmic (external) surface. *Proceedings of the National Academy of Science USA* 90: 620-624

Bakos É, Klein I, Welker E, Szabó K, Müller M, Sarkadi B and Váradi A (1997) Characterization of the Human Multidrug Resistance Protein Containing Mutations in the ATP-binding cassette signature region. *Biochemical Journal* 323: 777-783

Barber GN, Clegg JCS and Lloyd G (1990) Expression of the Lassa virus nucleocapsid protein in insect cells infected with a recombinant baculovirus: application to diagnostic assays for Lassa virus infection. *Journal of General Virology* 71: 19-28

Beadle GW and Ephrussi B (1936) The differentiation of eye pigments in *Drosophila* as studied by transplantation. *Genetics* 21: 225-247

Beadle GW and Law LW (1938) Influence on eye color of feeding diffusible substances to *Drosophila melanogaster. Proceedings of the Society for Experimental Biology & Medicine (Cambridge MA)* 37: 621-623

Bear CE, Li C, Galley K, Wang Y, Garami E and Ramjeesingh M (1997) Coupling of ATP hydrolysis with channel gating by purified, reconstituted CFTR. *Journal of Bioenergetics and Biomembranes* 1997: 465-473

Beck WT and Qian X-D (1992) Photoaffinity substrates for P-glycoprotein. *Biochemical Pharmacology* 43: 89-93

Bellamacina CR (1996) The nicotinamide dinucleotide binding motif: a comparison of nucleotide binding proteins. *FASEB* 10: 1257-1269

Bender W, Spierer P and Hogness DS (1983) Chromosomal walking and jumping to isolate DNA from the ace and rosy loci and the bithorax complex in *Drosophila melanogaster. Journal of Molecular Biology* 168: 17-33

Bergeron JJM, Brenner MB, Thomas DY and Williams DB (1994) Calnexin: a membrane-bound chaperone of the endoplasmic reticulum. *Trends in Biochemistry* 19: 124-128

Bernard GD and Stavenga DG (1979) Spectral sensitivities of retinular cells measured in intact, living flies by an optical method. *Journal of Comparative Physiology* 134: 95-107

Bianchet MA, Ko YH, Amzel LM and Pedersen PL (1997) Modeling of nucleotide binding domains of ABC transporter proteins based on a F_1-ATPase/recA topology: structural model of the nucleotide binding domains of the cystic fibrosis transmembrane conductance regulator (CFTR). *Journal of Bioenergetics and Biomembranes* 29: 503-524

Bonse A (1969) Uber das auftreten von pterinen, tryptophan und dessen derivate in verschiedenen Organen der mutante *white* von *Drosophila melanogaster*. *Z Naturf* 24b: 128-131

Bossemeyer D (1994) The glycine-rich sequence of protein kinases: a multifunctional element. *Trends in Biochemistry* 19: 201-205

Bourne HR, Sanders DA and McCormick F (1991) The GTPase superfamily: conserved structure and molecular mechanism. *Nature* 349: 117-127

Braig K, Otwinowski Z, Hegde R, Boisvert DC, Joachimiak A, Horwich AL and Sigler PB (1994) The crystal structure of the bacterial chaperonin GroEL at 2.8 Å. *Nature* 371: 578-586

Branden C and Tooze J (1991) Introduction to Protein Structure. Garland Publishing, Inc., New York and London.

Brandl CJ and Deber CM (1986) Hypothesis about the function of membrane-buried proline residues in transport proteins. *Proceedings of the National Academy of Science USA* 83: 917-921

Bridges (1935) *Drosophila Information Service* 3: 18

Browne BL, McClendon V and Bedwell DM (1996) Mutations within the first LSGGQ motif of Ste6p cause defects in **a**-Factor transport and mating in *Saccharomyces cerevisiae*. *Journal of Bacteriology* 178: 1712-1719

Bruggemann EP, Germann UA, Gottesman MM and Pastan I (1989) Two different regions of phosphoglycoprotein are photoaffinity-labeled by azidopine. *Journal of Biological Chemistry* 264: 15483-15488

Buckle PE, Davies RJ, Kinning T, Yeung D, Edwards PR, Pollard-Knight D and Lowe CR (1993) *Biosensors and Bioelectronics* 8: 355

Bullock TH and Horridge GA (1965) Structure and function of the nervous systems of invertebrates, San Francisco and London.

Buschman E and Gros P (1991) Functional analysis of chimeric genes obtained by exchanging homologous domains of the mouse mdr1 and mdr2 genes. *Molecular and Cellular Biology* 11: 595-603

Cagan RL and Ready DF (1989) The emergence of order in the *Drosophila* pupal retina. *Developmental Biology* 136: 346-362

Campbell S, Kim H, Doukas M and Haley B (1990) Photoaffinity labeling of ATP and NAD^+ binding sites on recombinant human interleukin 2. *Proceedings of the National Academy of Science USA* 87: 1243-1246

Canfield WM, Johnson KF, Ye RD, Gregory W and Kornfeld S (1991) Localisation of the signal for rapid internalisation of the bovine cation-independent mannose 6-phosphate/insulin-like growth factor-II receptor to amino acids 24-29 of the cytoplasmic tail. *Journal of Biological Chemistry* 266: 5682-5688

Carlson SD and Chi C (1979) The functional morphology of the insect photoreceptor. *Annual Review of Entomology* 24: 379-416

Carson MR and Welsh MJ (1995) Structural and functional similarities between the nucleotide-binding domains of CFTR and GTP-binding proteins. *Biophysical Journal* 69: 2443-2448

Carter DB, Thomsen DR, Im WB, Lennon DJ, Ngo D, Gale W, Im HK, Seeburg PH and Smith MW (1992) Functional expression of GABA-A chloride channels and benzodiazepine binding sites in baculovirus infected insect cells. *Bio/Technology* 10: 679-681

Castagna M, Shayakul C, Trotti D, Sacchi VF, Harvey WR and Hediger MA (1997) Molecular characteristics of mammalian and insect amino acid transporters: implications for amino acid homeostasis. *Journal of Experimental Biology* 200: 269-286

Chen H, Rossier C, Lalioti MD, Lynn A, Chakravarti A, Perrin G and Antonarakis SE (1996) Cloning of the cDNA for a human homologue of the Drosophila *white* gene and mapping to chromosome 21q22.3. *American Journal of Human Genetics* 59: 66-75

Chen WJ, Goldstein JL and Brown MS (1990) NPXY, a sequence often found in cytoplasmic tails is required for coated pit-mediated internalization of the low density lipoprotein receptor. *Journal of Biological Chemistry* 265: 3116-3123

Cheung M and Akabas MH (1996) Identification of CFTR channel-lining residues in and flanking the M6 membrane-spanning segment. *Biophysical Journal* 70: 2688-2695

Cheung M and Akabas MH (1997) Locating the anion-selectivity filter of the cystic fibrosis transmembrane conductance regulator (CFTR) chloride channel. *Journal of General Physiology* 109: 289-299

Choi K, Chen C-j, Kriegler M and Roninson IB (1988) An altered pattern of cross-resistance in multidrug resistant human cells results from spontaneous mutations in the *mdr*1 (P-glycoprotein) gene. *Cell* 53: 519-529

Chou PY and Fasman GD (1978) Empirical predictions of protein conformation. *Annual Review of Biochemistry* 47: 251-276

Collawn JF, Strangel M, Kuhn LA, Esekogwu V and Jing S (1990) Transferrin receptor internalization sequence YXRF implicates a tight turn as the structural recognition motif for endocytosis. *Cell* 63: 1061-1072

Cope DL, Holman GD, Baldwin SA and Wolstenholme AJ (1994) Domain assembly of the GLUT 1 glucose transporter. *Biochemical Journal* 300: 291-294

Cotten JF, Ostedgaard LS, Carson MR and Welsh MJ (1996) Effect of cystic fibrosis-associated mutations in the fourth intracellular loop of cystic fibrosis transmembrane conductance regulator. *Journal of Biological Chemistry* 271: 21279-21284

Cox GB, Webb D and Rosenberg H (1989) Specific amino acid residues in both the PstB and PstC proteins are required for phosphate transport by the *Escherichia coli* Pst system. *Journal of Bacteriology* 1989: 1531-1534

Croop JM (1998) Evolutionary relationships among ABC transporters. *Methods in Enzymology* 292: 101-116

Croop JM, Tiller GE, Fletcher JA, Lux ML, Raab E, Goldenson D, Son D, Arciniegas S and Wu RL (1997) Isolation and characterization of a mammalian homolog of the *Drosophila white* gene. *Gene (Amsterdam)* 185: 77-85

Cush R, Cronin JM, Stewart WJ, Maule CH, Molloy J and Goddard NJ (1993) The resonant mirror: a novel optical biosensor for direct sensing of biomolecular interactions. Part 1: principle and operation and associated instrumentation. *Biosensors and Bioelectronics* 8: 347-353

Cutting GR, Kasch LM, Rosenstein BJ, Zielenski J, Tsui L-C, Antonarakis SE and Kazazian HH (1990) A cluster of cystic fibrosis mutations in the first nucleotide-binding fold of the cystic fibrosis conductance regulator protein. *Nature* 346: 366-369

Czarnecki J, Geahlen R and Haley B (1979) Synthesis and use of azido photoaffinity analogs of adenine and guanine nucleotides. *Methods in Enzymology* LVI: 642-683

Davidson AL, Laghaeian SS and Mannering DE (1996) The maltose transport system of *Escherichia coli* displays positive cooperativity in ATP hydrolysis. *Journal of Biological Chemistry* 271: 4858-4863

Dayan G, Baubichon-Cortay H, Jault J-M, Cortay J-C, Deleage G and Pietro AD (1996) Recombinant N-terminal nucleotide-binding domain from mouse P-glycoprotein. *Journal of Biological Chemistry* 271: 11652-11658

Deber CM, Brandl CJ, Deber RB, Hsu LC and Young XK (1986) Amino acid composition of the membrane and aqueous domains of integral membrane proteins. *Archives of Biochemistry and Biophysics* 251: 68-76

Devine SE, Ling V and Melera PW (1992) Amino acid substitutions in the sixth transmembrane domain of P-glycoprotein alter multidrug resistance. *Proceedings of the National Academy of Science USA* 89: 4564-4568

Dhir R, Grizzuti K, Kajiji S and Gros P (1993) Modulatory effects on substrate specificity of independent mutations at the Serine $^{939/941}$ position in predicted transmembrane domain 11 of P-glycoprotein. *Biochemistry* 32: 9492-9499

Dhir R and Gros P (1992) Functional analysis of chimeric proteins constructed by exchanging homologous domains of two P-glycoproteins conferring distinct drug resistance profiles. *Biochemistry* 31: 6103-6110

Dong M, Penin F and Baggetto LG (1996) Efficient purification and reconstitution of P-glycoprotein for functional and structural studies. *Journal of Biological Chemistry* 271: 28875-28883

Dörk T, Wulbrand U, Richter T, Neumann T, Wolfes H, Wulf B, Maass G and Tummler B (1991) Cystic fibrosis with three mutations in the cystic fibrosis transmembrane regulator gene. *Human Genetics* 87: 441-446

Dreeson TD, Johnson DH and Henikoff S (1988) The Brown protein of *Drosophila melanogaster* is similar to the White protein and to components of active transport complexes. *Molecular and Cellular Biology* 8: 5206-5215

Dudler R and Hertig C (1992) Structure of an *mdr*-like gene from *Arabidopsis thaliana*. *Journal of Biological Chemistry* 267: 5882-5888

Dunn MF, Aguilar V, Brzovic P, Drew WF, Houben JKF, Leja CA and Roy M (1990) The tryptophan synthase bienzyme complex transfers indole between the α – and β– sites via a 25-30 angstrom long tunnel. *Biochemistry* 29: 8598-8607

Eakin RM (1972) Structure of invertebrate photoreceptors. In Dartnall HJA (ed) Handbook of Sensory Physiology. Springer Verlag, Berlin, Vol 7/1, pp 625-684

Endicott JA and Ling V (1989) The biochemistry of P-glycoprotein-mediated multidrug resistance. *Annual Review of Biochemistry* 58: 137-171

Engvall E and Perlmann P (1971) Enzyme-linked immunosorbent assay (ELISA) quantitative assay of immunoglobulin. *Immunochemistry* 8: 871-874

Ephrussi B (1942) Analysis of eye color differentiation in *Drosophila*. *Cold Spring Harbour Harbour Symposium of Quantitative Biology* 10: 40-48

Evans BA and Howells AJ (1978) Control of drosopterin synthesis in *Drosophila melanogaster*: mutants showing an altered pattern of GTP cyclohydrolase activity during development. *Biochemical Genetics* 16: 13-26

Ewart GD, Cannell D, Cox GB and Howells AJ (1994) Mutational analysis of the traffic ATPase (ABC) transporters involved in uptake of eye pigment precursors in *Drosophila melanogaster*. *Journal of Biological Chemistry* 269: 10370-10377

Ewart GD and Howells AJ (1998) ABC transporters involved in transport of eye pigment precursors in *Drosophila melanogaster*. *Methods in Enzymology* 292: 213-224

Ewart GD, Sutherland T, Gage PW and Cox GB (1996) The Vpu protein of human immunodeficiency virus type 1 forms cation-selective ion channels. *Journal of Virology* 70: 7108-7115

Fayle RH (1978) *Studies on the Mg-ATPase of E. coli*. Australian National University, Canberra.

Felgner JH, Kumar R, Sridhar CN, Wheeler CJ, Tsai YJ, Border R, Ramsey P, Martin M and Felgner PL (1994) Enhanced gene delivery and mechanism studies with a novel series of cationic lipid formulations. *Journal of Biological Chemistry* 269: 2550-2561

Fjose A, Polito LC, Weber U and Gehring WJ (1984) Developmental expression of the *white* locus of *Drosophila melanogaster*. *EMBO Journal* 3: 2087-2094

Fojo AT, Whang-Peng J, Gottesman MM and Pastan I (1985) Amplification of DNA sequences in human multidrug-resistant KB carcinoma cells. *Proceedings of the National Academy of Science USA* 82: 7661-7665

Forrest HS (1957) Pigment Cell Biology. Academic Press Inc., New York.

Fraser MJ (1992) The baculoviris-infected insect cell as a eukaryotic gene expression system. *Current Topics in Microbiolgy and Immunology* 158: 131-172

Freund and McDermott (1942) Sensitization to horse serum by means of adjuvants. *Proceedings of the Society for Experimental Biology & Medicine (Cambridge MA)* 49: 548-553

Garnier J, Osguthorpe DJ and Robson B (1978) Analysis of the accuracy and implications of simple methods for predicting the secondary structure of globular proteins. *Journal of Molecular Biology* 120: 97-120

Gentschev I and Goebel W (1992) Topological and functional studies on HlyB of *Escherichia coli* inner membrane. *Molecular and General Genetics* 232: 40-48

George AJ, French RR and Glennie MJ (1995) Measurement of kinetic binding constants of a panel of anti-saporin antibodies using a resonant mirror biosensor. *Journal of Immunological Methods* 183: 51-63

Georgopoulos C (1993) Role of the major heat shock proteins as molecular chaperones. *Annual Review of Cell Biology* 9: 601-634

Germann UA, Willingham MC, Pastan I and Gottesman MM (1990) Expression of the human multidrug transporter in insect cells by a recombinant Baculovirus. *Biochemistry* 29: 2295-2303

Gilmour D (1961) The Biochemistry of Insects. Academic Press, New York.

Goeddel DV (1990) Systems for heterologous gene expression. *Methods of Enzymology* 185: 3-195

Goloubinoff P, Gatenby AA and Lorimer GH (1989) GroE heat-shock proteins promote assembly of foreign prokaryotic ribulose bishphosphate carboxylase oligomers in *Escherichia coli*. *Nature* 337: 44-47

Gottesman MM and Pastan I (1988) The multidrug transporter, a double-edged sword. *Journal of Biological Chemistry* 263: 12163-12166

Gottesman MM and Pastan I (1993) Biochemistry of multidrug resistance mediated by the multidrug transporter. *Annual Review of Biochemistry* 62: 385-427

Green MM (1952) Mutant isoalleles at the *vermilion* locus in *Drosophila melanogaster*. *Proceedings of the National Academy of Science USA* 38: 300-305

Greenberger LM (1993) Major photoaffinity drug labeling sites for iodoaryl azidoprazosin in P-glycoprotein are within, or immediately C-terminal to, transmembrane domains 6 and 12. *Journal of Biological Chemistry* 268: 11417-11425

Greenberger LM, Lisanti CJ, Silva JT and Horwitz SB (1991) Domain mapping of the photoaffinity drug-binding sites in P-glycoprotein encoded by mouse *mdr*1b. *Journal of Biological Chemistry* 266: 20744-20751

Grisshammer R and Tate CG (1995) Overexpression of integral membrane proteins for structural studies. *Quarterly Reviews of Biophysics* 28: 315-422

Gruis DB and Price EM (1997) The nucleotide binding folds of the cystic fibrosis transmembrane conductance regulator are extracellularly accessible. *Biochemistry* 36: 7739-7745

Haley BE (1977) Adenosine 3',5'-cyclic monophosphate binding sites. *Methods of Enzymology* 46: 339-347

Hanna M, Brault M, Kwan T, Kast C and Gros P (1996) Mutagenesis of transmembrane domain 11 of P-Glycoprotein by alanine scanning. *Biochemistry* 35: 3625-3635

Harter C and Wieland F (1996) The secretory pathway: mechanisms of protein sorting and transport. *Biochimica et Biophysica Acta* 1286: 75-93

Hartle F-U, Hlodan R and Langer T (1994) Molecular chaperones in protein folding: the art of avoiding sticky situations. *Trends in Biochemical Science* 19: 20-25

Hazelrigg T (1987) The *Drosophila white* gene: a molecular update. *Trends in Genetics* 3: 43-46

Heuser JE and Keen JH (1988) Deep-etch visualization of proteins involved in clathrin assembly. *Journal of Cell Biology* 107: 877-886

Higgins CF (1992) ABC transporters: from microoganisms to man. *Annual Review of Cell Biology* 8: 67-113

Higgins CF, Hiles ID, Salmond GPC, Gill DR, Downie JA, Evans IJ, Holland IB, Gray L, Buckel SD, Bell AW and Hermodson MA (1986) A family of related ATP binding subunits coupled to many distinct biological processes in bacteria. *Nature* 323: 448-450

Higgins CF, Hiles ID, Whalley K and Jamieson DJ (1985) Nucleotide binding by membrane components of bacterial periplasmic binding protein-dependent transport systems. *EMBO Journal* 4: 1033-1040

Higgins DG, Thompson JD and Gibson TJ (1996) Using CLUSTAL for multiple sequence alignments. *Methods of Enzymology* 266: 383-402

Hobson AC, Weatherwax R and Ames GF-L (1984) ATP-binding sites in the membrane components of histidine permease, a periplasmic transport

system. *Proceedings of the National Academy of Science USA* 81: 7333-7337

Hoedemaeker FJ, Davidson AR and Rose DR (1998) A model for the nucleotide-binding domains of ABC transporters based on the large domain of aspartate aminotransferase. *Proteins: Structure, Function, and Genetics* 30: 275-286

Höning S, Sandoval IV and Figura Kv (1998) A di-leucine-based motif in the cytoplasmic tail of LIMP-II and tyrosinase mediates selective binding of AP-3. *EMBO Journal* 17: 1304-1314

Hoof T, Demmer A, Hadam MR, Riordan JR and Tümmler B (1994) Cystic fibrosis-type mutational analysis in the ATP-binding cassette transporter signature of human P-glycoprotein MDR1. *Journal of Biological Chemistry* 269: 20575-20583

Howells AJ and Ryall RL (1975) A biochemical study of the *scarlet* eye-color mutant of *Drosophila melanogaster*. *Biochemical Genetics* 13: 273-82

Howells AJ, Summers KM and Ryall RL (1977) Developmental patterns of 3-hydroxykynurenine accumulation in *white* and various other eye color mutants of *Drosophila melanogaster*. *Biochemical Genetics* 15: 1049-1059

Hung L-W, Wang IX, Nikaido K, Liu P-Q, Ames GF-L and Kim S-H (1998) Crystal structure of the ATP-binding subunit of an ABC transporter, the histidine permease of *Salmonella typhimurium*. *Nature* 396: 703-707

Hunziker W and Fumey C (1994) A di-leucine motif mediates endocytosis and basolateral sorting of macrophage IgG Fc receptors in MDCK cells. *EMBO Journal* 13: 2963-2967

Hyde CC, Ahmed SA, Padlan EA, Miles EW and Davies DR (1988) Three-dimensional structure of the tryptophan synthase $\alpha_2\beta_2$ multi-enzyme complex from *Salmonella typhimurium*. *Journal of Biological Chemistry* 263: 17857-17871

Hyde SC, Emsley P, Hartshorn MJ, Mimmack MM, Gileadi U, Pearce SR, Gallagher MP, Gill DR, Hubbard RE and Higgins CF (1990) Structural model of ATP-binding proteins associated with cystic fibrosis, multidrug resistance and bacterial transport. *Nature* 346: 362-365

Jameson BA and Wolf H (1988) The antigenic index: A novel algorithm, for predicting antigenic determinants. *Computer Apllications in the Biosciences* 4: 181-186

Janknecht R, Martynoff Gd, Lou J, Hipskind RA, Nordheim A and Stunnenberg HG (1991) Rapid and efficient purification of native histidine-tagged

protein expressed by recombinant vaccinia virus. *Proceedings of the National Academy of Science USA* 88: 8972-8976

Judd (1964) *Drosophila Information Service* 39: 59-60

Juranka PF, Zastawny RL and Ling V (1989) P-glycoprotein: multidrug-resistance and a superfamily of membrane-associated transport proteins. *FASEB Journal* 3: 2583-2592

Kang J, Lemaire H-G, Unterbeck A, Salbaum JM and Masters CL (1987) The precursor of Alzheimer's disease amyloid A4 protein resembles a cell-surface receptor. *Nature* 325: 733-736

Kartner N, Hanrahan JW, Jensen TJ, Naismith AL, Sun S, Ackerley CA, Reyes ER, Tsui L-C, Rommens JM, Bear CE and Riordan JR (1991) Expression of the cystic fibrosis gene in non-epithelial invertebrate cells produces a regulated anion conductance. *Cell* 64: 681-691

Kast C, Canfield V, Levenson R and Gros P (1996) Transmembrane organisation of mouse P-glycoprotein determined by epitope insertion and immunofluorescence. *Journal of Biological Chemistry* 271: 9240-9248

Keeton WT and Gould JL (1986) *Biological Science*. W.W. Norton & Company, New York.

Kerem BS, Zielenski J, Markiewicz D, Bozon D, Gazit E, Yahaf J, Kennedy D, Riordan JR, Collins FS, Rommens JR and Tsui L-C (1990) Identification of mutations in regions corresponding to the two putative nucleotide (ATP)-binding folds of the cystic fibrosis gene. *Proceedings of the National Academy of Science USA* 87: 8447-8451

Kerppola R and Ames G (1992) Topology of the hydrophobic membrane-bound components of the histidine periplasmic permease. Comparison with other members of the family. *J Biol Chem* 267: 2329-36

Kerppola RE, Shyamala VK, Klebba P and Ames GF-L (1991) The membrane-bound proteins of periplasmic permeases form a complex. *Journal of Biological Chemistry* 266: 9857-9865

King LA and Possee RD (1992) The Baculovirus Expresssion System, A laboratory Guide. Chapman & Hall, London.

Kitts PA and Possee RD (1993) A method for producing recombinant baculovirus expression vectors at high frequency. *Biotechniques* 14: 810-817

Ko Y and Pedersen P (1995) The first nucleotide binding fold of the cystic fibrosis transmembrane conductance regulator can function as an active ATPase. *Journal of Biological Chemistry* 270: 22093-22096

Ko YH, Delannoy M and Pedersen PL (1997) Cystic fibrosis transmembrane conductance regulator: the first nucleotide binding fold targets the membrane with retention of its ATP binding function. *Biochemistry* 36: 5053-5064

Koronakis V, Hughes C and Koronakis E (1993) ATPase activity and ATP/ADP-induced conformational change in the soluble domain of the bacterial protein translocator HlyB. *Molecular Microbiology* 8: 1163-1175

Kunkel TA (1985) Rapid and efficient site-specific mutagenesis without phenotypic selection. *Proceedings of the National Academy of Science USA* 82: 488-492

Kunkel TA (1988) *Nucleic Acids Molecular Biology* 12: 124

Kunkel TA, Bebenek K and McClary J (1991) Efficient Site-Directed Mutagenisis using uracil-containing DNA. *Methods in Enzymology* 204: 125-139

Kurkulos M, Weinberg JM, Pepling ME and Mount SM (1991) Polyadenylation in *copia* requires unusually distant upstream sequences. *Proceedings of the National Academy of Science USA* 88: 3038-3042

Kyte J and Doolittle RF (1982) A simple method for displaying the hydropathic character of a protein. *Journal of Molecular Biology* 157: 105-132

Laemmli UK (1970) Cleavage of structural proteins during the assembly of the head of bacteriophage T4. *Nature* 227: 680-685

Lang K, Schmid FX and Fischer G (1987) Catalysis of protein folding by prolyl isomerase. *Nature* 329: 268-270

Laughlin SB (1975) The function of the lamina ganglionaris. In Horridge GA (ed) The compound eye and vision of insects. Clarendon Press, Oxford, pp 341-358

Lee SC and Olins P (1992) Effect of overproduction of heat shock chaperones GroESL and DnaK on human procollagenase production in *Escherichia coli*. *Journal of Biological Chemistry* 267: 2849-2852

Lenhard T and Reiländer H (1997) Engineering the folding pathway of insect cells: generation of a stably transformed insect cell line showing improved folding of a recombinant membrane protein. *Biochemical and Biophysical Research Communications* 238: 823-830

Letourneur F and Klausner RD (1992) A novel di-leucine motif and a tyrosine-based motif independently mediate lysosomal targeting and endocytosis of CD3 chains. *Cell* 69: 1143-1157

Levis R, Hazelrigg T and Rubin GM (1985) Effects of genomic position on the expression of transduced copies of the *white* gene of *Drosophila*. *Science* 229: 558-561

Li C, Ramjeesingh M and Bear CE (1996a) Purified cystic fibrosis transmembrane conductance regulator (CFTR) does not function as an ATP channel. *Journal of Biological Chemistry* 271: 11623-11626

Li C, Ramjeesingh M, Wang W, Garami E, Hewryk M, Lee D, Rommens JM, Gallery K and Bear CE (1996b) ATPase activity of the cystic fibrosis transmembrane conductance regulator. *Journal of Biological Chemistry* 271: 28463-28468

Linzen B (1974) The tryptophan to ommochrome pathway in insects. *Advances in Insect Physiology* 10: 117-245

Lis H and Sharon N (1993) Protein glycosylation. Structural and functional aspects. *European Journal of Biochemistry* 218: 1-27

Lloyd V, Ramaswami M and Krämer H (1998) Not just pretty eyes: *Drosophila* eye-colour mutations and lysosomal delivery. *Trends in Cell Biology* 8: 257-259

Lo MC and Pak WL (1981) Light induced pigment granule migration in the retinular cells of *Drosophila melanogaster*. *Journal of General Physiology* 155: 155-175

Loo TW and Clarke DM (1993) Functional consequences of phenylalanine mutations in the predicted transmembrane domain of P-glycoprotein. *Journal of Biological Chemistry* 268: 19965-19972

Loo TW and Clarke DM (1994a) Functional consequencess of glycine mutations in the predicted cytoplasmic loops of P-glycoprotein. *Journal of Biological Chemistry* 269: 7243-7248

Loo TW and Clarke DM (1994b) Mutations to amino acids located in predicted transmembrane segment 6 (TM6) modulate the activity and substrate specificity of human P-glycoprotein. *Biochemistry* 33: 14049-14057

Loo TW and Clarke DM (1995a) Covalent modification of human P-glycoprotein mutants containing a single cysteine in either nucleotide-binding fold abolishes drug-stimulated ATPase activity. *Journal of Biological Chemistry* 270: 22957-22961

Loo TW and Clarke DM (1995b) Membrane topology of a cysteine-less mutant of human P-glycoprotein. *Journal of Biological Chemistry* 270: 843-848

Loo TW and Clarke DM (1995c) P-glycoprotein. *Journal of Biological Chemistry* 270: 21839-21844

Lu Y-A, Clavijo P, Galantino M, Shen Z-Y, Liu W and Tam JP (1991) Chemically unambiguous peptide immunogen: preparation, orientation and antigenicity of purified peptide conjugated to the multiple antigen peptide system. *Molecular Immunology* 28: 623-630

Mackenzie S, Brooker MR, Gill TR, Cox GB, Howells AJ and Ewart GD (1999) Mutations in the *white* gene of *Drosophila melanogaster* affecting ABC transporters that determine eye colouration. *In press*

Manavalan P, Smith AE and McPherson JM (1993) Sequence and Structural Homology Among Membrane-Associated Domains of CFTR and Certain Transporter Proteins. *Journal of Protein Chemistry* 12: 279-290

Mannheim B Detergents for Membrane Research. *Technical Manual*

Matsuura Y, Possee RD, Overton HA and Bishop DHL (1987) Baculovirus expression vectors: the requirements for high level expression of proteins, including glycoproteins. *Journal of General Virology* 68: 1233-1250

McCarty NA, McDonough S, Cohen BN, Riordan JR, Davidson N and Lester HA (1993) Voltage-dependent block of the cystic fibrosis transmembrane conductance regulator channel by two closely related arylaminobenzoates. *Journal of General Physiology* 102: 1-23

McDonough S, Davidson N, Lester HA and McCarty NA (1994) Novel pore-lining residues in CFTR that govern permeation and open-channel block. *Neuron* 13: 623-634

McGivan JD and Pastor-Anglada M (1994) Regulatory and molecular aspects of mammalian amino acid transport. *Biochemical Journal* 299: 321-334

Meyer TH, van Endert PM, Uebel S, Ehring B and Tampe R (1994) Functional expression and purification of the ABC transporter complex associated with antigen processing (TAP) in insect cells. *FEBS Letters* 351: 443-7

Mimura CS, Holbrook SR and Ames GF-L (1991) Structural model of the nucleotide binding conserved component of periplasmic permeases. *Proceedings of the National Academy of Science USA* 88: 84-88

Moore GP and Sullivan DT (1978) Biochemical and genetic characterisation of kynurenine formamidase from *D. melanogaster*. *Biochemical Genetics* 16: 619-633

Morgan TH (1910) Sex limited inheritance in Drosophila. *Science* 32: 120-122

Morris DI, Greenberger LM, Bruggemann EP, Cardarelli C, Gottesman MM, Pastan I and Seamon KB (1994) Localisation of the forskolin labeling sites to both halves of P-glycoprotein: similarity of the sites labeled by forskolin and prazosin. *Molecular Pharmacology* 46: 329-337

Morris DI, Speicher LA, Ruoho AE, Tew KD and Seamon KB (1991) Interaction of Forskolin with the P-glycoprotein multidrug transporter. *Biochemistry* 30: 8371-8379

Mosser J, Douar A-M, Sarde C-O, Kioschis P, Feil R, Moser H, Poustka A-M, Mandel J-L and Aubourg P (1993) Putative X-linked adrenoleukodystrophy gene shares unexpected homology with ABC transporters. *Nature* 361: 726-730

Mourez M, Hofnung M and Dassa E (1997) Subunit interactions in ABC transporters: a conserved sequence in hydrophobic membrane proteins of periplasmic permeases defines an important site of interaction with the ATPase subunits. *EMBO Journal* 16: 3066-3077

Mullis KB and Faloona FA (1987) Specific synthesis of DNA in vitro via a polymerase-catalyzed chain reaction. *Methods in Enzymology* 155: 335-350

Nakai K and Horton P (1999) PSORT: a program for detecting sorting signals in proteins and predicting their subcellular localisation. *Trends in Biochemistry* 24: 34-35

Newman LS, McKeever MO, Okano HJ and Darnell RB (1995) Beta-NAP, a cerebellar degeneration antigen, is a neuron-specific vesicle coat protein. *Cell* 82: 773-783

Neyfakh AA, Bidnenko VE and Chen LB (1991) Efflux-mediated multidrug resistance in *Bacillus subtilis*: similarities and dissimilarities with the mammalian system. *Proceedings of the National Academy of Science USA* 88: 4781-4785

Nicoletti (1960) *Drosophila Information Service* 34: 52-53

Nikaido K, Liu P-Q and Ames GF-L (1997) Purification and characterization of HisP, the ATP-binding subunit of a traffic ATPase (ABC transporter), the histidine permease of *Salmonella typhimurium*. *Journal of Biological Chemistry* 272: 27745-27752

Nissani M (1975) Cell lineage analysis of kynurenine producing organs in *Drosophila melanogaster*. *Genetic Research Camb* 26: 63-72

Odorizzi G, Cowles CR and Emr SD (1998) The AP-3 complex: a coat of many colours. *Trends in Cell Biology* 8: 282-288

O'Hare K, Murphy C, Levis R and Rubin GM (1984) DNA Sequence of the *white* locus of *Drosophila melanogaster*. *Journal of Molecular Biology* 180: 437-455

Ooi CE, Moreira JE, Dell'Angelica EC, Poy G, Wassarman DA and Bonifacino JS (1997) Altered expression of a novel adaptin leads to defective pigment granule biogenesis in the *Drosophila* eye colour mutant *garnet*. *EMBO Journal* 16: 4508-4518

O'Riordan CR, Erickson A, Bear C, Li C, Manavalan P, Wang KX, Marshall J, Scheule RK, McPherson JM, Cheng SH and Smith AE (1995) Purification and characterisation of recombinant CFTR from Chinese Hamster Ovary and Insect Cells. *Journal of Biological Chemistry* 270: 17033-17043

Pacholczyk T, Blakely RD and Amara SG (1991) Expression cloning of a cocaine- and antidepressant-senstive human noradrenaline transporter. *Nature* 350: 350-354

Page LJ and Robinson MS (1995) Targeting signals and subunit interactions in coated vesicle adaptor complexes. *Journal of Cell Biology* 131: 619-630

Pai EF, Kabsch W, Krengel U, Holmes KC, John J and Wittinghofer A (1989) Structure of the guanine-nucleotide-binding domain of the Ha-*ras* oncogene product p21 in the triphosphate conformation. *Nature* 341: 209-214

Pai EF, Krengel U, Petsko GA, Goody RS, Kabsch W and Wittinghofer A (1990) Refined crystal structure of the triphosphate conformation of H-ras p21 at 1.35 angstom resolution: implications for the mechanism of GTP hydrolysis. *EMBO Journal* 9: 2351-2359

Pastink A, Schalet A, Vreeken C, Paradi E and Eeken J (1987) The nature of radiation-induced mutations at the white locus of Drosophila melanogaster. *Mutation Research* 177: 101-15

Pastink A, Vreeken C, Schalet A and Eeken J (1988a) DNA sequence analysis of X-ray-induced deletions at the white locus of Drosophila melanogaster. *Mutat Res* 207: 23-8

Pastink A, Vreeken C and Vogel EW (1988b) The nature of N-ethyl-N-nitrosourea-induced mutations at the *white* locus of *Drosophila melanogaster*. *Mutation Research* 199: 47-53

Paton DR and Sullivan DT (1978) Mutagenesis at the *cinnabar* locus in *D. melanogaster*. *Biochemical Genetics* 16: 855-863

Pawagi AB, Wang J, Silverman M, Reithmeier RAF and Deber CM (1994) Transmembrane aromatic amino acid distribution in P-glycoprotein. *Journal of Molecular Biology* 235: 554-564

Pearce SR, Mimmack ML, Gallagher MP, Gileadi U and Hyde SC (1992) Membrane topology of the integral membrane components, OppB and

OppC, of the oligopeptide permease of *Salmonella typhimurium*. *Molecular Microbiology* 6: 47-57

Peeler JS, Donzell WC and Anderson RGW (1993) The appendage domain of the AP-2 subunit is not reqired for assembly or invagination of clathrin-coated pits. *Journal of Cell Biology* 120: 47-54

Pepling M and Mount SM (1990) Sequence of a cDNA from the *Drosophila melanogaster white* gene. *Nucleic Acids Research* 18: 1633

Petronilli V and Ames GF-L (1991) Binding protein-independent histidine permease mutants. Uncoupling of ATP hydrolysis from transmembrane signaling. *Journal of Biological Chemistry* 266: 16293-16296

Phillips JP and Forrest HS (1980) Ommochromes and pteridines. In Ashburner M and Wright TRF (eds) The Genetics and Biology of *Drosophila*. Academic Press, New York and London, Vol 2d, pp 542-611

Piller SC, Ewart GD, Jans DA, Gage PW and Cox GB (1999) The amino-terminal region of Vpr from human immunodeficiency virus type 1 forms ion channels and kills neurons. *Journal of Virology* 73: 4230-4238

Potterf SB, Muler J, Bernardini I, Tietze F, Kobayashi T, Hearing VJ and Gahl WA (1996) Characterization of a melanosomal transport system in murine melanocytes mediating entry of the melanogenic substrate tyrosine. *Journal of Biological Chemistry* 271: 4002-4008

Quinton PM (1990) Cystic fibrosis: a disease in electrolyte transport. *The FASEB Journal* 4: 2709-2717

Randak C, Roscher AA, Hadorn H-B, Assalg-Machleidt I, Auerswald EA and Machleidt W (1995) Expression and functional properties of the second nucleotide binding fold of the cystic fibrosis transmembrane conductance regulator fused to glutathione-S-transferase. *FEBS Letters* 363: 189-194

Raviv Y, Pollard HB, Bruggemann EP, Pastan I and Gottesman MM (1990) Photosensitized labeling of a functional multidrug transporter in living drug-resistant tumor cells. *Journal of Biological Chemistry* 265: 3975-3980

Reinemer P, Dirr HW, Ladenstein R, Schaeffer J, Gallay O and Huber R (1991) The three-dimensional structure of class π glutathione S-transferase in complex with glutathione sulfonate at 2.3 angstrom resolution. *EMBO Journal* 10: 1997-2005

Renfranz P and Benzer S (1989) Monoclonal antibody probes discriminate early and late mutant defects in development of the *Drosophila* retina. *Developmental Biology* 136: 411-429

Riordan JR, Rommens JM, Kerem B-S, Alon N, Rozmahel R, Grzelczak Z, Zielenski J, Lok S, Plavsic N, Chou J-L, Drumm ML, Iannuzzi MC, Collins FS and Tsui L-C (1989) Identification of the cystic fibrosis gene: cloning and characterisation of complementary DNA. *Science* 245: 1066-1073

Rizki MTM (1961) Intracellular localisation of kynurenine in the fat body of *Drosophila*. *Journal of Biochemistry Biophysical Cytology* 9: 567-572

Rizki TM (1980) Fat Body. In Ashburner M and Wright TRF (eds) The Genetics and Biology of *Drosophila*. , Vol 2b, pp 561-601

Roberts DB (1986) Drosophila: a practical approach. IRL Press Limited, Oxford.

Robson B and Suzuki E (1976) Conformational properties of amino acid residues in globular proteins. *Journal of Molecular Biology* 107: 327-356

Roepe PD (1995) The role of the MDR protein in altered drug translocation across tumor cell membranes. *Biochimica et Biophysica Acta* 1241: 385-406

Roepe PD, Wei L, Hoffman MM and Fritz F (1996) Altered drug transclocation mediated by the MDR protein: direct, indirect or both? *Journal of Bioenergetics and Biomembranes* 28: 541-555

Rommens JM, Iannuzzi MC, Kerem B-S, Drumm ML, Melmer G, Dean M, Rozmahel R, Cole JL, Kennedy D, Hidaka N, Zsiga M, Buchwald M, Riordan JR, Tsui L-C and Collins FS (1989) Identification of the cystic fibrosis gene: chromosome walking and jumping. *Science* 245: 1059-1065

Roninson IB, Chin JE, Choi K, Gros P, Housman DE, Fojo A, Shen D-W, Gottesman MM and Pastan I (1986) Isolation of human *mdr* DNA sequences amplified in multidrug-resistant KB carcinoma cells. *Proceedings of the National Academy of Science USA* 83: 4538-4542

Roninson IB, Pastan I and Gottesman MM (1991) Molecular and cellular biology of multidrug resistance in tumor cells. In Roninson IB (ed) . Plenum, New York, pp 91-106

Rossman MG, Moras D and Olsen KW (1974) Chemical and biological evolution of a nucelotide-binding protein. *Nature* 250: 194-199

Rubin G and Spradling A (1983) Vectors for P element-mediated gene transfer in *Drosophila*. *Nucleic Acids Research* 11: 6341-6351

Ryall RL and Howells AJ (1974) Ommochrome biosynthetic pathway of *Drosophila melanogaster*. Variations in the levels of enzyme activities and intermediates during adult development. *Insect Biochemistry* 6: 135-142

Safa AR, Stern RK, Choi K, Agresti M, Tamai I, Mehta ND and Roninson IB (1990) Molecular basis of preferential resistance to colchicine in multidrug-resistant human cells conferred by Gly185 to Val substitution in

P-glycoprotein. *Proceedings of the National Academy of Science USA* 87: 7225-7229

Saiki RK, Scharf S, Faloona F, Mullis KB, Horn GT, Erlich HA and Arnheim N (1985) Enzymatic amplification of beta-globin genomic sequences and restriction site analysis for diagnosis of sickle cell anemia. *Science* 230: 1350-1354

Salamero J, LeBorgne R, Saudrais C, Goud B and Hoflack B (1996) Expression of major histocompatibility complex class II molecules in HeLa cells promotes the recruitment of AP-1 golgi-specific assembly proteins on golgi membranes. *Journal of Biological Chemistry* 271: 30318-30321

Sambrook J, Fritsch EF and Maniatis T (1989) Molecular Cloning: A Laboratory Manual. Cold Spring Harbor Laboratory, Cold Spring Harbor, NY.

Sankaran B, Bhagat S and Senior AE (1997) Inhibition of P-Glycoprotein ATPase Activity by Procedures Involving Trapping of Nucleotide in Catalytic sites. *Archives of Biochemistry and Biophysics* 341: 160-169

Saraste M, Sibbald PR and Wittinghofer A (1990) The P-loop - a common motif in ATP- and GTP-binding proteins. *Trends in Biochemstry* 15: 430-434

Sarkadi B, Price EM, Boucher RC, Germann UA and Scarborough GA (1992) Expression of the human multidrug resistance cDNA in insect cells generates a high activity drug-stimulated membrane ATPase. *Journal of Biological Chemistry* 267: 4854-4858

Saurin W, Koster W and Dassa E (1994a) Bacterial binding protein-dependent permeases: characterization of distinctive signatures for functionally related integral cytoplasmic membrane proteins. *Mol Microbiol* 12: 993-1004

Saurin W, Köster W and Dassa E (1994b) Bacterial binding protein-dependent permeases: characterization of distinctive signatures for functionally related integral cytoplasmic membrane proteins. *Molecular Microbiology* 12: 993-1004

Savary S, Denizot F, Luciani M-F, Mattei M-G and Chimini G (1996) Molecular cloning of a mammalian ABC transporter homologous to *Drosophila white* gene. *Mammalian Genome* 7: 673-676

Schmid SL (1997) Clathrin-coated vesicle formation and protein sorting: an integrated process. *Annual Review of Biochemistry* 66: 511-548

Schneuwly S, Shortridge RD, Larrivee DC, Ono T, Ozaki M and Pak WL (1989) *Drosophila ninaA* gene encodes an eye-specific cyclophilin (cyclosporine A binding protein). *Proceedings of the National Academy of Science USA* 86: 5390-5394

Schraermeyer U and Dohms M (1993) Atypical granules in the eyes of *white* mutant *Drosophila melanogaster* are lysosome-related organelles. *Pigment Cell Research* 6: 73-84

Seibert FS, Jia Y, Mathews CJ, Hanrahan JW, Riordan JR, Loo TW and Clarke DM (1997) Disease-associated mutations in cytoplasmic loops 1 and 2 of cystic fibrosis transmembrane conductance regulator impede processing or opening of the channel. *Biochemistry* 36: 11966-11974

Senior AE, Al-Shawi MK and Urbatsch IL (1995) Mini-review. The catalytic cycle of P-glycoprotein. *FEBS Letters* 377: 285-289

Shani N, Sapag A and Valle D (1996) Characterisation and analysis of conserved motifs in a peroxisomal ATP-binding cassette transporter. *Journal of Biological Chemistry* 271: 8725-8730

Shani N, Watkins PA and Valle D (1995) *PXA1*, a possible *Saccharomyces cerevisiae* ortholog of the human adrenoleukodystrophy gene. *Proceedings of the National Academy of Science USA* 92: 6012-6016

Shapiro AB and Ling V (1995) Using purified P-glycoprotein to understand multidrug resistance. *Journal of Bioenergetics and Biomembranes* 27: 7-13

Sheppard DN, Travis SM, Ishihara H and Welsh MJ (1996) Contribution of proline residues in the membrane-spanning domains of cystic fibrosis transmembrane conductance regulator to chloride channel function. *Journal of Biological Chemistry* 271: 14995-15001

Shieh BH, Stamnes MA, Seavello S, Harris GL and Zuker CS (1989) The *ninaA* gene required for visual transduction in *Drosophila* encodes a homologue of cyclosporin A-binding protein. *Nature* 338: 67-70

Shotwell MA and Oxender DL (1983) The regulation of neutral amino acid transport by amino acid availability in animal cells. *Trends in Biochemical Science* 8: 314-316

Shoup JR (1966) The development of pigment granules in the eyes of wild type and mutant *Drosophila melanogaster*. *Journal of Cell Biology* 29: 223-249

Shyamala V, Baichwal V, Beall E and Ames GF-L (1991) Structure-functional analysis of the histidine permease and comparison with cystic fibrosis mutations. *Journal of Biological Chemistry* 266: 18714-18719

Simpson F, Peden AA, Christopoulou L and Robinson MS (1997) Characterisation of the Adaptor-related protein complex, AP-3. *Journal of Cell Biology* 137: 835-845

Smith DB and Johnson KS (1988) Single-step purification of polypeptides expressed in *Escherichia coli* as fusions with glutathione S-transferase. *Gene (Amsterdam)* 67: 31-39

Solomon KA, Hsu DK and Brusilow WS (1989) Use of lacZ fusions to measure in vivo expression of the first three genes of the *Escherichia coli* unc operon. *Journal of Bacteriology* 171: 3039-3045

Stamnes MA, Shieh BH, Chuman L, Harris GL and Zuker CS (1991) The cyclophilin homolog ninaA is a tissue-specific integral membrane protein required for the proper synthesis of a subset of *Drosophila* rhodopsins. *Cell* 65: 219-227

Stark WS and Sapp R (1988) Eye color pigment granules in wild-type and mutant *Drosophila melanogaster*. *Canadian Journal of Zoology* 66: 1301-1308

Stark WS and Wasserman GS (1972) Transient and receptor potentials in the electroretinogram of *Drosophila*. *Vision Research* 12: 1771-1775

Stark WS and Wasserman GS (1974) Wavelength specific ERG characteristics of pigmented- and white-eyed strains of *Drosophila*. *Journal of Comparative Physiology* 91: 427-441

Story RM and Steitz TA (1992) Structure of the recA protein-ADP complex. *Nature* 355: 318-324

Stratakis E (1981) Submitochondrial localization of kynurenine 3-hydroxylase from ovaries of *Ephestia kuhniella*. *Insect Biochemistry* 11: 735-741

Sullivan DT, Bell La, Paton DR and Sullivan MC (1979) Purine transport by malpighian tubules of pteridine-deficient eye color mutants of *Drosophila melanogaster*. *Biochemical Genetics* 17: 565-573

Sullivan DT, Bell LA, Paton DR and Sullivan MC (1980) Genetic and functional analysis of tryptophan transport in malpighian tubules of *Drosophila*. *Biochemical Genetics* 18: 1109-1131

Sullivan DT, Grillo SL and Kitos RJ (1974) Subcellular localization of the first three enzymes of the ommochrome synthetic pathway in *Drosophila melanogaster*. *Journal of Experimental Zoology* 188: 225-234

Sullivan DT and Kitos RJ (1976) Developmental regulation of tryptophan catabolism in *Drosophila*. *Insect Biochemistry* 6: 649-655

Sullivan DT, Kitos RJ and Sullivan MC (1973) Developmental and genetic studies on kynurenine hydroxylase from *Drosophila melanogaster*. *Genetics* 75: 651-661

Sullivan DT and Sullivan MC (1975) Transport defects as the physiological basis for eye color mutants of *Drosophila melanogaster*. *Biochemical Genetics* 13: 603-613

Summers KM, Howells AJ and Pyliotis NA (1982) Biology of eye pigmentation in insects. *Advances in Insect Physiology* 16: 119-166

Tabcharani JA, Rommens JM, How YX, Chang XB, Tsui LC, Riordan JR and Hanrahan JW (1993) Multi-ion pore behaviour in the CFTR chloride channel. *Nature* 366: 79-82

Tam JP (1988) Synthetic peptide vaccine design: synthesis and properties of a high-density multiple antigen peptide system. *Proceedings of the National Academy of Science USA* 85: 5409-5413

Tate CG and Blakely RD (1994) The effect of N-linked glycosylation on activity of the Na^+ - and Cl^-- dependent serotonin transporter expressed using recombinant baculovirus in insect cells. *Journal of Biological Chemistry* 269: 26303-26310

Taylor ME, Conary JT, Lennartz MR, Stahl PD and Drickamer K (1990) Primary structure of the mannose receptor contains multiple motifs resembling carbohydrate recognition domains. *Journal of Biological Chemistry* 265: 12156-12162

Tearle RG, Belote JM, McKeown M, Baker BS and Howells AJ (1989) Cloning and characterisation of the *scarlet* gene of *Drosophila melanogaster*. *Genetics* 122: 595-606

Teem JL, Berger HA, Ostedgaard LS, Rich DP, Tsui L-C and Welsh MJ (1993) Identification of revertants for the cystic fibrosis deltaF508 mutation using STE6-CFTR chimeras in yeast. *Cell* 73: 335-346

Thiem SM and Miller LK (1989) Identification, sequence, and transcriptional mapping of the major capsid protein gene of the baculovirus *Autographa californica* nuclear polyhedrosis virus. *Journal of Virology* 63: 2008-2018

Thompson ST, Cass KH and Stellwagen E (1975) Blue dextran-sepharose: an affinity column for the dinucleotide fold in proteins. *Proceedings of the National Academy of Science USA* 72: 669-672

Tobler J, Bowman JT and Simmons JR (1971) Gene modulation in *Drosophila*. Dosage compensation and relocated v^+ genes. *Biochemical Genetics* 5: 111-117

Tong L, Milburn MV, Vos AMD and Kim S-H (1989) Structure of *ras* protein. *Science* 245: 244

Tordo N, Bourhy H, Sather S and Ollo R (1993) Structure and expression in baculovirus of the mokola virus glycoprotein: an efficient recombinant vaccine. *Virology* 194: 59-69

Towbin H, Staehelin T and Gordon J (1979) Electrophoretic transfer of proteins from polyacrylamide gels to nitrocellulose sheets: procedure and some applications. *Proceedings of the National Academy of Science USA* 76: 4350-4354

Trowbridge IS and Collawn JF (1993) Signal-dependent membrane protein trafficking in the endocytic pathway. *Annual Review of Cell Biology* 9: 129-161

Tweeten KA, Bulla LA and Consigli RA (1980) Characterisation of an extremely basic protein derived from granulosis virus nucleocapsids. *Journal of Virology* 33: 866-876

Uhlen M and Moks T (1990) Gene Fusions for purpose of expression: an introduction. *Methods of Enzymology* 185: 129-143

Urbatsch IL, Al-Shawi MK and Senior AE (1994) Characterization of the ATPase activity of purified Chinese hamster P-glycoprotein. *Biochemistry* 33: 7069-7076

Urbatsch IL, Sankaran B, Bhagat S and Senior AE (1995a) Both P-glycoprotein nucleotide-binding sites are catalytically active. *Journal of Biological Chemistry* 270: 26956-26961

Urbatsch IL, Sankaran B, Weber J and Senior AE (1995b) P-glycoprotein is stably inhibited by vanadate-induced trapping of nucleotide at a single catalytic site. *Journal of Biological Chemistry* 270: 19383-19390

Walker AR, Howells AJ and Tearle RG (1986) Cloning and characterisation of the *vermilion* gene of *D. melanogaster*. *Molecular and General Genetics* 202: 102-107

Walker JE, Saraste M, Runswick MJ and Gay NJ (1982) Distantly related sequences in the alpha and beta-subunits of ATP synthase, myosin, kinases and other ATP-requiring enzymes and a common nucleotide binding fold. *EMBO Journal* 1: 945-951

Walter C, Bentrup KHz and Schneider E (1992) Large scale purification, nucleotide binding properties, and ATPase activity of the MalK subunit of *Salmonella typhimurium* maltose transport complex. *Journal of Biological Chemistry* 267: 8863-8869

Webb DC, Rosenberg H and Cox GB (1992) Mutational analysis of the *Escherichia coli* Phosphate-specific transport system, a member of the traffic ATPase (or ABC) family of membrane transporters. *Journal of Biological Chemistry* 267: 24661-24668

Weinbaum G and Markman R (1966) A rapid technique for distinguishing enzymatically active proteins in the cell "envelope" of *Escherichia coli* B. *Biochimica et Biophysica Acta* 124: 207-209

Welsh MJ, Robertson AD and Ostedgaard LS (1998) The ABC of a versatile engine. *Nature* 396: 623-624

Weyer U and Possee RD (1991) A baculovirus dual expression vector derived from the *Autographa californica* nuclear polyhedrosis virus polyhedrin and

p10 promoters: co-expression of two influenza virus genes in insect cells. *Journal of General Virology* 72: 2967-2974

Wiederrecht G and Brown G (1984) Purification and properties of the enzymes from *Drosophila melanogaster* that catalyze the conversion of dihydroneopterin triphosphate to the pyrimidodiazepine precursor of the drosopterins. *Journal of Biological Chemistry* 259: 14121-14127

Wigglesworth VB (1972) The Principles of Insect Physiology. Methuen, London.

Wiley K and Forrest HS (1981) Terminal synthesis of xanthommatin in *Drosophila melanogaster*. IV. enzymatic and nonenzymatic catalysis. *Biochemical Genetics* 19: 1211-1221

Williams GV, Rohel DZ, Kuzio J and Faulkner P (1989) A cytopatholgical investigation of *Autographa californica* nuclear polyhedrosis virus p10 gene function using insertion/deletion mutants. *Journal of General Virology* 70: 187-202

Williams MA and Fukuda M (1990) Accumulation of membrane glycoproteins in lysosomes requires a tyrosine residue at a particular position in the cytoplasmic tail. *Journal of Cell Biology* 111: 955-966

Xie J, Drumm ML, Ma J and Davis PB (1995) Intracellular loop between transmembrane segments IV and V of cystic fibrosis transmembrane conductance regulator is involved in regulation of chloride channel conductance state. *Journal of Biological Chemistry* 270: 28084-28091

Yagi S and Ogawa H (1996) Effect of tryptophan metabolites on fluorescent granules in the malpighian tubules of eye color mutants of *Drosophila melanogaster*. *Zoological Science* 13: 97-104

Yoshida M and Amano T (1995) A common topology of proteins catalyzing ATP-triggered reactions. *FEBS Letters* 359: 1-5

Zachar Z and Bingham PM (1982) Regulation of *white* locus expression: the structure of mutant alleles at the *white* locus of *Drosophila melanogaster*. *Cell* 30: 529-541

Zeigler I (1961) Genetic aspects of ommochrome and pterin pigments. *Advances in Genetics* 10: 349-403

Zhang S and Odenwald W (1995) Misexpression of the *white (w)* gene triggers male-male courtship in *Drosophila*. *Proceedings of the National Academy of Science USA* 92: 5525-5529

Zhang X, Collins KI and Greenberger LM (1995a) Functional evidence that transmembrane 12 and the loop between transmembrane 11 and 12 form part of the drug-binding domain in P-glycoprotein encoded by *MDR1*. *Journal of Biological Chemistry* 270: 5441-5448

Zhang X, Collins KI and Greenberger LM (1995b) Functional Evidence that Transmembrane 12 and the Loop between Transmembrane 11 and 12 Form Part of the Drug-binding Domain in P-glycoprotein encoded by *MDR 1*. *Journal of Biological Chemistry* 270: 5441-5448

Zwiebel LJ, Saccone G, Zacharopoulou A, Besansky NJ, Favia G, Collins FH, Louis C and Kafatos FC (1995) The *white* gene of *Ceratitis capitata*: a phenotypic marker for germline transformation. *Science* 270: 2005-2007